

Using Protease Structure to Design New Enantioselective Reactions

by

Christopher K. Savile

*A thesis submitted to McGill University in partial fulfillment of the requirements of the
degree of Doctor of Philosophy*

Department of Chemistry
McGill University
Montréal, Québec
Canada
November 2005

© Christopher K. Savile, 2005



Library and
Archives Canada

Bibliothèque et
Archives Canada

Published Heritage
Branch

Direction du
Patrimoine de l'édition

395 Wellington Street
Ottawa ON K1A 0N4
Canada

395, rue Wellington
Ottawa ON K1A 0N4
Canada

Your file Votre référence

ISBN: 978-0-494-25249-9

Our file Notre référence

ISBN: 978-0-494-25249-9

NOTICE:

The author has granted a non-exclusive license allowing Library and Archives Canada to reproduce, publish, archive, preserve, conserve, communicate to the public by telecommunication or on the Internet, loan, distribute and sell theses worldwide, for commercial or non-commercial purposes, in microform, paper, electronic and/or any other formats.

The author retains copyright ownership and moral rights in this thesis. Neither the thesis nor substantial extracts from it may be printed or otherwise reproduced without the author's permission.

AVIS:

L'auteur a accordé une licence non exclusive permettant à la Bibliothèque et Archives Canada de reproduire, publier, archiver, sauvegarder, conserver, transmettre au public par télécommunication ou par l'Internet, prêter, distribuer et vendre des thèses partout dans le monde, à des fins commerciales ou autres, sur support microforme, papier, électronique et/ou autres formats.

L'auteur conserve la propriété du droit d'auteur et des droits moraux qui protègent cette thèse. Ni la thèse ni des extraits substantiels de celle-ci ne doivent être imprimés ou autrement reproduits sans son autorisation.

In compliance with the Canadian Privacy Act some supporting forms may have been removed from this thesis.

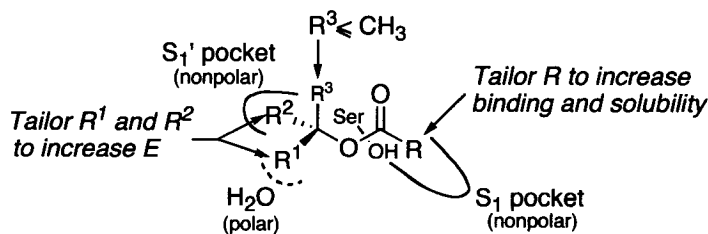
Conformément à la loi canadienne sur la protection de la vie privée, quelques formulaires secondaires ont été enlevés de cette thèse.

While these forms may be included in the document page count, their removal does not represent any loss of content from the thesis.

Bien que ces formulaires aient inclus dans la pagination, il n'y aura aucun contenu manquant.


Canada

Abstract



The X-ray crystal structure of the protease subtilisin shows its active site is on the surface. It binds substrate in an extended conformation and reacts only with soluble substrates. Subtilisin has a large nonpolar pocket (the S_1 pocket) to bind acyl group and a shallow crevice (the S_1' pocket) to bind one substituent of a secondary alcohol group, while the other substituent remains in solvent. The reactivity and enantioselectivity of subtilisin toward nonpolar secondary alcohol esters is low. Based on its structure, we hypothesized that subtilisin would be highly reactive if the acyl group anchored the substrate to the active site and highly enantioselective if there was a large hydrophobicity difference between alcohol substituents.

To test our first hypothesis, we show that an anchoring acyl group increases protease reactivity and extends subtilisin E to a new class of substrates, *N*-acyl sulfinamides. Subtilisin E did not catalyze hydrolysis of *N*-acetyl arylsulfinamides, but did catalyze a highly enantioselective hydrolysis of *N*-dihydrocinnamoyl arylsulfinamides. The *N*-dihydrocinnamoyl group mimics phenylalanine and thus binds the sulfinamide to the active site. We then use the 3-(3-pyridyl)propionyl group as anchoring group to increase substrate solubility. We use this group to resolve multi-gram quantities of three important compounds and isolate the enantiomers without the use of chromatography.

Next, we use different anchoring acyl groups to extend several proteases to tertiary alcohol esters. We show that a *syn*-pentane-like interaction destabilizes the transition state for reaction of tertiary alcohols, but that the addition of an anchor group that binds substrate to the protease stabilizes transition state and enables proteases to catalyze hydrolysis of tertiary alcohol esters.

To test our second hypothesis, we show subtilisin enantioselectivity stems from a favourable hydrophobic interaction between nonpolar substituent and S_1' pocket residues and favourable solvation of polar substituent in water. The enantioselectivity of a series of secondary alcohols in water varied linearly with the difference in hydrophobicity ($\log P/P_0$) of the substituents. The larger the $\log P/P_0$ difference the higher the enantioselectivity. Consistent with our hypothesis, the enantioselectivity of subtilisin toward *N*-acyl arylsulfonamides is high because of the large difference in substituent hydrophobicity.

Résumé

Le site actif de la protéase subtilisine est situé sur sa surface. La subtilisine se lie dans une conformation étendue et réagit seulement avec des substrats solubles. La subtilisine a une large poche non polaire (la poche S_1) utile pour lier des groupes acyles et une cavité peu profonde (la poche S_1') utile pour lier un substituant d'un groupe d'alcool secondaire, alors que l'autre substituant reste dans le solvant. L'activité et l'énantiosélectivité de la subtilisine envers les esters d'alcool secondaire non polaire est faible. Notre hypothèse est que les protéases seraient très réactives si le groupe acyle était structuré pour encrer un substrat et très énantiosélectives s'il y avait une grande différence d'hydrophobie entre les substituants du groupe alcool.

Pour vérifier notre première hypothèse, nous avons démontré qu'un groupe d'encrage acyle augmente l'activité de la protéase et augmente l'activité de la subtilisine E envers une nouvelle classe de substrats, les *N*-acyle sulfinamides. La subtilisine E n'a pas catalysé l'hydrolyse des *N*-acyle arylesulfinamides, mais a catalysé une hydrolyse hautement énantiosélective des *N*-dihydrocinnamoyl arylesulfinamides. Le groupe *N*-dihydrocinnamoyl mime le groupe phénylalanine et par conséquent entraîne la liaison du sulfinamide au site actif. Nous avons ensuite utilisé le groupe 3-(3-pyridine)propionyle comme groupe d'encrage pour augmenter la solubilité du substrat. Nous avons utilisé ce groupe pour obtenir des quantités à l'échelle de plusieurs grammes de trois composés importants et isoler les énantiomères sans avoir recours à la chromatographie.

Ensuite, nous avons utilisé différents groupes d'encrage acyle pour augmenter l'activité de plusieurs protéases envers des esters d'alcool tertiaire. L'activité est élevée mais par contre l'énantiosélectivité est de faible à moyenne avec des substrats non polaires. Nous avons démontré que le petit substituant occupe le même espace que l'atome d'hydrogène des alcools secondaires et que l'activité est élevée lorsque ce groupe est plus petit qu'un méthyle.

Pour vérifier notre deuxième hypothèse, nous avons démontré que l'énantiosélectivité de la subtilisine est due à une interaction hydrophobe favorable entre un substituant non polaire et des résidus de la poche S_1' et à la solvation du substituant polaire dans l'eau. L'énantiosélectivité de différents alcools secondaires dans l'eau varie

de façon linéaire avec la différence d'hydrophobie ($\log P/P_0$) des substituants. Plus grande est la différence $\log P/P_0$ plus grande est l'énantiosélectivité. En accord avec notre hypothèse, l'énantiosélectivité de la subtilisine envers les *N*-acyle arylesulfinamides est élevée due à la grande différence d'hydrophobie du substituant.

Acknowledgements

There are many people I wish to thank for helping me during the past four years. First, I wish to express my deepest gratitude to my supervisor, Dr. Romas J. Kazlauskas, for his guidance and support and for always letting me try silly experiments, even when he knew they would probably fail. I am also grateful to Dr. Karl Hult for his guidance during the three months I spent in his laboratory at the Royal Institute of Technology (KTH) in Stockholm, Sweden. I also thank Dr. Seongsoon Park and Dr. Johanna C. Rotlicci-Mulder for teaching me molecular biology techniques while working at KTH. As well, I must thank Magnus Eriksson for showing me there is a lot more to do than molecular biology when in Stockholm.

I am indebted to Dr. Fred Schendel and Rick Dillingham for their assistance with the large-scale fermentation and purification of subtilisin E and BPN', the University of Minnesota Super Computing Institute for access and assistance with the molecular modeling software and the University of Minnesota for providing access to so much state-of-the-art equipment. I am grateful to the Natural Science and Engineering Research Council of Canada, McGill University and the Walter C. Sumner Memorial Foundation for financial support.

I thank Dr. Peter H. Buist, Dr. Gemma Fabrias, Dr. David N. Harpp and Dr. John Shanklin for helpful discussions and constant encouragement.

I thank Chantal Marotte and Kristi Iskierka for administrative assistance at McGill University and University of Minnesota, respectively.

I also wish to thank my McGill University and University of Minnesota lab mates, past and present, Alessandra, Clarisse, David, Jeremy, Krista, Matt, Paul, Peter and Vladimir for their friendship and assistance during all these years. I am also grateful to my friends, April, Brad, Brandon, Christine, Cedric, Gerald, Hyung, J. P., Kristina, Matt, Trish and Oleh for their friendship and support.

Last, I am grateful to my family, who don't really understand why I am still in school, for their constant and unwavering support.

Contributions of authors

This thesis consists of one introduction, two publications (Chapters 2 and 3) and three drafts (Chapters 4, 5 and 6). The first draft (Chapter 4) has been submitted for publication, the second draft (Chapter 5) will be submitted for publication shortly and the third draft (Chapter 6) may be included in a future article. All the work described in these manuscripts was carried out as part of my research for the degree of Doctor of Philosophy.

Although Chapters 2 and 5 have co-authors, I was the primary researcher and first author. I wrote the manuscripts in their entirety under the supervision of Professor Romas J. Kazlauskas. Other co-authors did not write the manuscripts but carefully proofread them.

Co-authorship of manuscripts

Professor Romas J. Kazlauskas, supervisor throughout my doctoral degree, is a co-author for each manuscript.

Chapter 2: Vladimir P. Magloire synthesized *N*-butyl- and *N*-chloroacetyl-*p*-toluenesulfinamide and screened commercial enzymes for activity with these substrates. I synthesized all other substrates, expressed and purified subtilisin, performed all small-scale reactions with subtilisin, performed molecular modelling experiments and interpreted results.

Chapter 3: I was responsible for all research.

Chapter 4: I was responsible for all research.

Chapter 5: Paul F. Mugford synthesized two substrate esters and performed some enzymatic experiments. I synthesized the remaining substrates, performed small-scale reactions with proteases, performed molecular modelling experiments and interpreted results.

Chapter 6: I was responsible for all research.

Table of contents

Abstract.....	ii
Résumé.....	iv
Acknowledgements.....	vi
Contributions of authors.....	vii
Co-authorship of manuscripts.....	vii
Table of contents.....	viii
List of figures.....	xii
List of schemes.....	xv
List of tables.....	xvii
Glossary of frequently used symbols and abbreviations.....	xix
 Chapter 1: Introduction.....	 1
1.1 Chirality and enantiopure materials.....	2
1.2 Strategies for preparing enantiopure compounds.....	4
1.3 Hydrolase-catalyzed kinetic resolutions.....	7
1.4 Enzyme catalysis and anchor groups.....	9
1.5 Enzyme enantioselectivity <i>E</i>	13
1.6 General features of hydrolases – lipases and proteases.....	18
1.6.1 Lipases.....	19
1.6.2 Serine proteases – subtilisin and α -chymotrypsin.....	21
1.7 Molecular basis for hydrolase enantioselectivity.....	25
1.7.1 Models for rationalizing enantiomer discrimination.....	25
1.7.2 Enantioselectivity of lipases toward secondary alcohols.....	27
1.7.3 Enantioselectivity of subtilisin toward secondary alcohols.....	32
1.7.4 Using molecular modelling to rationalize enantioselectivity of hydrolases.....	34
1.8 Strategies for improving enzyme enantioselectivity.....	35
1.8.1 Increasing <i>E</i> by substrate engineering.....	35
1.8.2 Increasing <i>E</i> by medium engineering.....	36

1.8.3 Increasing <i>E</i> by protein engineering.....	38
1.9 New targets for hydrolase-catalyzed kinetic resolution.....	41
1.9.1 Chiral sulfur compounds – sulfinamides.....	41
1.9.2 Sterically hindered substrates – tertiary alcohols.....	46
1.10 Using protease structure to design new enantioselective reactions – thesis outline...50	
References.....	52

Chapter 2: Subtilisin-catalyzed resolution of *N*-acyl arylsulfinamides.....

Bridging passage to Chapter 2.....	62
Abstract.....	63
2.1 Introduction.....	64
2.2 Results.....	65
2.2.1 Synthesis of substrates.....	65
2.2.2 Initial screening.....	66
2.2.3 Optimization of <i>N</i> -acyl group for enantioselectivity and reactivity.....	68
2.2.4 Sulfinamide substrate range and enantioselectivity.....	70
2.2.5 Gram-scale resolutions.....	72
2.2.6 Molecular basis for higher reactivity of 1c and 1h	74
2.2.7 Molecular basis for enantioselectivity of subtilisin E with 1h	76
2.3 Discussion.....	79
2.4 Experimental section.....	81
2.4.1 General.....	81
2.4.2 Synthesis of substrates.....	81
2.4.3 Hydrolase library.....	82
2.4.4 Screening of commercial hydrolases with pH indicators.....	82
2.4.5 Small-scale reactions with commercial hydrolases to determine enantioselectivity.....	83
2.4.6 Cultivation and isolation of subtilisin E.....	83
2.4.7 Hydrolysis of <i>N</i> -acylsulfinamides with subtilisin E.....	84
2.4.8 Gram-scale resolution of <i>N</i> -acylsulfinamides.....	84

2.4.9 Modelling of tetrahedral intermediates bound to subtilisin E.....	85
Acknowledgements.....	86
References.....	87
Chapter 2 – Appendix.....	92

Chapter 3: How substrate solvation contributes to the enantioselectivity of subtilisin toward secondary alcohols.....	109
Bridging passage to Chapter 3.....	109
Abstract.....	110
3.1 Communication.....	111
Acknowledgements.....	116
References.....	116
Chapter 3 – Appendix.....	118

Chapter 4: The 3-(3-pyridyl)propionyl anchor group for large-scale protease-catalyzed resolution of <i>p</i>-toluenesulfinamide and sterically hindered secondary alcohols.....	146
Bridging passage to Chapter 4.....	146
Abstract.....	147
4.1 Introduction.....	148
4.2 Results and discussion.....	149
4.3 Conclusion.....	159
4.4 Experimental section.....	159
4.4.1 General.....	159
4.4.2 Synthesis of substrates.....	160
4.4.3 Small-scale protease-catalyzed hydrolysis of 2a and 3a	164
4.4.4 Large-scale protease-catalyzed hydrolysis of 1a , 3a and 3a	164
4.4.5 Absolute configuration of 2,2-dimethylcyclopentanol, 3	166
4.4.6 Modelling of tetrahedral intermediates bound to α -chymotrypsin.....	166
Acknowledgements.....	167

References.....	167
Chapter 5: Tailoring anchor group extends proteases to tertiary alcohol esters.....	171
Bridging passage to Chapter 5.....	171
Abstract.....	172
5.1 Communication.....	173
Acknowledgements.....	179
References.....	179
Chapter 5 – Appendix.....	181
 Chapter 6: New chromogenic reference compounds for Quick E.....	 198
Bridging passage to Chapter 6.....	198
Abstract.....	199
6.1 Introduction.....	200
6.2 Results and discussion.....	203
6.3 Experimental section.....	208
6.3.1 General.....	209
6.3.2 Synthesis of substrates.....	208
6.3.3 Synthesis of reference compounds.....	209
6.3.4 Quick E measurements.....	210
Acknowledgements.....	211
References.....	211
 Summary, conclusions and future work.....	 213
Contribution to knowledge.....	217
 <i>Appendices</i>	
Appendix I – Copyright waivers.....	219
Appendix II – Reprints of published articles.....	222

List of figures

Figure 1.1. Diagram of chirality.....	2
Figure 1.2. Enantiomers of the drugs dopa, Naproxen and propoxyphene.....	3
Figure 1.3. Effect of binding on enzyme catalysis.....	9
Figure 1.4. Substrates containing anchoring groups that bind to the active site and orient the reaction sites.....	11
Figure 1.5. Split-site model in which an active site is subdivided into a binding region and a reactive region.....	11
Figure 1.6. Dependence of optical purity on conversion.....	17
Figure 1.7. Energy diagram for a hypothetical enzyme-catalyzed enantioselective resolution.....	18
Figure 1.8. Schematic drawing of the α/β -hydrolase fold.....	19
Figure 1.9. A close up view of a complex of a lipase (<i>Pseudomonas cepacia</i> lipase) with a transition state analogue of 1-phenoxy-2-acetoxybutane.....	20
Figure 1.10. Schematic drawing of the α/β -subtilase fold.....	22
Figure 1.11. Naming of the binding site of proteases.....	23
Figure 1.12. A close up view of a complex of subtilisin (subtilisin Carlsberg) with a non-covalently bound protease inhibitor (Eglin C).....	24
Figure 1.13. Schematic representation of enantiomer discrimination by an enzyme via the “three-point attachment rule”.....	26
Figure 1.14. Schematic representation of enzymatic enantiomer discrimination via the “four location model”.....	26
Figure 1.15. A close up view of a complex of a lipase (<i>Candida rugosa</i> lipase) with a transition state analogue of (<i>R</i>)-menthyl hexylphosphonate.....	27
Figure 1.16. An empirical rule to predict which enantiomer of a secondary alcohol reacts faster in lipase-catalyzed reactions.....	28
Figure 1.17. Schematic representation of both enantiomers of the menthol inhibitor bound to the active site of CRL.....	29
Figure 1.18. Schematic representation of the productive binding modes of secondary alcohols with CALB.....	30

Figure 1.19. Schematic representation of the proposal by Ema and coworkers.....	31
Figure 1.20. Electronic effects can influence enantioselectivity.....	31
Figure 1.21. An empirical rule to predict which enantiomer of a secondary alcohol reacts faster in subtilisin-catalyzed reactions.....	32
Figure 1.22. Schematic representation of the binding modes of (<i>S</i>)- and (<i>R</i>)-1-phenethyl alcohol with subtilisin Carlsberg, as described by Klibanov and coworkers.....	32
Figure 1.23. Comparison of rational protein design and directed evolution.....	38
Figure 1.24. Sulfinic acid and its derivatives.....	41
Figure 1.25. Hydrolase-catalyzed resolution of sulfoxides with pendant acyl groups.....	42
Figure 1.26. Tertiary alcohols.....	46
Figure 1.27. Resolution of highly substituted compounds.....	48
Figure 1.28. Resolution of tertiary alcohol stereocentres by hydrolysis at a less-hindered remote site.....	48
Figure 1.29. Screening identified hydrolases that resolve tertiary alcohol stereocentres.....	49
Figure 1.30. Model rationalizing the enantioselectivity of lipases toward tertiary acetylenic alcohols.	49
Figure 1.31. Schematic of how an ester binds to the active site of subtilisin.....	50
Figure 2.1. Empirical rules that predict the enantiopreference of subtilisins toward secondary alcohols and sulfinamides.....	76
Figure 2.2. Catalytically productive tetrahedral intermediates for the subtilisin E catalyzed hydrolysis of fast-reacting (<i>R</i>)- 1h (I) and slow-reacting (<i>S</i>)- 1h (II) as identified by molecular modelling.....	78
Figure A2.1. SDS-polyacrylamide gel electrophoresis of subtilisin E from <i>B. subtilis</i> DB104 carrying pBE3.....	103
Figure A2.2. Catalytically productive tetrahedral intermediates for the subtilisin E catalyzed hydrolysis of (<i>R</i>)- 7c (I) and (<i>S</i>)- 7c (II) as identified by molecular modelling.....	106
Figure 3.1. Empirical rules that predict the enantiopreference of subtilisins toward secondary alcohols.....	111
Figure 3.2. Enantioselectivity varies with the substituent hydrophobicity difference of secondary alcohols.....	114

Figure A3.1. SDS-polyacrylamide gel electrophoresis of subtilisin BPN' and E from <i>B. subtilis</i> DB104 carrying pBE3 and subtilisin Carlsberg.....	130
Figure A3.2. Catalytically competent orientation of the tetrahedral intermediates for the subtilisin E catalyzed hydrolysis of (<i>R</i>)- 1a (I) and (<i>S</i>)- 1a (II) as identified by molecular modelling.....	134
Figure 4.1. Catalytically productive tetrahedral intermediates for the α -chymotrypsin-catalyzed hydrolysis of (<i>S</i>)- 1a (I) and (<i>S</i>)- 1a (II) as identified by molecular modelling.....	156
Figure 5.1. Schematic representation of the proposed conformation of the first tetrahedral intermediate of subtilisin- or α -chymotrypsin-catalyzed ester hydrolysis.....	177
Figure A5.1. Catalytically competent orientation of the tetrahedral intermediates for subtilisin Carlsberg catalyzed hydrolysis of (<i>R</i>)- 2a (I) and (<i>S</i>)- 2a (II) as identified by molecular modelling.....	192
Figure 6.1. Structures of achiral chromogenic reference compounds 1-3 and chiral substrates (<i>R</i>)- 4 and (<i>S</i>)- 4	203

List of schemes

Scheme 1.1. An example of a chiral pool synthesis.....	4
Scheme 1.2. An example of an asymmetric synthesis.....	5
Scheme 1.3. An example of a chemical kinetic resolution.....	5
Scheme 1.4. An example of an enzyme-catalyzed kinetic resolution.....	6
Scheme 1.5. Dynamic kinetic resolution of 1-phenethyl alcohol.....	6
Scheme 1.6. Mechanism of subtilisin Carlsberg-catalyzed ester hydrolysis.....	8
Scheme 1.7. Substrates for biocatalysis containing anchor groups.....	12
Scheme 1.8. Substrates for biocatalysis containing anchor groups.....	12
Scheme 1.9. Secondary alcohol esters of <i>N</i> -acetylglycine were not substrates for α -chymotrypsin-catalyzed hydrolysis.....	13
Scheme 1.10. Variation of enantioselectivity for PCL-catalyzed acylation of 2-[(<i>N,N</i> -dimethylcarbamoyl)methyl]-3-cyclopenten-1-ol with acylating agent.....	35
Scheme 1.11. Increasing the enantioselectivity of PCL-catalyzed hydrolysis via substrate modification to increase the relative substituent size difference.....	36
Scheme 1.12. Influence of organic solvent on subtilisin Carlsberg-catalyzed transesterification of 1-phenethyl alcohol with vinyl acetate.....	37
Scheme 1.13. Lipase AH-catalyzed hydrolysis of a prochiral diester shows opposite enantiopreference in isopropyl ether versus cyclohexane.....	37
Scheme 1.14. PAL-catalyzed hydrolysis of <i>p</i> -nitrophenyl ester of 2-methyldecanoic acid.....	40
Scheme 1.15. Directed evolution to improve the enantioselectivity of <i>Aspergillus niger</i> epoxide hydrolase toward glycidyl phenyl ether.....	40
Scheme 1.16. Synthesis of enantiopure amines from sulfinamides and the proposed transition state for nucleophilic addition.....	43
Scheme 1.17. Synthesis of enantiopure amines from <i>tert</i> -butylsulfinimine.....	43
Scheme 1.18. Synthesis of α - and β -amino acids from sulfinimines.....	44
Scheme 1.19. Synthesis of amino alcohols from <i>tert</i> -butylsulfinimine.....	44
Scheme 1.20. Synthesis of α -aminophosphonic acid from <i>p</i> -toluenesulfinimine.....	44

Scheme 1.21. Synthesis of enantiopure <i>p</i> -toluenesulfinamide from menthyl- <i>p</i> -toluenesulfinate.....	45
Scheme 1.22. Enantioselective oxidation of <i>tert</i> -butyldisulfide to give enantiopure <i>tert</i> -butylsulfinamide.....	45
Scheme 1.23. Synthesis of enantiopure sulfinamides from <i>endo</i> -1,2,3-oxathiazolidine-2-oxide derived from <i>N</i> -sulfonyl indanol.....	46
Scheme 1.24. Phenylation of ketones using enantioselective organozinc reagents.....	47
Scheme 2.1. Synthesis of enantiopure amines from sulfinamides.....	64
Scheme 2.2. Subtilisin-catalyzed kinetic resolution of sulfinamides.....	65
Scheme 2.3. Synthesis of sulfinamides 1-8 and <i>N</i> -acylsulfinamides.....	66
Scheme 2.4. Gram-scale kinetic resolution of sulfinamides 1 , 3 and 5	73
Scheme A3.1. Synthesis of esters 1a-13a , 10c , 11b and 12b and secondary alcohols 4-10 and 12	119
Scheme 4.1. Synthesis of racemic <i>N</i> -3-(3-pyridyl)propionyl- <i>p</i> -toluenesulfinamide 1a	152
Scheme 4.2. α -Chymotrypsin-catalyzed resolution of 1a and 1c	152
Scheme 4.3. Subtilisin Carlsberg-catalyzed resolution of 3a	153
Scheme 4.4. <i>Aspergillus melleus</i> protease-catalyzed resolution of 4a	154
Scheme 4.5. Synthesis of enantiopure amines from sulfinamides.....	158
Scheme A5.1. Synthesis of tertiary alcohol esters 1a-7a , 1b and 6b , 1c and tertiary alcohols 3-5 and 7	182
Scheme 6.1. Enzymatic hydrolysis of the pseudo-enantiomers (<i>S</i>)-glycidyl phenyl ether and (<i>R</i>)- <i>d</i> ₅ -glycidyl phenyl ether.....	200
Scheme 6.2. The Quick E screening method for rapid determination of hydrolase enantioselectivity.....	201

List of tables

Table 2.1. Screening of hydrolases for enantioselective hydrolysis of 1c	67
Table 2.2. Reactivity and enantioselectivity of subtilisin E toward 1a-m	69
Table 2.3. Enantioselectivity of subtilisin E toward 2c-5c and 2h-5h	71
Table 2.4. Minimized structures for the tetrahedral intermediate of subtilisin E-catalyzed hydrolysis of 1h , 1c and 7c	75
Table A2.1. Enantioselectivity of <i>Bacillus subtilis</i> var. biotecnus A with 2c-5c	104
Table 3.1. Enantioselectivity of subtilisin BPN'-, Carlsberg- and E-catalyzed hydrolysis of 1a-13a	112
Table A3.1. Minimized structures for the tetrahedral intermediate for the subtilisin E-catalyzed hydrolysis of 1a	135
Table A3.2. Enantioselectivity of BPN'-catalyzed hydrolysis of 1a-13a and transesterification of 1-13 with a vinyl ester in dioxane.....	136
Table A3.3. Enantioselectivity of subtilisin Carlsberg-catalyzed hydrolysis of 1a-13a and transesterification of 1-13 with a vinyl ester in dioxane.....	138
Table A3.4. Enantioselectivity of subtilisin E-catalyzed hydrolysis of 1a-13a and transesterification of 1-13 with a vinyl ester in dioxane.....	139
Table A3.5. Enantioselectivity of PCL-catalyzed hydrolysis of 1a-13a or transesterification of 1-13 with a vinyl ester in dioxane.....	142
Table 4.1. Specific activity of proteases toward secondary alcohol esters 2a , 2b and 2c	150
Table 4.2. Reactivity and enantioselectivity of subtilisin BPN' and α -chymotrypsin toward 1a , 1b and 1c	151
Table 5.1. Reactivity and enantioselectivity of proteases toward 1a-1c	174
Table 5.2. Reactivity and enantioselectivity of subtilisin Carlsberg and α -chymotrypsin toward 1a-9a	176
Table A5.1. Minimized structures of tetrahedral intermediates for subtilisin Carlsberg-catalyzed hydrolysis of 2a	193
Table A5.2. Reactivity and enantioselectivity of proteases toward 1,1,1-trifluoro-2-phenyl-but-3-yn-ol esters 1a , 1b and 1c (complete details).....	194

Table A5.3. Reactivity and enantioselectivity of subtilisin Carlsberg and α -chymotrypsin toward 1a-9a (complete details).....	195
Table 6.1. Specific activity of hydrolases toward different reference compounds.....	205
Table 6.2. Enantioselectivity of hydrolases toward 1-phenethyl acetate 4 using the quick E method with reference compound 1, 2 or 3	206

Glossary of symbols and abbreviations

A or Ala	alanine
Å	Ångstrom
AMBER	assisted model building with energy refinement
AMP	<i>Aspergillus melleus</i> protease
AOP	<i>Aspergillus oryzae</i> protease
ASL	<i>Alcaligenes species</i> lipase
BES	<i>N, N</i> -bis[2-hydroxyethyl]-2-aminoethanesulfonic acid
c	conversion
C	Celsius
CALA	<i>Candida antarctica</i> Lipase A
CALB	<i>Candida antarctica</i> Lipase B
CRL	<i>Candida rugosa</i> lipase
C or Cys	cysteine
CE	cholesterol esterase
d	day
d	doublet (NMR)
<i>D</i>	dextrorotary
D or Asp	aspartate
DCC	1,3-dicyclohexylcarbodiimide
δ	chemical shift (NMR)
DKR	dynamic kinetic resolution
EDC	<i>N</i> -(3-dimethylaminopropyl)- <i>N'</i> -ethylcarbodiimide
ΔG	Gibbs free energy change
ΔH	enthalpy difference
ΔS	entropy difference
ε	extinction coefficient (M ⁻¹ cm ⁻¹)
<i>E</i>	enantiomeric ratio
E or Glu	glutamate
ee	enantiomeric excess

EI	electron ionization
F or Phe	phenylalanine
g	gram
G	Gibbs free energy
G or Gly	glycine
GC	gas chromatography
h	hour
H or His	histidine
HPLC	high performance liquid chromatography
HRMS	high-resolution mass spectroscopy
Hz	Hertz
I or Ile	isoleucine
J	coupling constant (NMR)
k	kilo
K or Lys	lysine
k_{cat}	turnover number
K_M	Michaelis-Menten constant
K_S	dissociation constant
l	path length
L	large substituent
L	lævorotatory
L or Leu	leucine
m	metre
μ	micron
M or Met	methionine
	medium substituent
MeCN	acetonitrile
MD	molecular dynamics
min	minute
MM	molecular mechanics
mol	mole(s)

MS	mass spectroscopy
<i>m/z</i>	mass-to-charge ratio
n	nano
N or Asn	asparagine
n.a.	not applicable
n.d.	not determined
NMR	nuclear magnetic resonance
n.p.	not performed
n.r.	no reaction
Nu	nucleophile
%	percent
<i>p</i>	para
P	product
	<i>n</i> -octanol-water partition coefficient
PAL	<i>Pseudomonas aeruginosa</i> lipase
PCL	<i>Pseudomonas cepacia</i> lipase
PFE	<i>Pseudomonas fluorescens</i> esterase
pH	negative logarithm of hydrogen ion concentration
pKa	negative logarithm of equilibrium constant for association
PLE	pig liver esterase
PPL	porcine pancreatic lipase
q	quartet (NMR)
Q or Gln	glutamine
R or Arg	arginine
	alkyl or aryl group
r.m.s.	root mean square
ROL	<i>Rhizopus oryzae</i> lipase
s	singlet (NMR)
S or Ser	serine
	substrate
SDS-PAGE	sodium dodecyl sulfate polyacrylamide gel electrophoresis

sec	second
S ₁	S ₁ acyl binding pocket of proteases
S ₁ '	S ₁ ' alcohol/amine binding pocket of proteases
t	triplet (NMR)
T _{d1}	first tetrahedral intermediate
T _{d2}	second tetrahedral intermediate
THF	tetrahydrofuran
T or Thr	threonine
TLC	thin-layer chromatography
TRIS	tris(hydroxymethyl)aminomethane
U	unit
U/mg	μmol of substrate released per minute per mg protein
v	initial velocity
V or Val	valine
V _{max}	maximum velocity
W or Trp	tryptophan
Y or Tyr	tyrosine

Chapter 1

Introduction

Introduction

1.1 Chirality and enantiopure materials

A chiral object is one that cannot be superimposed on its mirror image. The word chiral comes from the Greek word for “hand”. Our hands are chiral because they are mirror images of each other and you cannot superimpose your left hand on your right hand. Similarly, molecules can be chiral (Figure 1.1). The molecules depicted in Figure 1.1 are mirror images and cannot be superimposed on one another. These mirror-image molecules are called enantiomers. Similar to our hands, enantiomers have the same physical and chemical properties in achiral environments, but have different properties in chiral environments such as biological systems.

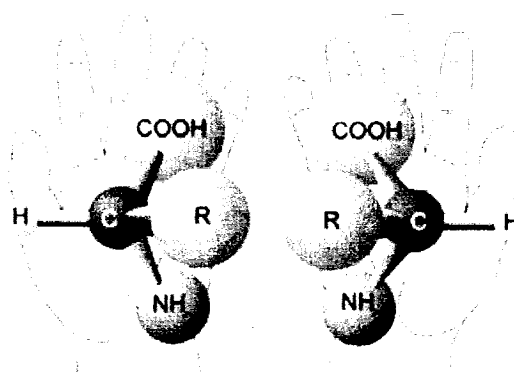


Figure 1.1. Diagram of chirality. Molecules, just like our hands, can be mirror images and thus, cannot be superimposed on one another. Reproduced from Sarfati.¹

Natural products generally exist exclusively in one biologically active chiral form. For example, most proteins are formed of L-enantiomers of amino acids while natural sugars exist as the D-enantiomers. We also see that most naturally occurring medicinal agents exist in a single isomer form, such as (-)-morphine and (+)-digitoxin.² Consequently, individual enantiomers of a synthetic pharmaceutical drug can have different therapeutic or toxicological effects in biological systems.

Many drugs are developed as single enantiomers because of unwanted side effects caused by the antipode (Figure 1.2). For example, it was noted during development that many of the unwanted side effects of L-dopa were due to the D-isomer.² The drug Naproxen (Aleve[®]) is marketed as the single (*S*)-enantiomer product because the unbound

(*R*)-enantiomer is a liver toxin.³ In contrast to unwanted effects of an antipode, it was discovered that D-propoxyphene is an analgesic, while L-propoxyphene is a cough suppressant. As a result, Lilly marketed them separately and gave them tradenames that are “mirror images” of one another, Darvon® and Novrad®.²

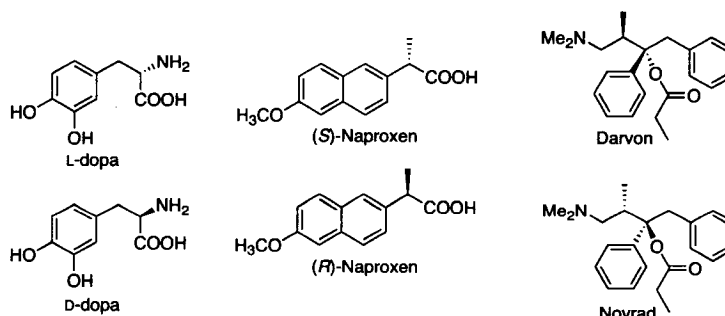


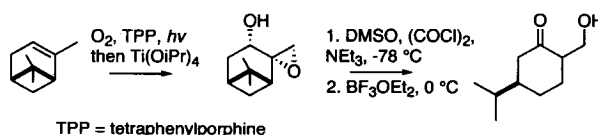
Figure 1.2. Enantiomers of the drugs dopa, Naproxen and propoxyphene. L-dopa is used to treat Parkinson’s disease, but D-dopa reduces white blood cell counts. (*S*)-Naproxen is an effective NSAID, but (*R*)-Naproxen is a liver toxin. Darvon® is an analgesic; its antipode Novrad® is a cough suppressant.

The life science industry is an important market for the chemical industry. The total revenue from sales to the pharmaceutical and agrochemical industries for the year 2000 was in excess of US \$20 billion, with the greatest share from the pharmaceutical industry.⁴ Optically active intermediates used as chemical building blocks, auxiliaries, or advanced intermediates make up 15% of the total market and sales are increasing at about 10% annually. Currently, about 80% of active pharmaceuticals in the pipeline are chiral, and it is estimated that this fraction will increase, as the development of active substances continues. The introduction of enantiopure active substances is also enforced through the ever-stricter regulations of the US Food and Drug Administration (FDA). Recognizing that enantiomers have different therapeutic properties, both the FDA and the European Committee for Proprietary Medicinal Products have stipulated that the physiological action of each enantiomer of a drug must be individually characterized.⁵

Thus, the production of enantiomerically pure drugs has become an important process in the pharmaceutical industry. As a result, chemists are faced with the challenge of developing novel synthetic strategies for the preparation of enantiopure chemicals.

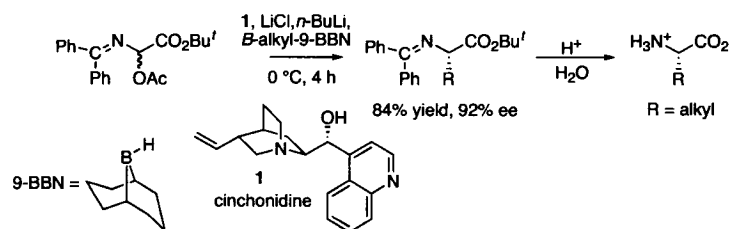
1.2 Strategies for preparing enantiopure compounds

There are three basic ways to synthesize a chiral compound in the form of a single enantiomer. The first way, which is most common, is to begin with a single stereoisomer obtained from nature, since many compounds are present in a single enantiomeric form (e.g., amino acids, sugars, steroids and terpenes). These compounds are chiral pool; that is, readily available starting materials. A recent example is the synthesis of (*R*)-7-hydroxycarvone,⁶ an important building block for organic synthesis, from α -pinene, which is an abundant terpene (Scheme 1.1).⁷ The chiral pool approach is often unbeatable when the requisite starting material is abundant or because the target itself is a complex natural product. However, nature is limited with respect to structure and stereochemistry, and for this reason other strategies are necessary.



Scheme 1.1. An example of a chiral pool synthesis. Synthesis of (*R*)-7-hydroxycarvone from α -pinene.

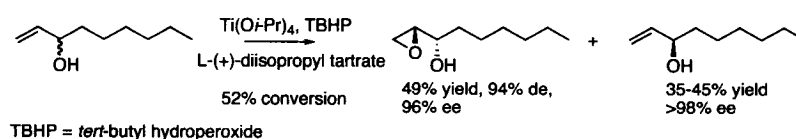
The second strategy is called asymmetric synthesis. Asymmetric synthesis involves the transformation of an achiral molecule into a chiral molecule by means of a chiral catalyst or chiral auxiliary. Over the past several years, enormous advances have been made in asymmetric synthesis,⁸ with particular emphasis on the development of enantioselective catalytic reactions.⁹ For example, O'Donnell and coworkers¹⁰ synthesized a variety of nonnatural α -amino acids using an organoborane reagent coupled with a *Cinchona* alkaloid chiral complexation agent (Scheme 1.2).



Scheme 1.2. An example of an asymmetric synthesis. Enantioselective synthesis of nonnatural α -amino acids via organoboranes and cinchonidine.

Another route to enantiopure compounds is resolution of a racemic mixture. This method dates back to when Pasteur¹¹ first resolved a racemate, sodium ammonium tartrate, via crystallization and manual separation of the two crystalline forms. However, this is seldom a practical method, since few compounds crystallize in this manner. A more common strategy is to convert a racemic mixture into diastereomers and separate them via fractional crystallization. Although the starting enantiomers have the same properties, the diastereomers have different chemical and physical properties. The property most often used for separation is differential solubility.

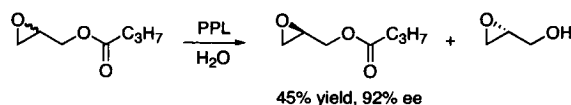
Kinetic resolution is another strategy for resolving enantiomers. Kinetic resolutions occur when one enantiomer reacts faster with a chiral catalyst, such as a metal-chiral ligand complex or enzyme. An excellent example is the resolution of an allylic alcohol by a titanium alkoxide tartrate epoxidation catalyst (Scheme 1.3).¹² The (*S*)-enantiomer is converted to the epoxide, while the (*R*)-enantiomer reacts slowly.



Scheme 1.3. An example of a chemical kinetic resolution. Kinetic resolution of allylic alcohols by enantioselective epoxidation.

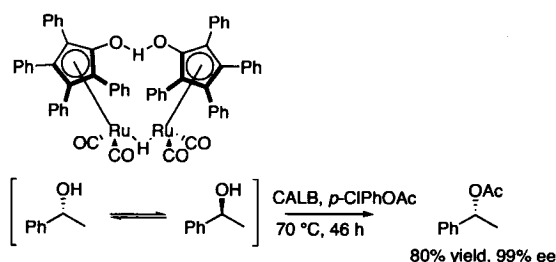
Enzymes are also excellent chiral catalysts for enantiomer resolution. For example, hydrolysis of racemic glycidylbutyrate with porcine pancreatic lipase (PPL) gives (*R*)-glycidylbutyrate in 45% yield with 92% ee (Scheme 1.4).¹³ This process was devel-

oped further by Andeno-DSM and implemented for the production of (*R*)-glycidylbutyrate and (*R*)-glycidol on the multi-ton scale.¹⁴



Scheme 1.4. An example of an enzyme-catalyzed kinetic resolution. Resolution of (*R*)-glycidylbutyrate and (*R*)-glycidol by porcine pancreatic lipase (PPL) catalyzed hydrolysis.

The key drawback to kinetic resolution is the 50% maximum yield of the desired enantiomer. This is often not satisfactory, especially if only one enantiomer is required. This 50% maximum yield can be overcome using a dynamic kinetic resolution (DKR). In a DKR, the substrate must rapidly racemize during resolution, the product must be stable to racemization and the enzyme must be highly selective. For example, Bäckvall *et al.*^{15,16} coupled a ruthenium catalyst-catalyzed secondary alcohol racemization process with *Candida antarctica* lipase B (CALB)-catalyzed transesterification. In this way, they resolved several secondary alcohols with yields from 60% to 88% with 79% ee to 99% ee. The best result was the DKR of 1-phenethyl alcohol, where they recovered (*R*)-1-phenethyl acetate in 80% yield with 99% ee (Scheme 1.5).



Scheme 1.5. Dynamic kinetic resolution of 1-phenethyl alcohol via ruthenium-catalyzed racemization coupled with CALB-catalyzed transesterification.

Park and coworkers increased the yield of (*R*)-1-phenethyl alcohol to 95% by employing a different racemization catalyst, aminocyclopentadienyl ruthenium chloride.^{17,18} This catalyst functions at room temperature and tolerates conventional acyl donors such

as vinyl acetate, which extends this strategy to enzymes that have lower thermally stability and substrate tolerance.¹⁹ Recently, they developed a polymer-bound racemization catalyst that is air stable and easily recyclable.²⁰

1.3 Hydrolase-catalyzed kinetic resolutions

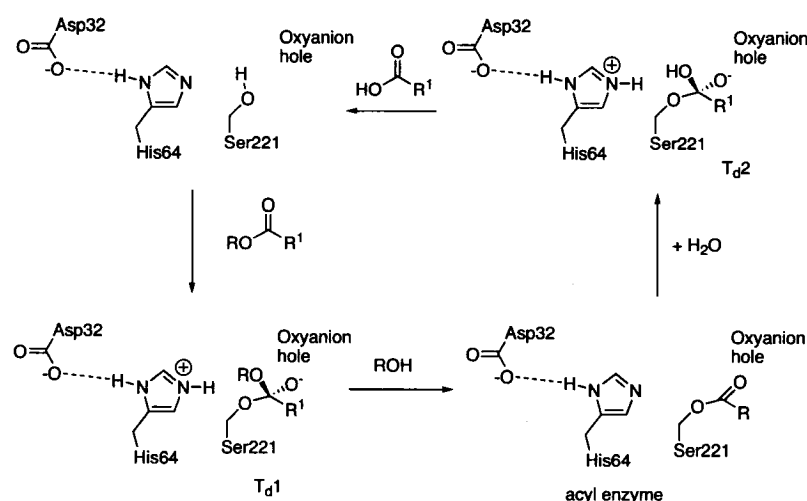
Kinetic resolution of enantiomers can be accomplished using enzymes. Many enzymes are useful for kinetic resolutions because they are stable to temperature, solvent and pH changes, are simple to use and can often increase the rate of reaction, compared to non-enzymatic processes, by a factor of 10^8 - 10^{10} . As well, the amount of enzyme required generally ranges from 10^{-3} to 10^{-4} % mole fraction, while chemical catalysts usually range from 0.1 up to 1% mole fraction. Most importantly, from an industrial aspect, enzymes usually work under mild conditions (pH 5 to 8; $T = 20\text{ }^{\circ}\text{C}$ to $40\text{ }^{\circ}\text{C}$), which can minimize substrate decomposition and/or racemization. Enzymes often show a wide substrate range, but with high chemo-, regio-, diastereo- and enantioselectivity.²¹

The worldwide sales for industrial enzymes are estimated to be \$2 billion and at least 75% of these are hydrolases.⁴ Hydrolases are a group of enzymes that catalyze bond cleavage by reaction with water. Generally speaking, they are used to catalyze the hydrolysis or formation of esters and amides. The main industrial application of hydrolases are in detergents, oil processing and dairy products, but they have emerged as the most common type of biocatalyst used for the production of chiral compounds for organic chemistry.²²

Lipases, esterases and proteases are the three main classes of hydrolytic enzymes used as biocatalysts. This group of enzymes also includes some lesser-known enzymes such as, epoxide hydrolases, dehalogenases and phospholipases. All hydrolases use a nucleophile in their active site to attack substrate. Lipases, esterases and serine proteases use a serine residue to attack the carbonyl group of an ester or amide. Epoxide hydrolases and dehalogenases use an aspartate residue as nucleophile for epoxide hydrolysis and dehalogenation, respectively, and thiol proteases use a cysteine residue as nucleophile.

The catalytic machinery of a serine hydrolases consists of a triad – serine, histidine and aspartate (glutamate) – and oxyanion-stabilizing residues. This catalytic triad was first observed in α -chymotrypsin,²³ but has since been observed in many other hydro-

lases.^{24,25} The reaction proceeds in two steps. The first step of the catalytic mechanism is nucleophilic attack of an ester or amide by the hydroxyl group of serine to form the first tetrahedral intermediate, T_d1 . Alcohol is then released, thus, formation or collapse of this intermediate determines the selectivity of hydrolases toward alcohols. This gives the acyl-enzyme intermediate, which is then attacked by water to form the second tetrahedral intermediate, T_d2 . When deacylation is rate limiting, this step determines the selectivity of hydrolases toward carboxylic acids. Collapse of the second tetrahedral intermediate releases the carboxylic acid and the free enzyme (Scheme 1.6.). The research in this thesis involves enantioselective resolution of leaving groups, such as secondary alcohols, and will focus on the first step of this catalytic mechanism.



Scheme 1.6. Mechanism of subtilisin Carlsberg-catalyzed ester hydrolysis. The catalytic triad is composed of Asp32, His 64 and Ser221. The mechanism of hydrolysis involves formation of an acyl enzyme intermediate and two negatively charged tetrahedral intermediates, which are stabilized by residues forming an oxyanion hole.

Due to the chirality of the active site, one enantiomer may fit better in the active and react faster. This difference in reaction rate is the basis for using hydrolases as chiral biocatalysts. Enzyme enantioselectivity is discussed in section 1.5 and how hydrolases distinguish enantiomers is discussed in section 1.7.

1.4 Enzyme catalysis and anchor groups

The first step of catalysis is the formation of a reversible ES complex, or Michaelis complex (see Section 1.5). The Michaelis complex then undergoes rearrangement to one or several transition states before product is formed (Figure 1.3).²⁶ The transition state is the highest energy species on the reaction pathway and occurs at the peak of the reaction coordinate. In the transition state, chemical bonds are in the process of being made and broken. In contrast, intermediates, such as the tetrahedral intermediate formed during ester hydrolysis, whose bonds are fully formed, occupy the troughs in the diagram (Figure 1.3, inset). Energy is required for these rearrangements and formation of intermediates. The input energy required is at the highest transition state and is called the activation free energy of the reaction. The more than one million-fold rate enhancement achieved by enzyme catalysis is a result of the ability of the enzyme to decrease the activation energy of the reaction.

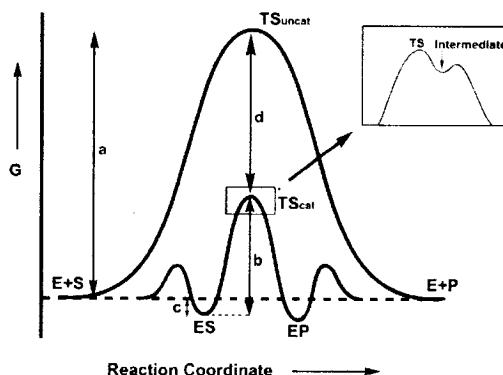


Figure 1.3. Effect of binding on enzyme catalysis. Enzymes accelerate chemical reactions by decreasing activation energy. The activation energy is higher for a noncatalyzed reaction *a* than for the same reaction catalyzed by an enzyme *b*. Binding of substrate and transition state to the enzyme can lower the activation energy by amounts *c* and *d*, respectively. Transition states occur at the peaks of the energy profile of a reaction, and intermediates occupy the troughs (inset).

Linus Pauling²⁷ first formulated the basic principle underlying enzyme catalysis; that is, an enzyme reduces the activation free energy and hence, increases the rate of reac-

tion by strongly binding the transition state of a specific substrate. This decrease in activation energy is achieved by enzyme in several ways: for example, by providing catalytically competent groups for a specific reaction mechanism and by binding and/or distorting substrate in an orientation appropriate for reaction.²⁶ Binding involves multiple weak interactions such as electrostatic interaction, hydrogen bonding and/or hydrophobic interaction at reaction site or at a remote site.²⁶ Maximum binding of substrate and enzyme occurs when each binding group on the substrate matches a binding site on the enzyme. In this case the enzyme is said to be complementary in structure to the substrate (transition state). The activation energy for the conversion of ES to E + P will be lowered only if the enzyme binds more tightly to the transition state of S than in its ground state structure.

Enzymes often use an anchoring group to bind and orient a substrate for reaction. For example, orotidine 5'-monophosphate decarboxylase is an efficient catalyst.²⁸ Although reaction occurs entirely in the orotic acid base, the ribosyl phosphate moiety is essential for activity (Figure 1.4a). Orotic acid ($2.5 \times 10^{-5} \text{ M}^{-1} \text{ s}^{-1}$) alone shows 12 orders of magnitude lower activity than orotidine 5'-monophosphate ($6.3 \times 10^7 \text{ M}^{-1} \text{ s}^{-1}$), even though orotic acid binds to the enzyme active site ($K_i = 9.5 \text{ mM}$). Similarly, a coenzyme A moiety accelerates 10^7 -fold the acyl transfer of thiol esters by CoA transferase over short linear thiol esters (Figure 1.4b).²⁹ In a third case, lipoic acid is a poor substrate for the pyruvate dehydrogenase multi-enzyme complex, but the lipoyl domain (lipoic acid bound to protein) is a 10^4 -fold better substrate.³⁰ In all three cases, the enzyme holds one portion of the substrate (phosphoribosyl, pantothenoyl-ADP, or protein domain) tightly in a non-reactive or binding subsite. This binding orients the reactive portion of the substrate (carboxylate, thioester, thiol) into a critical distance, orientation and conformation for chemical transformation.

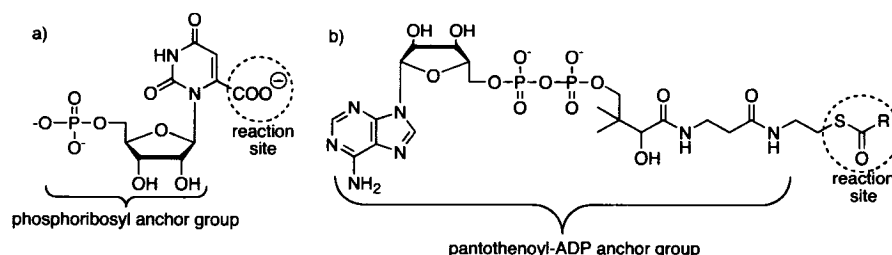


Figure 1.4. Substrates containing anchoring groups that bind to the active site and orient the reaction sites. (a) decarboxylation of orotidine 5'-monophosphate, (b) acyl transfer to coenzyme A.

So, how does this binding of an anchor group contribute to stabilization of the transition state? When one thinks about transition state stabilization, one first thinks of direct involvement in the catalytic mechanism at a reaction site (e.g., polarization or activation of groups). However, Jencks³¹ and Menger³² showed that remote binding interactions between enzyme and substrate also stabilize transition states and increase reactivity. Menger proposed a split-site model that considers the influence of binding a remote site (Figure 1.5). The remote binding of an anchor group brings the reactive sites in contact and lowers the free energy of the transition state by favouring its formation through a combination of stabilizing interactions that are stronger in the transition state than the ground state. Thus, it favours a catalytically productive orientation. However, due to dynamic effects in proteins it can be difficult or impossible to dissect enzyme-substrate interaction into purely ground state binding vs. transition state binding contributions.³³

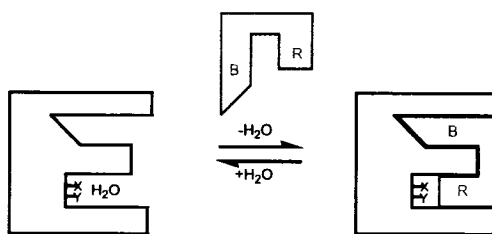
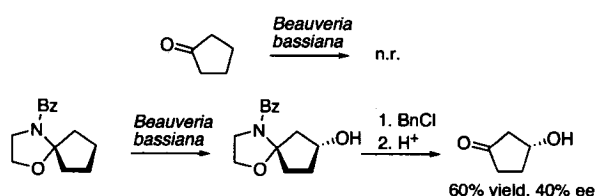


Figure 1.5. Split-site model in which an active site is subdivided into a binding region and a reactive region. The regions associate with B (Binding) and R (Reactive) of the substrate, respectively. Catalytic groups on the enzyme (X and Y) are brought into con-

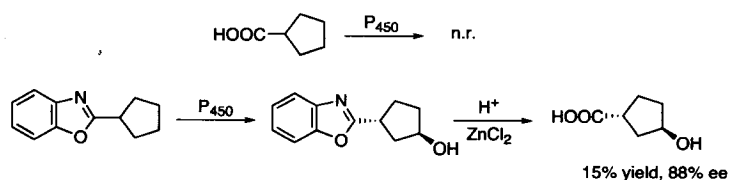
tact distances with the labile group of the substrate when the enzyme/substrate complex is formed. It is assumed that, $ES = ES_R + ES_B$. Adapted from Menger.³²

In a few cases, researchers have used anchor groups to enhance biocatalysis. Without an anchor group, there was no reaction; with the group there was a reaction. This change indicates >100-fold change in reactivity due to the anchor group. For example, the fungus *Beauveria bassiana* did not hydroxylate cyclopentanone, but did hydroxylate the *N*-benzoylspirooxazolidine derivative with moderate yield and diastereoselectivity (Scheme 1.7).³⁴



Scheme 1.7. Substrates for biocatalysis containing anchor groups. Cyclopentanone was not a substrate for hydroxylation, but the *N*-benzoylspirooxazolidine derivative was a good substrate.

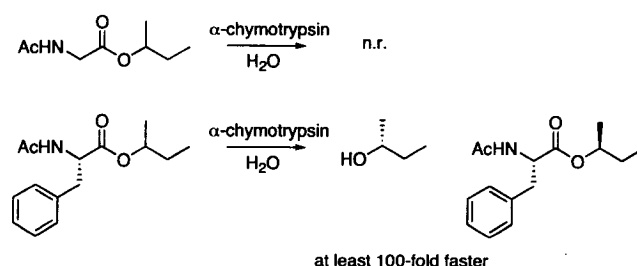
In a second example, cyclopentanecarboxylic acids were not substrates for hydroxylation by P₄₅₀, but the benzoxazole derivative showed moderate reactivity (Scheme 1.8).³⁵



Scheme 1.8. Substrates for biocatalysis containing anchor groups. Cyclopentanecarboxylic acids were not substrates for hydroxylation by P₄₅₀, but the benzoxazole derivative showed moderate reactivity.

Fonken and coworkers³⁶ highlighted the importance of anchoring groups for monooxygenases by developing a model predicting the regioselectivity of oxidation. They showed that an electron rich centre, such as carbonyl oxygen of an amide anchored cycloalkanol derivatives to the active site of monooxygenase from *Beauveria bassiana* and directed oxidation between 4.5-6.2 Å from the carbonyl. Other groups have since tailored anchor groups to favour oxidation at a particular reaction site.³⁷

Anchor groups are also useful for hydrolase-catalyzed reactions. For example, Jones and coworkers³⁸ showed α -chymotrypsin catalyzed the hydrolysis of a variety of secondary alcohol esters of *N*-acetyl-L-phenylalanine, α -hydroxy- β -phenyl-propionic acid, dihydrocinnamic acid and hippuric acid, but did not react with the *N*-acetylglycine derivative (Scheme 1.9).



Scheme 1.9. Secondary alcohol esters of *N*-acetylglycine were not substrates for α -chymotrypsin-catalyzed hydrolysis, but *N*-acetylphenylalanine was a good substrate.

1.5 Enzyme enantioselectivity *E*

Enzymes are chiral catalysts that exhibit enantioselectivity. The degree of enantioselectivity of an enzyme is defined as the ratio of specificity constants (k_{cat}/K_M) of the (*R*)- and (*S*)-enantiomer in an enzyme-catalyzed reaction.³⁹ The kinetic constants, k_{cat} and K_M , describe the reaction of each enantiomer with enzyme. Sih and coworkers⁴⁰ later defined the ratio of specificity constants as a dimensionless parameter called the enantiomeric ratio, *E*. This ratio measures the ability of an enzyme to distinguish between two enantiomers and is widely accepted as the parameter for quantifying the enantioselectivity of an enzyme. The value of *E* cannot change unless the values of the kinetic constants

change. The basis for the enantiomer ratio can be found in the kinetic equations that describe enzyme-catalyzed hydrolysis.

A simple, irreversible hydrolase-catalyzed single substrate hydrolysis can be described by the Michaelis-Menton mechanism where E is the free enzyme; S is the substrate; ES is the enzyme-substrate complex; P is the product; and k_1 , k_{-1} and k_2 are the rate constants.²⁶



Since no chemical changes occur in the first reversible step, and the second step is assumed to be irreversible if [P] is very low, which is the case when the velocity is measured at initial stages of the reaction, the initial rate equation can be expressed as:

$$v = d[P]/dt = k_2[ES] \quad (1.1)$$

From the steady state assumption, the rate of formation of the ES complex is equal to its rate of destruction which is true if $[S] \gg [E]$. Therefore:

$$+d[ES]/dt = -d[ES]/dt \quad (1.2)$$

The concentration [ES] can be defined as:

$$k_1[E][S] = (k_2 + k_{-1})[ES] \quad (1.3)$$

During the reaction, the enzyme is either bound to the substrate as an ES complex or free in solution. Therefore:

$$[E]_0 = [E] + [ES] \quad (1.4)$$

where $[E]_0$ is the total enzyme concentration and [E] is the free enzyme in solution.

Combining equations 1.3 and 1.4 gives:

$$[ES] = \frac{[E]_0[S]}{\left(\frac{k_2 + k_{-1}}{k_1}\right) + [S]} \quad (1.5)$$

Equation 1.1 now becomes:

$$v = \frac{k_2[E]_0[S]}{\left(\frac{k_2 + k_{-1}}{k_1}\right) + [S]} \quad (1.6)$$

Defining V_{max} as the maximum velocity at saturating substrate concentration ($V_{max} = k_2[E]_0$) and K_M as the substrate concentration at 50% of maximum velocity ($S = K_M$ if $v = V_{max}/2$):

$$\frac{V_{\max}}{2} = \frac{V_{\max} K_M}{\left(\frac{k_2 + k_{-1}}{k_1} \right) + K_M} \quad (1.7)$$

Therefore:

$$K_M = \frac{k_2 + k_{-1}}{k_1} \quad (1.8)$$

and equation 1.6 becomes:

$$v = \frac{k_2 [E]_0 [S]}{K_M + [S]} \quad (1.9)$$

This basic equation of enzyme kinetics is called the Michaelis-Menton equation. It is true under steady-state conditions with no product inhibition.

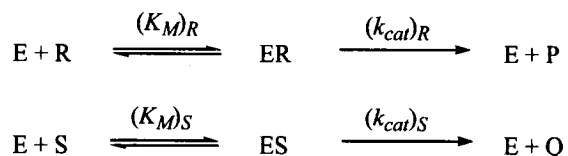
Defining V_{\max} as:

$$k_2 [E_0] = V_{\max} \quad (1.10)$$

Equation 1.9 can also be expressed as:

$$v = \frac{V_{\max} [S]}{K_M + [S]} \quad (1.11)$$

In a kinetic resolution, the (*R*)- and (*S*)-enantiomers compete for the enzyme active site where k_{cat} is the enzyme turnover number:



Combining equation 1.1 and 1.9 gives:

$$K_M = \frac{[E][S]}{[ES]} \quad (1.12)$$

Substituting equation 1.12 into equation 1.1 gives:

$$v_R = \left(\frac{k_{cat}}{K_M} \right)_R [E][R] \quad (1.13)$$

$$v_S = \left(\frac{k_{cat}}{K_M} \right)_S [E][S] \quad (1.14)$$

Dividing 1.13 by 1.14 gives:

$$\frac{v_R}{v_S} = \frac{\left(\frac{k_{cat}}{K_M}\right)_R [R]}{\left(\frac{k_{cat}}{K_M}\right)_S [S]} \quad (1.15)$$

Considering there is equal amounts of the two enantiomers in a racemic mixture, we obtain equation 1.16, the enantiomeric ratio E :

$$E = \frac{\left(\frac{k_{cat}}{K_M}\right)_R}{\left(\frac{k_{cat}}{K_M}\right)_S} \quad (1.16)$$

K_M is the Michaelis constant and approximates the dissociation constant (K_S) of the enzyme-substrate complex when the subsequent step, k_2 , is slow, as is the case with hydrolase-catalyzed reactions. It is a direct reflection of substrate binding; lower values indicate better binding. The kinetic constant, k_{cat} , is the apparent first order rate constant for conversion of the enzyme-substrate complex to product.

Determining the kinetic constants of both enantiomers with an enzyme is time consuming. A more convenient way of measuring enzyme enantioselectivity consists of measuring the enantiomer excess (ee) of either the product or substrate at a particular conversion. The enantiomeric excess (ee) is calculated from the concentration of both enantiomers as:

$$ee = \frac{[R] - [S]}{[R] + [S]} \quad (1.17)$$

where $[R]$ is the concentration of the (R)-enantiomer and $[S]$ is the concentration of (S)-enantiomer. E_p indicates the enantiomeric excess of product and ee_s indicates the enantiomeric excess of substrate. Sih *et al.*⁴⁰ developed formulas that relate the enantiomeric purity of reactant and product and conversion to the enantiomeric ratio, E . This is commonly referred to as the end point method. Integration of equation 1.15 gives the enantiomeric ratio E , where $[R_0]$ and $[S_0]$ are the initial concentration of both enantiomers and $[R]$ and $[S]$ are the remaining concentration after a given reaction time.

$$\frac{\ln([R]/[R_0])}{\ln([S]/[S_0])} = \frac{(k_{cat}/K_M)_R}{(k_{cat}/K_M)_S} = E \quad (1.18)$$

Expressing the extent of conversion c and the enantiomer excess of substrates (ee_s) and products (ee_p) as:

$$c = 1 - \frac{[R] + [S]}{[R_0] + [S_0]} ee_s = \frac{[R] - [S]}{[R] + [S]} ee_p = \frac{[P] - [Q]}{[P] + [Q]} \quad (1.19)$$

the enantioselectivity E can be rewritten as a logarithmic function of c and ee_s , c and ee_p or ee_s and ee_p :

$$E = \frac{\ln[1 - c(1 + ee_p)]}{\ln[1 - c(1 - ee_p)]} = \frac{\ln[(1 - c)(1 - ee_s)]}{\ln[(1 - c)(1 + ee_s)]} = \ln \left(\frac{\frac{1 - ee_s}{1 + \frac{ee_s}{ee_p}}}{\frac{1 + ee_s}{1 + \frac{ee_s}{ee_p}}} \right) \quad (1.20)$$

The end point method is the current standard to measure the enantiomeric ratio E of an enzyme-catalyzed kinetic resolution. This ratio serves as measure of the performance of a hydrolase. For synthetic purposes, an enantiomeric ratio of less than $E = 20$ is not acceptable for preparative reactions, but $E = 100$ is considered excellent. However, once the E value for an enzyme toward a substrate is determined, plots of % ee versus % conversion can be useful to determine % conversion where you can obtain at least one enantiomer in high optical purity. For example, if the enzyme $E = 10$ one has to stop the reaction at 62% conversion to obtain 90% ee_s . In this case, 55% ee_p is obtained. When the enzyme $E = 100$, at 50% conversion it is possible to obtain 93% ee_s and 93% ee_p (Figure 1.6).

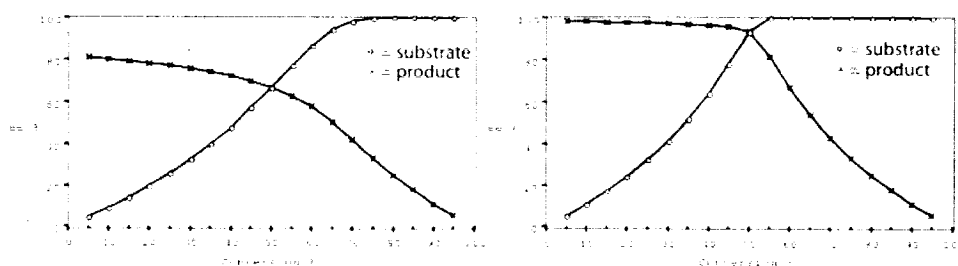


Figure 1.6. Dependence of optical purity on conversion. Left: $E = 10$; right: $E = 100$. Generated using “Enantiomeric Ratio”.⁴¹

The enantioselectivity of a kinetic resolution may also be expressed as the difference in activation free energy, $\Delta\Delta G^\ddagger$, between the diastereomeric transition states of the two enantiomers during reaction (Figure 1.7):

$$\Delta\Delta G^\ddagger = \Delta G^\ddagger_R - \Delta G^\ddagger_S = -RT\ln E \quad (1.21)$$

From equation 1.21, we can calculate that a high enantioselectivity, $E = 100$, corresponds to a $\Delta\Delta G^\ddagger = 2.7 \text{ kcal mol}^{-1}$ at 298 K.

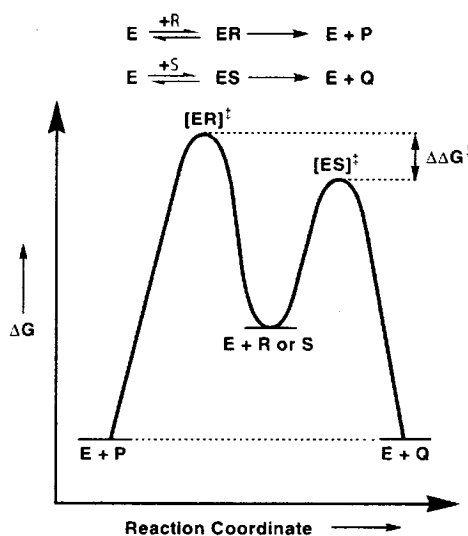


Figure 1.7. Energy diagram for a hypothetical enzyme-catalyzed enantioselective resolution. The two peaks ($[ER]^\ddagger$ and $[ES]^\ddagger$) indicate the transition states for reaction of the enzyme (E) with the two enantiomers ($R = (R)$ -enantiomer; $S = (S)$ -enantiomer) of a substrate. $[ER]$ and $[ES]$ = enzyme-substrate complexes and ‡ symbolizes a transition state. Enantioselectivity originates from the difference in activation free energy ($\Delta\Delta G^\ddagger$) for the two enantiomers. Adapted from Faber.²¹

1.6 General features of hydrolases – lipases and proteases

Several characteristics make hydrolases useful for organic chemistry. First, because of their broad substrate specificity, hydrolases often accept as substrates various synthetic intermediates. Second, hydrolases often show high stereoselectivity. Third, besides hydrolysis, they can also catalyze condensations (e.g. transesterification). Finally, they do not require cofactors, they tolerate water-miscible organic co-solvents and hun-

dreds are commercially available. In this section, I will highlight the structural features of lipases and proteases, how they bind substrate and what types of substrates and reactions they are best suited.

1.6.1 Lipases

Lipases belong to the α/β -hydrolase super-family and to the α/β -hydrolase fold, as identified by Ollis and coworkers⁴² from the comparison of five different enzymes. It is comprised of a central β -sheet, formed by eight mostly-parallel β -strands, which are flanked on either side by α -helices (Figure 1.8). The catalytic triad residues, serine, histidine and aspartate acid, are in the same order in the amino acid sequence of all lipases. Consequently, they have the same orientation in the three-dimensional structure of each enzyme because of the common α/β -fold. The catalytic triad is situated at the C-terminal edge of the β -sheet. The nucleophilic serine is situated at the elbow of a sharp turn of the loop between strand 5 and helix C, the aspartate is in a loop following strand 7 and the histidine is the first amino acid after a reverse turn following strand 8. The “oxyanion hole” residues are located between strand 3 and helix A.

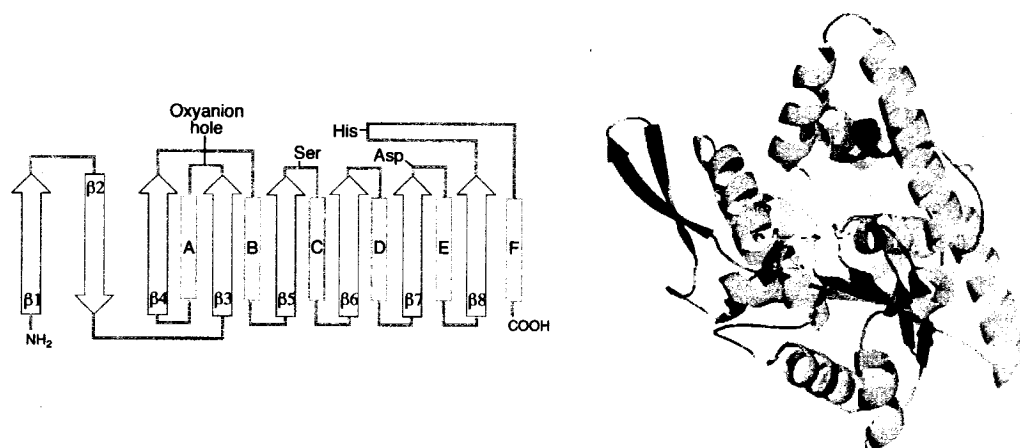


Figure 1.8. Schematic drawing of the α/β -hydrolase fold showing the relative position of the catalytic site residues, and a ribbon diagram of an X-ray crystal structure of an α/β -hydrolase (*Pseudomonas cepacia* lipase). The residues are coloured as follows: alpha helices (green), beta strands (magenta), loops (grey). The catalytic residues are shown in lines and coloured according to CPK.

The specific arrangement of the catalytic machinery and α/β -fold provide a chiral environment within the active site that is common to the lipases. X-ray crystal structures of transition state analogues bound to the active site of lipases show a buried active site with distinct binding sites for the alcohol and acid portion of esters.²⁴ The alcohol-binding site is a well-defined binding site that is similar for all lipases. It is a crevice containing two regions – a large hydrophobic pocket which is open to solvent and a medium-sized pocket (stereoselectivity pocket). As a result, lipases exhibit a common enantioselectivity toward secondary alcohols. This will be further discussed in section 1.7. The binding site for the acid portion of the ester varies among the lipases. For some lipases, the acyl group binds in a short trough that extends into the large hydrophobic region of the alcohol-binding site. In others like *Candida rugosa* lipase (CRL) the acyl group binds in a long tunnel. In most lipases, the substrate binds in a folded conformation, where the acyl group and alcohol group are in close contact (Figure 1.9).⁴³ For this reason, the size and substitution pattern of the acyl group can affect the selectivity of lipases toward alcohols.⁴⁴

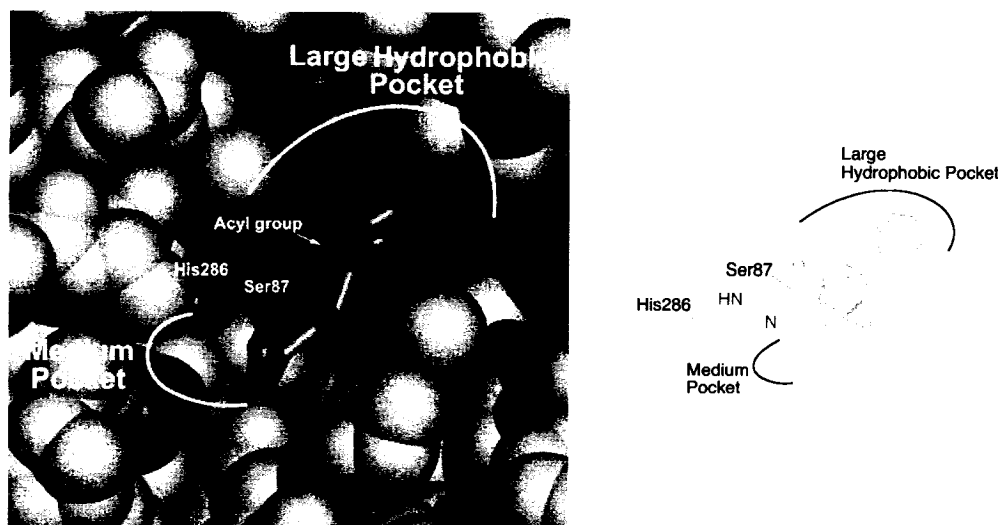


Figure 1.9. A close up view of a complex of a lipase (*Pseudomonas cepacia* lipase) with a transition state analogue of 1-phenoxy-2-acetoxybutane (pdb: 1HQD).⁴³ The substrate analogue and active site residues (Ser87, His286 and Asp264) are shown as sticks. The atoms are coloured as follows: orange (alcohol portion of substrate), blue (acyl portion of substrate), red (enzyme oxygen), blue (enzyme nitrogen). Surrounding atoms (space fill) of *Pseudomonas cepacia* lipase are shown in the colour wheat; large pocket residues

(Val266, Val 267, Leu167, Phe119 and Pro113) are shown in green; medium pocket residue (Leu287) is shown in red. For clarity, all hydrogen atoms and water molecules are hidden. The medium substituent (CH_3CH_2-) of the secondary alcohol binds in the medium-sized pocket, while the large substituent (PhOCH_2-) of the secondary alcohol binds adjacent to the acyl group (C(O)CH_3) in the large hydrophobic pocket. Because of this orientation, the substrate is said to bind in a folded conformation.

The catalytic activity of most lipases increases in contact with lipid-soluble substrate at a lipid/water interface.⁴⁵ The X-ray crystal structures of lipases usually show the “closed” conformation where the active site is completely buried by a “lid” on the surface.⁴⁶ However, X-ray crystal structures with bound transition state analogues show the “open” conformation. For this reason, researchers believe a lipid-induced change in the lid orientation causes interfacial activation. Lipases show poor activity toward soluble substrates in aqueous solution because the lid is closed. Upon contact with a hydrophobic interface, the lid opens and the catalytic activity increases. This property distinguishes them from serine proteases, which react only with soluble substrates. As well, it makes them very useful for organic synthesis because they can act on nonpolar organic molecules that are poorly soluble in aqueous solutions.

Lipases show high enantioselectivity toward a wide range of substrates. However, lipase substrate specificity stems mainly from the alcohol-binding site. For this reason, they are most suited for resolution of nonpolar secondary alcohols and derivatives.

1.6.2 Serine proteases – subtilisin and α -chymotrypsin

Subtilisins are a family of bacterial serine proteases secreted by a various *Bacillus* species that can cleave both amides and esters. Subtilisins are secreted as a pro-peptide complex that undergoes autolysis to yield active subtilisin.⁴⁷ The mature protein is a single polypeptide chain that consists of ca. 270 amino acids and contains at least one structural Calcium ion.⁴⁸ The core secondary structure of subtilisin is folded in what is known as the α/β -subtilase fold (Figure 1.10).⁴⁹ This fold is not, however, the same as the α/β -hydrolase fold of lipases. This fold consists of a β -sheet comprised of five parallel β -strands flanked by four α -helices. Unlike the α/β -hydrolases, the catalytic residues,

Ser221, His64, Asp32, are not located on the loops but rather within the secondary structure. Histidine and serine are located on the first turn of helix B and helix E, respectively. Aspartate is found within strand 1 and Asn155, which along with the backbone amide of Ser221 forms the oxyanion hole, is on the tip of the carboxy end of strand 5.

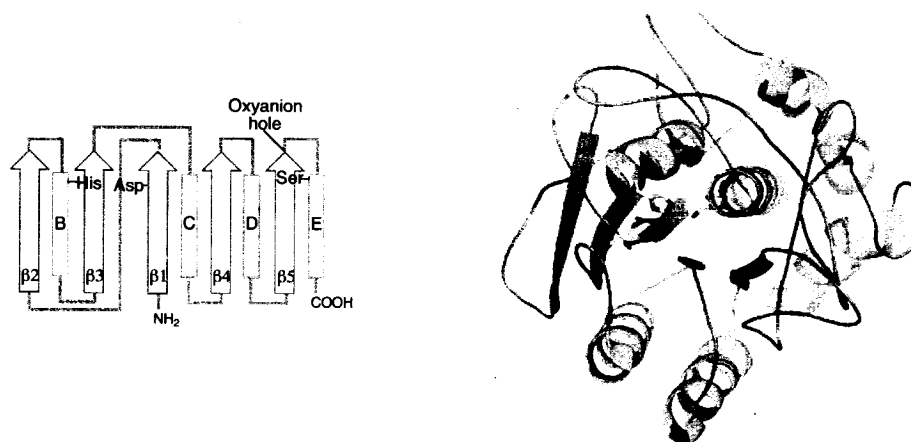


Figure 1.10. Schematic drawing of the α/β -subtilase fold showing the relative position of the catalytic site residues, and a ribbon diagram of an X-ray crystal structure of an α/β -subtilase (subtilisin Carlsberg). The residues are coloured as follows: alpha helices (green), beta strands (magenta), loops (grey). The catalytic residues are shown in lines and coloured according to CPK.

α -Chymotrypsin (241 amino acids) from bovine pancreas is the most widely studied chymotrypsin.²⁵ The pancreas secretes inactive chymotrypsinogen A. Proteases then remove two peptides yielding active α -chymotrypsin. Mature α -chymotrypsin consists of three polypeptide chains linked by five disulfide bonds. The catalytic residues in both subtilisin and α -chymotrypsin have a similar three-dimensional arrangement, but their protein folds are not related. α -Chymotrypsin has a β/β fold – two anti-parallel β -barrel domains.

Although the catalytic triad residues of subtilisin and α -chymotrypsin are the same as those found in lipases, the serine nucleophile lies on the opposite side of the plane formed by the imidazole ring of the histidine. Therefore, the three-dimensional ori-

entations of the catalytic machinery, including the oxyanion hole, in lipases and most proteases are approximately mirror images.⁵⁰

Schechter and Berger⁵¹ suggested numbering the different regions within the peptide channel of a protease according to the amino acid residues that bind there and the distance of these amino acids from the amide link to be cleaved (Figure 1.11). Thus, the acyl group of the amino acid undergoing cleavage is the P_1 residue, which binds in the S_1 site. The amine group to be released belongs to the P_1' amino acid, which binds in the S_1' site. The S_1 site is analogous to the acyl binding site of lipases and the S_1' site is analogous the alcohol binding site of lipases.

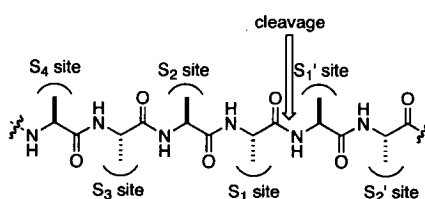


Figure 1.11. Naming of the binding site of proteases according to Schechter and Berger.⁵¹ The acyl portion of the amide peptide bond to be cleaved lies in the S_1 , S_2 , S_3 , etc. binding sites, while the amine portion of the peptide bond to be cleaved lies in the S_1' , S_2' , etc. binding sites. The substrate residues are called P_1 , P_2 , P_3 , etc. and P_1' , P_2' , etc. according to their location relative to the amide link being cleaved. Adapted from Bornscheuer and Kazlauskas.²²

The active site of subtilisin and α -chymotrypsin is an open-to-solvent active site located on the surface of protein in the peptide channel (Figure 1.12). The active site has two distinct, and separate, regions – the acyl binding site and the amine (alcohol) binding site. Proteases bind peptide substrate in an extended conformation,⁵² unlike the lipases that bind substrate in a folded conformation.

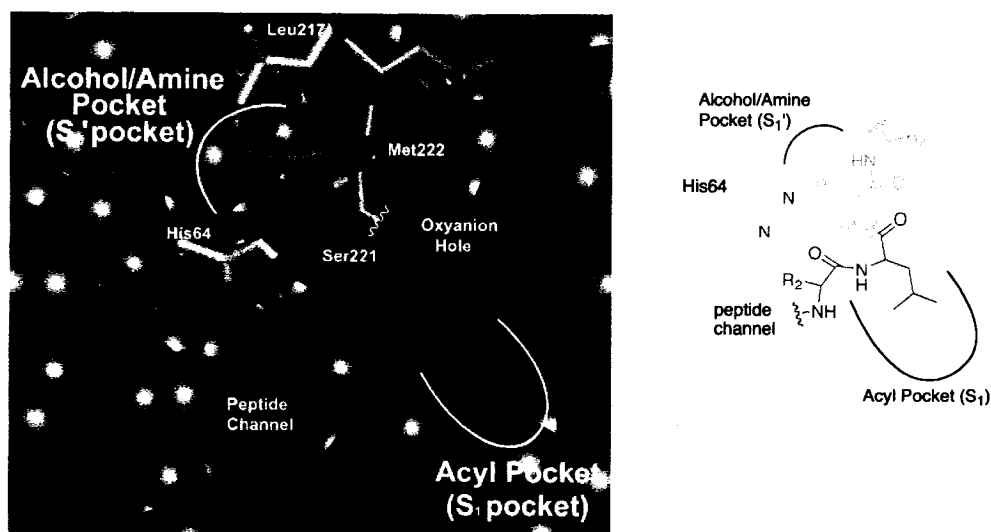


Figure 1.12. A close up view of a complex of subtilisin (subtilisin Carlsberg) with a non-covalently bound protease inhibitor (Eglin C) (pdb: 1CSE).⁵³ The substrate and catalytic residues (Ser221, His64 and Asp32) and key active site residues (Asn155, Leu217 and Met222) are shown as sticks. The atoms are coloured as follows: orange (alcohol portion of substrate), blue (acyl portion of substrate), red (enzyme oxygen), blue (enzyme nitrogen) and orange (enzyme sulfur). Surrounding atoms (space fill) of subtilisin Carlsberg are shown in the colour blue. For clarity, all hydrogen atoms and water molecules are hidden and the first 30 and last 22 residues of Eglin are removed. The peptide backbone binds in the peptide channel. The side chain of amino acid P_1' (amine portion) binds in the S_1' leaving-group pocket and the side chain of amino acid P_1 (acyl portion) binds in the S_1 pocket. Because of this orientation, the substrate is said to bind in an extended conformation.

Subtilisin shows broad substrate specificity; however, it favours large uncharged residues, such as phenylalanine, at the P_1 position.⁵⁴ Subtilisin shows little preference for amino acids at P_2 and P_3 , but favours hydrophobic residues at P_4 . α -Chymotrypsin also favours large non-polar amino acids, such as phenylalanine, at P_1 . Unlike subtilisin, α -chymotrypsin reacts slowly with small and/or polar amino acids at P_1 . The specificity of α -chymotrypsin correlates with the hydrophobicity of the P_1 residue, with phenylalanine preferred over alanine by ca. 50,000.⁵⁵ Proteases usually show little preference for amino acids at P_1' and P_2' .

Unlike lipases, proteases react only with dissolved substrates. To dissolve nonpolar substrates in aqueous solutions, researchers usually add organic co-solvents. However, organic solvents tend to decrease the rate of reaction of subtilisin and chymotrypsin by reducing hydrophobic interaction between P_1 side chain and S_1 pocket residues.⁵⁶

Since subtilisin and α -chymotrypsin substrate specificity stems mainly from the acyl-binding site, not the amine-binding site, subtilisin usually shows higher stereoselectivity toward acids and lower, broader selectivity toward the amine or alcohol.²² However, since the active site is on the surface and substrate is bound in an extended conformation, they accept sterically hindered substrates.⁵⁷ In addition, they readily accept polar, water-soluble substrates⁵⁸ that react slowly with lipases.²²

The catalytic mechanism for lipases and proteases is similar (see Scheme 1.6). Kinetic studies indicate that the breakdown of the first tetrahedral intermediate is rate determining for lipase-catalyzed hydrolysis of esters and protease-catalyzed hydrolysis of amides.⁵⁹ However, the rate-determining step of protease-catalyzed ester hydrolysis can be the second deacylation step.⁶⁰

1.7 Molecular basis for hydrolase enantioselectivity

The building blocks of enzymes are L-amino acids. Their chirality and position in the protein sequence determine the three-dimensional shape of each enzyme and give an enzyme its ability to distinguish enantiomers. There are several proposals rationalizing hydrolase enantioselectivity toward secondary alcohols. Most of these proposals are based on simple models for enzyme enantioselectivity. These models for enzyme enantioselectivity and a summary of recent developments regarding molecular basis of hydrolase enantioselectivity toward secondary alcohols will be discussed in this section.

1.7.1 Models for rationalizing enantiomer discrimination

Ogston⁶¹ suggested a three-point attachment rule to rationalize the enantioselectivity of enzymes. To get a high degree of enantioselection, a substrate must be held firmly in three-dimensional space. As a consequence, there must be at least three different points of attachment of the substrate in the active site. This is exemplified for the enantiodiscrimination of a racemic substrate with its chirality on a sp^3 -carbon atom in Figure 1.13.

The favoured enantiomer is a good substrate by allowing optimal interaction of its groups (A, B, C) with their complementary binding sites in the enzyme active site (A', B', C'). It ensures an optimal orientation of the reactive group (D) toward the chemical operator, which is required for reaction. This model suggests two substituents at stereocentre exchange and the disfavoured enantiomer is a poor substrate because optimal binding and orientation is not possible.

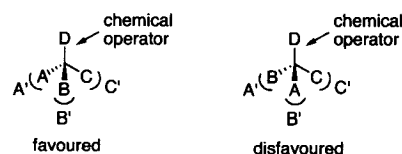


Figure 1.13. Schematic representation of enantiomer discrimination by an enzyme via the “three-point attachment rule”. Adapted from Faber.²¹

Recently, Mesecar and Koshland⁶² suggested that the three-point attachment rule works only when the substrate approaches from the top of a flat enzyme surface. If, however, binding sites are in an enzyme cleft an additional interaction point is necessary to discriminate enantiomers because the binding sites can be approached from two directions (Figure 1.14). They show an umbrella-like inversion at stereocentre for the two enantiomers of isocitrate in the catalytic pocket of isocitrate dehydrogenase, where three of the four substituents occupy the same position and the fourth is pointing in a different direction. This interaction with enzyme is responsible for enantiodiscrimination. This is known as the “four location model” to explain enzyme enantioselectivity. This model suggests substituents at stereocentre do not exchange. Instead, there is an umbrella-like inversion at stereocentre.

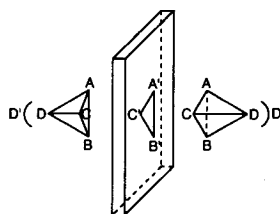


Figure 1.14. Schematic representation of enzymatic enantiomer discrimination via the “four location model”. Adapted from Koshland.⁶³

1.7.2 Enantioselectivity of lipases toward secondary alcohols

Although lipases show high enantioselectivity toward a wide range of substrates, the most common substrates are secondary alcohols. All lipases have a common enantio-preference toward secondary alcohols, although the degree of enantioselectivity is variable. It is suggested that this common enantio-preference is due to common characteristics of the alcohol-binding site: a large hydrophobic pocket and medium-sized (stereoselectivity) pocket. In this site, the large substituent will bind in the large hydrophobic pocket and the medium-sized substituent will bind in the stereoselectivity pocket. For example, Cy-gler and coworkers²⁴ showed the transition state analogue of menthyl hexanoate binds menthol in the alcohol-binding site with its large substituent in the large hydrophobic pocket and its smaller substituent in the medium pocket (Figure 1.15).

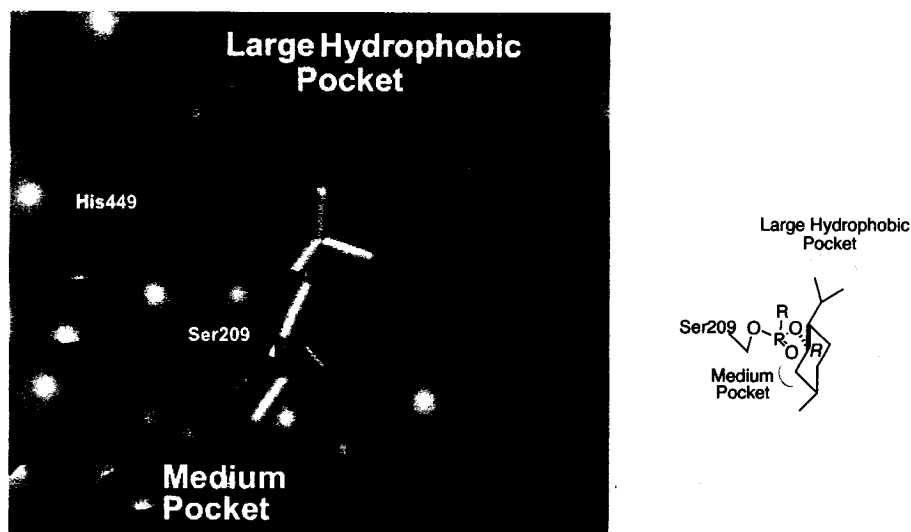


Figure 1.15. A close up view of a complex of a lipase (*Candida rugosa* lipase) with a transition state analogue of (*R*)-menthyl hexylphosphonate (pdb: 1LPM)²⁴ and schematic diagram showing orientation of substituents in the active site pocket.²⁴ The substrate analogue and active site residues (Ser209, His449 and Glu341) are shown as sticks. The atoms are coloured as follows: grey (substrate carbon), green (enzyme carbon), red (oxygen), blue (nitrogen) and pink (phosphorous). Surrounding atoms (space fill) of *Candida rugosa* lipase are shown in grey; large pocket residues (Phe296, Ile297, Phe344, Phe345) are shown in green; medium pocket residues (Glu208, Gly122) are shown in red. For clarity, all hydrogen atoms and water molecules are hidden. The methylene group binds in the

medium-sized pocket (red residues) and the isopropyl group binds in the large hydrophobic pocket (green residues).

Based on the observed enantioselectivity of lipases, chemists have developed models to predict the enantipreference of lipases toward secondary alcohols and their esters. The rule is based on the relative size difference of the substituents at the stereocentre and suggests that lipases distinguish between enantiomers of secondary alcohols primarily by comparing the sizes of these two substituents (Figure 1.16).⁶⁴ Indeed, researchers have increased the enantioselectivity of lipase-catalyzed reactions by increasing the size difference of the two substituents (see Section 1.8.1).

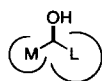


Figure 1.16. An empirical rule to predict which enantiomer of a secondary alcohol reacts faster in lipase-catalyzed reactions, where M is the medium-sized substituent and L is the large substituent.

Several researchers have proposed explanations for the enantioselectivity of lipases toward secondary alcohols. Models based on the three-point attachment model, where two substituents exchange, the four-location model, where there is an inversion at stereocentre, and stereoelectronic effects have been used to rationalize hydrolase enantioselectivity. The explanations are based on X-ray crystal structures of transition state analogues, kinetic experiments, molecular modelling and substrate mapping studies.

X-ray structures of transition state analogues containing a secondary alcohol, menthol, bound to CRL identified the alcohol-binding pocket.²⁴ This pocket resembled the empirical rule: a large hydrophobic pocket and a smaller pocket for the medium-sized substituent. A comparison of the structures of the fast-reacting (*R*)-enantiomer and slow-reacting (*S*)-enantiomer of menthol showed that in both cases the large substituent binds in the large hydrophobic pocket and the medium substituent binds in the smaller pocket, suggesting enantiorecognition follows the four location model. In the slow-reacting (*S*)-enantiomer, the isopropyl moiety is directed toward the catalytic histidine. This distorts

the orientation of the imidazole ring, permitting only the hydrogen bond to the catalytic serine O_γ to form (Figure 1.17).ⁱ Thus, the (*R*)-enantiomer is favoured. This suggests that enantiomers differ mainly in their rate of reaction and not in their relative affinity to the lipase.

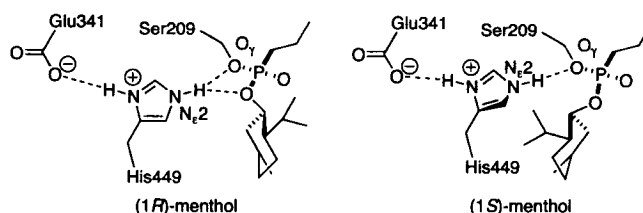


Figure 1.17. Schematic representation of both enantiomers of the menthol inhibitor bound to the active site of CRL. The alcohol oxygens of the two enantiomers point in different directions. The slightly different orientation of the large group of the slow-reacting enantiomer within the hydrophobic pocket disrupts the catalytically essential hydrogen bond between $N_{\epsilon 2}$ and O_{alcohol} .

Consistent with the above results, Nishizawa and coworkers⁵⁹ measured the kinetic constants with PCL for two the different enantiomers of a secondary alcohol and found similar values for the apparent K_M , but very different values for k_{cat} . They proposed that the large substituent of both enantiomers bind tightly to the same site and that the orientation of smaller substituent hinders hydrogen bond formation between $N_{\epsilon 2}$ of catalytic histidine and O_{alcohol} .

Modelling of the transition state for ester hydrolysis in CALB, combined with substrate experiments, suggested an explanation similar to the three point attachment model.^{65,66} Hult and coworkers show the transition states for hydrolysis of the enantiomers of 1-phenethyl alcohol have different binding modes. In the fast enantiomer the large substituent binds in the large pocket and the medium in the medium pocket, but in the slow enantiomer the large substituent binds in the medium pocket and the medium

ⁱ For a hydrolase catalyzed hydrolysis to occur, the substrate must be in a productive conformation in the first tetrahedral intermediate. That is, the oxyanion should be oriented to hydrogen bond with “oxyanion hole” residues, the $N_{\epsilon 2}$ hydrogen of catalytic histidine should be hydrogen bonded to catalytic serine O_γ and substrate O_{alcohol} , and $N_{\delta 1}$ should be hydrogen bonded to catalytic aspartate (glutamate).

substituent in the large pocket (Figure 1.18). Consistent with this explanation, increasing the size of large substituent resulted in higher enantioselectivity toward the favoured enantiomer because the large substituent could no longer be accommodated in the medium-sized pocket.⁶⁷

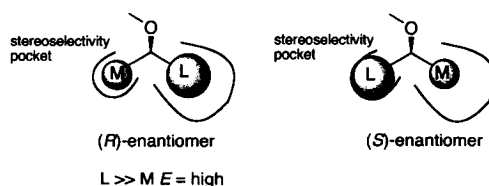


Figure 1.18. Schematic representation of the productive binding modes of secondary alcohols with CALB.

Ema and coworkers⁶⁸ suggested that enantiomer discrimination is solely dependent on the relative stability of the transition states of each enantiomer, while ignoring the size, shape and electronic characteristics of the substrate. In the transition state, the conformation along the $C_{\text{alcohol}}-O_{\text{alcohol}}-C_{\text{C=O}}-O_{\gamma}$ dihedral adopts a *gauche* conformation. According to the stereoelectronic theory,^{ii,69} this is necessary for efficient cleavage of the ester C-O bond. When the fast-reacting enantiomer adopts this conformation, the large substituent is directed toward solvent and the hydrogen at stereocentre forms a *syn-syn* interaction with oxyanion. When the slow enantiomer adopts this *gauche* conformation, the large substituent is positioned toward the “protein wall”, causing severe steric strain between substrate and enzyme. To reduce steric strain the substrate adopts a conformation where the medium substituent forms a *syn*-pentane-like interaction with oxyanion or an *anti* conformation along $C_{\text{alcohol}}-O_{\text{alcohol}}-C_{\text{C=O}}-O_{\gamma}$. In either of these conformations this enantiomer is less stable than the antipodal enantiomer (Figure 1.19). However, X-ray crystal structures of phosphonate transition-state analogues containing secondary alcohols do not support this theory. The fast-reacting enantiomer of menthol bound to *Candida rugosa* lipase did not adopt the predicted *gauche* conformation (130°). On the other hand,

ⁱⁱ According to the stereoelectronic theory, for efficient cleavage of the ester C-O bond to occur the two other oxygens in the tetrahedral intermediate must have their lone pair electrons antiperiplanar to the breaking C-O bond. In this arrangement the oxygen lone pair n orbital overlaps with the breaking bond σ^* orbital, facilitating cleavage of the bond.

the slow-reacting enantiomer did adopt a *gauche* conformation (71°), again contrary to predictions.²⁴

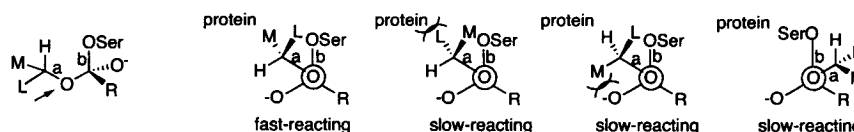


Figure 1.19. Schematic representation of the proposal by Ema and coworkers. The view along bond *a* for the fast-reacting enantiomer and the slow-reacting enantiomer. The conformation along the $C_{\text{alcohol}}-O_{\text{alcohol}}-C_{\text{C=O}}-O_{\gamma}$ dihedral adopts a *gauche* due to the stereoelectronic effect. In the fast reacting enantiomer the large substituent points toward external solvent without severe steric hindrance and the hydrogen forms a *syn-syn* interaction with oxyanion. In the slow-reacting enantiomer the large substituent encounters severe steric strain with protein backbone and adopts a conformation where the medium-sized group forms an unfavourable *syn*-pentane-like interaction with oxyanion or an *anti* conformation along $C_{\text{alcohol}}-O_{\text{alcohol}}-C_{\text{C=O}}-O_{\gamma}$. In either case, the slower reacting enantiomer is less stable.

Although steric interactions are the most important determinant of lipase enantio-preference, electronic interactions also contribute. For example, CALB shows high enantioselectivity toward 3-nonanol ($E = >300$), but low enantioselectivity toward 1-bromo-2-octanol ($E = 7.6$) under the same conditions (Figure 1.20). Both an ethyl and a $-\text{CH}_2\text{Br}$ group are similar size, so the difference suggests that an electronic interaction lowers enantioselectivity.^{66,70}

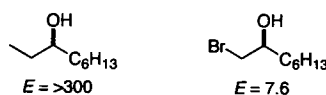


Figure 1.20. Electronic effects can influence enantioselectivity. CALB-catalyzed acylation with ethyl thiooctanoate shows high enantioselectivity toward 3-nonanol, but low enantioselectivity toward its isostere, 1-bromo-2-octanol.

1.7.3. Enantioselectivity of subtilisin toward secondary alcohols

Like the lipases, subtilisin is enantioselective toward secondary alcohols, but favours the enantiomer opposite to the one favoured by lipases. An empirical rule based on the size of substituents at stereocentre to predict the favoured enantiomer has also been proposed for subtilisin (Figure 1.21).^{50,71}

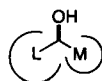


Figure 1.21. An empirical rule to predict which enantiomer of a secondary alcohol reacts faster in subtilisin-catalyzed reactions, where M is the medium-sized substituent and L is the large substituent.

Many of the studies to determine how subtilisin distinguishes enantiomers of secondary alcohols used the same rationale to those for lipases. For example, Klibanov and coworkers⁷² used computational molecular modelling to study the enantioselectivity of subtilisin Carlsberg-catalyzed acylation of 1-phenethyl alcohol. Modelling of the favoured (*S*)-enantiomer shows the medium-sized methyl group bound in a small pocket and the large phenyl group in a spacious opening. Modelling with the slow-reacting (*R*)-enantiomer switches these substituents and places the methyl group in the spacious opening and the phenyl group in the small pocket where it makes close contact with residues lining this pocket. This suggests a rationale similar to the three-point attachment model, where steric hindrance between phenyl group of the slow-reacting (*R*)-enantiomer with active site residues in this small pocket slow its reaction (Figure 1.22). However, X-ray crystal structures show there is only one pocket – the *S*₁' pocket – that is slightly larger than a phenyl group.

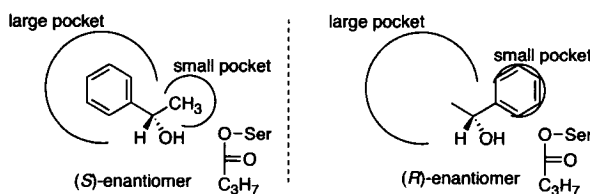


Figure 1.22. Schematic representation of the binding modes of (*S*)- and (*R*)-1-phenethyl alcohol with subtilisin Carlsberg, as described by Klibanov and coworkers.⁷² Steric hin-

drance between phenyl group of (*R*)-1-phenethyl alcohol with “small pocket” residues slow its reaction and thus, the (*S*)-enantiomer is favoured.

Using molecular modelling, Colombo et al.⁷³ suggested that steric hindrance between the large phenyl group of the slow-reacting (*R*)-1-phenethyl alcohol with enzyme active site residues disrupted catalytically relevant hydrogen bonds between His64 N_{ε2} and O_γ of Ser221 and O_{alcohol}. In addition, they suggested there was a favourable stacking interaction between the phenyl group of the fast-reacting (*S*)-enantiomer with the imidazole ring of catalytic His64. However, the calculated energy difference ($\Delta\Delta G^\ddagger$) between enantiomers was 1-2 orders of magnitude higher than the experimental, suggesting the slow-reacting enantiomer complex was not a fully minimized conformer.

Ema and coworkers⁷⁴ also proposed their transition state theory to rationalize the enantioselectivity of subtilisin toward secondary alcohols. Again, they claim the conformation along the C_{alcohol}-O_{alcohol}-C_{C=O}-O_γ dihedral adopts a *gauche* conformation due to the stereoelectronic effect. The faster-reacting enantiomer adopts a conformation that directs the large substituent into open solvent, whereas the slower-reacting enantiomer directs the large substituent toward the “protein wall” causing severe steric repulsion and destabilizing its transition state. However, a recent molecular modelling study with subtilisin by Mugford and coworkers⁷⁵ suggests the fast-reacting enantiomer of a secondary alcohol cannot adopt this *gauche* orientation along the C_{alcohol}-O_{alcohol}-C_{C=O}-O_γ dihedral because the medium substituent encounters severe clash with catalytic histidine and loses catalytically essential hydrogen bonds. Instead, it must adopt an *anti* conformation along this bond to make catalytically essential hydrogen bonds.

Kazlauskas and Weissfloch⁵⁰ proposed that the reverse enantiopreference of subtilisin is because the active site is a mirror image of the lipases. This mirror-image relationship places the catalytic histidine on opposite sides of the stereoselectivity pocket in lipases and subtilisin (the S₁' pocket) and results in opposite enantiopreference toward secondary alcohols. It is important to note that an isolated catalytic triad cannot impart stereoselectivity toward secondary alcohols; the pockets created by folding L-amino acids of the protein are essential to create a chiral environment. This is a qualitative model that rationalizes the enantiopreference, but not the degree of enantioselectivity.

Although there are many different proposals rationalizing hydrolase enantioselectivity toward secondary alcohols and related compounds, it is still not clear how enantio-differentiation occurs and what determines the degree of enantioselectivity. It seems as though there is a balance between the many structural and electronic characteristics of the both the substrate and hydrolase. Thus, it is very likely that there is a different explanation for different substrates and different hydrolases and one rationale may only apply to one enzyme substrate complex.

1.7.4 Using molecular modelling to rationalize enantioselectivity of hydrolases

Recent advances in solving the three-dimensional structure of proteins have opened up the possibility of using computational techniques for understanding enzyme selectivity.⁷⁶ One of the most popular techniques for studying proteins is molecular mechanics (MM). In molecular mechanics, classical mechanics describes the structure and dynamics of molecules. Atoms are treated as classical particles and bonds as springs and hence, molecules are sets of vibrating spheres. The energy functions are the sum of steric interactions and non-bonded interactions and contain constants that are obtained from experimental or *ab initio* methods.⁷⁷ This method is simple, which allows for its application to large molecules such as proteins.

Molecular mechanics can be used to model transition state intermediates, such as the tetrahedral intermediate formed during ester hydrolysis. Thus, it can be effective for understanding enzyme-catalyzed reactivity and selectivity and for predicting the influence of amino acid or substrate changes. For example, a molecular mechanics simulation was used to predict amino acid substitutions to improve enantioselectivity of *Candida antarctica* lipase B (CALB) toward 1-chloro-2-octanol.⁷⁸ Molecular modelling of the two enantiomers revealed unfavourable interactions between the chloromethyl substituent of the fast-reacting enantiomer and residues in the medium-sized alcohol-binding pocket. Virtual mutation of residues in this pocket indicated several amino acid substitutions with increased affinity for the chloromethyl substituent. Based on these predictions, two residues with electronegative side chains, S47 and T42, were mutated to alanine and valine, respectively, using site-directed mutagenesis. Enantioselectivity improved from $E = 14$

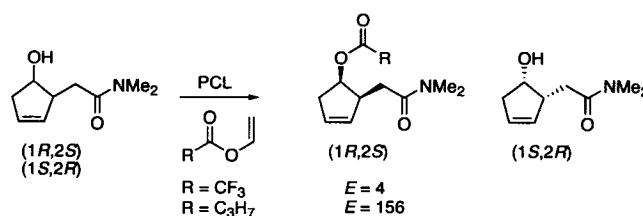
for wild-type CALB to $E = 28$ for the S47A mutant. No increase was observed for the T42V mutant. This is an example of rational protein design (see Section 1.8.3).

1.8 Strategies for improving enzyme enantioselectivity

Hydrolases are frequently used in the synthesis of optically pure compounds. However, natural enzymes do not always show sufficiently high enantioselectivity (e.g., $E = >20$). The enantioselectivity of an enzyme-catalyzed reaction can be optimized by alteration of the substrate, the reaction medium or by protein engineering.

1.8.1 Increasing E by substrate engineering

Modifying the substrate in a reaction can increase the E . This is known as substrate engineering. For example, using vinyl esters of carboxylic acids instead of commonly used ethyl esters can enhance enantioselectivity.⁷⁹ In the CALB catalyzed kinetic resolution of ibuprofen, the E value increased from $E < 2$ for the ethyl ester to $E = 39$ for the vinyl ester.⁸⁰ Variation of the chain length and polarity of the acyl donor in the resolution of secondary alcohols also changes the E value. For example, the enantioselectivity of PCL-catalyzed acylation of 2-[(*N,N*-dimethylcarbamoyl)methyl]-3-cyclopenten-1-ol varied from $E = 4$ to 156 depending on the acylating agent (Scheme 1.10).⁸¹



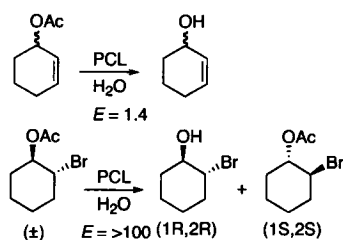
Scheme 1.10. Variation of enantioselectivity for PCL-catalyzed acylation of 2-[(*N,N*-dimethylcarbamoyl)methyl]-3-cyclopenten-1-ol with acylating agent.

Ottosson and Hult⁸² found that the E value decreased for shorter vinyl esters in the CALB-catalyzed transesterification of 3-methyl-2-butanol. The lowest E value was with vinyl butanoate ($E = 390$) and the highest E value was with vinyl octanoate ($E = 810$).

This phenomenon was mainly attributed to changes in the entropic component except for reaction of vinyl propionate, which differed from the others in the enthalpic component.

Waldmann and coworkers⁸³ showed that the acyl group also influences protease-catalyzed reactions. They found that changing from the 2-pyridylacetyl to the 4-pyridylacetyl group increased the rate eight-fold and the enantioselectivity three-fold for a penicillin G acylase-catalyzed hydrolysis of 1-phenethyl esters.

To improve the enantioselectivity of lipases toward cyclic secondary alcohols, Gupta and Kazlauskas⁸⁴ increased the size of one substituent at stereocentre compared to the other, according to the empirical rule previously proposed by Kazlauskas (Scheme 1.11).⁶⁴ While acetates of the allylic secondary alcohols 2-cyclopentenol, 2-cyclohexenol and 2-cycloheptenol could not be resolved with PCL, the larger 2-bromo cycloalkanol derivatives were resolved with high enantioselectivity ($E = 80$ to >100). Base-catalyzed elimination of HBr of enantiopure 2-bromo cycloalkyl esters, followed by reduction of the ester gave the corresponding enantiopure 2-cycloalkenols.

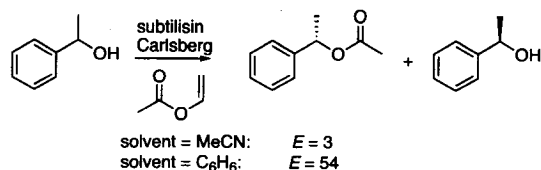


Scheme 1.11. Increasing the enantioselectivity of PCL-catalyzed hydrolysis via substrate modification to increase the relative substituent size difference.

1.8.2 Increasing E by medium engineering

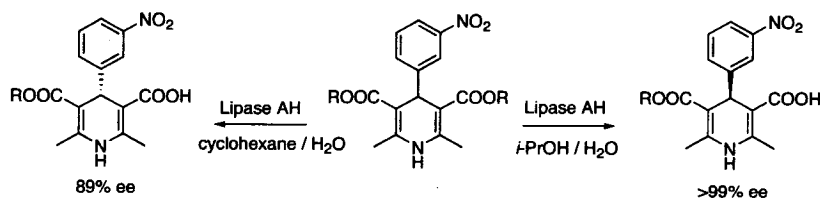
Another strategy to improve enzyme enantioselectivity is medium engineering, where the solvent is changed in the reaction. Although the effect of solvent or additive can be difficult to predict, it can still be a useful approach for increasing enantioselectivity. For example, Klibanov and coworkers^{71,72} increased the enantioselectivity of subtilisin Carlsberg-catalyzed transesterification of 1-phenethyl alcohol from $E = 3$ to $E = 54$ toward the (*S*)-enantiomer simply by switching solvent from acetonitrile to benzene (Scheme 1.12). They rationalized that the enantioselectivity of subtilisin was higher in nonpolar organic solvent because the enzyme has a tighter, more rigid structure, which

increases steric interactions between active site residues and the slow-reacting (*S*)-enantiomer. However, the crystal structure of subtilisin Carlsberg, where crystals have been soaked in acetonitrile or dioxane, is nearly indistinguishable from the structure determined in water.⁸⁵



Scheme 1.12. Influence of organic solvent on subtilisin Carlsberg-catalyzed transesterification of 1-phenethyl alcohol with vinyl acetate.

Another example where changing the solvent affected enantioselectivity was for lipase AH-catalyzed hydrolysis of prochiral diesters, 4-aryl-1,4-dihydro-2,6-dimethyl-3,5-pyridine diester (Scheme 1.13).⁸⁶ By changing the solvent from water-saturated cyclohexane to water-saturated isopropyl ether they reversed the enzyme enantiopreference. A similar solvent-induced reversal of enantioselectivity with other substrates has also been reported for PCL⁸⁷ and *Aspergillus oryzae* protease.⁸⁸ In the latter example, preferential solvation of a nonpolar substituent in nonpolar media instead of the enzyme active site resulted in reversal of enantiopreference.



Scheme 1.13. Lipase AH-catalyzed hydrolysis of a prochiral diester shows opposite enantiopreference in isopropyl ether versus cyclohexane.

Hult and coworkers⁸⁹ suggested a correlation between enantioselectivity and solvent size for CALB-catalyzed transesterification of 3-methyl-2-butanol after thermodynamic analysis of CALB enantioselectivity in nine different solvents. A plot of CALB enantioselectivity versus the van der Waals volume of the solvent showed a direct corre-

lation. The larger the solvent the higher the enantioselectivity. This suggests the difference in activation energy of the enantiomers is partly attributed to the different transition state entropy of the substrate or protein and the different number of solvent molecules displaced from the active site.

1.8.3 Increasing E by protein engineering

The final strategy to improve the enantioselectivity of an enzyme-catalyzed reaction is to modify the enzyme at the genetic level (DNA), also referred to as protein engineering. Two strategies exist to improve enzyme enantioselectivity: rational design and directed evolution (Figure 1.23).

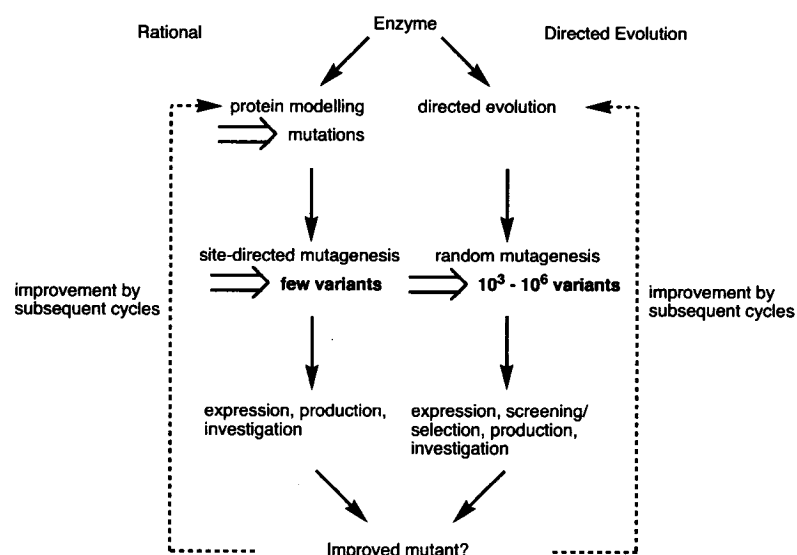


Figure 1.23. Comparison of rational protein design and directed evolution.

In rational design, researchers try to improve the enzyme enantioselectivity by first studying its X-ray crystal structure and then modifying amino acids by site-directed mutagenesis. Crystal structures of transition state analogues or virtual models are often used to identify active site residues that may influence substrate binding. For example, Janssen and coworkers⁹⁰ used rational design to improve the enantioselectivity of epoxide hydrolase from *Agrobacterium radiobacter* AD1. They chose two tyrosines (Y152 and Y215) in the active site of epoxide hydrolase that not only contact substrate, but also participate in the reaction mechanism.⁹¹ A Y215F showed up to a four-fold increase in enan-

tioselectivity toward substituted styrene epoxides. The Y215 mutant, which binds epoxide and facilitates proton donation during ring opening, yields an enzyme with that shows reduced k_{cat} for the slow-reacting (*S*)-enantiomer and hence, increased enantioselectivity for the (*R*)-enantiomer. This Y215F mutant can resolve a variety of styrene epoxides, some on the gram-scale.⁹²

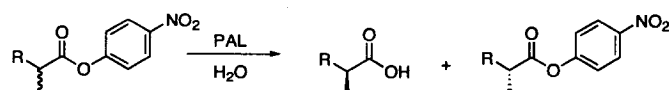
Recently, a W104A mutation in the stereoselectivity pocket of CALB converted the *R*-selective wild-type enzyme into an *S*-selective enzyme.⁹³ Molecular modelling showed that mutation of tryptophan to the smaller alanine residue would create a larger stereoselectivity pocket, which could accommodate the phenyl substituent of the (*S*)-enantiomer and thus favour its reaction. Consistent with their hypothesis, wild-type CALB showed an enormously high enantioselectivity toward (*R*)-1-phenethyl alcohol ($E = 1,300,000$), while the W104A mutant showed low enantioselectivity toward (*S*)-1-phenethyl alcohol ($E = 6.6$). This impressive result represents an 8.3×10^6 change in enantioselectivity.

One advantage of rational design is that it produces a small number of mutants and thus avoids screening of large mutant libraries. However, this strategy requires an enzyme X-ray crystal structure and information regarding the molecular basis of its enantioselectivity.

An alternate approach is directed evolution. Directed evolution is the iterative generation of mutants combined with high-throughput screening. In contrast to rational design, directed evolution does not require a crystal structure or detailed knowledge of the enzyme mechanism. In this strategy, mutations are made in a random fashion throughout the enzyme using error-prone PCR⁹⁴ or DNA shuffling.⁹⁵ The mutant libraries are then screened for improved enantioselectivity using high-throughput screening.⁹⁶ The improved mutant from the first round of mutagenesis is the starting point for the next round of evolution and the whole process is repeated until a suitable catalyst is obtained.

For example, Reetz and Jaeger used directed evolution to improve the enantioselectivity of *Pseudomonas aeruginosa* lipase (PAL) toward *p*-nitrophenyl 2-methyldecanoate (Scheme 1.14).⁹⁷ After four rounds of random mutagenesis by error-prone PCR and screening of approximately 8000 mutants, enantioselectivity increased from $E = 1.1$ to $E = 11$ in favour of the (*S*)-enantiomer. They further improved the enanti-

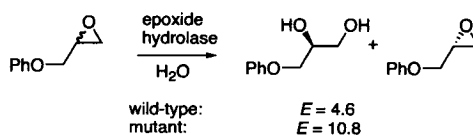
oselectivity to $E = 26$ by applying one round of saturation mutagenesis – mutation of one amino acid to all possible amino acids – at a key position, followed by another round of error-prone PCR.⁹⁸



Scheme 1.14. PAL-catalyzed hydrolysis of *p*-nitrophenyl ester of 2-methyldecanoic acid.

In another example, directed evolution was used to convert a D-hydantoinase into an L-hydantoinase.⁹⁹ After one round of error-prone PCR and screening of 10,000 clones, the enantioselectivity of D-hydantoinase toward D,L-5-(2-methylthioethyl)hydantoin was inverted from $E = 2.7$ in favour of the D-enantiomer to $E = 1.2$ in favour of the L-enantiomer.

Reetz and coworkers¹⁰⁰ used directed evolution with error-prone PCR to improve the enantioselectivity of epoxide hydrolase from *Aspergillus niger* toward glycidyl phenyl ether ($E_{wt} = 4.6$) (Scheme 1.15). They screened at least 20,000 mutants and found that ca. 20% had activity with their pretest. The active mutants were then screened using an ESI-MS-based ee assay with a deuterated pseudo-enantiomer.¹⁰¹ Their best mutant showed a moderate two-fold increase in enantioselectivity ($E = 10.8$). Sequence analysis revealed three amino acid exchanges – two amino acids being far from the active site (K332E and A390E), while one was somewhat closer (A217V; ca. 9 Å from active site). The researchers proposed the larger side-chain of valine disfavors the slow-reacting (*R*)-enantiomer due to steric interaction. The small increase in enantioselectivity is not surprising considering all mutations were relatively far from the active site (ca. 10 Å or greater).



Scheme 1.15. Directed evolution to improve the enantioselectivity of *Aspergillus niger* epoxide hydrolase toward glycidyl phenyl ether.

Directed evolution is an ideal strategy when little is known about the enzyme structure and function. However, one requires a rapid and efficient screening assay to effectively screen large mutant libraries. As well, depending on the experimental design, there may be a bias for distant, less-effective mutations.¹⁰²

1.9 New targets for hydrolase-catalyzed kinetic resolution

For biocatalysis to remain relevant, we must identify new targets and develop new routes for their preparation. Although strategies exist for hydrolase-catalyzed resolution of secondary alcohols, amines and carboxylic acids, there are few strategies for resolution of chiral heteroatoms, such as sulfinamides, and sterically hindered substrates such as tertiary alcohols. Both, as you will discover, are important compounds for organic synthesis.

1.9.1 Chiral sulfur compounds – sulfinamides

Sulfur forms a variety of organic compounds showing different structural and stereochemical properties.¹⁰³ Organosulfur with three different ligands and a lone pair form a distorted tetrahedron that is chiral and configurationally stable.¹⁰⁴ Many chiral sulfur compounds of this class are derived from sulfinic acid, which is not chiral because of rapid proton exchange. Sulfinic acid derivatives include sulfinates, thiosulfinates, sulfoxides, sulfinamides and sulfinimines (Figure 1.24).

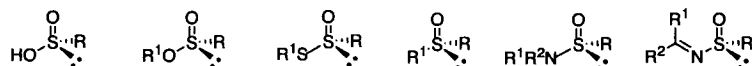


Figure 1.24. Sulfinic acid and its derivatives. Sulfinic acid, sulfinate, thiosulfinates, sulfoxide, sulfinamide and sulfinimine.

Chiral sulfinyl-containing compounds are useful chiral auxiliaries.¹⁰⁵ For example, chiral sulfoxides direct the formation of carbon-carbon bonds,^{106,107} including electrophilic additions to anions at the α - or β -position, nucleophilic addition to the C=C bond of vinyl sulfoxides or carbonyl to the sulfoxide, radical reactions at the α -carbon, and Diels-Alder reactions of vinyl sulfoxides.

Two classes of enantioselective syntheses are the best current routes to enantiomerically pure sulfinyl compounds:¹⁰⁸ stereospecific displacements at sulfites, sulfinates and related compounds with established chirality and enantioselective oxidations at sulfur. Stereospecific displacements of menthol from menthyl-*p*-toluenesulfinate remain the most common synthetic methods because the starting material is easily prepared.¹⁰⁹ However, there are alternate starting materials that can yield sulfoxides after one or two displacements at sulfur stereocentre.¹¹⁰ Examples of enantioselective oxidations of sulfides that yield sulfoxides with high enantiopurity include oxidation with modified Sharpless reagent,¹¹¹ chiral oxaziridines,¹¹² peroxidases¹¹³ and microorganisms.¹¹⁴

Another route to enantiomerically pure sulfinyl compounds is resolution. The most successful resolutions use hydrolase-catalyzed reactions. Researchers have resolved sulfoxides by hydrolyzing pendant ester groups. Ohta *et al.*¹¹⁵ resolved sulfinylacetates and sulfinylpropanoates by microbe-catalyzed hydrolysis. Burgess *et al.*¹¹⁶ resolved these compounds using a *Pseudomonas* species lipase. Cardellicchio *et al.*¹¹⁷ resolved methyl (*Z*)-3-arylsulfinylpropenoates with CRL or α -chymotrypsin. Allenmark and Andersson¹¹⁸ resolved a series of 2-(alkylsulfinyl)benzoates with CRL, while Serreqi and Kazlauskas¹¹⁹ used cholesterol esterase (CE) to resolve 2-(methylsulfinyl)phenyl acetate (Figure 1.25). Indeed, hydrolase-catalyzed resolution of sulfinyl compounds is a useful strategy to prepare enantiopure compounds.

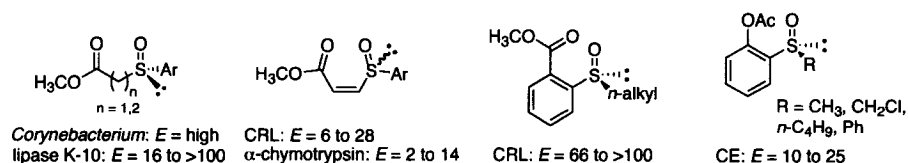
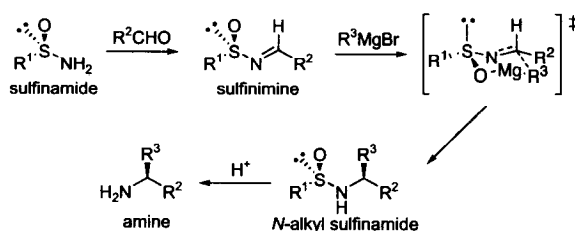


Figure 1.25. Hydrolase-catalyzed resolution of sulfoxides with pendant acyl groups. Example one from Burgess *et al.*¹¹⁶ Example two from Cardellicchio *et al.*¹¹⁷ Example three from Allenmark and Andersson.¹¹⁸ Example four from Serreqi and Kazlauskas.¹¹⁹

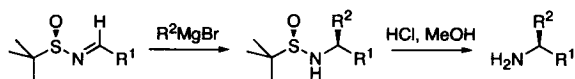
An important class of chiral sulfinyl reagents is the sulfinamides.¹²⁰ While chiral sulfoxides have long been employed for stereoselective carbon-carbon bond-forming reactions, the sulfinamides are only recently being used as versatile nitrogen intermediates for the preparation of chiral amines and derivatives.¹²¹ When a sulfinamide is condensed

with an aldehyde or ketone to give the sulfinimine, the sulfinyl group directs nucleophilic addition across the C=N bond. Nucleophilic addition proceeds through a six-membered ring Zimmerman-Traxler-type transition state with the metal coordinated to the oxygen of the sulfinyl group.¹²² In this transition state the bulky alkyl or aryl group occupies the less hindered equatorial position resulting in preferential attack from the same face for all additions. This yields the *N*-alkyl sulfinamide, which upon hydrolysis of the S-N link yields an enantiopure amine (Scheme 1.16).



Scheme 1.16. Synthesis of enantiopure amines from sulfinamides and the proposed transition state for nucleophilic addition.

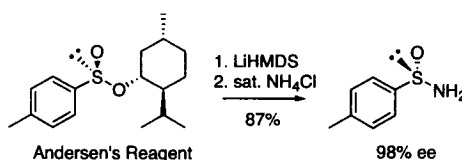
Enantioselective syntheses using sulfinimines derived from sulfinamides include preparations of amines,¹²³ α -¹²⁴ and β -amino acids,¹²⁵ amino alcohols,¹²⁶ aziridines¹²⁷ and amino phosphonic acids.¹²⁸ For example, Ellman applied *tert*-butylsulfinimine to the asymmetric synthesis of α -branched amines. Nucleophilic addition of Grignard reagents to the sulfinimine proceeded with high yield and diastereoselectivity and removal of the sulfinyl auxiliary with mild acid gave the enantiopure amine (Scheme 1.17).¹²³



Scheme 1.17. Synthesis of enantiopure amines from *tert*-butylsulfinimine.

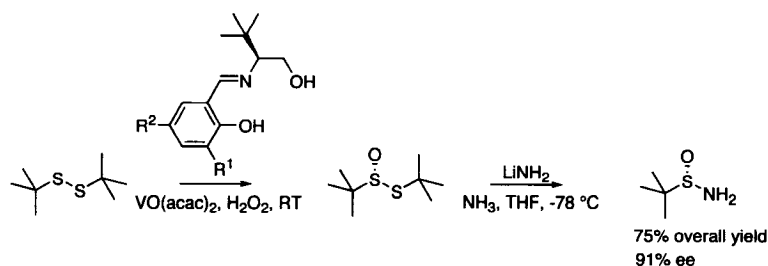
Enantiopure sulfinimines are useful for preparation of α - and β -amino acids. Nucleophilic addition of ethyl(alkoxy)aluminum cyanide to *p*-toluenesulfinimine, followed by hydrolysis of the sulfinyl moiety and the cyano group gave the enantiopure α -amino acid (Scheme 1.18a).¹²⁴ Titanium enolate addition to sulfinimines proceeded with high yield and diastereoselectivity. Hydrolysis of the *tert*-butylsulfinyl group gave the enantiopure β -amino acid (Scheme 1.18b).¹²⁵

preparation of Andersen's reagent relies on the crystallization of diastereomers epimeric at sulfur, and only *p*-toluenesulfinate and close analogues efficiently crystallize as the menthyl derivative.¹²⁹ Thus, this route is limited to *p*-toluenesulfinamide and close analogues.



Scheme 1.21. Synthesis of enantiopure *p*-toluenesulfinamide from menthyl-*p*-toluenesulfinate.

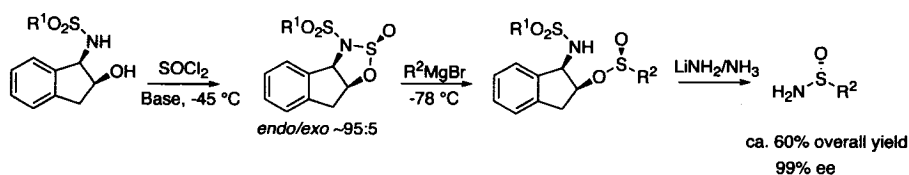
Ellman and co-workers¹³¹ developed a route to enantiopure *tert*-butylsulfinamide via enantioselective oxidation of *tert*-butyldisulfide (Scheme 1.22). Oxidation using H_2O_2 as stoichiometric oxidant in the presence of $\text{VO}(\text{acac})_2$ and a chiral Schiff base ligand gave chiral *tert*-butylthiosulfinate. Displacement by lithium amide in liquid ammonia yields enantiopure *tert*-butylsulfinamide. Their strategy relies on the high selectivity exhibited only with *tert*-butyldisulfide and the stability of the oxidation product, *tert*-butylthiosulfinate, to racemization and is thus limited to *tert*-butylsulfinamide.



Scheme 1.22. Enantioselective oxidation of *tert*-butyldisulfide to give enantiopure *tert*-butylsulfinamide.

Recently, Senanayake and co-workers¹³² described a double displacement route to a variety of enantiopure sulfinamides from *N*-sulfonyl-1,2,3-oxathiazolidine-2-oxide intermediates (Scheme 1.23). Preparation of *endo*-1,2,3-oxathiazolidine-2-oxide from *N*-sulfonyl indanol and thionyl chloride, followed by nucleophilic displacement with a

Grignard reagent and treatment with lithium amide in liquid ammonia gave enantiopure alkyl and aryl sulfinamides. This route yields a variety of novel sulfinamides, but includes complicated steps requiring low temperatures and moisture- and air-sensitive reagents.



Scheme 1.23. Synthesis of enantiopure sulfinamides from *endo*-1,2,3-oxathiazolidine-2-oxide derived from *N*-sulfonyl indanol.

The importance of these useful chiral auxiliaries warrants design of new routes for their preparation. Kinetic resolution of racemic sulfinamides may be a viable strategy for preparation of enantiopure sulfinamides.

1.9.2 Sterically hindered substrates – tertiary alcohols

Tertiary alcohols and their esters are an important class of compounds, which are found in numerous natural products (e.g., linalool, which is a flavour compound) and are also a useful group of building blocks (e.g., 3-methylpent-1-yn-3-ol and 2-phenylbut-3-yn-2-ol) (Figure 1.26).^{133,134,135,136}

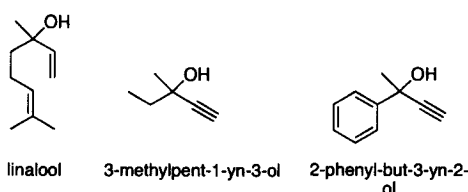
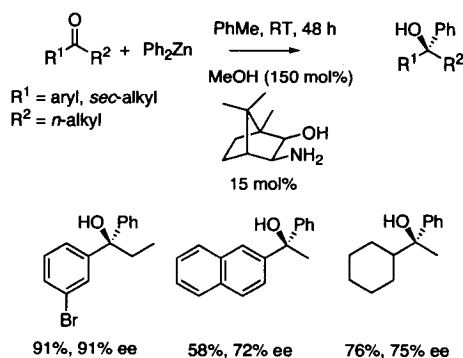


Figure 1.26. Tertiary alcohols.

The preparation of chiral tertiary alcohols is a challenge in synthetic organic chemistry because there are few synthetic methods that offer a general strategy. The simplest approach for the preparation of chiral tertiary alcohols is the enantioselective addition of an organometallic reagent to a ketone.¹³⁷ Although there are several examples of the addition of organolithium¹³⁸ and Grignard reagents¹³⁹ to ketones, at least one equiva-

lent of a chiral ligand is required. To reduce the amount of chiral ligand, an organometallic reagent with lower nucleophilic character is usually considered. Organozinc reagents are the ideal candidates for this reaction since their nucleophilic character is very low. This behavior has permitted the development of a plethora of chiral promoters¹⁴⁰ such as amino alcohols, diols and disulfonamides. In this way, the catalyzed enantioselective addition of organozinc reagents to aldehydes has been achieved with excellent enantioselectivity. However, enantioselective addition to ketones is more difficult. Ketones are less reactive electrophiles than aldehydes and the addition does not take place even when promoters are used and the reaction is conducted at high temperatures.¹⁴¹ This was the status until Dosa and Fu¹⁴² reported the catalytic enantioselective addition of diphenylzinc to ketones promoted by 3-*exo*-(dimethylamino)isoborneol in the presence of methanol to yield the corresponding chiral benzyl alcohols with reasonable enantioselectivity (Scheme 1.24). Since then, variations of this strategy have been used to facilitate enantioselective addition of alkyl and alkynyl groups to ketones.¹⁴³ However, a large excess of organozinc reagent, 10-20 mol% of chiral promoter and long reaction times are required and most importantly, enantioselectivities are generally moderate.



Scheme 1.24. Phenylation of ketones using enantioselective organozinc reagents.

The kinetic resolution of racemic esters using hydrolytic enzymes is a well-established protocol for the synthesis of secondary and chiral primary alcohols and carboxylic acids.²² Resolutions of more highly substituted tertiary systems are limited although a number of examples of α,α -disubstituted carboxylic acid esters¹⁴⁴ and α -fluorinated malonate diesters¹⁴⁵ have been successfully resolved using a variety of differ-

ent hydrolases. Substituted *N*-acylamino acids have also been hydrolytically cleaved using acylases to generate α -substituted amino acids¹⁴⁶ (Figure 1.27).

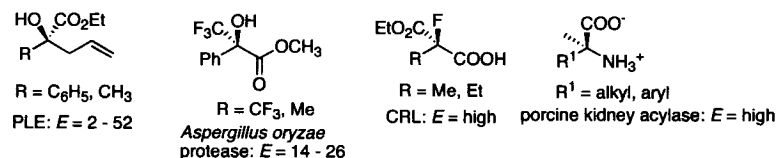


Figure 1.27. Resolution of highly substituted compounds. Example one from Moorlag *et al.*^{144d} Example two from Feichter *et al.*^{144e} Example three from Kitazume *et al.*¹⁴⁵ Example four from Chenault *et al.*^{146a}

Examples of the resolution of tertiary alcohol esters are rare. One attempt to resolve tertiary alcohols was reaction at a less-hindered remote site (Figure 1.28). For example, oxalate¹⁴⁷ or alkoxymethyl alkanoates¹⁴⁸ moved the reactive carbonyl two bonds further away from the tertiary alcohol stereocentre. Unfortunately, the enantioselectivity was low, likely because the stereocentre is far from the reactive carbonyl. Another approach was to react at a nearly primary alcohol reaction site.¹⁴⁹ The enantioselectivity was much better, but this approach is restricted to special substrates.

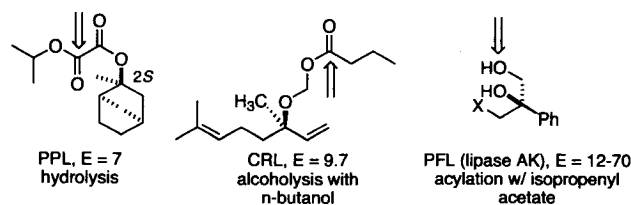


Figure 1.28. Resolution of tertiary alcohol stereocentres by hydrolysis at a less-hindered remote site. Example one from Brackenridge *et al.*¹⁴⁷ Example two from Franssen *et al.*¹⁴⁸ Example three from Chen *et al.*¹⁴⁹

Another attempt was to screen for enzymes that can accept hindered alcohols as substrates, but the enantioselectivities were low and the substrate range was limited (Figure 1.29). For example, *Pichia miso* IAM 4682 resolved 1-cyano-1-methylalkyl and alkenyl acetates,¹⁵⁰ CRL^{133,151} resolved several tertiary acetylenic acetate esters with low to moderate enantioselectivity and several lipases resolved 1-bicyclo[4.1.0]-heptyl acetate

and chloroacetate with moderate enantioselectivity.¹⁵² Various lipases and esterases catalyzed the hydrolysis of linalyl acetate and methyl-1-pentyn-1-yl acetate, but with low enantioselectivity.¹⁵³ The only practical resolution is *Candida antarctica* lipase A (CALA)-catalyzed resolution 2-phenylbut-3-yn-2-ol.¹³⁵

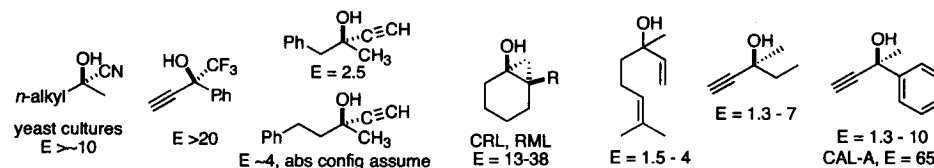


Figure 1.29. Screening identified hydrolases that resolve tertiary alcohol stereocentres: cyanohydrin acetates;¹⁵⁰ acetylenic acetates;^{133,151} bicyclic derivatives;¹⁵² linalyl acetate, methyl-1-pentyn-1-yl acetate and 2-phenyl-3-butyn-2-yl acetate.^{135,153}

O'Hagen and Zaidi¹³³ proposed a model rationalizing the enantioselectivity of CRL toward α -acetylenic tertiary alcohols (Figure 1.30). They noted that replacement of the acetylene functionality with methyl, vinyl or nitrile resulted in compounds that did not react with lipase and that the *R*-selectivity was consistent with CRL selectivity toward secondary alcohols. From this they deduced that acetylene must occupy the same space in the active site as the α -hydrogen in secondary alcohols and the favoured enantiomer will have the shape shown in Figure 1.30.

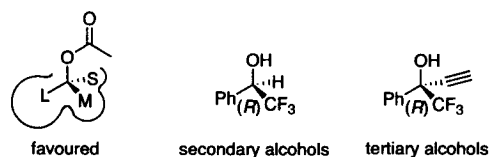


Figure 1.30. Model rationalizing the enantioselectivity of lipases toward tertiary acetylenic alcohols. The small site 'S' accepts only hydrogen and acetylene; the medium site 'M' accommodates CF_3 or methyl; and the large site 'L' accepts a wide variety of substituents.

Henke and coworkers¹⁵³ showed that lipases possessing a GGGX motif, such as CRL, in their active sites catalyze hydrolysis of tertiary alcohol esters. X-ray structures show that this GGGX sequence motif creates a larger binding site for the alcohol moiety.

They propose that this flexible loop allows binding of a third substituent. Molecular modelling with a *Bacillus* species esterase, which possesses this flexible GGGX loop, suggests the acetylene binds in the medium-sized binding site, while the methyl group occupies a small binding site and the large substituent occupies a large hydrophobic gorge. Steric hindrance between the phenyl group of the slow-reacting (*S*)-enantiomer and residues in the small binding site favour reaction of the (*R*)-enantiomer. However, the enantioselectivity was low ($E = 3$). Recent unpublished work suggests that the GGGX motif may be only part of the story because adding this motif to an esterase by site-directed mutagenesis did not enable it to hydrolyze esters of tertiary alcohols. Thus, researchers have not found a good route for resolving tertiary alcohols.

1.10 Using protease structure to design new enantioselective reactions – thesis outline

For typical lipase substrates, proteases, such as subtilisin, generally show low reactivity and enantioselectivity. We show structure-based substrate design can increase the reactivity and enantioselectivity of subtilisin and other proteases.

The active site of subtilisin is on its surface and binds substrate in an extended conformation. Subtilisin has a large nonpolar pocket (the S_1 pocket) to bind acyl group and a shallow crevice (the S_1' pocket) to bind one substituent of a secondary alcohol group, while the other substituent remains in solvent. We hypothesized that proteases would be highly reactive if the acyl group anchored the substrate to the active site and highly enantioselective if there was a large hydrophobicity difference between alcohol substituents (Figure 1.31).

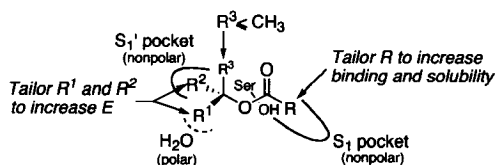


Figure 1.31. Schematic of how an ester binds to the active site of subtilisin. We show the R group can be tailored to increase binding and solubility; the hydrophobicity difference between the R^1 and R^2 groups can be tailored to increase enantioselectivity; and proteases can be highly reactive toward tertiary alcohols when the R^3 group is methyl or smaller.

To test our hypothesis, we show that an anchoring acyl group extends subtilisin E to a new class of substrates, *N*-acyl sulfinamides. Subtilisin E did not catalyze hydrolysis of *N*-acetyl arylsulfinamides, but did catalyze a highly enantioselective hydrolysis of *N*-dihydrocinnamoyl arylsulfinamides. The *N*-dihydrocinnamoyl group mimics phenylalanine and thus binds the sulfinamide to the active site. Further, we show that the enantio-preference of subtilisin toward sulfinamides is based on a favourable hydrophobic interaction with active site residues

Next, we show subtilisin enantioselectivity toward secondary alcohols and related substrates stems from a favourable hydrophobic interaction between nonpolar substituent and S₁' pocket residues and favourable solvation of polar substituent in water. The enantioselectivity of a series of secondary alcohols in water varied linearly with the difference in hydrophobicity ($\log P/P_0$) of the substituents. The larger the $\log P/P_0$ difference the higher the enantioselectivity. Based on our results, we proposed a new structure-based model for predicting the enantiopreference of subtilisin toward secondary alcohol esters and related substrates.

We then use 3-(3-pyridyl)propionate as anchoring acyl group to increase the reaction rate of subtilisin and α -chymotrypsin by up to six hundred-fold versus acetate and allow separation of substrate and product via mild acid extraction. We use this group to resolve multi-gram quantities of three important compounds and isolate the enantiomers without the use of chromatography.

Next, we use different anchoring acyl groups to extend several proteases to tertiary alcohol esters. We show that a *syn*-pentane-like interaction destabilizes the transition state for reaction of tertiary alcohols, but that the addition of an anchor group that binds substrate to the protease stabilizes transition state and enables proteases to catalyze hydrolysis of tertiary alcohol esters. We then rationalize this hypothesis using molecular modelling and propose strategies to increase the enantioselectivity of these new reactions.

Last, we use our anchor group strategy to decrease the activity of chromogenic reference compounds for Quick E. Our slower reacting reference compounds can measure high *E* values because we can add more enzyme and/or extend measurement time to determine reaction rates of slow reacting enantiomeric substrates.

References

- ¹ Sarfati, J. *Tech. J.* **1998**, *12*, 263-266.
- ² Brown, C. *Chirality in Drug Design and Synthesis*; Academic Press: London, 1990, chap. 1.
- ³ Geneve, J.; Hayat-Bonan, B.; Labbe, G.; DeGott, C.; Letteron, P.; Freneaux, E.; Le Dinh, T.; Larrey, D.; Pessayre, D. *J. Pharmacol. Exp. Ther.* **1987**, *242*, 1133-1137.
- ⁴ Breuer, M.; Ditrich, K.; Habicher, T.; Hauer, B.; Keßeler, M.; Stürmer, R.; Zelinski, T. *Angew. Chem. Int. Ed.* **2004**, *43*, 788-824.
- ⁵ FDA's policy statement for the development of new stereoisomer drugs *Chirality* **1992**, *4*, 338-340.
- ⁶ Ho, T.-L. *Enantioselective Synthesis: Natural Products from Chiral Terpenes*; Wiley: New York, 1992; chap. 1.
- ⁷ Lakshmi, R.; Bateman, T. D.; McIntosh, M. C. *J. Org. Chem.* **2005**, *70*, 5313-5315.
- ⁸ *Asymmetric Synthesis, Vols. 1-5*; Morrison, J. D., Ed.; Academic Press: Orlando, 1983-1985.
- ⁹ *Comprehensive Asymmetric Catalysis, Vols. I-III*; Jacobsen, E. N.; Pfaltz, A.; Yamamoto, H., Eds.; Springer: New York, 1999.
- ¹⁰ O'Donnell, M. J.; Drew, M. D.; Cooper, J. T.; Delgado, F.; Zhou, C. *J. Am. Chem. Soc.* **2002**, *124*, 9348-9349.
- ¹¹ Pasteur, L. *Compt. Rend. Acad. Sci.* **1849**, *29*, 297-300.
- ¹² Martin, V. S.; Woodard, S. S.; Katsuki, T.; Yamada, Y.; Ikeda, M.; Sharpless, K. B. *J. Am. Chem. Soc.* **1981**, *103*, 6237-6240.
- ¹³ Ladner, W. E.; Whitesides, G. M. *J. Am. Chem. Soc.* **1984**, *106*, 7250-7251.
- ¹⁴ Sheldon, R. A. In *Speciality Chemicals*, Elsevier, London, 1991.
- ¹⁵ Larsson, A. L. E.; Persson, B. A.; Bäckvall, J.-E. *Angew. Chem. Int. Ed.* **1997**, *36*, 1211-1212.
- ¹⁶ Persson, B. A.; Larsson, A. L. E.; Le Ray, M.; Bäckvall, J.-E. *J. Am. Chem. Soc.* **1999**, *121*, 1645-1650.

- ¹⁷ Choi, J. H.; Kim, Y. H.; Nam, S. H.; Shin, S. T.; Kim, M.-J.; Park, J. *Angew. Chem. Int. Ed.* **2002**, *41*, 2372-2376.
- ¹⁸ Choi, J. H.; Choi, Y. K.; Kim, Y. H.; Park, K. E.; Kim, E. J.; Kim, M.-J.; Park, J. *J. Org. Chem.* **2004**, *69*, 1972-1977.
- ¹⁹ Kim, M. -J.; Chung, Y. I.; Choi, Y. K.; Lee, H. K.; Kim, D.; Park, J. *J. Am. Chem. Soc.* **2003**, *125*, 11494-11495.
- ²⁰ Kim, N.; Ko, S.-B.; Kwon, M. S.; Kim, M.-J.; Park, J. *Org. Lett.* **2005**, *7*, 4523-4526.
- ²¹ Faber, K. *Biotransformations in Organic Chemistry*, 3rd edition; Springer-Verlag: Berlin, 1995; chap. 1 and 2.
- ²² Bornscheuer, U. T.; Kazlauskas, R. J. *Hydrolases in Organic Synthesis*; Wiley-VCH: Weinheim, 1999; pp. 1-31, 65-129 and 178-193.
- ²³ Blow, D. M.; Birktoft, J. J.; Hartley, B. S. *Nature*, **1969**, *221*, 337-340.
- ²⁴ Cygler, M.; Grochulski, P.; Kazlauskas, R. J.; Schrag, J. D.; Bouthillier, F.; Rubin, B.; Serreqi, A. N.; Gupta, A. K. *J. Am. Chem. Soc.* **1994**, *116*, 3180-3186.
- ²⁵ Jones, J. B.; Beck, J. F. In *Applications of Biochemical Systems in Organic Chemistry*, Jones, J. B.; Sih, C. J.; Perlman, D., eds.; Wiley, New York, part I, pp 107-401.
- ²⁶ Fersht, A. *Structure and Mechanism in Protein Science*; W. H. Freeman and Co.: New York, 1999; chap. 2,3, 11 and 12.
- ²⁷ Pauling, L. *Chem. Eng. News.* **1946**, *24*, 1375-1380.
- ²⁸ Miller, B. G.; Snider, M. J.; Short, S. A.; Wolfenden, R. *Biochemistry* **2000**, *39*, 8113-8118.
- ²⁹ Whitty, A.; Fierke, C. A.; Jencks, W. P. *Biochemistry* **1995**, *34*, 11678-11689.
- ³⁰ Perham, R. N.; Jones, D. D.; Chauhan, H. J.; Howard, M. J. *Biochem. Soc. Trans.* **2002**, *30*, 47-51.
- ³¹ Jencks, W. P. *Adv. Enzymol. Relat. Areas Mol. Biol.* **1975**, *43*, 219-410.
- ³² Menger, F. M. *Biochemistry* **1992**, *31*, 5368-5373.
- ³³ Cannon, W. R.; Singleton, S. F.; Benkovic, S. J. *Nature Struct. Biol.* **1996**, *3*, 821-833.
- ³⁴ (a) Braunegg, G.; de Raadt, A.; Feichtenhofer, S.; Griengl, H.; Kopper, I.; Lehman, A.; Weber, H.-J. *Angew. Chem. Int. Ed.* **1999**, *38*, 2763-2766. (b) de Raadt, A.; Griengl, H.; Weber, H. *Chem. Eur. J.* **2001**, *7*, 27-31.

- ³⁵ Münzer, D. F.; Meinhold, P.; Peters, M. W.; Feichtenhofer, S.; Griengl, H.; Arnold, F. H.; Glieder, A.; de Raadt, A. *Chem. Commun.* **2005**, 2597-2599.
- ³⁶ Fonken, G. S.; Herr, M. E.; Murray, H. C.; Reineke, L. M. *J. Am. Chem. Soc.* **1967**, *89*, 672-675.
- ³⁷ (a) Pietz, S.; Fröhlich, R.; Haufe, G.; *Tetrahedron* **1997**, *53*, 17055-17066. (b) Pietz, S.; Fröhlich, R.; Haufe, G.; *Tetrahedron* **1997**, *53*, 17067-17078. (c) Haufe, G.; Wölker, D.; Fröhlich, R. *J. Org. Chem.* **2002**, *67*, 3022-3028.
- ³⁸ Lin, Y. Y.; Palmer, D. N.; Jones, J. B. *Can. J. Chem.* **1974**, *52*, 469-476.
- ³⁹ Hein, G. E.; Niemann, C. *J. Am. Chem. Soc.* **1962**, *84*, 4487-4494.
- ⁴⁰ Chen, C.-S.; Fujimoto, Y.; Girdaukas, G.; Sih, C. J. *J. Am. Chem. Soc.* **1982**, *104*, 7294-7299.
- ⁴¹ Faber, K.; Hönig, H.; Kleewein, A. In *Preparative Biotransformations*; Roberts, S. M., Ed.; Wiley: New York, 1995; pp. 0:075-0:076.
- ⁴² Ollis, D. L.; Cheah, E.; Cygler, M.; Dijkstra, B.; Frolow, F.; Franken, S. M.; Harel, M.; Remington, S. J.; Silman, I.; Schrage, J.; Sussman, J. L.; Verschueren, K. H. G.; Goldman, A. *Protein Eng.* **1992**, *5*, 197-211.
- ⁴³ Luic, M.; Tomic, S.; Lescic, I.; Ljubovic, E.; Sepac, D.; Sunjic, V.; Vitale, L.; Saenger, W.; Kojic-Prodic, B. *Eur. J. Biochem.* **2001**, *268*, 3964-3973.
- ⁴⁴ Lavandera, I.; Fernández, S.; Magdalena, J.; Ferrero, M.; Grewal, H.; Savile, C. K.; Kazlauskas, R. J.; Gotor, V. *ChemBioChem* **2006**, *7*, 693-698.
- ⁴⁵ Verger, R. *Trends in Biotechnology* **1997**, *15*, 32-38.
- ⁴⁶ Rubin, B. *Nat. Struct. Biol.* **1994**, *1*, 568-572.
- ⁴⁷ (a) Ikemura, H.; Takagi, H.; Inouye, M. *J. Biol. Chem.* **1987**, *262*, 7859-7864. (b) Jain, S. C.; Shinde, U.; Li, Y.; Inouye, M.; Berman, H. M. *J. Mol. Biol.* **1998**, *284*, 137-144.
- ⁴⁸ Alexander, P. A.; Ruan, B.; Bryan, P. N. *Biochemistry* **2001**, *40*, 10634-10639.
- ⁴⁹ Branden, C.; Tooze, J. *Introduction to Protein Structure*; Garland: New York, 1991; chap. 15.
- ⁵⁰ Kazlauskas, R. J.; Weissfloch, A. N. E. *J. Mol. Catal. B: Enz.* **1997**, *3*, 65-72.
- ⁵¹ Schechter, I.; Berger, A. *Biochem. Biophys. Res. Commun.* **1967**, *27*, 157-162.
- ⁵² Tyndall, J. D. A.; Nall, T.; Fairlie, D. P. *Chem. Rev.* **2005**, *105*, 973-999.

- ⁵³ Bode, W.; Papamokos, E.; Musil, D.; Seemueller, U.; Fritz, H. *EMBO J.* **1986**, *5*, 813-818.
- ⁵⁴ (a) Estell, D. A.; Graycar, T. P.; Miller, J. V.; Powers, D. B.; Burnier, J. P.; Ng, P. G.; Wells, J. A. *Science* **1986**, *233*, 659-663. (b) Wells, J. A.; Powers, D. B.; Bott, R. R.; Graycar, T. P.; Estell, D. A. *Proc. Natl. Acad. Sci. USA* **1987**, *84*, 1219-1223.
- ⁵⁵ (a) Knowles, J. R. *J. Theor. Biol.* **1965**, *9*, 213-228. (b) Dorovskaya, V. N.; Varfolomeyev, S. D.; Kazanskaya, N. F.; Klyosov, A. A.; Martinek, K. *FEBS Lett.* **1972**, *23*, 122-124.
- ⁵⁶ Zaks, A.; Klibanov, A. M. *J. Am. Chem. Soc.* **1986**, *108*, 2767-2768.
- ⁵⁷ Bordusa, F. *Chem. Rev.* **2002**, *102*, 4817-4867.
- ⁵⁸ Muchmore, D. C. *US Patent*, US 5,215,918.
- ⁵⁹ Nishizawa, K.; Ohgami, Y.; Matsuo, N.; Kisida, H.; Hirohara, H. *J. Chem. Soc., Perkin Trans. 2* **1997**, 1293-1298.
- ⁶⁰ (a) Bonneau, P. R.; Graycar, T. P.; Estell, D. A.; Jones, J. B. *J. Am. Chem. Soc.* **1991**, *113*, 1026-1030. (b) Stein, R. L.; Strimpler, A. M.; Hori, H.; Powers, J. C. *Biochemistry* **1987**, *26*, 1301-1305.
- ⁶¹ Ogston, A. G. *Nature* **1948**, *162*, 963.
- ⁶² Mesecar, A. D.; Koshland, D. E. *Nature* **2000**, *403*, 614-615.
- ⁶³ Koshland, D. E. *Biochem. Mol. Biol. Edu.* **2002**, *30*, 27-29.
- ⁶⁴ Kazlauskas, R. J.; Weissfloch, A. N. E.; Rappaport, A. T.; Cuccia, L. A. *J. Org. Chem.* **1991**, *56*, 2656-2665.
- ⁶⁵ Uppenberg, J.; Öhrner, N.; Norin, M.; Hult, K.; Kleywegt, G. J.; Patkar, S.; Waagen, V.; Anthonsen, T.; Jones, T. A. *Biochemistry* **1995**, *34*, 16838-16851.
- ⁶⁶ Orrenius, C.; Öhrner, N.; Rotticci, D.; Mattson, A.; Hult, K.; Norin, T. *Tetrahedron: Asymmetry* **1995**, *6*, 1217-1220.
- ⁶⁷ Rotticci, D.; Haeffner, F.; Orrenius, C.; Norin, T.; Hult, K. *J. Mol. Catal. B.: Enz.* **1998**, *5*, 267-272.
- ⁶⁸ (a) Ema, T.; Kobayashi, J.; Maeno, S.; Sakai, T.; Utaka, M. *Bull. Chem. Soc. Jpn.* **1998**, *71*, 443-453. (b) Ema, T.; Jittani, M.; Furuie, K.; Utaka, M.; Sakai, T. *J. Org. Chem.* **2002**, *67*, 2144-2151.

- ⁶⁹ Deslongshamps, P. *Stereoelectronic Effects in Organic Chemistry*; Pergamon Press: Oxford, 1983.
- ⁷⁰ Rotticci, D. Orrenius, C.; Hult, K.; Norin, T. *Tetrahedron: Asymmetry* **1997**, *8*, 359-362.
- ⁷¹ Fitzpatrick, P.A.; Klivanov, A. M. *J. Am. Chem. Soc.* **1991**, *113*, 3166-3171.
- ⁷² Fitzpatrick, P. A.; ringe, D.; Klivanov, A. M. *Biotechnol. Bioeng.* **1992**, *40*, 735-742.
- ⁷³ Colombo, G.; Ottolina, G.; Carrea, G.; Bernardi, A.; Scolastico, C. *Tetrahedron: Asymmetry* **1998**, *9*, 1205-1214.
- ⁷⁴ (a) Ema, T.; Okada, R.; Fukumoto, M.; Jittani, M.; Ishida, M.; Furuie, K.; Yamaguchi, K.; Sakai, T.; Utaka, M. *Tet. Lett.* **1999**, *40*, 4367-4370. (b) Ema, T.; Yamaguchi, K.; Wakasa, Y.; Yabe, A.; Okada, R.; Fukumoto, M.; Yano, F.; Korenaga, T.; Utaka, M.; Sakai, T. *J. Mol. Catal. B: Enzymatic* **2003**, *22*, 181-192.
- ⁷⁵ Mugford, P. F.; Lait, S. M.; Keay, B. A.; Kazlauskas, R. J. *ChemBioChem* **2004**, *5*, 980-987.
- ⁷⁶ Kazlauskas, R. J. *Science* **2001**, *293*, 2277-2279.
- ⁷⁷ Rossi, K. A.; Merz, K. M.; Smith, G. M.; Baldwin, J. J. *J. Med. Chem.* **1995**, *38*, 2061-2069.
- ⁷⁸ Rotticci, D.; Rotticci-Mulder, J. C.; Denman, S.; Norin, T.; Hult, K. *ChemBioChem*. **2001**, *2*, 766-770.
- ⁷⁹ Borscheuer, U. T. *Curr. Opin. Biotechnol.* **2002**, *13*, 543-547.
- ⁸⁰ Henke, E.; Schister, S.; Yang, H.; Bornscheuer, U. T. *Chem. Month* **2000**, *131*, 633-638.
- ⁸¹ Ema, T.; Maeno, S.; Takaya, Y.; Sakai, T.; Utaka, M. *J. Org. Chem.* **1996**, *61*, 8610-8616.
- ⁸² Ottosson, J.; Hult, K. *J. Mol. Catal. B: Enz.* **2001**, *11*, 1025-1028.
- ⁸³ Pohl, T.; Waldmann, H. *Tetrahedron Lett.* **1995**, *36*, 2963-2966.
- ⁸⁴ Gupta, A. K.; Kazlauskas, R. J. *Tetrahedron: Asymmetry* **1993**, *4*, 879-888.
- ⁸⁵ (a) Fitzpatrick, P. A.; Steinmetz, A. C. U.; Ringe, D.; Klivanov, A. M. *Proc. Natl. Acad. Sci. U.S.A.* **1993**, *90*, 8653-8657. (b) Schmitke, J. L.; Stern, L. J.; Klivanov, A. M. *Proc. Natl. Acad. Sci. U.S.A.* **1997**, *94*, 4250-4255.

- ⁸⁶ Hirose, Y.; Kariya, K.; Sasaki, I.; Kurono, Y.; Ebiike, H.; Achiwa, K. *Tetrahedron Lett.* **1992**, *33*, 7157-7160.
- ⁸⁷ Bornscheuer, U.; Herar, A.; Kreye, L.; Wendel, V.; Capewell, A.; Meyer, H. H.; Scheper, T.; Kollis, F. N. *Tetrahedron: Asymmetry* **1993**, *4*, 1007-1016.
- ⁸⁸ Tawaki, S.; Klivanov, A. M. *J. Am. Chem. Soc.* **1992**, *114*, 1882-1884.
- ⁸⁹ Ottosson, J.; Fransson, L.; King, J. W.; Hult, K. *Biochim. Biophys. Acta* **2002**, *1594*, 325-334.
- ⁹⁰ Rink, R.; Lutje Spelberg, J. H.; Pieters, R. J.; Kingma, J.; Nardini, M.; Kellogg, R. M.; Dijkstra, B. W.; Janssen, D. B. *J. Am. Chem. Soc.* **1999**, *121*, 7417-7418.
- ⁹¹ Rink, R.; Fennema, M.; Smids, M.; Dehmel, U.; Janssen, D. B. *J. Biol. Chem.* **1997**, *272*, 14650-14657.
- ⁹² Lutje Spelberg, J. H.; Rink, R.; Kellogg, R. M.; Janssen, D. B. *Tetrahedron: Asymmetry* **1998**, *9*, 459-466.
- ⁹³ Magnusson, A. O.; Takwa, M.; Hamberg, A.; Hult, K. *Angew. Chem. Int. Ed.* **2005**, *44*, 4582-4585.
- ⁹⁴ Cadwell, R. C.; Joyce, G. F. *PCR Meth. Appl.* **1992**, *2*, 28-33.
- ⁹⁵ Stemmer, W. P. C. *Proc. Natl Acad. Sci. USA* **1994**, *91*, 10747-10751.
- ⁹⁶ Jaeger, K.-E.; Eggert, T. *Curr. Opin. Biotechnol.* **2004**, *15*, 305-313.
- ⁹⁷ Reetz, M. T.; Zonta, A.; Schimossek, K.; Liebeton, K.; Jaeger, K.-E. *Angew. Chem. Int. Ed. Engl.* **1997**, *36*, 2830-2832.
- ⁹⁸ Liebeton, K.; Zonta, A.; Schimossek, K.; Nardini, M.; Lang, D.; Dijkstra, B. W.; Reetz, M. T.; Jaeger, K.-E. *Chem. Biol.* **2000**, *7*, 709-718.
- ⁹⁹ May, O.; Nguyen, P. T.; Arnold, F. H. *Nat. Biotech.* **2000**, *18*, 317-320.
- ¹⁰⁰ Reetz, M. T.; Torre, C.; Eipper, A.; Lohmer, R.; Hermes, M.; Brunner, B.; Maichele, A.; Bocola, M.; Arand, M.; Cronin, A.; Genzel, Y.; Archelas, A.; Furstoss, R. *Org. Lett.* **2004**, *6*, 177-180.
- ¹⁰¹ Schrader, W.; Eipper, A.; Pugh, D. J.; Reetz, M. T. *Can. J. Chem.* **2002**, *80*, 626-632.
- ¹⁰² Morley, K. L.; Kazlauskas, R. J. *Trends Biotechnol.* **2005**, *23*, 231-237.
- ¹⁰³ Oae, S. *Organic Sulfur Chemistry: Structure and Mechanism*, CRC Press, Boca Raton, USA, 1991, chap. 3.

- ¹⁰⁴ Mikolajczk, M.; Drabowicz, J.; Kielbasinski, P. *Chiral Sulfur Reagents: Applications in Asymmetric and Stereoselective Synthesis*; CRC Press: New York, 1997; pp 1-5.
- ¹⁰⁵ K. K. Andersen. In *The Chemistry of Sulphones and Sulphoxides*. Patai, S.; Rappaport, Z.; Stirling, C. J. M., Eds.; Wiley: New York, 1988; pp. 55-94.
- ¹⁰⁶ Carreño, M. C. *Chem. Rev.* **1995**, *95*, 1717-1760.
- ¹⁰⁷ Fernández, I.; Khier, N. *Chem. Rev.* **2003**, *103*, 3651-3705.
- ¹⁰⁸ Kagan, H. B.; Rebiere, F. *Synlett* **1990**, 643-650.
- ¹⁰⁹ (a) Andersen, K. K. *Tetrahedron Lett.* **1962**, 93-95. (b) Drabowicz, J.; Bujinicki, B.; Mikolajczyk, M. *J. Org. Chem.* **1982**, *47*, 3325-3327. (c) Solladié, G. *Synthesis* **1981**, 185-196.
- ¹¹⁰ (a) Marino, J. P.; Bogdan, S. Kimura, K. *J. Am. Chem. Soc.* **1992**, *114*, 5566-5572. (b) Evans, D. A.; Faul, M. M.; Colombo, L.; Bisaha, J. J.; Clardy, J.; Cherry, D. *J. Am. Chem. Soc.* **1992**, *114*, 5977-5985. (c) Rebiere, F.; Samuel, O.; Ricard, L.; Kagan, H. B. *J. Org. Chem.* **1991**, *56*, 5991-5999.
- ¹¹¹ Di Furia, F.; Modena, G.; Seraglia, R. *Synthesis* **1984**, 325-326 (b) Pitchen, P.; Deshmukh, M.; Dunach, E.; Kagan, K. B. *J. Am. Chem. Soc.* **1984**, *106*, 8188-8193.
- ¹¹² Davis, F. A.; Reddy, R. T.; Han, W.; Carroll, P. J. *J. Am. Chem. Soc.* **1992**, *114*, 1428-1437.
- ¹¹³ (a) Colonna, S.; Gaggero, N.; Manfredi, A.; Casella, L.; Gullotti, M. Carrea, G.; Pasta, P. *Biochemistry* **1990**, *29*, 10465-10468. (b) Colonna, S.; Gaggero, N.; Casella, L.; Carrea, G.; Pasta, P. *Tetrahedron: Asymmetry* **1992**, *3*, 95-106. (c) van Deurzen, M. P. J.; van Rantwijk, F.; Sheldon, R. A. *Tetrahedron* **1997**, *39*, 13183-13220. (d) ten Brink, H. B.; Holland, H. L.; Shoemaker, H. E.; van Lingen, H.; Wever, R. *Tetrahedron: Asymmetry* **1999**, *10*, 4563-4572.
- ¹¹⁴ Holland, H. L. *Chem. Rev.* **1988**, *88*, 473-485.
- ¹¹⁵ Ohta, H.; Kata, Y.; Tsuchihashi, G. *Chem. Lett.* **1986**, 217.
- ¹¹⁶ (a) Burgess, K.; Henderson, I. *Tetrahedron Lett.* **1989**, *30*, 3633-3636. (b) Burgess, Henderson, I.; Ho, K.-K. *J. Org. Chem.* **1992**, *57*, 1290-1295.
- ¹¹⁷ Cardellicchio, C.; Naso, F.; Scilimati, A. *Tetrahedron Lett.* **1994**, *35*, 4635-
- ¹¹⁸ Allenmark, S. G.; Andersson, A. C. *Tetrahedron: Asymmetry* **1993**, *4*, 2371-2376.

- ¹¹⁹ Serreqi, A. N.; Kazlauskas, R. J. *Can. J. Chem.* **1995**, *73*, 1357-1367.
- ¹²⁰ Nudelman, A. In *The Chemistry of Sulphinic Acids, Esters and their Derivatives*; Patai, S., Ed.; John Wiley & Sons; New York, 1990; pp 35-85.
- ¹²¹ Davis, F. A.; Zhou, P.; Chen, B.-C. *Chem. Soc. Rev.* **1998**, *27*, 13-18.
- ¹²² (a) Davis, F. A.; Reddy, R. T.; Reddy, R. E. *J. Org. Chem.* **1992**, *57*, 6387-6389. (b) Cogan, D. A.; Liu, G.; Ellman, J. *Tetrahedron* **1999**, *55*, 8883-8904. (c) Tang, T. P.; Ellman, J. A. *J. Org. Chem.* **1999**, *64*, 12-13.
- ¹²³ Liu, G.; Cogan, D. A.; Ellman, J. A. *J. Am. Chem. Soc.* **1997**, *119*, 9913-9914.
- ¹²⁴ Davis, F. A.; Portonovo, P. S.; Reddy, R. E.; Chiu, Y. *J. Org. Chem.* **1996**, *61*, 440-441.
- ¹²⁵ Tang, T. P.; Ellman, J. A. *J. Org. Chem.* **1999**, *64*, 12-13.
- ¹²⁶ Kochi, T.; Tang, T. P.; Ellman, J. A. *J. Am. Chem. Soc.* **2002**, *124*, 6518-6519.
- ¹²⁷ Davis, F. A.; Zhou, P.; Reddy, G. V. *J. Org. Chem.* **1994**, *58*, 3243-3245.
- ¹²⁸ Lefebvre, I. M.; Evans, S. A. *J. Org. Chem.* **1997**, *62*, 7532-7535.
- ¹²⁹ (a) Anderson, K. K. In *The Chemistry of Sulphones and Sulfoxides*; Patai, S. Rappoport, Z.; Stirling, C. J. M., Eds.; John Wiley & Sons: New York, 1988; pp 55-94. (b) Phillips, H. *J. Chem. Soc.* **1925**, *127*, 2552-2587. (c) Hulce, M.; Mallamo, J. P.; Frye, L. L.; Kogan, T. P.; Posner, G. A. *Org. Synth.* **1986**, *64*, 196-206. (d) Drabowicz, J.; Kielbasinski, P.; Mikolajczyk, M. In *The Chemistry of Sulphones and Sulfoxides*; Patai, S. Rappoport, Z.; Stirling, C. J. M., Eds.; John Wiley & Sons: New York, 1988; Chapter 3, pp 233-378.
- ¹³⁰ Davis, F. A.; Reddy, R. T.; Reddy, R. E. *J. Org. Chem.* **1999**, *64*, 1403-1406.
- ¹³¹ (a) Liu, G.; Cogan, D. A.; Ellman, J. A. *J. Am. Chem. Soc.* **1997**, *119*, 9913-9914. (b) Cogan, D. A.; Liu, G.; Kim, K.; Backes, B. J.; Ellman, J. A. *J. Am. Chem. Soc.* **1998**, *120*, 8011-8019.
- ¹³² Han, Z.; Krishnamurthy, D.; Grover, P.; Fang, Q. K.; Senanayake, C. H. *J. Am. Chem. Soc.* **2002**, *124*, 7880-7881.
- ¹³³ O'Hagan, D.; Zaidi, N. A. *J. Chem. Soc., Perkin Trans. 1* **1992**, 947-949.
- ¹³⁴ O'Hagan, D.; Zaidi, N. A.; Lamont, R. B. *Tetrahedron: Asymmetry* **1993**, *4*, 1703-1708.

- ¹³⁵ Krishna, S. H.; Persson, M.; Bornscheuer, U. T. *Tetrahedron: Asymmetry* **2002**, *13*, 2693-2696.
- ¹³⁶ Pogorevc, M.; Strauss, U. T.; Hayn, M.; Faber, K. *Monatshefte für Chemie* **2000**, *131*, 639-644.
- ¹³⁷ (a) Yus, M.; Ramón, D. J. *Recent Res. Dev. Org. Chem.* **2002**, *6*, 297-378. (b) Ramón, D. J.; Yus, M. *Angew. Chem. Int. Ed.* **2004**, *43*, 284-287.
- ¹³⁸ (a) Thompson, A. S.; Corley, E. G.; Huntington, M. F.; Grobowski, E. J. J.; Remenar, J. F.; Collum, D. B. *J. Am. Chem. Soc.* **1998**, *120*, 2028-2038. (b) Thompson, A. S.; Corley, E. G.; Huntington, M. F.; Grobowski, E. J. J.; *Tetrahedron Lett.* **1995**, *36*, 8937-8940.
- ¹³⁹ Weber, B.; Seebach, D. *Angew. Chem. Int. Ed. Engl.* **1992**, *31*, 84-86.
- ¹⁴⁰ Pu, L.; Yu, H.-B. *Chem. Rev.* **2001**, *101*, 757-824.
- ¹⁴¹ Watanabe, M.; Soai, K. *J. Chem. Soc. Perkin Trans. 1* **1994**, 3125-3128.
- ¹⁴² Dosa, P. I.; Fu, G.C. *J. Am. Chem. Soc.* **1998**, *120*, 445-446.
- ¹⁴³ (a) Cozzi, P. G. *Angew. Chem. Int. Ed.* **2003**, *115*, 3001-3004. (b) Jiang, B.; Chen, Z.; Tang, X. *Org. Lett.* **2002**, *4*, 3451-3453. (c) Ramón, D. J.; Yus, M. *Tetrahedron Lett.* **1998**, *39*, 1239-1242. (d) DiMauro, E. F.; Kozlowski, M. C. *J. Am. Chem. Soc.* **2002**, *124*, 12668-12669.
- ¹⁴⁴ (a) Schneider, M.; Engel, N.; Boensmann, H. *Angew. Chem. Int. Ed. Engl.* **1984**, *23*, 66. (b) Sugai, T.; Kakeya, H.; Ohta, H. *J. Org. Chem.* **1990**, *55*, 4643-4647. (c) Pottie, M.; Van der Eycken, J.; Vandewalle, M.; Dewanckele, J. M.; Roper, H. *Tetrahedron Lett.* **1989**, *30*, 5319-5322. (d) Moorlag, H.; Kellogg, R. M.; Kloosterman, M.; Kaptein, B.; Kamphuis, J.; Shoemaker, H. E. *J. Org. Chem.* **1990**, *55*, 5878-5881. (e) Feichter, C.; Faber, K.; Griengl, H. *J. Chem. Soc., Perkin Trans. 1* **1991**, 653-654.
- ¹⁴⁵ Kitazume, T.; Sato, T.; Kobayashi, T.; Lin, J. T. *J. Org. Chem.* **1986**, *51*, 1003-1006.
- ¹⁴⁶ (a) Chenault, H. K.; Dahmer, J.; Whitesides, G. M. *J. Am. Chem. Soc.* **1989**, *111*, 6354-6364. (b) Keller, J. W.; Hamilton, B. J. *Tetrahedron Lett.* **1986**, 1249-1250.
- ¹⁴⁷ Brackenridge, I.; McCague, R.; Roberts, S. M.; Turner, N. J. *J. Chem. Soc., Perkin Trans. 1* **1993**, 1093-1094.
- ¹⁴⁸ Franssen, M. C. R.; Goetheer, E. L. V.; Jongejan, H. de Groot, A. *Tetrahedron Lett.* **1998**, *39*, 8345-9348.

- ¹⁴⁹ Chen, S. T., Fang, J. M. *J. Org. Chem.* **1997**, *62*, 4349-4357.
- ¹⁵⁰ Ohta, H., Kimura, Y., Sugano, Y., Sugai, T. *Tetrahedron* **1989**, *45*, 5469-5476.
- ¹⁵¹ O'Hagan, D.; Zaidi, N. A. *Tetrahedron: Asymmetry* **1994**, *5*, 1111-1118.
- ¹⁵² Barnier, J.-P.; Blanco, L.; Rousseau, G.; Guibé-Jampel, E.; Fresse, I. *J. Org. Chem.* **1993**, *58*, 1570-1574.
- ¹⁵³ (a) Henke, E.; Pleiss, J.; Bornscheuer, U. T. *Angew. Chem. Int. Ed.* **2002**, *41*, 3211-3213. (b) Henke, E.; Bornscheuer, U. T.; Schmid, R. D.; Pleiss, J. *ChemBioChem* **2003**, *4*, 485-493.

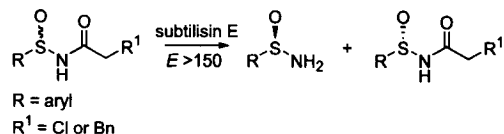
Chapter 2

For biocatalysis to remain relevant in organic chemistry, we must identify new targets and develop new routes for their preparation. In this chapter, we extend the protease subtilisin to a novel class of substrates, *N*-acyl arylsulfonamides, by using an acyl group that anchors substrate to the active site. We then use molecular modelling to identify the basis for the high reactivity and enantioselectivity. This new biocatalytic route is a simple, inexpensive strategy to these useful chiral auxiliaries.*

* This chapter is a copy of a published article and is reproduced with permission from the *Journal of the American Chemical Society*, Vol. 127, Christopher K. Savile, Vladimir P. Magloire and Romas J. Kazlauskas, "Subtilisin-Catalyzed Resolution of *N*-Acyl Arylsulfonamides", 2104-2113, Copyright 2005, American Chemical Society (see Appendix II for reprint).

Subtilisin-catalyzed resolution of *N*-acyl arylsulfinamides

Abstract

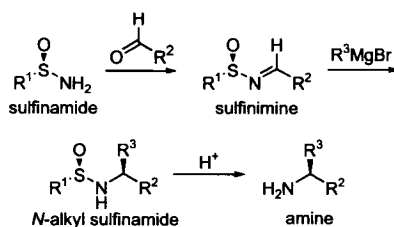


We report the first biocatalytic route to sulfinamides (R-S(O)-NH_2), whose sulfur stereocentre makes them important chiral auxiliaries for the asymmetric synthesis of amines. Subtilisin E did not catalyze hydrolysis of *N*-acetyl or *N*-butanoyl arylsulfinamides, but did catalyze a highly enantioselective ($E > 150$ favouring the (*R*)-enantiomer) hydrolysis of *N*-chloroacetyl- and *N*-dihydrocinnamoyl arylsulfinamides. Gram-scale resolutions using subtilisin E overexpressed in *B. subtilis* yielded, after recrystallization, three synthetically useful auxiliaries: (*R*)-*p*-toluenesulfinamide (42% yield, 95% ee), (*R*)-*p*-chlorobenzenesulfinamide (30% yield, 97% ee) and (*R*)-2,4,6-trimethylbenzenesulfinamide (30% yield, 99% ee). Molecular modelling suggests that the *N*-chloroacetyl and *N*-dihydrocinnamoyl groups mimic a phenylalanine moiety and thus bind the sulfinamide to the active site. Molecular modelling further suggests that enantioselectivity stems from a favourable hydrophobic interaction between the aryl group of the fast-reacting (*R*)-arylsulfinamide and the S_1' leaving group pocket in subtilisin E.

2.1 Introduction

The chiral sulfinyl group (R-S(O)-) is an important functional group for asymmetric synthesis because it effectively transfers chirality to a wide range of centres.¹⁻³ This efficacy stems from the steric and stereoelectronic differences between the substituents: a lone pair, an oxygen and an alkyl or aryl group. As well, the sulfinyl group is configurationally stable.²

Sulfinamides (R-S(O)-NH₂) are useful sulfinyl chiral auxiliaries for synthesis of amines, Scheme 2.1.^{4,5} When condensed with an aldehyde or ketone to give the sulfinimine, the *N*-sulfinyl group directs nucleophilic addition across the C=N bond. This yields the *N*-alkyl sulfinamide, which upon hydrolysis of the S-N link yields an amine. Enantioselective syntheses using sulfinimines include preparations of amines,⁶ α - and β -amino acids,⁵ amino alcohols,⁷ aziridines⁸ and amino phosphonic acids.⁹



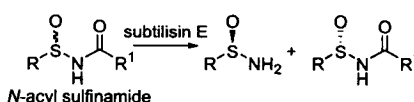
Scheme 2.1. Synthesis of enantiopure amines from sulfinamides.

The best route to enantiopure aryl sulfinyl moieties is via menthyl-*p*-toluenesulfonate (Andersen's reagent).^{2,10,11} Nucleophilic displacement of menthol at chiral sulfur leads to enantiopure arylsulfinyl compounds⁴ including *p*-toluenesulfinamide.¹² However, preparation of Andersen's reagent relies on the crystallization of diastereomers epimeric at sulfur and only *p*-toluenesulfonate and close analogs efficiently crystallize as the menthyl derivative.^{2,4,13} Thus, this route is limited to *p*-toluenesulfinamide and close analogs. Asymmetric oxidation using one equivalent of (+)- or (-)-*N*-(phenylsulfonyl)(3,3-dichlorocamphoryl)oxaziridine also yields enantiopure aryl sulfinyl moieties.¹⁴

The two other routes to enantiopure sulfinamides use either an enantioselective oxidation of *tert*-butyl disulfide^{6,15} or a double displacement using a chiral auxiliary derived from indanol.¹⁶ The enantioselective oxidation developed by Ellman and coworkers

relies on the stability of the oxidation product – thiosulfinate (*t*-Bu-S(O)-S-*t*-Bu) – to racemization and is thus limited to *tert*-butylsulfonamide. The double displacement route developed by Senanayake and coworkers uses *N*-sulfonyl-1,2,3-oxathiazolidine-2-oxide intermediates. This route yields a variety of enantiopure sulfonamides, but includes complicated steps requiring low temperatures and moisture- and air-sensitive reagents.

Many groups have reported biocatalytic routes to sulfinyl stereocentres, but not to sulfonamides. A direct biocatalytic route to sulfinyl compounds is oxidation. For example, enantioselective oxidation of unsymmetrical sulfides yields sulfoxides.^{11,17} These direct oxidation routes may not be suitable routes to sulfonamides because oxidation of unsubstituted sulfenamides (RSNH₂) can involve nitrene intermediates.¹⁸ Another biocatalytic route to enantiopure sulfinyl groups is lipase-catalyzed hydrolysis of a pendant ester group.¹⁹ Enantioselectivity can be high even when the stereocentre is remote from the reacting carbonyl. Ellman and coworkers tested the hydrolase-catalyzed acylation of the sulfonamide amino group, but did not observe any reaction.¹⁵ In this paper, we explore the reverse reaction – hydrolase-catalyzed hydrolysis of *N*-acyl sulfonamides, Scheme 2.2, and find that subtilisin E shows high enantioselectivity toward many arylsulfonamides. Further, molecular modelling suggests that the high enantioselectivity of subtilisin toward sulfonamides compared to the moderate enantioselectivity toward the isosteric secondary alcohols likely stems from the polar nature of the oxygen substituents in sulfonamides, Figure 2.1.

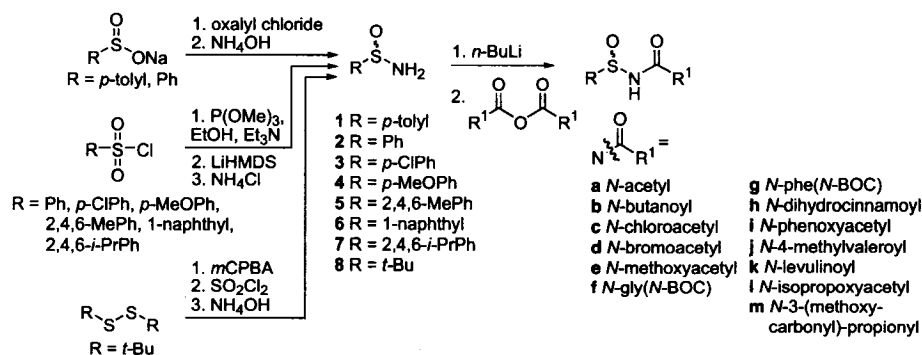


Scheme 2.2. Subtilisin-catalyzed kinetic resolution of sulfonamides.

2.2 Results

2.2.1 Synthesis of substrates

We prepared racemic sulfonamides **1–8** by one of three established routes, Scheme 2.3. The simplest route, from the corresponding sulfinic acid, yielded *p*-toluenesulfonamide **1** and benzenesulfonamide **2**. Treating the sulfinic acid with oxalyl chloride followed by ammonolysis yielded the sulfonamides in 56–59% yield.²⁰



Scheme 2.3. Synthesis of sulfinamides **1-8** and *N*-acylsulfinamides.

To prepare sulfinamides for which no sulfinic acid precursors were available – *p*-chlorobenzenesulfinamide **3**, *p*-methoxybenzenesulfinamide **4**, 2,4,6-trimethylbenzenesulfinamide **5**, 1-naphthylenesulfinamide **6** and 2,4,6-triisopropylbenzenesulfinamide **7** – we used the sulfonyl chlorides. Reduction of the sulfonyl chloride with $\text{P}(\text{OMe})_3$ in ethanol gave the respective sulfinate ethyl esters.²¹ Displacement of ethanol with lithium bis(trimethylsilyl)amide followed by desilylation gave the corresponding sulfinamides in 21-55% overall yield.²⁰

We prepared *tert*-butylsulfinamide **8** from *tert*-butyldisulfide in three steps. Oxidation of *tert*-butyldisulfide with 3-chloroperoxybenzoic acid followed by addition of sulfonyl chloride gave *tert*-butylsulfinyl chloride,²² which reacted with NH_4OH to give **8** in 21% overall yield.²⁰

To prepare *N*-acylsulfinamides **a-m**, we treated the appropriate sulfinamide with two equiv. of *n*-butyllithium in THF at -78°C followed by rapid addition of the necessary symmetrical carboxylic acid anhydride (15-90% yield).²⁰

2.2.2 Initial screening

Initial screening of the *N*-butanoyl derivative **1b** with fifty hydrolases revealed no active hydrolases, but screening the more reactive *N*-chloroacetyl derivative **1c** identified four moderately to highly active proteases, one lipase and one esterase (Table 2.1).²³ To determine enantioselectivities, we carried out small-scale reactions and measured the enantiomeric purity of the starting materials and products by HPLC using a column with a chiral stationary phase.

Table 2.1. Screening of hydrolases for enantioselective hydrolysis of **1c**

Hydrolases	wt ^a	%C _{app} ^b	ee _s % ^{c,d}	ee _p % ^{c,d}	E _{app} ^{d,e}	x(sp) ^f %	E _{true} ^{e,g}	enantio- preference ^h
<i>B. subtilis</i> var. biotectus A protease	16	50	92	93	90	3	>150	<i>R</i>
subtilisin E	n.d.	37 ⁱ	56	97	115	2	>150	<i>R</i>
subtilisin Carlsberg	34	56	82	64	n.d. ^j	n.d.	n.d. ^j	<i>R</i>
<i>A. oryzae</i> protease	90	56	88	68	14	3	17	<i>R</i>
<i>A. melleus</i> protease/acylase	250	29 ^k	30	75	9	10	29	<i>R</i>
<i>Candida antarctica</i> lipase A	137	14	11	65	5	3	6	<i>S</i>
bovine cholesterol esterase	80	29 ^k	27	67	7	10	11	<i>R</i>

^aWeight of enzyme in mg. ^b% Conversion: amount of sulfinamide formed in 6 h except where noted. ^c% Enantiomeric excess. Enantiomeric excess of substrate and product were determined by HPLC analysis on Daicel Chiralcel OD or AD columns at 238 nm or 222 nm. ^dee_p, ee_s and E_{app} (apparent enantioselectivity) are with no correction for chemical hydrolysis. n.d. = not determined. ^eEnantiomeric ratio: the enantiomeric ratio *E* measures the relative rate of hydrolysis of the fast enantiomer as compared to the slow enantiomer as defined by Sih (Chen, C.S.; Fujimoto, Y.; Girdaukas, G.; Sih, C.J. *J. Am. Chem. Soc.* **1982**, *104*, 7294.). ^fx(sp) refers to % spontaneous chemical hydrolysis. ^gE_{true} is the enantioselectivity corrected for chemical hydrolysis.²⁴ ^hThe absolute configuration was determined by comparison to authentic samples prepared by the method of Davis and coworkers.¹² ⁱReaction for 3 h. ^jThis reaction was complicated by competing sulfinyl hydrolysis. Accurate determination of E_{app} and E_{true} was more complicated and will be reported elsewhere. ^kReaction for 24 h.

Proteinase from *Bacillus subtilis* var. biotectus A showed the highest true enantioselectivity (E_{true} >150). At 50% conversion the product, (*R*)-**1**, had 93% ee while the unreacted starting material, (*S*)-**1c**, had 92% ee corresponding to an apparent enantioselectivity (E_{app}) of 90. However, this substrate also underwent ca. 1-3% spontaneous chemical hydrolysis. After correction for this chemical hydrolysis,²⁴ the true enantioselectivity (E_{true}) was >150.

A related protease, subtilisin Carlsberg, also catalyzed hydrolysis of **1c** with low apparent enantioselectivity (E_{app}). However, the amount of product sulfinamide was much lower than the amount of **1c** that disappeared. Further analysis revealed that in addition to

the expected C-N bond hydrolysis, this protease also catalyzed S-N bond hydrolysis.²⁵ Details of this unprecedented reaction will be reported separately.


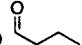
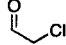
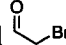
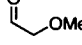
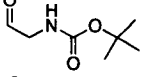
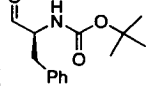
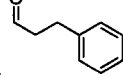
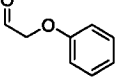
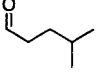
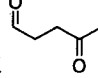
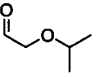
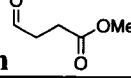
The two other proteases – protease from *Aspergillus oryzae* and protease/acylase from *Aspergillus melleus* – as well as a lipase, *Candida antarctica* lipase A, and bovine cholesterol esterase also catalyzed the hydrolysis of **1c**, but showed only low to moderate enantioselectivity (E_{true} = 6 to 29). All hydrolases except lipase A from *Candida antarctica* favoured the (*R*)-enantiomer.

Although this initial screen identified *Bacillus subtilis* var. biotecus A as the best commercial enzyme for hydrolysis of **1c**, it is, unfortunately, expensive (US\$725/gram) and its amino acid sequence is not available from the supplier. We suspected that subtilisin E might be a similar or even the same enzyme. Subtilisin E is an alkaline serine protease produced by *Bacillus subtilis* that has been cloned and overexpressed²⁶ and its structure has been elucidated by X-ray crystallography.²⁷ Confirming our hunch, subtilisin E showed similar enantioselectivity (E_{true} >150) to *Bacillus subtilis* var. biotecus A in the hydrolysis of **1c** (Table 2.1) as well as four other substrates (see below and Chapter 2 – Appendix Table A2.1). We focused further experiments on subtilisin E because it showed high enantioselectivity, it was inexpensive to produce by fermentation and the X-ray crystal structure permitted a molecular-level interpretation of results.

2.2.3 Optimization of *N*-acyl group for enantioselectivity and reactivity

The *N*-acetyl derivative **1a** and *N*-butanoyl derivative **1b** showed no reaction with subtilisin E,²⁸ but several acyl groups with electron withdrawing functional groups similar to **1c** showed enantioselective hydrolysis (Table 2.2). The *N*-bromoacetyl derivative **1d** reacted similarly to **1c**. It showed high enantioselectivity (E_{true} >150) and conversion (53% c_{app} in 3 h), but also underwent a similar spontaneous chemical hydrolysis (4% after 3 h). The *N*-methoxyacetyl derivative **1e** showed at least six-fold lower enantioselectivity (E_{true} = 26), ten-fold lower conversion (28% c_{app} after 24 h) and a slower spontaneous chemical hydrolysis (4% after 24 h). A glycine derivative **1f** showed at least three-fold lower enantioselectivity (E_{true} = 54) than **1c** and eleven-fold lower conversion (26% c_{app} after 24 h).

Table 2.2. Reactivity and enantioselectivity of subtilisin E toward **1a-m**

<i>N</i> -acyl group	% <i>c</i> _{app} ^a	relative rate (% <i>c</i> _{app} /h) ^b	ee _s (%) ^c	ee _p (%) ^c	<i>E</i> _{true} ^d
1a 	n.r.	n.a.	n.a.	n.a.	n.a.
1b 	n.r.	n.a.	n.a.	n.a.	n.a.
1c 	36 ^e	12	56	97	>150 ^f
1d 	53 ^e	18	99	89	>150 ^g
1e 	28	1.2	33	84	26 ^g
1f 	26	1.1	34	95	54
1g 	46	1.9	77	90	44
1h 	47	2.0	89	99	>150
1i 	n.r.	n.a.	n.a.	n.a.	n.a.
1j 	13	0.5	14	91	24
1k 	8	0.3	8	90	20
1l 	5	0.2	4	75	7
1m 	24	1.0	30	95	52

^a% Conversion: amount of sulfinamide formed in 24 h except where noted. ^b% Conversion per hour (assumes linear rate throughout course of reaction). n.a. = not applicable. ^c% Enantiomeric excess. Enantiomeric excess of substrate and product were determined by HPLC analysis on Daicel Chiralcel OD or AD columns at 238 nm or 222 nm. n.d. = not determined. ^dEnantiomeric ratio: the enantiomeric ratio *E* measures the relative rate of hydrolysis of the fast enantiomer as compared to the slow enantiomer as defined by Sih (Chen, C.S.; Fujimoto, Y.; Girdaukas, G.; Sih, C.J. *J. Am. Chem. Soc.* **1982**, *104*, 7294-7299). ^eReaction for 3 h. ^fCorrected for ca. 2% chemical hydrolysis. ^gCorrected for ca. 4% chemical hydrolysis.

Since subtilisin favours hydrolysis of peptides with aromatic or large non-polar residues at the P₁ position,²⁹ we prepared several phenylalanine derivatives or analogs. The phenylalanine derivative **1g** demonstrated at least three-fold lower enantioselectivity ($E_{true} = 46$) and six-fold lower conversion (46% c_{app} after 24 h) than **1c**. However, the *N*-dihydrocinnamoyl derivative **1h** showed very high enantioselectivity ($E_{true} > 150$) similar to **1c**, but with six-fold lower conversion (47% c_{app} after 24 h).³⁰ Surprisingly, the closely related *N*-phenoxyacetyl derivative **1i** did not react with enzyme.

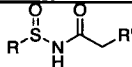
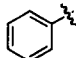
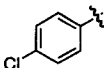
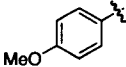
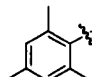
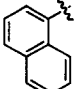
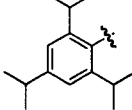

Three non-polar substrates structurally related to leucine, **1j**, **1k** and **1l**, showed at least six, eight and twenty-one-fold lower enantioselectivity ($E_{true} = 7$ to 24) and twenty-four, forty and sixty-fold lower conversion (5-13% c_{app} after 24 h), respectively, than **1c**. A similar compound, **1m**, demonstrated at least three-fold lower enantioselectivity ($E_{true} = 52$) and twelve-fold lower conversion (24% c_{app} after 24 h) than **1c**.

The *N*-dihydrocinnamoyl derivative **1h** and *N*-chloroacetyl derivative **1c** were the best acyl groups for *p*-toluenesulfonamide since they showed the highest enantioselectivity and reactivity. Thus, compounds **1c** and **1h**, which contain these groups, reacted at least 100 times faster than the simplest *N*-acyl sulfonamide, **1a**.²⁸ The conversion was six-fold lower for **1h**, as compared to **1c**, but it did not suffer spontaneous chemical hydrolysis. Although the reactivity and enantioselectivity of **1d** was comparable to that of the **1c**, its synthesis was less efficient (max. yield 20% for **1d** vs. 50% for **1c**).

2.2.4 Sulfonamide substrate range and enantioselectivity

To determine the substrate range of subtilisin E, we tested seven additional arylsulfonamides with enzyme (Table 2.3). Subtilisin E catalyzed the hydrolysis of **2c** and *para*-substituted benzenesulfonamides, **3c** and **4c**, with high enantioselectivity ($E_{true} > 150$), but the enantioselectivity decreased with the more substituted sulfonamide, **5c** ($E_{true} = 98$), and the more hindered sulfonamides, **6c** ($E_{true} = 13$) and **7c** ($E_{true} = 1.2$). Compound **8c** did not react with subtilisin E.

Table 2.3. Enantioselectivity of subtilisin E toward **2c-5c** and **2h-5h**

							
Sulfonamide	R'	%c _{app} ^a	ee _s (%) ^b	ee _p (%) ^b	E _{app}	E _{true} ^c	
	2c Cl	14	16	97	76	>150 ^{d,e}	
	2h Bn	14	16	99	>150	>150	
	3c Cl	35	52	97	110	>150 ^{d,e}	
	3h Bn	9	10	99	>150	>150	
	4c Cl	21	25	94	41	>150 ^{d,f}	
	4h Bn	40	65	98	>150	>150	
	5c Cl	41	67	94	65	98 ^{d,e}	
	5h Bn	0.5	n.d.	n.d.	n.d.	n.d.	
	6c Cl	19 ^g	20	73	13	13	
	6h Bn	n.r.	n.a.	n.a.	n.a.	n.a.	
	7c Cl	30 ^g	3	9	1.2	1.2	
	8c Cl	n.r.	n.a.	n.a.	n.a.	n.a.	
	8h Bn	n.r.	n.a.	n.a.	n.a.	n.a.	

^a% Conversion: conversion refers to the amount of sulfonamide formed. All reactions as *N*-chloroacetyl were 3 h and as *N*-dihydrocinnamoyl were 24 h except where noted. n.r. = no reaction. ^b% Enantiomeric excess. Enantiomeric excess of substrate and product were determined by HPLC analysis on Daicel Chiralcel OD or AD columns at 238 nm or 222 nm. n.d. = not determined, n.a. = not applicable. ^cEnantiomeric ratio: the enantiomeric ratio *E* measures the relative rate of hydrolysis of the fast enantiomer as compared to the slow enantiomer as defined by Sih (Chen, C.S.; Fujimoto, Y.; Girdaukas, G.; Sih, C.J. *J. Am. Chem. Soc.* **1982**, *104*, 7294-7299). ^dSimilar *E* results were obtained with *B. subtilis* var. biotocus A (see Chapter 2 - Appendix 2 Table A2.1). ^eCorrected for ca. 1% chemical hydrolysis. ^fCorrected for ca. 3% chemical hydrolysis. ^gReaction for 24 h.

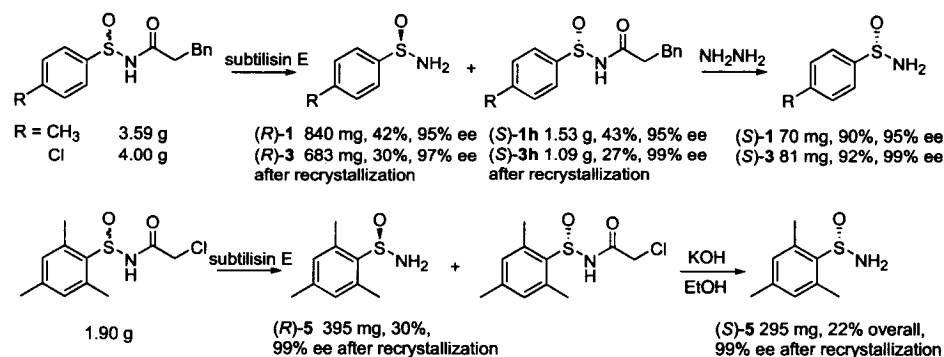
Subtilisin E showed moderate to high conversion with **2c**, **3c**, **4c** and **5c** (c_{app} = 14%, 35%, 21% and 41%, respectively after 3 h), but the conversion decreased with the more hindered arylsulfonamides, **6c** and **7c** (c_{app} = 19% and 30%, respectively after 24 h). Competing chemical hydrolysis (1-3%) occurred with all *N*-chloroacetyl derivatives; however, reducing the reaction temperature to 10 °C reduced spontaneous hydrolysis to <1% after 24 h. *Bacillus subtilis* var. biotecus A gave similar conversions and enantioselectivity (see Chapter 2 – Appendix Table A2.1).

The *N*-dihydrocinnamoyl sulfonamides showed similar enantioselectivity to the *N*-chloroacetyl sulfonamides, but lower conversion and no spontaneous chemical hydrolysis. *N*-Dihydrocinnamoyl derivatives **2h**, **3h**, and **4h** showed high enantioselectivity, (E_{true} >150) and low to moderate conversion, c_{app} = 14% (eight-fold lower than **2c**), 9% (thirty-fold lower than **3h**) and 40% (four-fold lower than **4c**) after 24 h, respectively. Compound **5h** reacted very slowly (0.5% c_{app} after 24 h) and **6h** and **8h** did not react. This lack of reaction may be due to either poor solubility³¹ or poor fit in the enzyme active site. We resolved the more hindered substrates using the more reactive *N*-chloroacetyl group, but used the *N*-dihydrocinnamoyl group for all other sulfonamides to avoid spontaneous chemical hydrolysis.

Comparing the HPLC traces of the product sulfonamides to samples of known absolute configuration prepared using either Davis and coworkers' method¹² for toluene-sulfonamide or Senanayake and coworkers' method¹⁶ for all other sulfonamides (see Appendix) established the absolute configurations. Subtilisin E favoured the (*R*)-enantiomer in all cases.

2.2.5 Gram-scale resolutions

To demonstrate the synthetic usefulness of this reaction, we resolved sulfonamides **1**, **3** and **5** on a multi-gram scale with subtilisin E, Scheme 2.4. We chose these sulfonamides for preparative reactions because sulfonamide **1** is widely used as a chiral auxiliary,⁵ the aryl group of **3** has different electronic properties than **1** and might be a useful alternative and 2,4,6-trimethylbenzenesulfonamide **5** is more hindered than **1** and gives fewer by-products during nucleophilic addition.³²



Scheme 2.4. Gram-scale kinetic resolution of sulfinamides **1**, **3** and **5**.

Resolution of **1h** (3.59 g) with subtilisin E gave (*R*)-**1** (840 mg, 42% yield; the maximum yield is 50% in a resolution) with 95% ee and (*S*)-**1h** (1.53 g, 43% yield) with 95% ee at ca. 50% conversion (3 d). If desired, both product and starting material can be recrystallized to >99% ee. Base- or acid-catalyzed hydrolysis of the *N*-dihydrocinnamoyl group proved unsuccessful. The substrate either did not react or under forcing conditions underwent decomposition. However, hydrazine hydrate³³ efficiently cleaved the *N*-dihydrocinnamoyl. Treating (*S*)-**1h** (144 mg) with hydrazine hydrate gave (*S*)-**1** (70 mg, 90% yield) with 95% ee.

We resolved **3h** (4.00 g) to give (*R*)-**3** (683 mg, 30% yield) with 97% ee and (*S*)-**3h** (2.42 g, 60% yield) with 64% ee at ca. 40% conversion (3 d). For unknown reasons, this resolution stopped at 40% conversion, but recrystallization of unreacted starting material gave (*S*)-**3h** (1.09 g, 27%) with 99% ee. Treating (*S*)-**3h** (155 mg) with hydrazine hydrate gave (*S*)-**3** (81 mg, 92%) with 99% ee.

We used the *N*-chloroacetyl group to resolve 2,4,6-trimethylbenzenesulfinamide **5** (1.90 g) because the *N*-dihydrocinnamoyl derivative reacted very slowly. The resolution yielded (*R*)-**5** (520 mg, 39% yield) with 90% ee at ca. 48% conversion (6 h). Recrystallization of (*R*)-**5** gave 395 mg (30%) with 99% ee. The unreacted starting material, (*S*)-**5c**, was isolated with 45% yield (860 mg, 82% ee). The *N*-chloroacetyl group cleaved in ethanolic KOH. Hydrolysis, followed by recrystallization gave (*S*)-**5** (295 mg, 22% yield) with 99% ee. Recrystallization was necessary because 5% of starting material spontaneously hydrolyzed during reaction. However, chemical hydrolysis could be reduced to

<1% at 10 °C while the enzymatic reaction was only three-fold slower (c_{app} = 16% at 10 °C vs. 41% at 37 °C after 3h).

These enzymatic resolutions are simple, convenient and avoid costly auxiliaries.^{12,16} The current synthetic route to enantiopure **1** relies on the starting material menthyl-*p*-toluenesulfinate (US\$15-40/g) and enantiopure **3** and **5** rely on the amino alcohol, *cis*-1-amino-2-indanol (US\$30/g), and gives low yields of the sterically hindered **5**.³⁴ This enzymatic resolution yields enantiopure *N*-acyl sulfinamides as intermediates. These may be useful for diastereoselective enolate alkylation reactions as a route to enantiopure α -substituted carboxylic acids.²⁰

2.2.6 Molecular basis for higher reactivity of **1c** and **1h**

To understand why (*R*)-**1h** and (*R*)-**1c** reacted with subtilisin E while (*R*)-**1a** did not, we modeled the first tetrahedral intermediate for hydrolysis of these substrates (see Experimental Section for modelling details). The modelling identified interactions that bind the *N*-acyl group of (*R*)-**1h** and (*R*)-**1c**, but not (*R*)-**1a**, to the S_1 pocket.

The (*R*)-**1h** tetrahedral intermediate fit well in the active site and all five catalytically relevant hydrogen bonds were normal length (<3.1 Å) (Table 2.4). The benzyl moiety of the dihydrocinnamoyl group bound in the S_1 pocket, as expected based on its similarity to phenylalanine.^{29,35} This benzyl moiety contacted hydrophobic portions of five out of eight residues lining this pocket (Leu126, Gly127, Gly128, Ala152 and Gly154). Using the incremental Gibbs free energy of transfer from *n*-octanol to water,^{36,37} we estimate the energy for this benzyl- S_1 pocket hydrophobic interaction to be 2.7-5.5 kcal/mol.³⁸ Thus, the hydrophobic interaction between the benzyl moiety and S_1 pocket likely improves binding of (*R*)-**1h**, as compared to (*R*)-**1a**.

Table 2.4. Minimized structures for the tetrahedral intermediate of subtilisin E-catalyzed hydrolysis of **1h**, **1c** and **7c**

Conformation	Group in S_1 ^a	H-bond $N_{\epsilon 2}$ - O_{γ} distance (Å) (N-H- O_{γ} angle, deg) ^b	Comments
(<i>R</i>)- 1h (Fig. 2)	tolyl	2.96 (155)	Steric contact with Tyr 217, His 64 and Met 222 in S_1 ' pocket
(<i>R</i>)- 1h	O_S ^c	3.08 (152)	Severe steric clash with Gly219 and Asn155
(<i>S</i>)- 1h (Fig. 2)	O_S	3.03 (154)	Unhindered in S_1 ' pocket
(<i>S</i>)- 1h	tolyl ^c	2.99 (157)	Steric clash with catalytic His 64
(<i>R</i>)- 1c	tolyl	2.98 (153)	Possible hydrogen bond with Thr 220 (Cl_{α} - $O_{\gamma 1}$ distance = 3.81 Å)
(<i>R</i>)- 1a	tolyl	2.97 (153)	No contact with S_1 residues
(<i>R</i>)- 7c (Fig. A2.2)	none	2.94 (157)	Binds above S_1 ' pocket
(<i>S</i>)- 7c (Fig. A2.2)	none	2.93 (156)	Binds above S_1 ' pocket

^aNarrow, hydrophobic pocket where leaving-group alcohol, amide or sulfinamide binds.

^bUnless otherwise noted, hydrogen bonds (His 64 $N_{\epsilon 2}$ - N or O, Ser 221NH - O⁻, and Asn155 NH₆₂ - O⁻) were present in all structures (N - N or O distance 2.7 - 3.1 Å, N-H-O or N-H-N angle 120- 175°). ^cGroup is forced out of S_1 ' because of steric clash with active site residues.

The (*R*)-**1c** tetrahedral intermediate also fit well in the active site and all five hydrogen bonds were normal length (<3.1 Å). The α -chloro atom of (*R*)-**1c** was bound in the S_1 pocket near the hydroxyl group ($O_{\gamma 1}$ -H) of Thr220 ($O_{\gamma 1}$ -Cl distance = 3.81 Å). This $O_{\gamma 1}$ -Cl distance was closer than the van der Waals contact (3.91 Å),³⁹ but longer than a hydrogen bond between a hydroxyl group and chlorine (2.91-3.52 Å).⁴⁰ A typical hydrogen bond between substrate and protein lowers the energy by 0.5-1.5 kcal/mol.⁴¹ This $O_{\gamma 1}$ -Cl interaction combined with the inductive effects of the α -chlorine atom, which increases the electrophilicity of the carbonyl carbon, may improve the binding and reactivity of (*R*)-**1c**.

Although the tetrahedral intermediate for (*R*)-**1a** also fits in the subtilisin active site and makes all five key hydrogen bonds, the small *N*-acyl group lacks contact with S_1

pocket residues. This lack of favourable interaction with S_1 residues to improve binding and an electron-withdrawing group to increase reactivity may account for its lack of reaction.⁴²

2.2.7 Molecular basis for enantioselectivity of subtilisin E with **1h**

Empirical rules based on substituent size can often predict the fast-reacting enantiomer in subtilisin-catalyzed reactions of secondary alcohols, Figure 2.1a.⁴³ Sulfinamides mimic secondary alcohols, where the aryl group is the large substituent and the oxygen is the medium substituent, because of their similar shape. However, the solvation of the medium group of a secondary alcohol (e.g. methyl group) and the sulfoxide oxygen differ. The incremental Gibbs free energy of transfer^{36,37} from *n*-octanol to water for a methyl group is +0.56 kcal/mol, while sulfoxide oxygen is -3.0 kcal/mol.⁴⁴ We hypothesized that subtilisin E favours the (*R*)-enantiomer because the sulfoxide oxygen favours a water-exposed orientation, while the aryl group binds in the S_1' leaving group pocket because of a favourable hydrophobic interaction, Figure 2.1b.

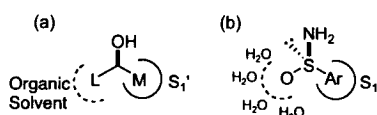


Figure 2.1. Empirical rules that predict the enantiopreference of subtilisins toward secondary alcohols and sulfinamides. (a) In organic solvent, subtilisins favour the secondary alcohol enantiomer with the shape shown where L is a large substituent such as phenyl and M is a medium substituent such as methyl. (b) In water, subtilisins favour the sulfinamide enantiomer with the shape shown where Ar is an aryl substituent. We suggest that a favourable hydrophobic interaction between the aryl substituent and S_1' pocket and good solvation of the polar sulfoxide oxygen in water explains the enantiopreference with sulfinamides.

To test this hypothesis, we modeled the first tetrahedral intermediate for hydrolysis of **1h**. The protein modelling molecular mechanics force field (AMBER) did not include parameters for the sulfinamide group, so we estimated these parameters using geometric information for methyl sulfinamide⁴⁵ from *ab initio* calculations and from force

field parameters for a sulfonamide-based inhibitor⁴⁶ also derived from *ab initio* calculations (see Chapter 2 - Appendix for details). Using these estimates, we expect only a qualitative rationalization of the enantioselectivity of subtilisin E with *N*-acyl sulfonamides.

Modelling **1h** with subtilisin E gave one productive conformation for each enantiomer, Table 2.4. The two other plausible conformations encountered severe steric clash with the protein.⁴⁷ The productive complex of (*R*)-**1h** had its *p*-tolyl group bound in the S₁' pocket and the sulfoxide oxygen exposed to solvent water, Figure 2.2. All hydrogen bond angles were >120° and all five hydrogen bond lengths were <3.1 Å (Table 2.4). The *p*-tolyl group appears to just fit in the S₁' pocket. Met222 in the bottom of the S₁' pocket, Tyr217 at the back of the S₁' pocket and catalytic His64 bumped the *p*-tolyl group.⁴⁷ This tight fit suggests a favourable hydrophobic interaction between the tolyl group and the S₁' residues.

The productive complex of the slower reacting (*S*)-**1h** had its sulfoxide oxygen in the S₁' pocket and tolyl group exposed to solvent water, Figure 2.2. All hydrogen bond angles were >120° and all five hydrogen bond lengths were <3.1 Å (Table 2.4). The sulfoxide oxygen fits well in the S₁' pocket and the protein does not hinder the *p*-tolyl group.⁴⁷ Unlike the favoured enantiomer, the smaller oxygen does not make steric contact with S₁' residues. Although the slow-reacting (*S*)-enantiomer avoids steric hindrances, it also lacks favourable hydrophobic interactions between the tolyl group and the S₁' residues. Using octanol-water partitioning data, we estimate that the hydrophobic interactions favour binding of (*R*)-**1h** by ~6.4 kcal/mol over the (*S*)-enantiomer in water.⁴⁴ The (*R*)-enantiomer places the hydrophobic aryl group in the S₁' pocket and the hydrophilic sulfoxide oxygen in the solvent (water), while the (*S*)-enantiomer does the opposite.

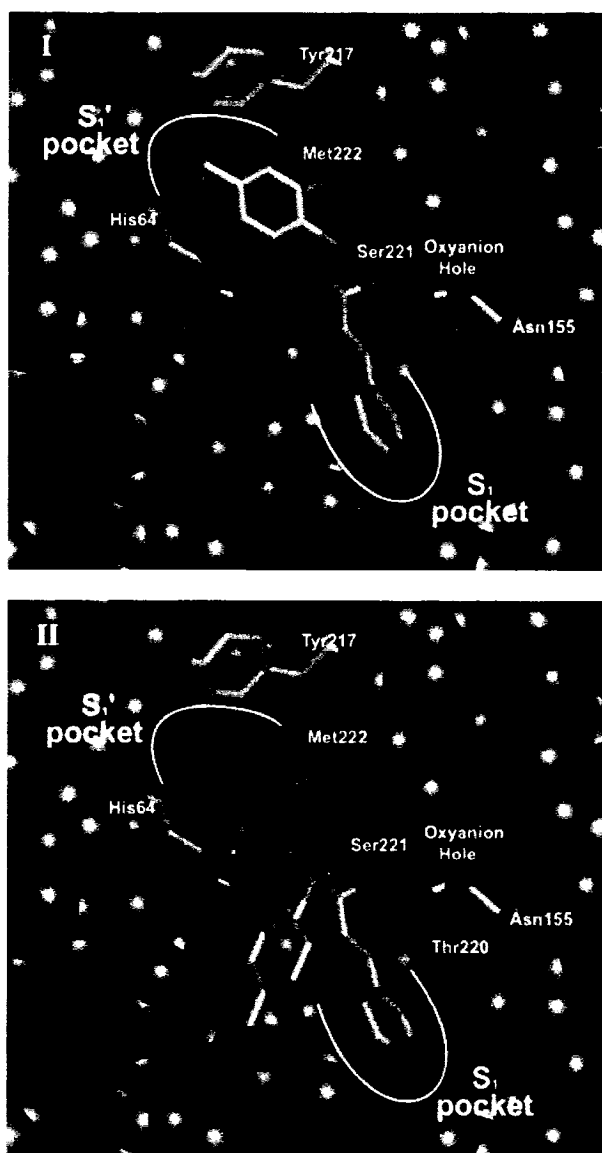


Figure 2.2. Catalytically productive tetrahedral intermediates for the subtilisin E catalyzed hydrolysis of fast-reacting (*R*)-**1h** (I) and slow-reacting (*S*)-**1h** (II) as identified by molecular modelling. The important active site and substrate atoms (sticks) are coloured as follows: grey (carbon), red (oxygen), blue (nitrogen) and orange (sulfur). Surrounding atoms (space fill) of subtilisin are shown in blue. For clarity, all hydrogen atoms and water molecules are hidden. Both I and II maintain all catalytically essential hydrogen bonds and the benzyl moiety of the dihydrocinnamoyl group binds in the S₁ pocket, as expected based on its similarity to phenylalanine.²⁹ In the fast-reacting enantiomer, (*R*)-**1h** (I), the *p*-tolyl group binds in the hydrophobic S_{1'} pocket and sulfoxide oxygen is exposed to sol-

vent water. In the slow-reacting enantiomer, (*S*)-**1h** (II), the sulfoxide oxygen binds in the hydrophobic S₁' pocket and the *p*-tolyl group is exposed to solvent water. The non-productive conformations (not shown) encountered severe steric clash with the active site residues.

Consistent with this explanation, the enantioselectivity of the subtilisin-E-catalyzed hydrolysis of **1h** decreased from $E > 150$ in 9:1 water: acetonitrile to $E = 12$ in 1:9 water: acetonitrile. Similarly, the enantioselectivity with **1c** decreased from $E > 150$ in 9:1 water: acetonitrile to $E = 41$ in 1:9 water: acetonitrile. The high concentration of acetonitrile favours the *p*-tolyl group in the solvent; thus, the enantiomer preference shifts toward the (*S*)-enantiomer, which orients with the oxygen in the S₁' pocket and the tolyl group in solvent. This result suggests that the enantioselectivity for acylation of sulfinamides in organic solvent would also be low, but we did not detect any acylation of *p*-toluenesulfinamide, consistent with Ellman's earlier report of no reaction.¹⁵

The decreasing enantioselectivity with the larger sulfinamides, **5c** ($E_{true} = 98$) and **6c** ($E_{true} = 13$), and loss of enantioselectivity with the very large sulfinamide, **7c** ($E_{true} = 1.2$), is also consistent with this explanation for enantioselectivity. Larger aryl substituents increase the steric hindrance in the S₁' pocket, which overwhelms the energy gained through a hydrophobic interaction between the pocket and the aryl group and therefore reduces the enantioselectivity. In other words, when either the aryl group or sulfoxide oxygen can fit in the S₁' pocket (**1** – **4**), a hydrophobic interaction favours the aryl group and the enantioselectivity is high. However, as the aryl group becomes larger, increased steric hindrance with S₁' residues oppose the hydrophobic interaction and lower the enantioselectivity (**5** – **7**). Modelling with **7c** suggests that this sulfinamide leaving-group is too large for the S₁' pocket and binds above it (see Chapter 2 – Appendix Figure A2.2).

2.3 Discussion

In this paper, we identified subtilisin E as the most suitable hydrolase of those examined for preparation of enantiopure arylsulfinamides. The reactivity and enantioselectivity of subtilisin E toward *N*-acyl arylsulfinamides depends on the *N*-acyl group. Simple *N*-acyl compounds such as *N*-acetyl and *N*-butanoyl did not react with subtilisin E. Mo-

lecular modelling suggests that the reactive acyl groups may mimic a phenylalanine moiety. Other research groups have also modified unreactive substrates to convert them into good substrates. For example, the fungus *Beauveria bassiana* did not hydroxylate cyclopentanone, but did hydroxylate the *N*-benzoylspirooxazolidine derivative with high yield and diastereoselectivity.⁴⁸ In a second example, changing from the 2-pyridylacetyl to the 4-pyridylacetyl increased the rate eight-fold and the enantioselectivity three-fold for a penicillin G acylase catalyzed hydrolysis of 1-phenethyl esters.⁴⁹ In a third example, the enantioselectivity of *Pseudomonas cepacia* lipase-catalyzed acylation of 2-[(*N,N*-dimethylcarbamoyl)methyl]-3-cyclopenten-1-ol varied from $E = 4$ to 156 depending on the acylating agent.⁵⁰

There are three synthetic routes to enantiopure sulfinamides: the method of Davis and coworkers¹² for *p*-toluenesulfinamide, the method of Ellman and coworkers⁶ for *tert*-butylsulfinamide and the method of Senanayake and coworkers¹⁶ for a variety of alkyl- and arylsulfinamides. Using subtilisin E, we resolved gram quantities of **1h**, **3h** and **5c**. These resolutions were simple, convenient and inexpensive. Our strategy does not provide as wide variety of enantiopure sulfinamides as reported by Senanayake, but the selectivity and mildness of the biocatalytic route make it the preferred route when there is a choice. This biocatalytic route is amenable to scale up, is environmentally acceptable and is performed under mild conditions. As well, the catalyst, subtilisin E, is inexpensive to produce and could be recycled.

Molecular modelling of the first tetrahedral intermediate for subtilisin E-catalyzed hydrolysis of **1h** suggests that the (*R*)-enantiomer reacts faster because of preferential binding of the nonpolar *p*-tolyl group in the hydrophobic S_1' pocket versus the polar sulfoxide oxygen, which prefers to be exposed to solvent water. Changing the solvent to 1:9 water: acetonitrile decreased the enantioselectivity. A similar decrease in enantioselectivity occurred for subtilisin-catalyzed reactions of amino acid derivatives.⁵¹ In water, subtilisin Carlsberg showed high enantioselectivity for the hydrolysis of a natural L-amino acid ester, but in organic solvent, transesterification was one to two orders of magnitude less enantioselective. Klivanov and coworkers suggested that the L-amino acid, but not the D-amino acid, binds to the hydrophobic S_1 pocket. Water as the solvent favours this interaction; thus, the enantioselectivity is higher in water. As expected, the difference in enzyme

enantioselectivity was greater for amino acid derivatives with more hydrophobic side chains.

Subtilisins usually show only low to moderate enantioselectivity with secondary alcohols and isosteric amines, but high enantioselectivity with the structurally related sulfinamides. For secondary alcohols and isosteric primary amines, the substituents are usually both hydrophobic, so the hydrophobic binding contribution differences are smaller than for arylsulfinamides where the substituents are the polar sulfoxide oxygen and the hydrophobic aryl group. This polarity difference between the two substituents appears to dominate subtilisin E enantioselectivity of arylsulfinamides resulting in high enantioselectivity.

2.4 Experimental section

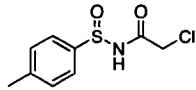
2.4.1 General

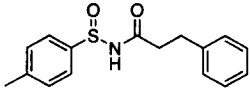
^1H and ^{13}C NMR spectra were obtained as dilute CDCl_3 solutions at 300 MHz and 75 MHz, respectively. Chemical shifts are expressed in ppm (δ) and are referenced to tetramethylsilane or trace CHCl_3 in CDCl_3 . Coupling constants are reported in Hertz (Hz). HPLC analyses were performed on a 4.6 x 250 mm Daicel Chiralcel OD or Chiralpak AD column (Chiral Technologies, Exton, USA) and monitored at 238 or 222 nm. Flash chromatography with silica gel (230-400 mesh) or preparative TLC (20 x 20 cm, 1000 μm) was used to purify all intermediates and substrates. Visualization of UV-inactive materials on TLC was accomplished using phosphomolybdic acid or ninhydrin followed by heating. All reagents, buffers, starting materials and anhydrous solvents were purchased from Sigma-Aldrich Canada (Oakville, Canada) and used without purification. All air- and moisture-sensitive reactions were performed under N_2 . The pBE3 *Escherichia coli*-*Bacillus subtilis* shuttle vector^{26b} containing the subtilisin E gene was kindly provided by Dr. F. Arnold (Caltech) and *Bacillus subtilis* strain DB104⁵² was a gift from Dr. S. L. Wong (University of Calgary).

2.4.2 Synthesis of substrates

Sulfinamides (1-8). We prepared racemic sulfinamides **1-8** using literature procedures (Scheme 2.3).²⁰⁻²² The relevant analytical data are in Chapter 2 - Appendix.

***N*-Acylsulfonamides.** We prepared *N*-acylsulfonamides by treating sulfonamides **1-8** with 2 equivalents of *n*-BuLi in THF, followed by rapid addition of the symmetrical anhydride of the appropriate carboxylic acid.⁵³ The relevant analytical data are given below or in Chapter 2 - Appendix.

 ***N*-Chloroacetyl-*p*-toluenesulfonamide (**1c**).** Obtained as a white solid (186 mg, 50%): mp 119-121 °C; ¹H NMR δ 2.43 (s, 3H, PhCH₃), 4.29 (s, 2H, C(O)CH₂Cl), 7.31 (d, *J* = 8.1, 2H), 7.63 (d, *J* = 8.1, 2H); ¹³C NMR δ 21.8 (PhCH₃), 42.5 (C(O)CH₂Cl), 124.8, 130.6, 139.9, 143.5 (phenyl), 167.2 (C=O); HRMS calcd for C₉H₁₀³⁵ClNO₂S (M⁺), 231.0120. Found: 231.0123. The enantiomers were separated by HPLC (Diacel Chiralcel OD column, 90:10 hexanes/EtOH, 0.5 mL/min, 238 nm; (*R*)-**1c**, *t*_R = 21.3 min; (*S*)-**1c**, *t*_R = 51.4 min).

 ***N*-Dihydrocinnamoyl-*p*-toluenesulfonamide (**1h**).** Obtained as a white solid (550 mg, 59%): mp 85-87 °C (lit.²⁰ mp 94-96 °C); ¹H NMR δ 2.43 (s, 3H, PhCH₃), 2.70 (m, 2H, C(O)CH₂), 3.01 (t, *J* = 7.8, 2H, CH₂Ph), 7.17-7.29 (m, 7H, phenyl), 7.41 (d, *J* = 8.1, 2H, phenyl), 7.81 (br s, 1H, NH); ¹³C NMR δ 21.9 (tolyl CH₃), 31.2 (CH₂Ph), 37.9 (C(O)CH₂), 124.9, 126.6, 128.7, 128.8, 130.1, 140.1, 140.3, 142.6 (phenyl), 173.6 (C=O). The enantiomers were separated by HPLC (Diacel Chiralcel OD column, 90:10 hexanes/EtOH, 0.5 mL/min, 238 nm; (*R*)-**1h**, *t*_R = 20.4 min; (*S*)-**1h**, *t*_R = 22.4 min).

2.4.3 Hydrolase library

All screening was performed at pH 7.2. The hydrolases were dissolved in BES buffer (5.0 mM, pH 7.2), at the concentration listed in Table 2.1, centrifuged for 10 min at 2000 rpm and titrated to pH 7.2. The supernatant was used for screening.

2.4.4 Screening of commercial hydrolases with pH indicators

The assay solution was prepared by mixing **1c** (1 mL of a 440 mM solution in CH₃CN), *p*-nitrophenol (6.71 mL of a 1.0 mM solution in 5.0 mM BES, pH 7.2) with BES buffer (5.14 mL of 5.0 mM solution, pH 7.2). Hydrolase solutions (10 μL/well) were transferred to a 96-well microtiter plate followed by assay solution (90 μL/well). The final concentration in each well was 3.1 mM substrate, 4.65 mM BES, 0.46 mM *p*-

nitrophenol in a total volume of 100 μ L 7% acetonitrile in buffer. The plate was shaken for 5 s on the microplate reader and the absorbance decrease was monitored at 404 nm for one hour. The assay was performed in quadruplicate at 25 °C and 37 °C.²³ The low pK_a of the *N*-acylsulfonamide NH group (ca. pK_a 6) reduced the sensitivity of the assay by protonating the pH indicator, *p*-nitrophenoxide, but a decrease in the absorbance could still be observed at pH 7.2.

2.4.5 Small-scale reactions with commercial hydrolases to determine enantioselectivity

Reactions of *N*-chloroacetylsulfonamides with commercial enzymes were carried out at 25 °C. For example, proteinase from *Bacillus subtilis* var. biotecnus A (16 mg) and substrate (5 mM in CH_3CN) in a total volume of 10 mL of buffer (20 mM BES, pH 7.2) were stirred together in reaction vials for 3-6 h. Upon completion, the aqueous phase was extracted with CH_2Cl_2 (2×10 mL). The combined organic layers were dried over anhydrous Na_2SO_4 and concentrated *in vacuo*. The residue was dissolved in 1 mL of EtOH, filtered through a nylon filter (0.45 μ m) and analyzed by HPLC (Diacel OD column, 90:10 hexanes/EtOH, 1.0 mL/min, 238 nm).

2.4.6 Cultivation and isolation of subtilisin E

Protease deficient *B. subtilis* DB104 was transformed with vector pBE3, as previously described.^{26b,54} Protease deficient *Bacillus subtilis* DB104 secretes proteases into the culture medium and accumulates them to a high level. Endogenous protease activity is less than 3%.⁵² Cells were grown in Schaeffer's sporulation medium (2XSG) supplemented with kanamycin (50 μ g/mL). Enzyme activity was monitored by adding 90 μ L of assay solution [0.2 mM succinyl-AAPF-*p*-nitroanilide (suc-AAPF-*p*NA) / 100 mM Tris pH 8.0 / 10 mM $CaCl_2$] to 10 μ L of supernatant and following the reaction at 410 nm at 37 °C for 15 min. When maximal activity was reached (48 h), the cells were centrifuged, the supernatant was filter sterilized and lyophilized. The residue was dissolved in 10 mM or 50 mM Tris buffer (pH 8.0, 10 mM $CaCl_2$) and the initial activity was assessed as above. Typical activity of the supernatant or prepared solution was 10-20 U/mL, with suc-AAPF-*p*NA.

2.4.7 Hydrolysis of *N*-acylsulfinamides with subtilisin E

Reactions of *N*-acyl sulfinamides with subtilisin E were carried out at 37 °C. Each mixture consisted of subtilisin E (solution in 10 mM Tris buffer (pH 8.0, 1 mM CaCl₂), 178 µL), CaCl₂ (1 M, 2 µL) and substrate (50 mM in CH₃CN, 20 µL). The reaction was allowed to continue for 3 h with *N*-bromoacetyl- and *N*-chloroacetyl sulfinamides and 24 h with all other substrates. The reaction was diluted with dH₂O (400 µL) and terminated with the addition of CH₂Cl₂ (500 µL). The organic layer was removed and the aqueous layer was twice extracted with CH₂Cl₂ (500 µL). The phases were separated by centrifugation, and the organic layers were collected. The combined organics were evaporated under a stream of N₂ and the residue was diluted with EtOH (150 µL) for analysis by HPLC (Brownlee Si-10 silica column followed by Diacel OD column, 90:10 hexanes/EtOH, 0.6 mL/min, 238 or 222 nm). Although the chiral column separated enantiomers, it did not separate the substrate and product. This two-column system separated the substrate and product in the silica column and the enantiomers of each in the chiral column.

2.4.8 Gram-scale resolution of *N*-acylsulfinamides

1h. Substrate (3.59 g, 12.5 mmol) in CH₃CN (50 mL) was added to enzyme solution (450 mL, ca. 20 U/mL with suc-AAPF-*p*NA) and incubated at 37 °C until ca. 50% conversion (3 d), as determined by HPLC. The mixture was filtered through Celite, extracted with CH₂Cl₂ (3 x 200 mL), dried over Na₂SO₄ and concentrated *in vacuo*. Separation of substrate and product on silica (1:1 EtOAc/hexanes to EtOAc) gave (*R*)-**1** (840 mg, 42%, 95% ee) and (*S*)-**1h** (1.53 g, 43%, 95% ee), as determined by HPLC. Remaining starting material (*S*)-**1h** (144 mg, 0.5 mmol) was treated with hydrazine hydrate (1 mL) at 0 °C followed by stirring at RT until the reaction was complete by TLC (3 h). The reaction mixture was diluted with CH₂Cl₂ (15 mL) and washed with 1 N HCl (2 x 10 mL), sat. NaHCO₃ (2 x 10 mL) and sat. NaCl (10 mL). The organic layer was dried over Na₂SO₄ and concentrated *in vacuo* to give (*S*)-**1** (70 mg, 90%, 95% ee).

3h. Substrate (4.00 g, 13.0 mmol) in MeCN (100 mL) was added to enzyme solution (900 mL, ca. 15 U/mL with suc-AAPF-*p*NA) and incubated at 37 °C until ca. 40% conversion (3 d), as determined by HPLC. The mixture was filtered through Celite, ex-

tracted with CH_2Cl_2 (3 x 200 mL), dried over Na_2SO_4 and concentrated *in vacuo*. Separation of substrate and product on silica (1:1 EtOAc/hexanes to EtOAc) gave (*R*)-**3** (683 mg, 30%, 97% ee) and (*S*)-**3h** (2.42 g, 60%, 64% ee). Recrystallization from EtOAc/hexanes gave (*S*)-**3h** (1.09 g, 27%, 99% ee), as determined by HPLC. Remaining starting material (*S*)-**3h** (155 mg, 0.5 mmol) was treated with hydrazine hydrate (1 mL) at 0 °C followed by stirring at RT until the reaction was complete by TLC (3 h). The reaction mixture was diluted with CH_2Cl_2 (15 mL) and washed with 1 N HCl (2 x 10 mL), sat. NaHCO_3 (2 x 10 mL) and sat. NaCl (10 mL). The organic layer was dried over Na_2SO_4 and concentrated *in vacuo* to give (*S*)-**3** (81 mg, 92%, 99% ee).

5c. Substrate (1.90 g, 7.30 mmol) in CH_3CN (30 mL) was added to enzyme solution (270 mL, ca. 20 U/mL with suc-AAPF-*p*NA) and incubated at 37 °C until ca. 49% conversion (6h), as determined by HPLC. The mixture was filtered through Celite, extracted with CH_2Cl_2 (3 x 200 mL), dried over Na_2SO_4 and concentrated *in vacuo* to give the crude mixture of substrate and product. Separation of substrate and product on silica (2:1 EtOAc/hexanes to EtOAc) gave (*R*)-**5** (520 mg, 39%, 90% ee) and (*S*)-**5c** (860 mg, 45%, 82% ee). Recrystallization from EtOAc/hexanes gave (*R*)-**5** (395 mg, 30%, 99% ee), as determined by HPLC. Remaining starting material was hydrolyzed in 1 N KOH (1:1 H_2O /EtOH) for 1 h at RT. The reaction mixture was extracted with CH_2Cl_2 (3 x 15 mL), dried over Na_2SO_4 , concentrated *in vacuo* to give (*S*)-**5** (295 mg, 22%, 99% ee) after recrystallization.

2.4.9 Modelling of tetrahedral intermediates bound to subtilisin E

All modelling was performed using *Insight II 2000.1 / Discover* (Accelrys, San Diego, CA, USA) on a SGI Octane UNIX workstation using the AMBER force field.⁵⁵ We used a nonbonded cutoff distance of 8 Å, a distance-dependent dielectric of 1.0 and scaled the 1-4 van der Waals interactions by 50%. Protein structures in Figures 2.2 and A2.2 were created using PyMOL (Delano Scientific, San Carlos, CA, USA). The X-ray crystal structure of subtilisin E (entry 1SCJ)²⁷ from the Protein Data Bank is a Ser221Cys subtilisin E-propeptide complex. Using the Builder module of *Insight II*, we replaced the Cys221 with a serine and removed the propeptide region. The hydrogen atoms were added to correspond to pH 7.0. Histidines were uncharged, aspartates and glutamates

were negatively charged, and arginines and lysines were positively charged. The catalytic histidine (His64) was protonated. The positions of the water hydrogens and then the enzyme hydrogens were optimized using a consecutive series of short (1 ps) molecular dynamic runs and energy minimizations.⁵⁶ This optimization was repeated until there was <2 kcal/mol in the energy of the minimized structures. Thereafter, an iterative series of geometry optimizations were performed on the water hydrogens, enzyme hydrogens and full water molecules. Finally, the whole system was geometry optimized.

The tetrahedral intermediates were built manually and covalently linked to Ser221. Since the parameters for the sulfinamide group were not included in the AMBER force field, they were assigned in analogy to existing parameters.^{45,46,47} The geometric properties of the sulfinamide moiety of minimized **1h** were compared to an available X-ray crystal structure⁵⁷ and adjusted as necessary. Nonstandard partial charges were calculated using a formal charge of -1 for the substrate oxyanion. Energy minimization proceeded in three stages. First, minimization of substrate with only the protein constrained (25 kcal mol⁻¹ Å⁻²); second, minimization with only the protein backbone constrained (25 kcal mol⁻¹ Å⁻²) and for the final stage the minimization was continued without constraints until the rms value was less than 0.0005 kcal mol⁻¹ Å⁻¹. A catalytically productive complex required all five hydrogen bonds within the catalytic machinery. We set generous limits for a hydrogen bond: a donor to acceptor atom distance of less than 3.1 Å with a nearly linear arrangement (>120° angle) of donor atom, hydrogen, and acceptor atom. Structures lacking any of the five catalytically relevant hydrogen bonds or encountering severe steric clash with enzyme were deemed nonproductive.

Acknowledgments

We thank the donors of the Petroleum Research Fund administered by the American Chemical Society and McGill University for financial support. CKS thanks the Natural Sciences and Engineering Research Council (Canada) for a postgraduate fellowship. We thank Dr. Frances Arnold (California Institute of Technology, USA) for the subtilisin E plasmid, Dr. S. L. Wong (University of Calgary, Canada) for the *B. subtilis* DB104 cells, Dr. Fred Schendel and Rick Dillingham (University of Minnesota Biotechnology Institute, USA) for the large-scale fermentation and purification of subtilisin E, Dr.

Ronghua Shu (McGill University) for the initial substrate synthesis and screening experiments, Linda Fransson (Royal Institute of Technology (KTH), Sweden) and the Minnesota Supercomputing Institute (University of Minnesota, USA) for assistance with the modelling software.

References

1. Carreña, M. C. *Chem. Rev.* **1995**, *95*, 1717-1760 and references therein.
2. Anderson, K. K. In *The Chemistry of Sulphones and Sulphoxides*; Patai, S. Rappoport, Z.; Stirling, C. J. M., Eds.; John Wiley & Sons: New York, 1988; pp 55-94.
3. Walker, A. J. *Tetrahedron: Asymmetry* **1992**, *3*, 961-998.
4. Nudelman, A. In *The Chemistry of Sulphinic Acids, Esters and their Derivatives*; Patai, S., Ed.; John Wiley & Sons; New York, 1990; pp 35-85.
5. Davis, F. A.; Zhou, P.; Chen, B.-C. *Chem. Soc. Rev.* **1998**, *27*, 13-18.
6. Liu, G.; Cogan, D. A.; Ellman, J. A. *J. Am. Chem. Soc.* **1997**, *119*, 9913-9914.
7. Kochi, T.; Tang, T. P.; Ellman, J. A. *J. Am. Chem. Soc.* **2002**, *124*, 6518-6519.
8. Davis, F. A.; Zhou, P.; Reddy, G. V. *J. Org. Chem.* **1994**, *59*, 3243-3245.
9. Lefebvre, I. M.; Evans, S. A. *J. Org. Chem.* **1997**, *62*, 7532-7533.
10. (a) Phillips, H. *J. Chem. Soc.* **1925**, *127*, 2552-2587. (b) Hulce, M.; Mallamo, J. P.; Frye, L. L.; Kogan, T. P.; Posner, G. A. *Org. Synth.* **1986**, *64*, 196-206.
11. Drabowicz, J.; Kielbasinski, P.; Mikolajczyk, M. In *The Chemistry of Sulphones and Sulphoxides*; Patai, S. Rappoport, Z.; Stirling, C. J. M., Eds.; John Wiley & Sons: New York, 1988; Chapter 3, pp 233-378.
12. Davis, F. A.; Xhang, Y.; Andemichael, Y.; Fang, T.; Fanelli, D. L.; Zhang, H. *J. Org. Chem.* **1999**, *64*, 1403-1406.
13. Herbranson, H. F.; Cusano, C. M. *J. Am. Chem. Soc.* **1961**, *83*, 2124-2128.
14. Davis, F. A.; Reddy, R. T.; Reddy, R. E. *J. Org. Chem.* **1992**, *57*, 6387-6389.
15. Cogan, D. A.; Liu, G.; Kim, K.; Backes, B. J.; Ellman, J. A. *J. Am. Chem. Soc.* **1998**, *120*, 8011-8019.
16. Han, Z.; Krishnamurthy, D.; Grover, P.; Fang, Q. K.; Senanayake, C. H. *J. Am. Chem. Soc.* **2002**, *124*, 7880-7881.

17. (a) Kagan, H. B. In *Catalytic Asymmetric Synthesis*; Ojima, I., Ed.; VCH; New York, 1993; pp. 203-226. (b) Holland, H. L. *Chem. Rev.* **1988**, *88*, 473-485. (c) ten Brink, H. B.; Holland, H. L.; Schoemaker, H. E.; van Lingen, H.; Wever, R. *Tetrahedron: Asymmetry* **1999**, *10*, 4563-4572.
18. (a) Capozzi, G.; Modena, G.; Pasquato, L. in *The Chemistry of Sulphenic Acids and Their Derivatives*, Patai, S., Ed. Wiley: Chichester, **1990**, pp 403-516. (b) Atkinson, R. S.; Judkins, B. D. *J. Chem. Soc., Perkin Trans. 1*, **1981**, 2615-2619.
19. (a) Allenmark, S. G.; Andersson, A. C. *Tetrahedron: Asymmetry* **1993**, *4*, 2371-2376. (b) Burgess, K.; Henderson, I. *Tetrahedron Lett.* **1989**, *30*, 3633-3636. (c) Burgess, Henderson, I.; Ho, K.-K. *J. Org. Chem.* **1992**, *57*, 1290-1295. (d) Serreqi, A. N.; Kazlauskas, R. J. *Can. J. Chem.* **1995**, *73*, 1357-1367.
20. Backes, B. J.; Dragoli, D. R.; Ellman, J. A. *J. Org. Chem.* **1999**, *64*, 5472-5478.
21. Klunder, J. M.; Sharpless, K. B. *J. Org. Chem.* **1987**, *52*, 2598-2602.
22. (a) Netscher, T.; Prinzbach, H. *Synthesis* **1987**, 683-686. (b) Gontcharov, A. V.; Liu, H.; Sharpless, K. B. *Org. Lett.* **1999**, *1*, 783-786.
23. Janes, L. E.; Löwendahl, C. P.; Kazlauskas, R. J. *Chem. Eur. J.* **1998**, *4*, 2324-2331.
24. A computer program, *Selectivity-KRESH*, was used for all calculations. For details, see: Faber, K.; Hönig, H.; Kleewein, A. in *Preparative Biotransformations*, Roberts, S. M. (ed.), John Wiley and Sons: New York, 1995, pp 0.079-0.084.
25. ¹H NMR and HRMS-EI identified *p*-toluenesulfinic acid as the primary product in this enzymatic reaction. Mugford, P. F.; Magloire, V. P.; Kazlauskas, R. J., in preparation.
26. (a) Park, S.-S.; Wong, S. -L.; Wang, L. -F.; Doi, R. H. *J. Bacteriol.* **1989**, *171*, 2657-2665. (b) Zhao, H.; Arnold, F. H. *Proc. Natl. Acad. Sci. USA* **1997**, *94*, 7997-8000.
27. Jain, S. C.; Shinde, U.; Li, Y.; Inouye, M.; Berman, H. M. *J. Mol. Biol.* **1998**, *284*, 137-144.
28. Based on a limit of detection of 0.1%.
29. (a) Estell, D. A.; Graycar, T. P.; Miller, J. V.; Powers, D. B.; Burnier, J. P.; Ng, P. G.; Wells, J. A. *Science* **1986**, *233*, 659-663. (b) Wells, J. A.; Powers, D. B.; Bott, R. R.; Graycar, T. P.; Estell, D. A. *Proc. Natl. Acad. Sci. USA*, **1987**, *84*, 1219-1223.

30. Additional screening with the *N*-dihydrocinnamoyl derivative **1h** showed chymotrypsin from bovine pancreas catalyzed its hydrolysis with good enantioselectivity ($E = 45$) favouring the *R*-enantiomer and high conversion ($\%c_{app} = 52\%$) after 6 h. This enzyme was missed in our initial activity screen because it reacted only slowly with the *N*-chloroacetyl derivative **1c**.

31. The solubility of both **5h** and **6h** in 10% MeCN/buffer were <5 mM. Organic co-solvents (1,4-dioxane, EtOH, DMSO) or additives (10 mM guanidium chloride) did not significantly improve solubility. Performing the reaction at 50 °C or using a biphasic reaction system with *tert*-butylmethyl ether also did not increase conversion. Using MeCN or 1,4-dioxane at higher concentrations (20-90%) improved substrate solubility, but did not increase conversion.

32. Han, Z.; Krishnamurthy, D.; Pflum, D.; Grover, P.; Wald, S. A.; Senanayake, C. H. *Org. Lett.* **2002**, *4*, 4025-4028.

33. Keith, D. D.; Tortora, J. A.; Yang, R. *J. Org. Chem.* **1978**, *43*, 3711-3713.

34. In our hands, the sodium bis(trimethylsilyl)amide displacement¹⁶ gave low yields of (*R*)-**2-4** and (*R*)-**6** (18-52%) and no yield for (*R*)-**5**. When LiNH₂/NH₃ was used in place of sodium bis(trimethylsilyl)amide, (*R*)-**5** formed in low yield (3%) and ee (68% ee).

35. Lee, T.; Jones, J. B. *J. Am. Chem. Soc.* **1996**, *118*, 502-508.

36. (a) Fujita, T.; Iwasa, J.; Hansch, C. *J. Am. Chem. Soc.* **1964**, *86*, 5175-5180. (b) Leo, A.; Hansch, C.; Elkins, D. *Chem. Rev.* **1971**, *71*, 525-616. (c) Hansch, C.; Coats, E. *J. Pharm. Sci.* **1970**, *59*, 731-743. (d) Hansch, C.; Leo, A. *Substituent Constants for Correlation Analysis in Chemistry and Biology*; John Wiley and Sons: New York, 1979; pp 48-51.

37. Fersht, A. *Structure and Mechanism in Protein Science*; W.H. Freeman and Company: New York, 1998; pp 324-348.

38. A hydrophobic interaction is the tendency of nonpolar compounds to transfer from an aqueous phase to an organic phase. The energy of a hydrophobic interaction is from the regaining of entropy by water after it is removed from a hydrophobic group and can be estimated using the incremental Gibbs free energy of transfer.³⁷ The incremental Gibbs free energy of transfer of a benzyl group from *n*-octanol to water is 2.7 kcal/mol using $\Delta G_{trans} = 2.303RT\pi$, where π is the hydrophobicity constant of the benzyl group ($\pi =$

2.01)^{36d} relative to hydrogen. However, binding of the benzyl group in the hydrophobic S₁ cavity removes two water-hydrophobic interfaces (ie. substrate and protein), so the value might be as high as 5.5 kcal/mol.³⁷ Since the S₁ pocket lies on the surface of the protein and the benzyl group is not completely buried, we estimate the energy for this hydrophobic interaction to be 2.7-5.5 kcal/mol.^{36ab, 37}

39. Estimated from the van der Waals radii of chlorine (1.75 Å) and hydrogen (1.20 Å) and the O-H bond length (0.96 Å) from Bondi, A. *J. Phys. Chem.* **1964**, 68, 441-451.

40. Jeffrey, G. A; Saenger, W. *Hydrogen Bonding in Biological Structures*; Springer-Verlag: Berlin, 1991; pp 29-31.

41. Removal of a hydrogen bond donor or acceptor in an enzyme active site weakens binding by 0.5-1.5 kcal/mol.³⁷ Although the hydrogen bond inventory is zero (ie. the number of hydrogen bonds is the same for both the free enzyme and the enzyme-substrate complex), hydrogen bonds between an enzyme and substrate increase the entropy due to the release of bound water molecules.

42. This reasoning predicts lower K_M values for **1h** and **1c** than for **1a**, but low solubility of these substrates (<5 mM) prevented testing this prediction.

43. (a) Fitzpatrick, P. A.; Klibanov, A. M. *J. Am. Chem. Soc.* **1991**, 113, 3166-3171. (b) Kazlauskas, R. J.; Weissfloch, A. N. E. *J. Mol. Catal. B: Enz.* **1997**, 3, 65-72.

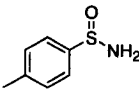
44. The incremental Gibbs free energy of transfer from *n*-octanol to water for the tolyl group was estimated to be ca. +3.4 kcal/mol and the sulfoxide oxygen was ca. -3.0 kcal/mol using $\Delta G_{trans} = 2.303RT\pi$, where π is the hydrophobicity constant of the group relative to hydrogen.^{36ab,37} Switching from (*S*)-**1h** to (*R*)-**1h** places the tolyl group into a hydrophobic pocket (3.4 kcal/mol for the tolyl group) and removes the sulfoxide group from the hydrophobic pocket (3.0 kcal/mol) for a total of 6.4 kcal/mol in water. The hydrophobicity constant of the tolyl group ($\pi = 2.52$) was estimated by adding π values of a phenyl and a methyl group.^{36d} The hydrophobicity constant of the sulfoxide oxygen ($\pi = -2.19$) was estimated by subtracting π values of a methyl sulfide group from a methyl sulfoxide group.^{36d} The energy difference may be higher if one includes the hydrophobic surface of the S₁' pocket.

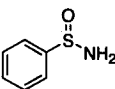
45. Bharatam, P. V.; Kaur, A.; Kaur, D. *J. Phys. Org. Chem.* **2002**, 15, 197-203.

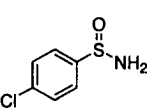
46. Rossi, K. A.; Merz, K. M., Jr.; Smith, G. M.; Baldwin, J. J. *J. Med. Chem.* **1995**, *38*, 2061-2069.
47. See Chapter 2 – Appendix for complete molecular modelling details.
48. (a) Braunegg, G.; de Raadt, A.; Feichtenhofer, S.; Griengl, H.; Kopper, I.; Lehman, A.; Weber, H. *-J. Angew. Chem. Int. Ed.* **1999**, *38*, 2763-2766. (b) de Raadt, A.; Griengl, H.; Weber, H. *Chem. Eur. J.* **2001**, *7*, 27-31.
49. Pohl, T.; Waldmann, H. *Tetrahedron Lett.* **1995**, *36*, 2963-2966.
50. Ema, T.; Maeno, S.; Takaya, Y.; Sakai, T.; Utaka, M. *J. Org. Chem.* **1996**, *61*, 8610-8616.
51. (a) Zaks, A.; Klibanov, A. M. *J. Am. Chem. Soc.* **1986**, *108*, 2767-2768. (b) Margolin, A. L.; Tai, D. –F. Klibanov, A. M. *J. Am. Chem. Soc.* **1987**, *109*, 7885-7887. (c) Sakurai, T.; Margolin, A. L.; Russell, A. J.; Klibanov, A. M. *J. Am. Chem. Soc.* **1988**, *110*, 7236-7237.
52. Kawamura, F.; Doi, R. H. *J. Bacteriol.* **1984**, *160*, 442-444.
53. Chen, F. M. F.; Kuroda, K.; Benoiton, N. L. *Synthesis* **1978**, *12*, 928-930.
54. Harwood, C. R.; Cutting, S. M. *Molecular Biological Methods for Bacillus*, John Wiley and Sons, England, 1990, pp 33-35, 391-402.
55. (a) Weiner, S. J.; Kollman, P. A.; Case, D. A.; Singh, U. C.; Ghio, C.; Alagona, G.; Profeta, S.; Weiner, P. *J. Am. Chem. Soc.* **1984**, *106*, 765-784. (b) Weiner, S. J.; Kollman, P. A.; Nguyen, D. T.; Case, D. A. *J. Comp. Chem.* **1986**, *7*, 230-252.
56. Raza, S.; Fransson, L.; Hult, K. *Protein Sci.* **2001**, *10*, 329-338.
57. Robinson, P. D. *Acta Cryst.* **1991**, *C47*, 594-596.

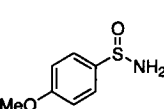
Chapter 2 – Appendix

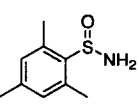
Synthesis of Racemic Sulfinamides. Racemic sulfinamides were prepared using literature procedures.¹ Analytical data are given below.

 ***p*-Toluenesulfinamide (1).** Obtained as white crystals (6.51 g, 56% overall yield): mp 115-117 °C (lit.¹ 117-118 °C); ¹H NMR δ 2.42 (s, 3H, PhCH₃), 4.30 (br s, 2H, -NH₂), 7.30 (d, *J* = 8.1, 2H, phenyl), 7.62 (d, *J* = 8.1, 2H, phenyl); ¹³C NMR δ 21.7 (PhCH₃), 125.6, 129.7, 141.5, 143.6 (phenyl). The enantiomers were separated by HPLC (Diacel OD column, 90:10 hexanes/EtOH, 0.5 mL/min, 238 nm; (*R*)-**1**, *t*_R = 21.0 min; (*S*)-**1**, *t*_R = 27.5 min).

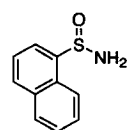
 **Benzenesulfinamide (2).** Obtained as white crystals (3.06 g, 59% overall yield): mp 104-106 °C; ¹H NMR δ 4.38 (br s, 2H, NH₂), 7.51 (m, 3H, phenyl), 7.75 (m, 2H, phenyl); ¹³C NMR (101 MHz) δ 125.6, 129.1, 131.3, 146.6 (phenyl). The enantiomers were separated by HPLC (Diacel OD column, 90:10 hexanes/EtOH, 0.5 mL/min, 238 nm; (*R*)-**2**, *t*_R = 22.6 min; (*S*)-**2**, *t*_R = 26.2 min).

 ***p*-Chlorobenzenesulfinamide (3).** Obtained as amber crystals (9.91 g, 53% overall yield): mp 130-132 °C; ¹H NMR (DMSO-*d*₆) δ 4.39 (br s, 2H, NH₂), 7.48 (d, *J* = 8.7, 2H, phenyl), 7.68 (d, *J* = 9.0, 2H, phenyl); ¹³C NMR (101 MHz) δ 127.3, 129.4, 137.8, 145.1 (phenyl). The enantiomers were separated by HPLC (Diacel OD column, 90:10 hexanes/EtOH, 0.5 mL/min, 238 nm; (*R*)-**3**, *t*_R = 24.7 min; (*S*)-**3**, *t*_R = 43.0 min).

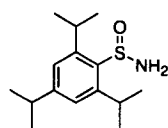
 ***p*-Methoxybenzenesulfinamide (4).** Obtained as white crystals (2.90 g, 35% overall yield): mp 129-131 °C (lit.² 135-136); ¹H NMR δ 3.86 (s, 3H, -OCH₃), 4.29 (br s, 2H, NH₂), 7.00 (d, *J* = 9.0, 2H, phenyl), 7.66 (d, *J* = 9.0, 2H, phenyl); ¹³C NMR (DMSO-*d*₆) δ 56.2 (-OCH₃), 114.7, 127.7, 140.2, 161.4 (phenyl). The enantiomers were separated by HPLC (Diacel OD column, 90:10 hexanes/EtOH, 0.5 mL/min, 238 nm; (*R*)-**4**, *t*_R = 28.8 min; (*S*)-**4**, *t*_R = 41.4 min).

 **2,4,6-Trimethylbenzenesulfinamide (5).** Obtained as a white crystals (6.03 g, 33% overall yield): mp 116-118 °C (lit.² 115-118 °C); ¹H NMR δ 2.29 (s, 3H, PhCH₃), 2.61 (s, 6H, 2 x PhCH₃), 4.41 (br s, 2H, NH₂), 6.86 (s, 2H, phenyl); ¹³C NMR (DMSO-*d*₆) δ 19.8 (2 x PhCH₃), 21.3 (PhCH₃), 130.8, 136.2, 139.8,

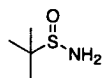
140.9 (phenyl). The enantiomers were separated by HPLC (Diacel OD column, 90:10 hexanes/EtOH, 0.5 mL/min, 238 nm; (*R*)-**5**, t_R = 26.8 min; (*S*)-**5**, t_R = 25.0 min).



1-Naphthylsulfonamide (6). Obtained as amber crystals (2.20 g, 55% overall yield): mp 166-168 °C; ^1H NMR (DMSO- d_6) δ 6.26 (br s, 2H, NH_2), 7.58-7.70 (m, 3H, phenyl), 8.01-8.08 (m, 3H, phenyl), 8.18-8.21 (m, 1H, phenyl); ^{13}C NMR (DMSO- d_6) δ 122.9, 123.8, 125.8, 127.0, 127.4, 129.2, 129.3, 131.6, 133.9, 143.8 (phenyl). The enantiomers were separated by HPLC (Diacel OD column, 90:10 hexanes/EtOH, 0.5 mL/min, 238 nm; (*R*)-**6**, t_R = 32.9 min; (*S*)-**6**, t_R = 39.5 min).



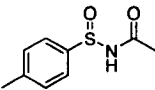
2,4,6-Triisopropylbenzenesulfonamide (7). Obtained as a white solid (2.51 g, 21% overall yield): mp (decomp.) 183-185 °C (lit.¹ 99-102 °C)³; ^1H NMR δ 1.24 (d, J = 6.9, 6H, 2 x CH_3), 1.27 (d, J = 6.6, 6H, 2 x CH_3), 1.32 (d, J = 7.2, 6H, 2 x CH_3), 2.88 (sept, J = 6.6, 1H, $\text{CH}(\text{CH}_3)$), 4.03 (sept, J = 6.7, 2H, 2 x $\text{CH}(\text{CH}_3)$), 4.48 (br s, 2H, NH_2), 7.07 (s, 2H, phenyl); ^{13}C NMR (DMSO- d_6) δ 24.6, 24.7, 25.1, 25.7, 28.7, 34.3, (*i*-Pr), 122.5, 141.5, 147.3, 149.5. The enantiomers were separated by HPLC (Diacel OD column, 90:10 hexanes/EtOH, 0.5 mL/min, 238 nm; (*R* or *S*)-**7**, t_R = 8.5 min; (*R* or *S*)-**7**, t_R = 10.5 min).

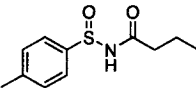


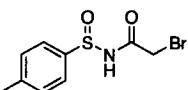
tert-Butylsulfonamide (8). *m*-CPBA (14 g, 62 mmol) in CH_2Cl_2 (100 mL) was added dropwise to a stirred solution of *tert*-butyldisulfide (10 g, 56 mmol) in CH_2Cl_2 (25 mL) at 0 °C over 15 min. The solution was stirred for 30 min at 0 °C and RT until the reaction was complete by TLC (3 h). The reaction mixture was poured into a separatory funnel containing CH_2Cl_2 (100 mL) and sat. NaHCO_3 (100 mL) and further extracted with CH_2Cl_2 (2 x 100 mL). The organic layer was removed and washed with sat. NaHCO_3 (3 x 100 mL), sat. NaCl (100 mL), dried over Na_2SO_4 and concentrated *in vacuo* to give 10.34 g (95%) of *tert*-butylthiosulfinate⁴; ^1H NMR (200 MHz) δ 1.32 (sulfide) 1.39 (s, 9H, $(\text{CH}_3)_3\text{S}$), 1.57 (s, 9H, $(\text{CH}_3)_3\text{S}=\text{O}$). This intermediate was dissolved in CH_2Cl_2 (25 mL) and a solution of SO_2Cl_2 (7.2 g, 53 mmol) in CH_2Cl_2 (10 mL) was added dropwise at 0 °C. The resulting yellow solution was stirred for 1 h allowing it to gradually reach RT.⁵ Excess SO_2Cl_2 was removed under vacuum and the resulting product, *tert*-butylsulfinyl chloride, was diluted in CH_2Cl_2 (100 mL) and added dropwise to NH_4OH (200 mL) at 0 °C over 30 min. After stirring for 30 min at RT, the reac-

tion mixture was saturated with NaCl and extracted with CH_2Cl_2 (3 x 100 mL). The combined organic layers were washed with sat. NaCl (150 mL), dried over Na_2SO_4 and concentrated *in vacuo* to give the crude sulfinamide. Purification using flash chromatography (12:1 $\text{CHCl}_3/\text{MeOH}$) gave the title compound (1.41 g, 22%) as a white solid: mp 98-100 °C (lit.⁶ 101-102 °C (*R*-enantiomer)); ^1H NMR (200 MHz) δ 1.23 (s, 9H, $-(\text{CH}_3)_3$), 3.72 (br s, 2 H, NH_2); ^{13}C NMR δ 22.6 ($-(\text{CH}_3)_3$), 55.4 ($\text{C}(\text{CH}_3)_3$). The enantiomers were separated by HPLC (Diacel OD column, 90:10 hexanes/EtOH, 0.5 mL/min, 222 nm; (*R*)-**8**, t_R = 12.6 min; (*S*)-**8**, t_R = 15.2 min).

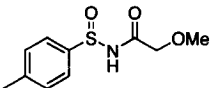
***N*-Acylsulfinamides.** *N*-Acylsulfinamides of **1-8** were prepared by treating sulfinamides **1-8** with two equivalents of *n*-BuLi in THF¹, followed by rapid addition of the symmetrical anhydride of the appropriate carboxylic acid.⁷ The relevant analytical data are given below:

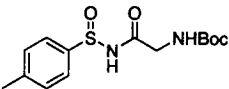
 ***N*-Acetyl-*p*-toluenesulfinamide (**1a**).** Obtained as white solid (95 mg, 30%): mp 125-127 °C; ^1H NMR δ 2.21 (s, 3H, $\text{C}(\text{O})\text{CH}_3$), 2.45 (s, 3H, PhCH_3), 7.35 (d, J = 8.4, 2H, phenyl), 7.59 (d, J = 8.1, 2H, phenyl); ^{13}C NMR δ 21.8 ($\text{C}(\text{O})\text{CH}_3$), 21.9 (PhCH_3), 124.9, 130.3, 140.3, 142.9 (phenyl), 171.3 ($\text{C}=\text{O}$); HRMS calcd for $\text{C}_9\text{H}_{12}\text{NO}_2\text{S}$ ($\text{M}+\text{H}^+$) 198.0589. Found: 198.0582. The enantiomers were separated by HPLC (Diacel OD column, 90:10 hexanes/EtOH, 0.5 mL/min, 238 nm; (*R* or *S*)-**1a**, t_R = 24.6 min; (*R* or *S*)-**1a**, t_R = 36.6 min).

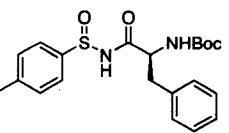
 ***N*-Butanoyl-*p*-toluenesulfinamide (**1b**).** Obtained as white solid (780 mg, 90%): mp 95-97 °C; ^1H NMR δ 1.0 (t, J = 7.0, 3H, $-\text{CH}_2\text{CH}_3$), 1.72 (m, 2H, $-\text{CH}_2\text{CH}_3$), 2.20 (m, 2H, $\text{C}(\text{O})\text{CH}_2$), 2.43 (s, 3H, PhCH_3), 7.32 (d, J = 8, 2H, phenyl), 7.57 (d, J = 8, 2H, phenyl); ^{13}C NMR δ 13.9 ($-\text{CH}_2\text{CH}_3$), 18.7 ($-\text{CH}_2\text{CH}_3$), 21.8 (PhCH_3), 37.2 ($\text{C}(\text{O})\text{CH}_2$), 124.9, 130.1, 139.9, 142.5 (phenyl), 174.7 ($\text{C}=\text{O}$); HRMS calcd for $\text{C}_{11}\text{H}_{16}\text{NO}_2\text{S}$ ($\text{M}+\text{H}^+$) 226.0902. Found: 226.0897. The enantiomers were separated by HPLC (Diacel Chiracel OD column, 90:10 hexanes/EtOH, 0.5 mL/min, 238 nm; (*R* or *S*)-**1b**, t_R = 12.9 min; (*R* or *S*)-**1b**, t_R = 17.4 min).

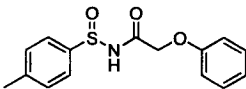
 ***N*-Bromoacetyl-*p*-toluenesulfinamide (**1d**).** Obtained as white solid (175 mg, 20%): mp 83-85 °C; ^1H NMR δ 2.46 (s, 3H, PhCH_3), 3.94 (s, 2H, $\text{C}(\text{O})\text{CH}_2\text{Br}$), 7.37 (d, J = 8.1, 2H, phenyl), 7.62 (d, J = 8.1, 2H, phenyl); ^{13}C

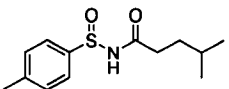
NMR δ 21.8 (PhCH₃), 29.6 (C(O)CH₂Br), 125.5, 130.4, 140.7, 142.6 (phenyl), 168.4 (C=O); HRMS calcd for C₉H₁₁⁷⁹BrNO₂S (M+H⁺) 275.9694. Found: 275.9698. The enantiomers were separated HPLC (Diacel Chiralcel OD column, 90:10 hexanes/EtOH, 0.5 mL/min, 238 nm; (*R*)-**1d**, *t_R* = 19.8 min; (*S*)-**1d**, *t_R* = 48.9 min).

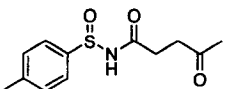
 ***N*-Methoxyacetyl-*p*-toluenesulfinamide (**1e**).** Obtained as white solid (304 mg, 42%); mp 57-59 °C; ¹H NMR δ 2.42 (s, 3H, PhCH₃), 3.37 (s, 3H, OCH₃), 4.00 (s, 2H, C(O)CH₂), 7.37 (d, *J* = 8.4, 2H, phenyl), 7.63 (d, *J* = 8.4, 2H) 8.29 (br s, 1H, NH); ¹³C NMR δ 21.9 (PhCH₃), 59.6 (OCH₃), 71.9 (C(O)CH₂), 124.8, 130.3, 140.4, 142.9 (phenyl), 170.7 (C=O); HRMS calcd for C₁₀H₁₄NO₃S (M+H⁺) 228.0694. Found: 228.0689. The enantiomers were separated by HPLC (Diacel OD column, 90:10 hexanes/EtOH, 0.5 mL/min, 238 nm; (*R*)-**1e**, *t_R* = 24.6 min; (*S*)-**1e**, *t_R* = 31.7 min).

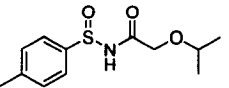
 ***N*-[*N*-(*tert*-Butoxycarbonyl)-glycine]-*p*-toluenesulfinamide (**1f**).** Obtained as white solid (290 mg, 29%); mp 128-130 °C; ¹H NMR δ 1.39 (s, 9H, -C(CH₃)₃), 2.43 (s, 3H, PhCH₃), 3.88 (m, 2H, C(O)CH₂), 5.29 (br s, 1H, NH), 7.32 (d, *J* = 7.8, 2H, phenyl), 7.57 (d, *J* = 8.1, 2H, phenyl), 8.65 (br s, 1H, NH); ¹³C NMR δ 21.8 (PhCH₃), 28.6 (C(CH₃)₃), 44.7 (C(O)CH₂), 80.6 (C(CH₃)₃), 124.9, 130.2, 139.8, 142.7 (phenyl), 156.4 (C=O, carbamate), 171.4 (C=O, amide); HRMS calcd for C₁₄H₂₁N₂O₄S (M+H⁺) 313.1222. Found: 313.1218. The enantiomers were separated by HPLC (Diacel OD column, 90:10 hexanes/EtOH, 0.5 mL/min, 238 nm; (*R*)-**1f**, *t_R* = 17.8 min; (*S*)-**1f**, *t_R* = 30.9 min).

 ***N*-[*N*-(*tert*-Butoxycarbonyl)-phenylalanine]-*p*-toluenesulfinamide (**1g**).** Obtained as white solid (660 mg, 51%); mp 111-113 °C; ¹H NMR δ 1.33-1.46 (m, 9H, (CH₃)₃), 2.42 (s, 3H, PhCH₃), 3.11 (m, 2H, CH₂Ph), 4.38 (bs s, 1H, NH), 4.99 (m, 1H, C(O)CH), 7.12-7.53 (m, 9H, phenyl), 8.33 (br s, 1H, NH); ¹³C NMR δ 21.8 (PhCH₃), 28.6 (C(CH₃)₃), 38.7 (CH₂Ph), 60.8 (C(O)CH), 80.6 (C(CH₃)₃), 125.0, 127.1, 128.8, 129.7, 130.2, 136.3, 139.8, 142.5, 155.8 (C=O, carbamate), 173.2 (C=O, amide); HRMS calcd for C₂₁H₂₇N₂O₄S (M+H⁺) 403.1691. Found: 403.1683. The enantiomers were separated by HPLC (Diacel OD column, 90:10 hexanes/EtOH, 0.5 mL/min, 238 nm; (*S,S*)-**1g**, *t_R* = 11.9 min; (*R,S*)-**1g**, *t_R* = 13.4 min).

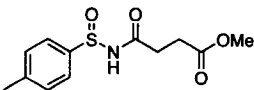
 **N-Phenoxyacetyl-*p*-toluenesulfinamide (1i).** Obtained as white solid (391 mg, 42%): mp 107-109 °C; ¹H NMR δ 2.45 (s, 3H, PhCH₃), 4.60 (s, 2H, C(O)CH₂), 6.83-7.06 (m, 3H, phenyl), 7.27-7.36 (m, 4H, phenyl), 7.58 (d, *J* = 8.1, 2H); ¹³C NMR δ 21.9 (PhCH₃), 67.5 (C(O)CH₂), 114.9, 122.7, 124.9, 130.0, 130.4, 140.2, 143.1, 156.8 (phenyl), 169.6 (C=O); HRMS calcd for C₁₅H₁₆NO₃S (M+H⁺) 290.0851. Found: 290.0843. The enantiomers were separated by HPLC (Diacel OD column, 90:10 hexanes/EtOH, 0.5 mL/min, 238 nm; (*R* or *S*)-**1i**, *t*_R = 31.4 min; (*R* or *S*)-**1i**, *t*_R = 43.8 min).

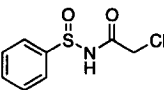
 **N-4-Methylvaleroyl-*p*-toluenesulfinamide (1j).** Obtained as white solid (160 mg, 20%): mp 123-125 °C; ¹H NMR δ 0.90 (s, 3H, CH₃), 0.93 (s, 3H, CH₃), 1.56-1.62 (m, 3H, CH₂CH(CH₃)₂), 2.40 (m, 2H, C(O)CH₂), 2.45 (s, 3H, PhCH₃), 7.35 (d, *J* = 8.6, 2H, phenyl), 7.59 (d, *J* = 8.2, 2H); ¹³C NMR δ 21.9 (PhCH₃), 22.6 ((CH₃)₂), 28.0 (CH(CH₃)₂), 33.9 (CH₂CH) or (C(O)CH₂), 34.4 (CH₂CH) or (C(O)CH₂), 124.9, 130.1, 140.4, 142.5 (phenyl), 174.6 (C=O); HRMS calcd for C₁₃H₂₀NO₂S (M+H⁺) 254.1215. Found: 254.1209. The enantiomers were separated by HPLC (Diacel OD column, 90:10 hexanes/EtOH, 0.5 mL/min, 238 nm; (*R*)-**1j**, *t*_R = 11.9 min; (*S*)-**1j**, *t*_R = 13.7 min).

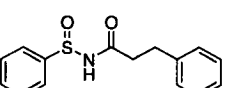
 **N-Levulinoyl-*p*-toluenesulfinamide (1k).** Obtained as white solid (399 mg, 49%): mp 74-76 °C; ¹H NMR δ 2.20 (s, 3H, C(O)CH₃), 2.44 (s, 3H, Ph CH₃), 2.61 (m, 2H, C(O)CH₂), 2.86 (m, 2H, CH₂C(O)CH₃), 7.33 (d, *J* = 8.6, 2H, phenyl), 7.60 (d, *J* = 8.2, 2H, phenyl), 8.08 (br s, 1H, NH); ¹³C NMR δ 21.8 (PhCH₃), 30.1 (C(O)CH₃), 30.2 (C(O)CH₂), 38.0 (CH₂C(O)CH₃), 125.0, 130.1, 140.2, 142.5 (phenyl), 173.4 (C=O, amide), 207.6 (C=O, ketone); HRMS calcd for C₁₂H₁₆NO₃S (M+H⁺) 254.0851. Found: 254.0857. The enantiomers were separated by HPLC (Diacel OD column, 90:10 hexanes/EtOH, 0.5 mL/min, 238 nm; (*R*)-**1k**, *t*_R = 30.4 min; (*S*)-**1k**, *t*_R = 42.9 min).

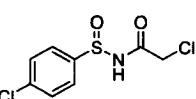
 **N-Isopropoxyacetyl-*p*-toluenesulfinamide (1l).** Obtained as white solid (289 mg, 35%): mp 68-70 °C; ¹H NMR (200 MHz) δ 1.13 (t, *J* = 6.0, 3H, CH₃), 1.23 (t, *J* = 5.8, 3H, CH₃), 2.46 (s, 3H, PhCH₃), 3.63 (m, 1H, CH(CH₃)₂), 4.03 (s, 2H, C(O)CH₂), 7.36 (d, *J* = 7.8, 2H, phenyl), 7.64 (d, *J* = 8.2, 2H, phenyl), 8.34 (br s, 1H, NH); ¹³C NMR δ 21.9 (PhCH₃), 22.1 (CH₃)₂, 22.2 (CH₃)₂, 67.8

(CH(CH₃)₂), 124.8, 130.3, 140.5, 142.9 (phenyl), 171.5 (C=O); HRMS calcd for C₁₂H₁₈NO₃S (M+H⁺) 256.1007. Found: 256.1012. The enantiomers were separated by HPLC (Diacel OD column, 90:10 hexanes/EtOH 0.5 mL/min, 238 nm; (*R* or *S*)-**1l**, *t*_R = 18.4 min; (*R* or *S*)-**1l**, *t*_R = 19.7 min).

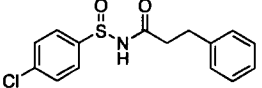
 **N-3-(Methoxycarbonyl)propionyl-*p*-toluenesulfinamide (1m).** Obtained as white solid (561 mg, 65%): mp 90-92 °C; ¹H NMR δ 2.43 (s, 3H, tolyl CH₃), 2.61 (m, 2H, CH₂C(O)CH₃) or (m, 2H, C(O)CH₂), 2.70 (m, 2H, CH₂C(O)CH₃) or (m, 2H, C(O)CH₂), 7.32 (d, *J* = 8.4, 2H, phenyl), 7.56 (d, *J* = 8.7, 2H, phenyl), 8.31 (br s, 1H, NH); ¹³C NMR δ 21.8 (tolyl CH₃), 28.8 (C(O)CH₂) or (CH₂C(O)OCH₃), 29.1 (C(O)CH₂) or (CH₂C(O)OCH₃), 52.3 (OCH₃), 125.0, 130.1, 140.1, 142.6 (phenyl), 172.9 (C=O, ester), 173.2 (C=O, amide); HRMS calcd for C₁₂H₁₆NO₄S (M+H⁺) 270.0800. Found: 270.0790. The enantiomers were separated by HPLC (Diacel OD column, 90:10 hexanes/EtOH, 0.5 mL/min, 238 nm; (*R*)-**1m**, *t*_R = 26.5 min; (*S*)-**1m**, *t*_R = 61.9 min).

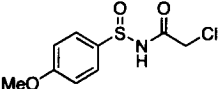
 **N-Chloroacetylbenzenesulfinamide (2c).** Obtained as white solid (216 mg, 56%): mp 92-94 °C; ¹H NMR δ 4.15 (s, 2H, C(O)CH₂Cl), 7.59 (m, 3H, phenyl), 7.75 (m, 2H, phenyl), 8.41 (br s, 1H, NH); ¹³C NMR δ 42.4 (C(O)CH₂), 124.9, 129.8, 132.7, 143.0 (phenyl), 167.3 (C=O); HRMS-EI calcd for C₈H₈³⁵Cl NO₂S (M⁺) 216.9964. Found: 216.9972. The enantiomers were separated by HPLC (Diacel OD column, 90:10 hexanes/EtOH; 0.5 mL/min, 238 nm; (*R*)-**2c**, *t*_R = 21.7 min; (*S*)-**2c**, *t*_R = 43.9 min).

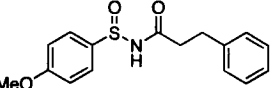
 **N-Dihydrocinnamoylbenzenesulfinamide (2h).** Obtained as white solid (185 mg, 48%): mp 94-96 °C; ¹H NMR δ 2.68 (m, 2H, C(O)CH₂), 3.02 (t, *J* = 7.8, 2H, CH₂Ph), 7.18-7.31 (m, 5H, phenyl), 7.49-7.57 (m, 5H, phenyl); ¹³C NMR (DMSO-*d*₆) δ 31.1 (CH₂Ph), 37.7 (C(O)CH₂), 125.6, 126.7, 128.9, 129.0, 129.9, 132.1, 141.2, 144.2 (phenyl), 174.1 (C=O); HRMS calcd for C₁₅H₁₆NO₂S (M+H⁺) 274.0902. Found: 274.0896. The enantiomers were separated by HPLC (Diacel AD column, 90:10 hexanes/EtOH; 0.5 mL/min, 238 nm; (*R*)-**2h**, *t*_R = 44.9 min; (*S*)-**2h**, *t*_R = 22.2 min).

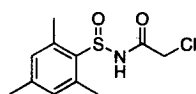
 **N-Chloroacetyl-*p*-chlorobenzenesulfinamide (3c).** Obtained as white solid (87 mg, 21%): mp 118-120 °C; ¹H NMR 4.16 (s, 2H,

C(O)CH₂Cl), 7.57 (d, J = 8.4, 2H, phenyl), 7.71 (d, J = 8.4, 2H, phenyl); ¹³C NMR δ 42.4 (C(O)CH₂Cl), 126.3, 130.2, 139.3, 141.5 (phenyl), 167.0 (C=O); HRMS calcd for C₈H₇³⁵Cl₂NO₂S (M⁺) 250.9574. Found: 250.9577. The enantiomers were separated by HPLC (Diacel OD column, 90:10 hexanes/EtOH; 0.5 mL/min, 238 nm; (*R*)-**3c**, t_R = 28.1 min; (*S*)-**3c**, t_R = 63.7 min).

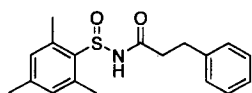
 ***N*-Dihydrocinnamoyl-*p*-chlorobenzenesulfinamide (3h).** Obtained as white solid (506 mg, 58%): mp 133-135 °C; ¹H NMR δ 2.69 (m, 2H, C(O)CH₂), 3.02 (t, J = 7.2, 2H, CH₂Ph), 7.18-7.31 (m, 7H, phenyl), 7.46 (s, 2H, phenyl); ¹³C NMR (DMSO-*d*₆) δ 31.0 (CH₂Ph), 37.7 (C(O)CH₂), 126.8, 127.6, 128.9, 129.0, 129.9, 136.9, 141.2, 143.2 (phenyl) 174.1 (C=O); HRMS calcd for C₁₅H₁₅³⁵ClNO₂S (M+H⁺) 308.0512. Found: 308.0505. The enantiomers were separated by HPLC (Diacel OD column, 90:10 hexanes/EtOH; 0.5 mL/min, 238 nm; (*R*)-**3h**, t_R = 25.1 min; (*S*)-**3h**, t_R = 27.9 min).

 ***N*-Chloroacetyl-*p*-methoxybenzenesulfinamide (4c).** Obtained as white solid (152 mg, 42%): mp 91-93 °C; ¹H NMR δ 3.89 (s, 3H, OCH₃), 4.14 (s, 2H, C(O)CH₂Cl), 7.06 (d, J = 8.7, 2H, phenyl), 7.68 (d, J = 9.3, 2H, phenyl), 8.28 (s, 1H, NH); ¹³C NMR δ 42.4 (C(O)CH₂), 55.9 (OCH₃), 115.2, 126.6, 133.9, 163.1 (phenyl), 167.2 (C=O); HRMS calcd for C₉H₁₁³⁵ClNO₃S (M+H⁺) 248.0148. Found: 248.0142. The enantiomers were separated by HPLC (Diacel OD column, 90:10 hexanes/EtOH; 0.5 mL/min, 238 nm; (*R*)-**4c**, t_R = 31.6 min; (*S*)-**4c**, t_R = 90.3 min).

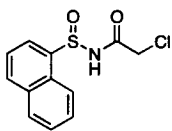
 ***N*-Dihydrocinnamoyl-*p*-methoxybenzenesulfinamide (4h).** Obtained as white solid (589 mg, 66%): mp 60-62 °C; ¹H NMR δ 2.67 (m, 2H, C(O)CH₂), 3.01 (t, J = 7.5, 2H, CH₂Ph), 3.86 (s, 3H, OCH₃), 6.98 (d, J = 8.7, 2H, phenyl), 7.18-7.31 (m, 5H, phenyl), 7.47 (d, J = 9.0, 2H, phenyl); ¹³C NMR (DMSO-*d*₆) δ 31.1 (CH₂Ph), 37.7 (C(O)CH₂), 56.4 (OCH₃), 115.3, 126.7, 127.3, 128.9, 129.0, 135.2, 141.3, 162.4 (phenyl), 174.0 (C=O); HRMS calcd for C₁₆H₁₈NO₃S (M+H⁺) 304.1007. Found: 304.1014. The enantiomers were separated by HPLC (Diacel OD column, 90:10 hexanes/EtOH; 0.5 mL/min, 238 nm; (*R*)-**4h**, t_R = 40.0 min; (*S*)-**4h**, t_R = 42.4 min).



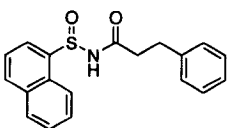
***N*-Chloroacetyl-2,4,6-trimethylbenzenesulfinamide (5c).** Obtained as white solid (195 mg, 28%): mp 89-91 °C; ^1H NMR δ 2.33 (s, 3H, PhCH_3), 2.62 (s, 6H, 2 x PhCH_3), 4.15 (m, 2H, $\text{C(O)CH}_2\text{Cl}$), 6.92 (s, 2H, phenyl); ^{13}C NMR δ 19.4 (2 x PhCH_3), 21.4 (PhCH_3), 42.6 ($\text{C(O)CH}_2\text{Cl}$), 131.5, 135.8, 138.1, 143.0 (phenyl), 166.7 (C=O); HRMS calcd for $\text{C}_{11}\text{H}_{14}^{35}\text{ClNO}_2\text{S}$ 259.0433 (M^+). Found: 259.0430. The enantiomers were separated by HPLC (Diacel OD column, 90:10 hexanes/EtOH, 0.5 mL/min, 238 nm; (*R*)-**5c**, t_R = 19.3 min; (*S*)-**5c**, t_R = 21.0 min).



***N*-Dihydrocinnamoyl-2,4,6-trimethylbenzenesulfinamide (5h).** Obtained as white solid (529 mg, 36%): mp 125-127 °C (lit.¹ 126-127 °C); ^1H NMR δ 2.31 (s, 3H, PhCH_3), 2.50 (s, 6H, 2 x PhCH_3), 2.68 (m, 2H, C(O)CH_2), 2.99 (t, J = 6.9, 2H, PhCH_2), 6.87 (s, 2H, phenyl), 7.16-7.29 (m, 5H, phenyl), 7.62 (br s, 1H, NH); ^{13}C NMR ($\text{DMSO}-d_6$) δ 19.6 (2 x PhCH_3), 21.4 (PhCH_3), 31.2 (CH_2Ph), 37.4 (C(O)CH_2), 126.7, 128.9, 128.9, 131.1, 136.2, 138.2, 141.4, 141.6 (phenyl), 174.1 (C=O). The enantiomers were separated by HPLC (Diacel OD column, 90:10 hexanes/EtOH, 0.5 mL/min, 238 nm; (*R*)-**5h**, t_R = 17.6 min; (*S*)-**5h**, t_R = 21.2 min).

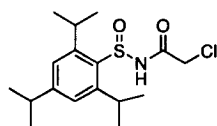


***N*-Chloroacetyl-1-naphthylsulfinamide (6c).** Obtained as white solid (92 mg, 22%): mp 117-119 °C; ^1H NMR δ 4.13 (d, J = 4.8, 2H, $\text{C(O)CH}_2\text{Cl}$), 7.61-7.72 (m, 3H, phenyl), 7.98 (m, 2H, phenyl), 8.08 (d, J = 8.1, 1H, phenyl), 8.28 (m, 1H, phenyl); ^{13}C NMR δ 43.2 ($\text{C(O)CH}_2\text{Cl}$), 122.4, 124.3, 126.0, 127.7, 128.5, 128.8, 129.6, 132.9, 133.9, 138.6 (phenyl), 168.4 (C=O); HRMS calcd for $\text{C}_{12}\text{H}_{11}^{35}\text{ClNO}_2\text{S}$ ($\text{M}+\text{H}^+$) 268.0199. Found: 268.0192. The enantiomers were separated by HPLC (Diacel OD column, 90:10 hexanes/EtOH, 0.5 mL/min, 238 nm; (*R*)-**6c**, t_R = 23.9 min; (*S*)-**6c**, t_R = 90.2 min).



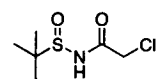
***N*-Dihydrocinnamoyl-1-naphthylsulfinamide (6h).** Obtained as white solid (302 mg, 36%): mp 113-115 °C; ^1H NMR δ 2.67 (t, J = 7.5, 2H, C(O)CH_2), 2.99 (m, 2H, CH_2Ph), 7.12-7.28 (m, 5H, phenyl), 7.54-7.65 (m, 3H, phenyl), 7.87-8.18 (m, 4H, phenyl); ^{13}C NMR δ 31.0 (CH_2Ph), 37.5 (C(O)CH_2), 122.4, 124.2, 126.0, 126.7, 127.5, 128.4, 128.9, 128.9, 129.6, 132.7, 133.9, 139.1, 141.2 (phenyl), 174.0 (C=O); HRMS calcd for $\text{C}_{19}\text{H}_{18}\text{NO}_2\text{S}$ ($\text{M}+\text{H}^+$) 324.1058. Found: 324.1053. The enantiomers were separated by HPLC (Diacel OD col-

umn, 90:10 hexanes/EtOH, 0.5 mL/min, 238 nm; (*R*)-**6h**, t_R = 24.2 min; (*S*)-**6h**, t_R = 37.4 min).



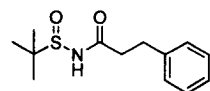
***N*-Chloroacetyl-2,4,6-triisopropylbenzenesulfinamide (7c).**

Obtained as white solid (140 mg, 15%): mp 119-121 °C; ^1H NMR δ 1.27 (d, J = 6.9, 12H, 2 x $\text{CH}(\text{CH}_3)_2$), 1.37 (d, J = 6.9, 6H, $\text{CH}(\text{CH}_3)_2$), 2.92 (sept, J = 6.9, 1H, $\text{CH}(\text{CH}_3)_2$), 3.93 (m, 2H, 2 x $\text{CH}(\text{CH}_3)_2$), 4.18 (s, 2H, $\text{C}(\text{O})\text{CH}_2\text{Cl}$), 7.14 (s, 2H, phenyl), 8.74 (br s, 1H, NH); ^{13}C NMR (DMSO- d_6) δ 24.3, 24.4, 24.5, 25.4, 28.8, 34.5, 39.5 (3 x *i*-Pr), 43.1 ($\text{C}(\text{O})\text{CH}_2\text{Cl}$), 123.5, 135.2, 149.6, 153.3 (phenyl); HRMS calcd for $\text{C}_{17}\text{H}_{27}^{35}\text{ClNO}_2\text{S}$ ($\text{M}+\text{H}^+$) 344.1451. Found: 344.1443. The enantiomers were separated by HPLC (Diacel OD column, 90:10 hexanes/EtOH, 0.5 mL/min, 238 nm; (*R* or *S*)-**7c**, t_R = 8.7 min; (*R* or *S*)-**7c**, t_R = 9.1 min).



***N*-Chloroacetyl-*tert*-butanesulfinamide (8c).**

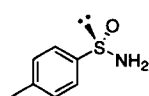
Obtained as white solid (191 mg, 29%): mp 56-58 °C; ^1H NMR (200 MHz) δ 1.32 (s, 9H, $(\text{CH}_3)_3$), 4.15 (m, 2H, CH_2Cl), 7.94 (br s, 1H, NH); ^{13}C NMR δ 22.3 ($(\text{CH}_3)_3$), 42.9 ($\text{C}(\text{O})\text{CH}_2\text{Cl}$), 58.1, ($\text{C}(\text{CH}_3)_3$), 167.3 ($\text{C}=\text{O}$); HRMS calcd for $\text{C}_6\text{H}_{13}^{35}\text{ClNO}_2\text{S}$ (MH^+) 198.0355. Found: 198.0360. The enantiomers were separated by HPLC (Diacel OD column, 90:10 hexanes/EtOH, 0.5 mL/min, 222 nm; (*R* or *S*)-**8c**, t_R = 13.6 min; (*R* or *S*)-**8c**, t_R = 16.9 min).



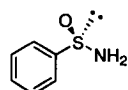
***N*-Dihydrocinnamoyl-*tert*-butanesulfinamide (8h).**

Obtained as white solid (450 mg, 71%): mp 63-65 °C; ^1H NMR (200 MHz) δ 1.17 (s, 9H, $(\text{CH}_3)_3$), 2.72 (m, 2H, $\text{C}(\text{O})\text{CH}_2$), 2.99 (t, J = 7.4, 2H, $\text{C}(\text{O})\text{Ph}$), 7.22-7.28 (m, 5H, phenyl), 7.62 (br s, 1H, NH); ^{13}C NMR δ 22.3 ($(\text{CH}_3)_3$), 31.3 (CH_2Ph), 37.1 ($\text{C}(\text{O})\text{CH}_2$), 57.7 ($\text{C}(\text{CH}_3)_3$), 126.6, 128.6, 128.8, 140.3 (phenyl), 173.6 ($\text{C}=\text{O}$). The enantiomers were separated by HPLC (Diacel OD column, 90:10 hexanes/EtOH, 0.5 mL/min, 222 nm; (*R* or *S*)-**8h**, t_R = 13.6 min; (*R* or *S*)-**8h**, t_R = 16.9 min).

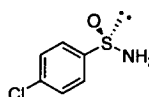
Synthesis of enantiopure sulfinamide standards. Enantiopure sulfinamides were prepared using literature procedures.^{8,9} These compounds of known absolute stereochemical configuration were used as HPLC standards to determine the enantioselectivity of enzymatic resolutions. Their relevant analytical data are given below:



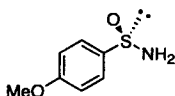
(S)-p-Toluenesulfinamide ((S)-1). Prepared from (1*R*,2*S*,5*R*)-(-)-menthyl (S)-*p*-toluenesulfinate as previously described.⁸ This was obtained as a white solid (620 mg, 59% overall yield): mp 111-113 °C; ¹H NMR (400 MHz) δ 2.42 (s, 3H, PhCH₃), 4.35 (br s, 2H, -NH₂), 7.30 (d, *J* = 8.0, 2H, phenyl), 7.61 (d, *J* = 8.4, 2H, phenyl); ¹³C NMR δ 21.8 (PhCH₃), 125.6, 129.8, 141.7, 143.6 (phenyl). The ee was determined to be 97% by HPLC (Diacel OD column, 90:10 hexanes/EtOH, 1.0 mL/min, 238 nm; (R)-1, *t*_R = 8.7 min; (S)-1, *t*_R = 10.3 min).



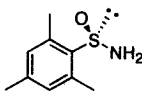
(R)-Benzenesulfinamide ((R)-2). Prepared from (1*R*,2*S*)-(+)-*cis*-1-amino-2-indanol as previously described.⁹ This was obtained as a white solid (180 mg, 37% overall yield): mp 91-93 °C; ¹H NMR (400 MHz) δ 4.38 (br s, 2H, NH₂), 7.50 (m, 3H, phenyl), 7.74 (m, 2H, phenyl); ¹³C NMR δ 125.6, 129.1, 131.3, 146.6 (phenyl). The ee was determined to be 96% by HPLC (Diacel AD column, 90:10 hexanes/EtOH, 1.0 mL/min, 238 nm; (R)-2, *t*_R = 20.4 min; (S)-2, *t*_R = 23.0 min).



(R)-p-Chlorobenzenesulfinamide ((R)-3). Prepared from (1*R*,2*S*)-(+)-*cis*-1-amino-2-indanol as previously described.⁹ This was obtained as a white solid (100 mg, 16% overall yield): mp 135-137 °C; ¹H NMR (400 MHz) δ 4.41 (s, 2H, NH₂), 7.47 (d, *J* = 8.8, 2H, phenyl), 7.66 (d, *J* = 8.4, 2H, phenyl); ¹³C NMR δ 127.3, 129.3, 137.7, 145.0. The ee was determined to be 95% by HPLC (Diacel OD column, 90:10 hexanes/EtOH, 1.0 mL/min, 238 nm; (R)-3, *t*_R = 22.4 min; (S)-3, *t*_R = 37.1 min).

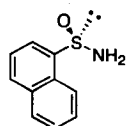


(R)-p-Methoxybenzenesulfinamide ((R)-4). Prepared from (1*R*,2*S*)-(+)-*cis*-1-amino-2-indanol as previously described.⁹ This was obtained as a white solid (80 mg, 14% overall yield): mp 111-113 °C; ¹H NMR (400 MHz) δ 3.85 (s, 3H, -OCH₃), 4.36 (s, 2H, NH₂), 6.98 (d, *J* = 7.6, 2H, phenyl), 7.64 (d, *J* = 7.6, 2H, phenyl); ¹³C NMR δ 55.9, 114.5, 127.3, 137.9, 161.9. The ee was determined to be 95% by HPLC (Diacel OD column, 90:10 hexanes/EtOH, 1.0 mL/min, 238 nm; (R)-4, *t*_R = 29.4 min; (S)-4, *t*_R = 43.9 min).



(R)-2,4,6-Trimethylbenzenesulfinamide ((R)-5). Prepared from (1*R*,2*S*)-(-)-*cis*-1-amino-2-indanol as previously described.⁹ This was obtained as a white solid (20 mg, 3% overall yield): mp 116-118 °C; ¹H NMR (400 MHz) δ 2.29 (s, 3H, PhCH₃), 2.61 (s, 6H, 2 x PhCH₃), 4.41 (br s, 2H, NH₂), 6.86 (s, 2H, phenyl);

^{13}C NMR δ 19.7 (2 x PhCH_3), 21.4 (PhCH_3), 131.1, 136.4, 139.0, 140.9 (phenyl). The ee was determined to be 68% by HPLC (Diacel OD column, 90:10 hexanes/EtOH, 0.5 mL/min, 238 nm; (*R*)-**5**, t_R = 13.4 min; (*S*)-**5**, t_R = 12.3 min).



(*R*)-1-Naphthylsulfinamide ((*R*)-6). Prepared from (1*R*,2*S*)-(+)-*cis*-1-amino-2-indanol as previously described.⁹ This was obtained as a white solid (160 mg, 25% overall yield): mp 151-153 °C; ^1H NMR (400 MHz) δ 4.40 (br s, 2H, NH_2), 7.56-7.64 (m, 3H, phenyl), 7.89-8.01 (m, 3H, phenyl), 8.22 (d, J = 8.0, 1H, phenyl); ^{13}C NMR ($\text{DMSO}-d_6$) δ 122.9, 123.8, 125.8, 127.0, 127.4, 129.2, 129.3, 131.6, 133.9, 143.8 (phenyl). The ee was determined to be 93% by HPLC (Diacel OD column, 90:10 hexanes/EtOH, 1.0 mL/min, 238 nm; (*R*)-**6**, t_R = 52.2 min; (*S*)-**6**, t_R = 49.9 min).

Cultivation and purification of subtilisin E. Protease deficient *B. subtilis* DB104 was transformed with vector pBE3, as previously described.^{10,11} Transformed cells were grown in 2XSG¹¹ media (500 mL) with shaking for 10 h at 37 °C. This culture was used to inoculate 14 L of 2XSG¹¹ media in a 20 L fermentor. After 42 hours (OD_{600} = 9.1), the culture was cooled and centrifuged. The cell pellet was discarded and the supernatant was concentrated using a 0.45 μm cartridge (8,000 MW cutoff) equipped with a 1.2 μm prefilter. The concentrate was brought to 70% saturation with NH_4SO_4 (472 g/L), stirred overnight and then centrifuged at 8,000 rpm for 1.5 h. The precipitate was resuspended and dialyzed for 48 h against 8 L of 10 mM HEPES (pH 7.5, 1 mM CaCl_2). The sample was passed through a bed of DE-52 anion exchange cellulose with vacuum. The clarified solution was then concentrated by passage through an 8,000 MW ultra filtration cartridge. The retentate was brought to 1.8 M NH_4SO_4 , centrifuged and the supernatant was passed through a 0.45 μm filter.

Subtilisin E was purified on a BioCad purification system (Applied Biosystems, Foster, USA) using a Poros 20HP2 (10 x 100) column.¹² The sample was loaded and washed with 1.8 M NH_4SO_4 in 20 mM HEPES (pH 7.0) and then eluted with a linear gradient of 1.8 M to 0 M NH_4SO_3 in 20 mM HEPES (pH 7.0). The enzyme activity was monitored by adding 90 μL of assay solution [0.2 mM succinyl-AAPF-*p*-nitroanilide (suc-AAPF-*p*NA) / 100 mM Tris pH 8.0 / 10 mM CaCl_2] to 10 μL of eluent and follow-

ing the reaction at 410 nm at 37 °C for 15 min. The specific activity toward suc-AAPF-*p*NA was 21 U/mg (lit.¹⁰ 17.2 U/mg). Fractions containing protein were concentrated by passage through an 8,000 MW cutoff ultrafiltration cartridge and diafiltered in 10 mM HEPES (pH 7.5, 1 mM CaCl₂). The final retentate was frozen and lyophilized to give ca. 300 mg of subtilisin E.

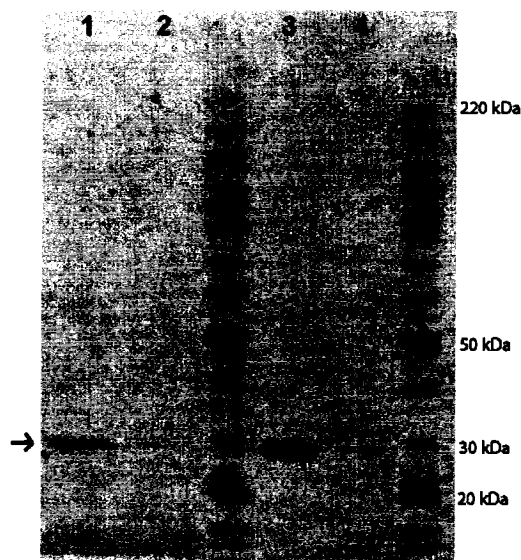
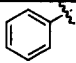
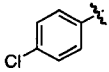
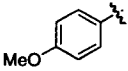
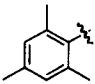


Figure A2.1. SDS-polyacrylamide gel electrophoresis of subtilisin E from *B. subtilis* DB104 carrying pBE3. The gel was stained by Coomassie Blue. To prevent autolysis, subtilisin E was treated with PMSF (phenylmethylsulfonylfluoride) before denaturation. PMSF (phenylmethylsulfonylfluoride) inhibited subtilisin E prepared from culture medium of *B. subtilis* DB104 carrying pBE3 is shown in *lane 1*. Subtilisin E prepared from culture medium of *B. subtilis* DB104 carrying pBE3 is shown in *lane 2*. Purified PMSF-inhibited subtilisin E is shown in *lane 3*. Purified subtilisin E is shown in *lane 4*.

Table A2.1. Enantioselectivity of *Bacillus subtilis* var. biotecnus A with **2c-5c**

$\begin{array}{c} \text{O} \\ \parallel \\ \text{R}-\text{S}-\text{N}-\text{C}(=\text{O})-\text{CH}_2-\text{Cl} \\ \\ \text{H} \end{array}$						
	R	%c _{app} ^a	ee _s (%) ^b	ee _p (%) ^b	E _{app}	E _{true} ^c
2c		47	81	90	48	>150 ^d
3c		45	77	96	103	>150 ^e
4c		49	87	90	53	>150 ^d
5c		41	66	94	64	97 ^e

^a% Conversion: amount of sulfinamide formed in 6 h. ^b% Enantiomeric excess. Enantiomeric excess of substrate and product were determined by HPLC analysis on Daicel Chiralcel OD or AD columns at 238 nm or 222 nm. ^cEnantiomeric Ratio: the enantiomeric ratio *E* measures the relative rate of hydrolysis of the fast enantiomer as compared to the slow enantiomer as defined by Sih (Chen, C.S.; Fujimoto, Y.; Girdaukas, G.; Sih, C.J. *J. Am. Chem. Soc.* **1982**, *104*, 7294-7299). ^dCorrected for ca. 4% chemical hydrolysis. ^eCorrected for ca. 1% chemical hydrolysis.

Molecular modelling details for (*R*)-1h and (*S*)-1h tetrahedral intermediates bound to subtilisin E. Modelling **1h** with subtilisin E gave one productive conformation for each enantiomer. The two other plausible conformations encountered severe steric clash with the protein.

Productive conformer of (*R*)-1h (Figure 2.2). The productive complex of (*R*)-1h had its *p*-tolyl group in the S₁' pocket and sulfoxide oxygen exposed to solvent (water). All hydrogen bond angles were >120° and all five hydrogen bond lengths were <3.1 Å. The *p*-tolyl group appears to just fit in the S₁' pocket. Met222 in the bottom of the S₁' pocket (C_{ortho}-C_e distance = 3.74 Å)¹³, Tyr217 at the back of the S₁' pocket (C_{para} -

$C_{\text{meta}}(\text{Tyr217})$ distance = 3.93 Å, $C_{\text{meta}} - C_{\text{para}}(\text{Tyr217})$ distance = 3.94 Å, $p\text{-CH}_3 - C_{\text{meta}}(\text{Tyr217})$ distance = 3.64 Å and $p\text{-CH}_3 - C_{\text{para}}(\text{Tyr217})$ distance = 3.93 Å)¹³ and catalytic His64 ($C_{\text{ortho}} - C_{\delta 2}$ distance = 3.72 Å and $C_{\text{meta}} - C_{\delta 2}$ distance = 3.83 Å)¹³ bumped the *p*-tolyl group. This tight fit suggests a favourable hydrophobic interaction between the *p*-tolyl group and the S_1' residues.

Non-productive conformer of (*R*)-1h. The *p*-tolyl group of non-productive (*R*)-1h encounters steric clash with Gly 219 ($C_{\text{ortho}} - C_{\alpha}$ distance = 3.43 Å)¹³ and catalytic Asn 155 ($C_{\text{ipso}} - N_{\delta 2}$ distance = 3.41 Å, $C_{\text{ortho}} - N_{\delta 2}$ distance = 3.10 Å, $C_{\text{meta}} - N_{\delta 2}$ distance = 3.37 Å)¹³. This steric clash results in the sulfoxide oxygen being forced out of the S_1' leaving-group pocket.

Productive conformer of (*S*)-1h (Figure 2.2). The productive complex of (*S*)-1h had its sulfoxide oxygen in the S_1' pocket and *p*-tolyl group exposed to solvent water. All hydrogen bond angles were >120° and all five hydrogen bond lengths were <3.1 Å. The sulfoxide oxygen fits well in the S_1' pocket ($O_s - C_{\epsilon}(\text{Met222})$ distance = 5.64 Å and $O_s - C_{\delta 2}(\text{His64})$ distance = 3.89 Å)¹³ and the protein does not hinder the *p*-tolyl group. Unlike the favoured enantiomer, the smaller oxygen does not make steric contact with S_1' residues. Although the slow-reacting (*S*)-enantiomer avoids steric hindrances, it also lacks favourable hydrophobic interactions between the *p*-tolyl group and the S_1' residues.

Non-productive conformer of (*S*)-1h The *p*-tolyl group of non-productive (*S*)-1h encounters steric clash with catalytic His 64 ($C_{\text{ortho}} - C_{\delta 2}$ distance = 3.58 Å, $C_{\text{meta}} - C_{\delta 2}$ distance = 3.62 Å)¹³. This steric clash results in the *p*-tolyl group being forced out of the S_1' leaving-group pocket.

Molecular modelling force field (AMBER) parameters for the sulfinamide group. (1) Atom labels: sulfur, SO; oxygen, OX. (2) Bond parameters: SO-OX, bond length = 1.48 Å, $K_r = 680 \text{ kcal/Å}$; SO-NT, bond length = 1.71 Å, $K_r = 230 \text{ kcal/Å}$; SO-CA, bond length = 1.78 Å, $K_r = 222 \text{ kcal/Å}$. (3) Angle parameters: SO-NT-H, $K_{\theta} = 35 \text{ kcal/rad}^2$, $\theta_{eq} = 108.9^\circ$; SO-CA-CA, $K_{\theta} = 100 \text{ kcal/rad}^2$, $\theta_{eq} = 118.8^\circ$; OX-SO-CA, $K_{\theta} = 74 \text{ kcal/rad}^2$, $\theta_{eq} = 107.6^\circ$; NT-SO-OX, $K_{\theta} = 100 \text{ kcal/rad}^2$, $\theta_{eq} = 112.2^\circ$; NT-SO-CA $K_{\theta} = 100 \text{ kcal/rad}^2$, $\theta_{eq} = 97.1^\circ$. (4) Dihedral angles parameters: X-NT-SO-X, $V_n = 5.0 \text{ kcal/rad}^2$, $\gamma = 0^\circ$, $n = 3$; NT-SO-CA-CA, $V_n = 0.0 \text{ kcal/rad}^2$, $\gamma = 0^\circ$, $n = 2$; OX-SO-CA-

CA, $V_n = 0.0 \text{ kcal/rad}^2$, $\gamma = 0^\circ$, $n = 2$. (5) Nonbonded parameters: SO, $R^* = 2.00 \text{ \AA}$, $\epsilon = 0.20 \text{ kcal/mol}$; OX, $R^* = 1.60 \text{ \AA}$, $\epsilon = 0.20 \text{ kcal/mol}$.

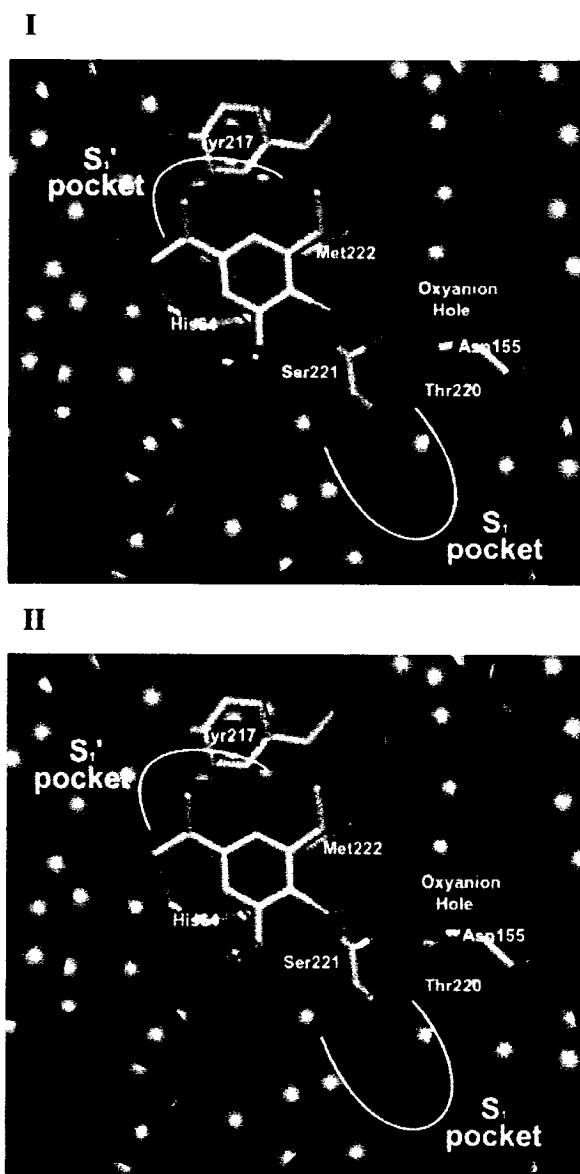


Figure A2.2. Catalytically productive tetrahedral intermediates for the subtilisin E catalyzed hydrolysis of (*R*)-**7c** (I) and (*S*)-**7c** (II) as identified by molecular modelling. The important active site and substrate atoms (sticks) are coloured as follows: grey (carbon), red (oxygen), blue (nitrogen), orange (sulfur) and pink (chlorine). Surrounding atoms (space fill) of subtilisin are shown in blue. For clarity, all hydrogen atoms and water

molecules are hidden. Both I and II maintain all catalytically essential hydrogen bonds and the chloroacetyl group binds in the S_1 pocket. The triisopropyl benzene group (Large) or sulfoxide oxygen (Medium) was bound in the leaving-group S_1' pocket. However, both groups were forced out of the S_1' pocket because of steric hindrance between the triisopropyl group and active site residues. The productive orientation of slow-reacting (*S*)-**7c** differs from (*S*)-**1h** because of steric clash between the triisopropyl group and the oxyanion residue Asn155 when the sulfoxide oxygen is bound in the S_1' pocket. This forces the substrate to rotate about the S-N bond, which places the triisopropyl group above the S_1' pocket. This conformation is similar to the productive orientation of fast-reacting (*R*)-**7c**. Since the aryl group of both (*R*)-**7c** and (*S*)-**7c** bind above the S_1' pocket, there is little difference in the binding conformations and the enantioselectivity is low ($E = 1.2$).

References (Chapter 2 – Appendix)

1. Backes, B. J.; Dragoli, D. R.; Ellman, J. A. *J. Org. Chem.* **1999**, *64*, 5472-5478.
2. Dahn, H.; Van Toan V.; Ung Truong, M. -N. *Magn. Reson. Chem.* **1991**, *29*, 897-903.
3. We are unable to account for the discrepancy with the previously reported mp value. However, the ^1H and ^{13}C NMR spectra correspond to the proposed structure of **7** and agree with the previously reported data.¹
4. Netscher, T.; Prinzbach, H. *Synthesis* **1987**, 683-686.
5. Gontcharov, A.V.; Liu, H.; Sharpless, K.B. *Org. Lett.* **1999**, *1*, 783-786.
6. Cogan, D.A.; Liu, G.; Kim, K.; Backes, B.J.; Ellman, J.A. *J. Am. Chem. Soc.* **1998**, *120*, 8011-8019.
7. Chen, F.M.F.; Kuroda, K.; Benoiton, N.L. *Synthesis* **1978**, 928-929.
8. Davis, F. A.; Xhang, Y.; Andemichael, Y.; Fang, T.; Fanelli, D. L.; Zhang, H. *J. Org. Chem.* **1999**, *64*, 1403-1406.
9. Han, Z.; Krishnamurthy, D.; Grover, P.; Fang, K.; Senanayake, C.H. *J. Am. Chem. Soc.* **2002**, *124*, 7880-7881.
10. Zhao, H.; Arnold, F. H. *Proc. Natl. Acad. Sci. USA* **1997**, *94*, 7997-8000.
11. Harwood, C. R.; Cutting, S. M. *Molecular Biological Methods for Bacillus*, John Wiley and Sons, England, 1990, pp 33-35, 391-402.

12. Cho, S.-J.; OH, S.-H.; Pridmore, R. D.; Juillerat, M. A.; Lee, C.-H. *J. Agric. Food Chem.* **2003**, *51*, 7664-7670.
13. The van der Waals distance for CH-C = 3.99 Å, CH-N = 3.84 Å, CH-S = 4.09 Å and O-HC = 3.81 Å. These were estimated from the van der Waals radii of carbon (1.70 Å), nitrogen (1.55 Å), sulfur (1.80 Å) or oxygen (1.52 Å) and hydrogen (1.20 Å) and the C-H bond length (1.09 Å) or O-H bond length (0.96 Å) from Bondi, A. *J. Phys. Chem.* **1964**, *68*, 441-451.

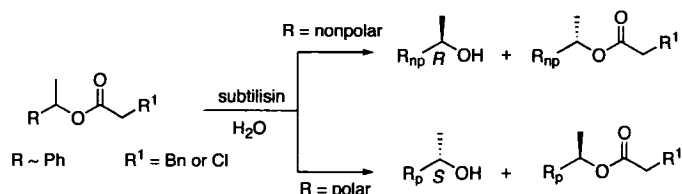
Chapter 3

Explaining the molecular basis for enzyme enantioselectivity is still a challenge in organic chemistry. In this chapter we decipher the molecular basis of subtilisin enantioselectivity toward secondary alcohols using a combination of substrate-mapping experiments and molecular modelling. Not only do we develop a qualitative model for rationalizing and predicting enantiopreference, we show a quantitative relationship between substituent polarity and subtilisin enantioselectivity. Our new model provides a strategy to increase enantioselectivity by modifying substrate.*

* This chapter is a copy of a published communication and is reproduced with permission from the *Journal of the American Chemical Society*, Vol. 127, Christopher K. Savile and Romas J. Kazlauskas, "How Substrate Solvation Contributes to the Enantioselectivity of Subtilisin toward Secondary Alcohols", 12228-12229, Copyright 2005, American Chemical Society (see Appendix II for reprint).

How substrate solvation contributes to the enantioselectivity of subtilisin toward secondary alcohols

Abstract



The current rule to predict the enantioselectivity of subtilisin toward secondary alcohols is based on the size of the substituents at the stereocenter and implies that the active site contains two differently sized pockets for these substituents. Several experiments are inconsistent with the current rule. First, the x-ray structures of subtilisin show there is only one pocket (the S_1' pocket) approximately the size of a phenyl group to bind secondary alcohols. Second, the rule often predicts the incorrect enantiomer for reactions in water. To resolve these contradictions, we refine the current rule to show that subtilisin binds only one substituent of a secondary alcohol and leaves the other in solvent. To test this refined empirical rule, we show that the enantioselectivity of a series of secondary alcohols in water varied linearly with the difference in hydrophobicity ($\log P/P_0$) of the substituents. This hydrophobicity difference accounts for the solvation of one substituent in water.

3.1 Communication

Enantioselective enzymes, especially hydrolases, are useful catalysts to make enantiomerically pure pharmaceuticals, agrochemicals, and fine chemicals.¹ Several empirical rules predict which substrate/hydrolase combinations work best. For example, a rule to predict the enantiopreference of subtilisin toward secondary alcohols is based on the size of the substituents at the stereocentre (Figure 3.1a).^{2,3} This model implies subtilisin has two differently-sized pockets for these substituents, but several experiments are inconsistent with this rule. First, the x-ray crystal structure shows only one pocket (the S_1' pocket) to bind secondary alcohols.⁴ Second, the rule often predicts the incorrect enantiomer for reactions in water. In this communication, we resolve this contradiction with a more general rule that shows subtilisin binds only one substituent of a secondary alcohol and leaves the other in solvent. This refined rule allows quantitative design of enantioselective reactions and rationalizes why solvent alters the enantioselectivity.

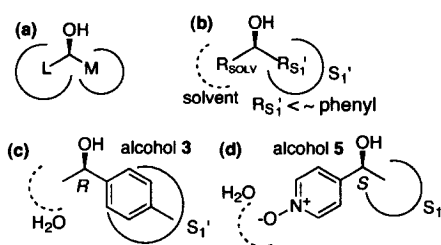


Figure 3.1. Empirical rules that predict the enantiopreference of subtilisins toward secondary alcohols. (a) A rule based on relative substituent size, where L is the large substituent and M is the medium substituent, is reliable in organic solvent. (b) A revised rule that is reliable in water as well. One substituent (R_{SOLV}) remains in solvent, while the other ($R_{S1'}$) binds in a hydrophobic pocket. (c) In water, the nonpolar aryl group of alcohol 3 favours binding in the S_1' pocket, thus favouring the (*R*)-enantiomer. (d) An isosteric substrate alcohol 5 contains a polar aryl group that favours the water-solvated orientation, thus favouring the (*S*)-enantiomer.

X-Ray crystal structures of subtilisin reveal one pocket – the S_1' pocket – that binds on substituent of the alcohol portion of an ester. Molecular modelling of a tetrahedral intermediate for subtilisin E-catalyzed hydrolysis of **1a** reveals that (*S*)-**1a** places the

methyl group in the S_1' pocket, while (*R*)-**1a** places the phenyl group in this pocket (see Chapter 3 - Appendix Figure A3.2). In both cases, the other substituent remains in the solvent. Binding the methyl group of (*S*)-**1a** in this pocket avoids some steric interactions between the pocket and the phenyl group, while binding the phenyl group of (*R*)-**1a** adds a good hydrophobic interaction between the pocket and the phenyl. The S_1' pocket is a shallow crevice large enough to accommodate *para*-substituted aryl groups, but too small for multi-substituted aryl groups.

Table 3.1. Enantioselectivity of subtilisin BPN', Carlsberg- and E-catalyzed hydrolysis of **1a-13a**^a

^a $R^1 = \text{CH}_2\text{-C}_6\text{H}_5$
^b $R^1 = \text{Cl}$

^{1a} $R = \text{C}_6\text{H}_5$
^{2a} $R = 4\text{-pyridyl}$
^{3a} $R = p\text{-tolyl}$
^{4a} $R = 4\text{-F}_3\text{C-C}_6\text{H}_4$
^{5a} $R = 4\text{-pyridine N-oxide}$
^{6a} $R = 4\text{-}i\text{-Pr-C}_6\text{H}_4$

^{7a} $R = 4\text{-O}_2\text{N-C}_6\text{H}_4$
^{8a} $R = 4\text{-HOOC-C}_6\text{H}_4$
^{9a} $R = 4\text{-}i\text{-Bu-C}_6\text{H}_4$
^{10b} $R = 2\text{-mesityl}$
^{11a} $R = 1\text{-naphthyl}$
^{12b} $R = 2,4,6\text{-}i\text{-Pr-C}_6\text{H}_2$
^{13a} $R = t\text{-Bu}$

Enantioselectivity, E^b					
entry	substrate	$\log P/P_0$ diff. ^c	subtilisin E	subtilisin Carlsberg	subtilisin BPN'
1	1a	+1.1	7.0 (<i>R</i>)	1.2 (<i>R</i>)	15 (<i>R</i>)
2	2a	-0.3	1.5 (<i>R</i>)	1.7 (<i>S</i>)	2.6 (<i>R</i>)
3	3a	+1.6	16 (<i>R</i>)	1.1 (<i>S</i>)	37 (<i>R</i>)
4	4a	+1.9	7.7 (<i>R</i>)	2.2 (<i>S</i>)	9.9 (<i>R</i>)
5	5a	-2.2	4.5 (<i>S</i>)	3.1 (<i>S</i>)	2.5 (<i>S</i>)
6	<i>N</i> -HCinn- <i>p</i> - TS ^d	+3.9	>150 (<i>R</i>) ^e	11 (<i>R</i>) ^e	50 (<i>R</i>) ^f
7	6a	+2.6	110 (<i>R</i>)	2.5 (<i>R</i>)	109 (<i>R</i>)
8	7a	+0.7	2.8 (<i>R</i>)	2.3 (<i>S</i>)	4.2 (<i>R</i>)
9	8a	-3.1	5.5 (<i>S</i>)	3.6 (<i>S</i>)	6.2 (<i>S</i>)
10	9a ^g		20 (<i>R</i>)	2.0 (<i>R</i>)	18 (<i>R</i>)
11	10b ^g		17 (<i>R</i>)	1.7 (<i>S</i>)	4.9 (<i>R</i>)
12	11a ^g		1.8 (<i>R</i>)	3.1 (<i>S</i>)	3.1 (<i>S</i>)
13	12b		n.r. ^h	n.r.	n.r.
14	13a		n.r.	n.r.	n.r.

^aSee Appendix Tables A3.2-A3.5 for complete details. ^bEnantioselectivity: the enantiomeric ratio E measures the relative rate of hydrolysis of the fast enantiomer as compared to the slow enantiomer as defined by Sih.⁵ ^cSubstituent hydrophobicity difference ($\log P/P_0$ $R_{\text{Large substituent}} - \log P/P_0$ $R_{\text{Medium substituent}}$). ^d*N*-dihydrocinnamoyl-*p*-toluenesulfonamide. This is a secondary alcohol ester isostere with the methine replaced

with sulfur and the methyl replaced with oxygen. ^eref. 6. ^fref 7. ^gNot included in Figure 3.2 because one substituent is much larger than phenyl. ^hNo reaction.

Although the rule in Figure 3.1a is reliable for reactions in organic solvents,^{2,3} it is not reliable in water. For the substrates in Table 3.1, the rule in Figure 3.1a predicts that the (*S*)-enantiomer will react faster. In organic solvent, the subtilisin-catalyzed transesterification of secondary alcohols **1-13** with dihydrocinnamic acid vinyl ester favoured the predicted (*S*)-enantiomer for twenty-six out of twenty-nine reactions with varying enantioselectivity ($E = 1.5$ to 66; see Chapter 3 - Appendix Tables A3.2-A3.5). In water, however, subtilisin favoured hydrolysis of the opposite (*R*)-enantiomer in most cases - twenty out of thirty-three reactions.

To resolve these contradictions, we propose a revised rule for the enantiopreference of subtilisins with secondary alcohols (Figure 3.1b). This rule places one substituent in solvent and limits the size of the other substituent to approximately the size of a phenyl group. This rule predicts that solvation of one substituent contributes to the enantiopreference of subtilisin. In particular, placing a nonpolar substituent in water is unfavourable. Reactions in water involving methyl and nonpolar aryl substituents will favour the nonpolar aryl substituent in the S_1' pocket, opposite to that predicted based on size alone. Thus, the revised rule predicts that subtilisin favours the (*R*)-enantiomer of **3a** in water, but the (*S*)-enantiomer in organic solvents. On the other hand, with a polar aryl group such as in **5a** (4-pyridine *N*-oxide), the (*S*)-enantiomer is favoured both in water, where solvation of the pyridine *N*-oxide is favourable, and in organic solvent, where placing the pyridine *N*-oxide in the solvent avoids steric interactions in the S_1' pocket.

The revised rule in Figure 3.1b correctly predicted the (*R*)-enantiomer for reactions in water for substrates with hydrophobic aryl groups (**1a**, **3a**, **6a**, **9a**, **10a** and **11b**) for fourteen out of eighteen reactions and the (*S*)-enantiomer for substrates with hydrophilic aryl groups (**2a**, **5a** and **8a**) for eight of nine reactions. It is difficult to predict the favoured enantiomer for moderately hydrophilic aryl groups (**4a** and **7a**) and indeed the enantioselectivity in these cases is low to moderate ($E = 2.2 - 9.9$). With nonpolar substituents and nonpolar solvents, the rule simplifies to the previous rule in Figure 3.1a.

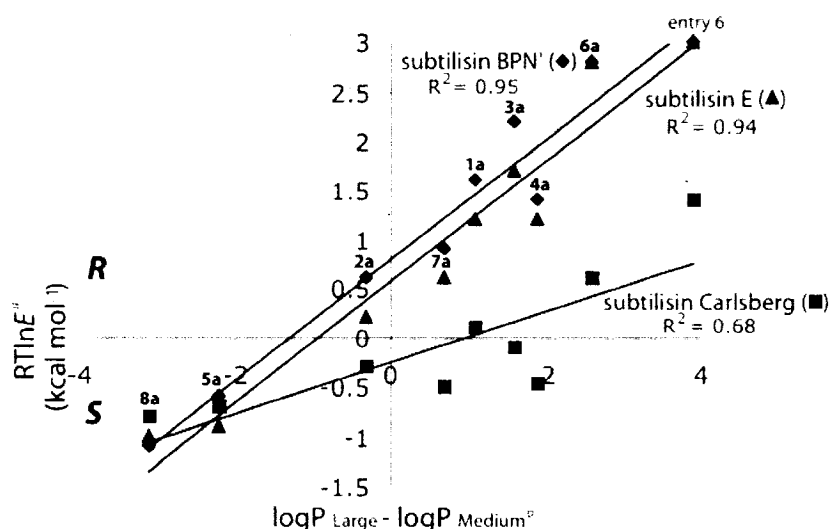


Figure 3.2. Enantioselectivity varies with the substituent hydrophobicity difference of secondary alcohols. This plot does not include substrates **9a–11a** because their substituted aryl groups are too large to fit in the S_1' pocket of subtilisins. ^aEnantioselectivity is given in energy using $\Delta\Delta G^\ddagger = -RT\ln E'$. ^bHydrophobicity partition coefficient ($\log P/P_0$).

The revised rule also suggests a quantitative link between enantioselectivity and solvation of the substituents. For example, reaction of dihydrocinnamoyl esters **1a–13a** with subtilisin E showed the enantioselectivity toward secondary alcohol esters in water varied linearly with the difference in hydrophobicity ($\log P/P_0$)⁸ between the large-sized aryl substituent and the methyl group (Figure 3.2). This hydrophobicity difference accounts for the solvation of one substituent in water and the other in the hydrophobic S_1' pocket. Increases in hydrophobicity of the aryl group favoured the (*R*)-enantiomer, while decreases favoured the (*S*)-enantiomer. For example, subtilisin E-catalyzed hydrolysis of **6a** containing the nonpolar 4-isopropylphenyl group gave (*R*)-**6** with $E = 110$, while **7a** containing the more polar, but similar sized 4-nitrophenyl group gave (*R*)-**7** with lower enantioselectivity ($E = 2.8$) and **8a** containing the hydrophilic carboxylate group gave the opposite enantiomer (*S*)-**8** with $E = 5.5$. Subtilisin BPN' showed similar enantioselectivity toward substrates **1a–13a** consistent with the similar S_1' pocket in both cases. On the other hand, subtilisin Carlsberg showed different behavior consistent with a slightly narrower and shorter S_1' pocket. The enantioselectivity of subtilisin Carlsberg was lower and the change in enantioselectivity (slope of the line in Figure 3.2) varied less with changes in

substituent hydrophobicity, presumably due to weaker interaction between substrate and S_1' pocket. All three subtilisins show slightly lower enantioselectivity toward the (*R*)-enantiomer of the *p*-CF₃ derivative **4a** than predicted using logP/*P*₀ values. This difference may be due to either stronger interaction of the CF₃ group with water than predicted from logP/*P*₀ values⁹ or weaker interaction of the CF₃ group with the S_1' pocket.

This revised model also predicts that increasing the polarity difference between the substituents will increase the enantioselectivity of subtilisins. Consistent with this prediction, subtilisin shows high enantioselectivity toward arylsulfonamides (entry 6).⁶ This toluenesulfonamide is a polar isostere of **3a**, where a polar oxygen replaces the methyl group and thereby increases the difference in polarity between the two substituents (logP difference = +1.6 for **3a** and +3.9 for the sulfonamide). The enantioselectivity of the subtilisin-E-catalyzed hydrolysis increases from *E* = 16 for **3a** to *E* = >150 for the sulfonamide.

Increasing the hydrophobicity difference by adding nonpolar substituents to the aryl group is not a good strategy to increase enantioselectivity because it creates a substituent too large for the S_1' pocket. For example, compounds **9a-11a** contain very large aryl groups. The poor fit of this aryl group in S_1' pocket destabilizes reaction of the (*R*)-enantiomer. Subtilisins favour the (*S*)-enantiomer in these cases, but the enantioselectivity is usually low.

This model also rationalizes how changing the organic solvent can increase the enantioselectivity of subtilisins. The enantioselectivity of subtilisin Carlsberg toward 1-phenethyl alcohol (**1**) increases from *E* = 3 (*S*) in acetonitrile to *E* = 54 (*S*) in benzene, likely due to better solvation of the solvent-exposed phenyl substituent in benzene as compared to acetonitrile.² Researchers previously explained changes in enantioselectivity of subtilisins toward chiral acids using a similar rationale for solvation of the solvent-exposed groups,^{10,11} but our model is the first to use this approach for chiral alcohols.

Unlike subtilisins, which bind substrate in an extended conformation,¹² lipases bind substrate in a folded conformation.¹³ This folding and the deeper hydrophobic pockets in lipases place both substituents of typical secondary alcohols in hydrophobic pockets that substantially shield the substituents from the solvent.¹⁴ For this reason, the enantioselectivity of lipase-catalyzed resolutions of secondary alcohols shows less variation with

changes in substituent polarity¹⁵ or solvent.¹⁶ Chapter 3 - Appendix Table A3.5 shows that lipase from *Burkholderia cepacia* (PCL) favours the (*R*)-enantiomer for all compounds in Table 3.1 and shows no reversal in enantiopreference upon changing from water to organic solvent.

In conclusion, this revised model of the enantioselectivity of subtilisins toward secondary alcohols is consistent with the structure of subtilisin, rationalizes why enantioselectivity changes and even reverses with changes in solvent, and provides a strategy to increase enantioselectivity by modifying the substrate.

Acknowledgements

We thank McGill University and University of Minnesota for financial support, Dr. F. Schendel and R. Dillingham (University of Minnesota Biotechnology Institute) for the large-scale fermentation and purification of subtilisins BPN' and E and the Minnesota Supercomputing Institute for access and support for molecular modelling computers and software.

References

1. Faber, K. *Biotransformations in Organic Chemistry*, 5th ed. Springer-Verlag, Berlin, 2004; Drauz, K.; Waldman, H., Eds. *Enzyme Catalysis in Organic Synthesis*, Wiley-VCH, Weinheim, 2002; Bornscheuer, U. T.; Kazlauskas, R. J. *Hydrolases in Organic Synthesis – Regio- and Stereoselective Biotransformations*, Wiley-VCH, Weinheim, 1999; Wong, C.-H.; Whitesides, G. M. *Enzymes in Synthetic Organic Chemistry*, Pergamon, New York, 1994.
2. Fitzpatrick, P. A.; Klibanov, A. M. *J. Am. Chem. Soc.* **1991**, *113*, 3166-3171.
3. Kazlauskas, R. J., Weissfloch, A. N. E. *J. Mol. Catal. B: Enzymatic* **1997**, *3*, 65-72.
4. (a) Jain, S. C.; Shinde, U.; Li, Y.; Inouye, M.; Berman, H. M. *J. Mol. Biol.* **1998**, *284*, 137-144. The crystal structure of subtilisin Carlsberg, where crystals have been soaked in acetonitrile or dioxane, is nearly indistinguishable from the structure determined in water: (b) Fitzpatrick, P. A.; Steinmetz, A. C. U.; Ringe, D.; Klibanov, A. M. *Proc. Natl. Acad. Sci. U.S.A.* **1993**, *90*, 8653-8657. (c) Schmitke, J. L.; Stern, L. J.; Klibanov, A. M. *Proc. Natl. Acad. Sci. U.S.A.* **1997**, *94*, 4250-4255.

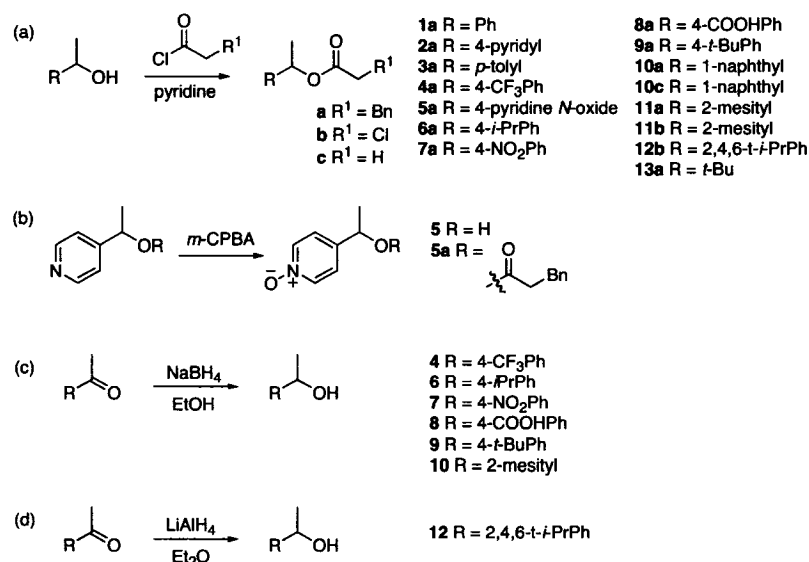
5. Chen, C.S.; Fujimoto, Y.; Girdaukas, G.; Sih, C.J. *J. Am. Chem. Soc.* **1982**, *104*, 7294-7299.
6. Savile, C. K.; Magloire, V. M.; Kazlauskas, R. J. *J. Am. Chem. Soc.* **2005**, *127*, 2104-2113.
7. Mugford, P. F.; Magloire, V. M.; Kazlauskas, R. J. *J. Am. Chem. Soc.* **2005**, *127*, 6536-6537.
8. LogP/P₀ is the substituent hydrophobicity partition coefficient relative to hydrogen.
9. Howard, J. A. K.; Hoy, V. J.; O'Hagan, D.; Smith, G. T. *Tetrahedron* **1996**, *38*, 12613-12622.
10. Margolin, A. L.; Tai, D.-F.; Klibanov, A. M. *J. Am. Chem. Soc.* **1987**, *109*, 7885-7887; Sakurai, T.; Margolin, A. L.; Russell, A. J.; Klibanov, A. M. *J. Am. Chem. Soc.* **1988**, *110*, 7236-7237; Tawaki, S.; Klibanov, A. M. *J. Am. Chem. Soc.* **1992**, *114*, 1882-1884.
11. Wangikar, P. P.; Rich, J. O.; Clark, D. S.; Dordick, J. S. *Biochemistry* **1995**, *34*, 12302-10.
12. Tyndall, J. D. A.; Tessa Nall, T.; Fairlie, D. P. *Chem. Rev.* **2005**, *105*, 973-1000.
13. Mezzetti, A.; Schrag, J.; Cheong, C. S.; Kazlauskas, R. J. *Chem. Biol.* **2005**, *12*, 427-437.
14. Cygler, M.; Grochulski, P.; Kazlauskas, R. J.; Schrag, J. D.; Bouthillier, F.; Rubin, B.; Serreqi, A. N.; Gupta, A. K. *J. Am. Chem. Soc.* **1994**, *116*, 3180-3186.
15. Hönig, H.; Shi, N.; Polanz, G. *Biocatalysis* **1994**, *9*, 61-69.
16. Parida, S.; Dordick, J. S. *J. Am. Chem. Soc.* **1991**, *113*, 2253-2259; Cernia, E.; Palocci, C.; Soro, C. *Chem. Phys. Lipids* **1998**, *93*, 157-168.

Chapter 3 – Appendix

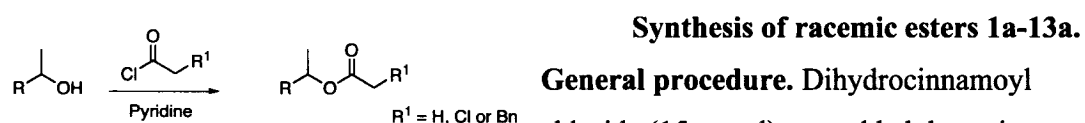
General. ^1H - and ^{13}C -NMR spectra were obtained as CDCl_3 solutions at 300 MHz and 75 MHz, respectively. Chemical shifts are expressed in ppm (δ) and are referenced to tetramethylsilane or solvent signal. Coupling constants are reported in Hertz (Hz). GC analyses were performed on a 25 m x 0.25 mm Chrompack CP-Chiralsil-Dex CB column (Varian Inc., Palo Alto, USA) with He as carrier gas using one of the three following temperature programs: **A** 17.5 psi, 50 °C, 5 °C min $^{-1}$, 150 °C held for 5 min, 2.5 °C min $^{-1}$; 175 °C held for 5 min, 5 °C min $^{-1}$, 200 °C held for 30 min); **B** 17.5 psi, 50 °C, 5 °C min $^{-1}$; 150 °C held for 10 min, 1.0 °C min $^{-1}$, 175 °C held for 10 min, 10 °C min $^{-1}$, 200 °C held for 7.5 min; **C** 17.5 psi, 50 °C, 10 °C min $^{-1}$, 200 °C held for 15 min). HPLC analyses were performed on a 4.6 x 250 mm Daicel Chiralcel OD or Chiralpak AD-H column (Chiral Technologies, Exton, USA) and monitored at 254 nm. Flash chromatography with silica gel (35-75 mesh) was used to purify all intermediates and substrates. All reagents, buffers, starting materials and anhydrous solvents were purchased from Sigma-Aldrich (Milwaukee, USA) and used without purification. All air- and moisture-sensitive reactions were performed under Ar.

Lipase from *Burkholderia cepacia* (PCL)¹ was purchased from Amano Enzyme USA (Troy, USA). The pBE3 *Escherichia coli*-*Bacillus subtilis* shuttle vector² containing the subtilisin E gene was kindly provided by Dr. F. Arnold (Caltech, USA) and *Bacillus subtilis* strain DB104³ was a gift from Dr. S. L. Wong (University of Calgary, Canada).

Synthesis of substrates. We synthesized esters **1a-13a**, **10c**, **11b** and **12b** by treating the corresponding secondary alcohol with the appropriate acid chloride in the presence of pyridine (Scheme A3.1a). *m*-CPBA oxidation of 1-(pyrid-4-yl) ethanol and **2a** gave the 4-pyridine *N*-oxide derivatives **5** and **5a**, respectively (Scheme A3.1b). We synthesized secondary alcohols by NaBH_4 (**4** and **6-10**) or LiAlH_4 (**12**) reduction of the corresponding ketone (Scheme A3.1c and A3.1d). The details for ester synthesis are presented first, followed by the secondary alcohols.



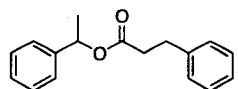
Scheme A3.1. Synthesis of esters **1a-13a**, **10c**, **11b** and **12b** and secondary alcohols **4-10** and **12**.



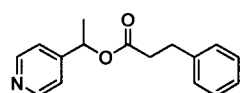
General procedure. Dihydrocinnamoyl

chloride (15 mmol) was added dropwise to a stirred solution of secondary alcohol (10 mmol) and pyridine (15 mmol) in CH₂Cl₂ (50 mL) at 0 °C. The ice bath was removed and stirred until the reaction was complete by TLC. The reaction was quenched with the addition of sat. NaHCO₃ (25 mL) (except **8a**). The layers were separated and the aqueous layer was extracted with CH₂Cl₂ (2 x 25 mL). The combined organic layers were washed with 1N HCl (2 x 25 mL) (except **2a**), sat. NaHCO₃ (2 x 25 mL) (except **8a**), sat. NaCl (25 mL) and dried over Na₂SO₄. The organic layer was concentrated *in vacuo* to give the crude ester. All substrates were purified on silica gel. The relevant analytical data are given below:

Dihydrocinnamic acid 1-phenyl-ethyl ester (**1a**).⁴

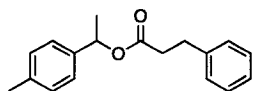
 Purification on silica gel (95:5 hexanes/EtOAc) to give a clear liquid (4.73 g, 75%): ¹H NMR δ 1.52 (d, *J* = 6.6, 3H, CH₃), 2.68 (m, 2H, C(O)CH₂), 2.97 (t, *J* = 7.8, 2H, CH₂Ph), 5.90 (q, *J* = 6.6, 1H, CH), 7.19-7.38 (m, 10H, phenyl); ¹³C NMR δ 22.2 (CH₃), 31.0 (CH₂Ph), 36.2 (C(O)CH₂), 72.4 (CH), 126.1, 126.3, 127.9, 128.4, 128.5, 140.5, 141.7 (phenyl), 172.2 (C=O); HRMS calcd for C₁₇H₁₈O₂Na [M+Na]⁺ 277.1209.

Found: 277.1202. The enantiomers were separated using GC (program A; (*S*)-**1a**, t_R = 40.8 min; (*R*)-**1a**, t_R = 41.0 min).



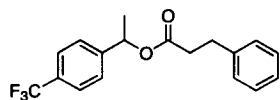
Dihydrocinnamic acid 1-pyridin-4-yl-ethyl ester (2a).

Purification on silica gel (3:1 to 2:1 hexanes/EtOAc) to give a viscous, yellow liquid (3.27 g, 85%): ^1H NMR δ 1.49 (d, J = 6.6, 3H, CH_3), 2.73 (m, 2H, C(O)CH_2), 2.99 (t, J = 7.5, 2H, CH_2Ph), 5.82 (q, J = 6.9, 1H, CH), 7.14 (d, J = 6.0, 2H, pyridyl), 7.19-7.32 (m, 7H, phenyl), 8.56 (d, J = 6.3, 2H, pyridyl); ^{13}C NMR δ 21.9 (CH_3), 30.9 (CH_2Ph), 35.9 (C(O)CH_2), 70.8 (CH), 120.6, 126.4, 128.3, 128.5, 140.2, 149.9, 150.4 (aromatic), 172.2 (C=O); HRMS calcd for $\text{C}_{16}\text{H}_{18}\text{NO}_2$ $[\text{M}+\text{H}]^+$ 256.1343. Found: 256.1342. The enantiomers were separated using GC (program A; (*S*)-**2a**, t_R = 45.0 min; (*R*)-**2a**, t_R = 45.2 min).



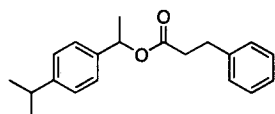
Dihydrocinnamic acid 1-*p*-tolyl-ethyl ester (3a).

Purification on silica gel (100% hexanes to 95:5 hexanes/EtOAc) to give a clear liquid (2.06 g, 77%): ^1H NMR δ 1.51 (d, J = 6.6, 3H, CH_3), 2.36 (s, 3H, CH_3), 2.66 (m, 2H, C(O)CH_2), 2.96 (t, J = 7.8, 2H, CH_2Ph), 5.88 (q, J = 6.6, 1H, CH), 7.15-7.32 (m, 9H, phenyl); ^{13}C NMR δ 21.2 (CH_3), 22.1 (CH_3), 31.0 (CH_2Ph), 36.2 (C(O)CH_2), 72.3 (CH), 126.1, 126.2, 128.4, 128.5, 129.2, 137.6, 138.7, 140.6 (phenyl), 172.2 (C=O); HRMS calcd for $\text{C}_{18}\text{H}_{20}\text{O}_2\text{Na}$ $[\text{M}+\text{Na}]^+$ 291.1366. Found: 291.1360. The enantiomers were separated using GC (program A; (*S*)-**3a**, t_R = 44.5 min; (*R*)-**3a**, t_R = 44.6 min).



Dihydrocinnamic acid 1-(4-trifluoromethylphenyl)-ethyl ester (4a).

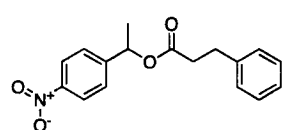
Purification on silica gel (100% hexanes to 95:5 hexanes/EtOAc) to give a clear liquid (960 mg, 76%): ^1H NMR δ 1.51 (d, J = 6.6, 3H, CH_3), 2.70 (m, 2H, C(O)CH_2), 2.97 (t, J = 7.5, 2H, CH_2Ph), 5.90 (q, J = 6.6, 1H, CH), 7.18-7.29 (m, 5H, phenyl), 7.37-7.61 (m, 4H, phenyl); ^{13}C NMR δ 22.3 (CH_3), 31.0 (CH_2Ph), 36.1 (C(O)CH_2), 71.7 (CH), 125.6 (q, CF_3), 126.3, 126.4, 128.4, 128.6, 140.3, 145.7, (phenyl), 172.1 (C=O); HRMS calcd for $\text{C}_{18}\text{H}_{18}\text{F}_3\text{O}_2$ $[\text{M}+\text{H}]^+$ 323.1258. Found: 323.1268. The enantiomers were separated using GC (program C; (*S*)-**4a**, t_R = 17.2 min; (*R*)-**4a**, t_R = 17.3 min).



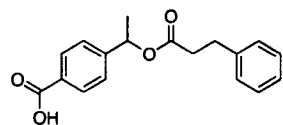
Dihydrocinnamic acid 1-(4-isopropylphenyl)-ethyl ester (6a).

Purification on silica gel (100% hexanes to 95:5

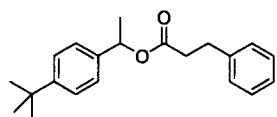
hexanes/EtOAc) to give a clear liquid (1.24 g, 84%): ^1H NMR δ 1.26 (d, J = 6.9, 6H, $\text{CH}(\text{CH}_3)_2$), 1.51 (d, J = 6.6, 3H, CH_3), 2.66 (m, 2H, $\text{C}(\text{O})\text{CH}_2$), 2.93 (hept, J = 6.6, 1H, $\text{CH}(\text{CH}_3)_2$), 2.97 (t, J = 7.8, 2H, CH_2Ph), 5.89 (q, J = 6.6, 1H, CH), 7.18-7.31 (m, 9H, phenyl); ^{13}C NMR δ 21.2 (CH_3), 24.1 ($\text{C}(\text{CH}_3)_2$), 31.1 (CH_2Ph), 34.0 ($\text{CH}(\text{CH}_3)_2$), 36.3 ($\text{C}(\text{O})\text{CH}_2$), 72.4 (CH), 126.3, 126.7, 128.4, 128.5, 128.6, 139.1, 140.7, 148.6 (phenyl), 172.3 ($\text{C}=\text{O}$); HRMS calcd for $\text{C}_{20}\text{H}_{24}\text{O}_2\text{Na}$ $[\text{M}+\text{Na}]^+$ 319.1673. Found: 319.1693. The enantiomers were separated using GC (program A; (*S*)-**6a**, t_R = 60.4 min; (*R*)-**6a**, t_R = 60.7 min).



Dihydrocinnamic acid 1-(4-nitrophenyl)-ethyl ester (7a). Purification on silica gel (9:1 hexanes/EtOAc) to give a yellow solid (2.64 g, 88%): mp 46-48 °C; ^1H NMR δ 1.52 (d, J = 6.9, 3H, CH_3), 2.72 (m, 2H, $\text{C}(\text{O})\text{CH}_2$), 2.98 (t, J = 7.5, 2H, CH_2Ph), 5.91 (q, J = 6.6, 1H, CH), 7.18-7.32 (m, 5H, phenyl), 7.39-8.20 (m, 4H, phenyl); ^{13}C NMR δ 22.3 (CH_3), 30.9 (CH_2Ph), 36.0 ($\text{C}(\text{O})\text{CH}_2$), 71.4 (CH), 123.9, 126.5, 126.8, 128.4, 128.6, 140.2, 147.5, 149.0 (phenyl), 172.0 ($\text{C}=\text{O}$); HRMS calcd for $\text{C}_{17}\text{H}_{17}\text{NO}_4\text{Na}$ $[\text{M}+\text{Na}]^+$ 322.1055. Found: 322.1051. The enantiomers were separated using GC (program A; (*S*)-**7a**, t_R = 59.9 min; (*R*)-**7a**, t_R = 60.8 min).

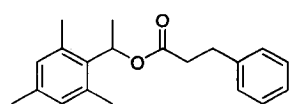


Dihydrocinnamic acid 1-(4-carboxyphenyl)-ethyl ester (8a). Purification on silica gel (95:5 to 90:10 hexanes/EtOAc) to give a white solid (316 g, 61%): mp 74-76 °C; ^1H NMR δ 1.53 (d, J = 6.9, 3H, CH_3), 2.74 (m, 2H, $\text{C}(\text{O})\text{CH}_2$), 2.98 (t, J = 7.8, 2H, CH_2Ph), 5.93 (q, J = 6.9, 1H, CH), 7.19-7.33 (m, 5H, phenyl), 7.37-8.10 (m, 4H, phenyl); ^{13}C NMR δ 22.3 (CH_3), 31.0 (CH_2Ph), 36.1 ($\text{C}(\text{O})\text{CH}_2$), 71.9 (CH), 126.1, 126.4, 128.4, 128.6, 130.6, 137.6, 138.7, 140.6, 147.8 (phenyl), 171.8 ($\text{C}=\text{O}$), 172.2 (COOH); HRMS calcd for $\text{C}_{18}\text{H}_{18}\text{O}_4\text{Na}$ $[\text{M}+\text{Na}]^+$ 321.1102. Found: 321.1036. The enantiomers were separated using HPLC (Chiralpak AD-H column, 75:25 hexanes/EtOH, 0.5 mL/min, 254 nm; (*R*)-**8a**, t_R = 17.5 min; (*S*)-**8a**, t_R = 19.0 min).



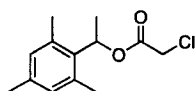
Dihydrocinnamic acid 1-(4-*tert*-butylphenyl) ethyl ester (9a). Purification on silica gel (100% hexanes to 95:5 hexanes/EtOAc) to give a clear liquid (1.01 g, 82%): ^1H NMR δ 1.34 (s, 9H, $\text{C}(\text{CH}_3)_3$), 1.52 (d, J = 6.6, 3H, CH_3), 2.67 (m, 2H, $\text{C}(\text{O})\text{CH}_2$), 2.97 (t, J = 7.8,

2H, CH_2Ph), 5.90 (q, $J = 6.6$, 1H, CH), 7.18-7.39 (m, 9H, phenyl); ^{13}C NMR δ 22.1 (CH_3), 31.1 (CH_2Ph), 31.5 ($\text{C}(\text{CH}_3)_3$), 34.6 ($\text{C}(\text{CH}_3)_3$), 36.3 ($\text{C}(\text{O})\text{CH}_2$), 72.3 (CH), 125.5, 126.0, 126.3, 128.4, 128.6, 138.6, 140.6, 150.9 (phenyl), 172.3 ($\text{C}=\text{O}$); HRMS calcd for $\text{C}_{21}\text{H}_{26}\text{O}_2\text{Na}$ $[\text{M}+\text{Na}]^+$ 333.1830. Found: 333.1852. The enantiomers were separated using GC (program A; (*S*)-**9a**, $t_R = 66.3$ min; (*R*)-**9a**, $t_R = 66.6$ min).



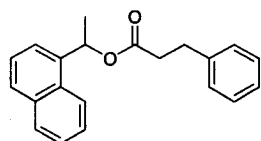
Dihydrocinnamic acid 1-(2,4,6-trimethylphenyl) ethyl ester (10a). Purification on silica gel (100% hexanes to 99:1 hexanes/EtOAc) to give a clear liquid (1.43 g, 70%): ^1H NMR δ

1.54 (d, $J = 6.9$, 3H, CH_3), 2.27 (s, 3H, $p\text{-CH}_3$), 2.42 (s, 6H, $o\text{-CH}_3$), 2.66 (m, 2H, $\text{C}(\text{O})\text{CH}_2$), 2.95 (t, $J = 7.8$, 2H, CH_2Ph), 6.30 (q, $J = 7.2$, 1H, CH), 6.84 (s, 2H, phenyl), 7.17-7.29 (m, 5H, phenyl); ^{13}C NMR δ 19.7 (CH_3), 20.6 (CH_3), 20.9 (CH_3), 31.1 (CH_2Ph), 36.2 ($\text{C}(\text{O})\text{CH}_2$), 69.7 (CH), 126.4, 128.4, 128.6, 130.1, 134.5, 136.1, 137.1, 140.7 (phenyl), 172.3 ($\text{C}=\text{O}$); HRMS calcd for $\text{C}_{20}\text{H}_{24}\text{O}_2\text{Na}$ $[\text{M}+\text{Na}]^+$ 319.1673. Found: 319.1409. The enantiomers could not be separated using GC or HPLC.



Chloroacetic acid 1-(2,4,6-trimethylphenyl) ethyl ester (10b). Purification on silica gel (100% hexanes to 95:5 hexanes/EtOAc) to

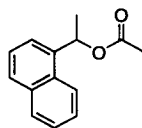
give a clear liquid (1.11 g, 90%): ^1H NMR δ 1.63 (d, $J = 6.9$, 3H, CH_3), 2.26 (s, 3H, $p\text{-CH}_3$), 2.45 (s, 6H, $o\text{-CH}_3$), 4.08 (d, $J = 2.4$, CH_2Cl), 6.37 (q, $J = 6.9$, 1H, CH), 6.85 (s, 2H, phenyl); ^{13}C NMR δ 19.6 (CH_3), 20.5 (CH_3), 20.9 (CH_3), 41.2 (CH_2Cl), 71.9 (CH), 130.2, 133.5, 136.1, 137.5 (phenyl), 166.7 ($\text{C}=\text{O}$); HRMS calcd for $\text{C}_{13}\text{H}_{17}^{35}\text{ClO}_2\text{Na}$ $[\text{M}+\text{Na}]^+$ 263.0814. Found: 263.0798. The enantiomers could not be separated using GC or HPLC.



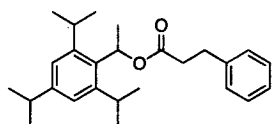
Dihydrocinnamic acid 1-(1-naphthyl) ethyl ester (11a).

Purification on silica gel (100% hexanes to 98:2 hexanes/EtOAc) to give a clear liquid (1.37 g, 75%): ^1H NMR δ 1.69 (d, $J = 6.6$, 3H, CH_3), 2.74 (m, 2H, $\text{C}(\text{O})\text{CH}_2$), 3.00 (t, $J = 7.8$, 2H, CH_2Ph), 6.67 (q, $J = 6.6$, 1H, CH), 7.20-8.10 (m, 12H, phenyl); ^{13}C NMR δ 21.8 (CH_3), 31.1 (CH_2Ph), 36.2 ($\text{C}(\text{O})\text{CH}_2$), 69.7 (CH), 123.3, 123.3, 125.5, 125.8, 126.4, 126.4, 128.4, 128.5, 128.6, 129.0, 130.3, 133.9, 137.5, 140.6 (phenyl), 172.3 ($\text{C}=\text{O}$); HRMS calcd for $\text{C}_{21}\text{H}_{20}\text{O}_2\text{Na}$ $[\text{M}+\text{Na}]^+$ 327.1360. Found: 327.1304. The enantiomers were separated using HPLC (Chiralcel OD column, 90:10 hexanes/EtOH, 0.75 mL/min, 254 nm; (*R*)-**11a**, $t_R = 6.7$ min; (*S*)-**11a**, $t_R =$

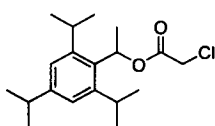
7.4 min).



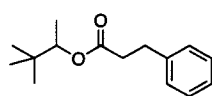
Acetic acid 1-(1-naphthyl) ethyl ester (11c). Purification on silica gel (100% hexanes to 95:5 hexanes/EtOAc) to give a clear liquid (860 mg, 80%): ^1H NMR δ 1.73 (d, J = 6.6, 3H, CH_3), 2.15 (s, 3H, $\text{C}(\text{O})\text{CH}_3$), 6.68 (q, J = 6.6, 1H, CH), 7.47-8.12 (m, 12H, phenyl); ^{13}C NMR δ 21.5 (CH_3), 21.8 (CH_3), 69.5 (CH), 123.3, 123.3, 125.5, 125.8, 126.4, 128.6, 129.0, 130.4, 133.9, 137.5 (phenyl), 170.5 ($\text{C}=\text{O}$); HRMS calcd for $\text{C}_{14}\text{H}_{14}\text{O}_2\text{Na}$ $[\text{M}+\text{Na}]^+$ 237.0891. Found: 237.0888. The enantiomers were separated using HPLC (Chiralcel OD column, 90:10 hexanes/EtOH, 0.75 mL/min, 254 nm; (*R*)-11c, t_R = 5.8 min; (*S*)-11c, t_R = 6.8 min).



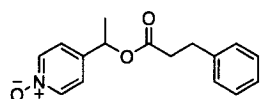
Dihydrocinnamic acid 1-(2,4,6-triisopropylphenyl) ethyl ester (12b). Purification on silica gel (100% hexanes to 98:2 hexanes/EtOAc) to give a white solid (819 mg, 87%): mp 80-82 °C; ^1H NMR δ 1.24 (d, J = 6.6, 6H, $\text{C}(\text{CH}_3)_2$), 1.26 (d, J = 6.9, 6H, $\text{C}(\text{CH}_3)_2$), 1.30 (d, J = 6.6, 6H, $\text{C}(\text{CH}_3)_2$), 1.69 (d, J = 6.9, 3H, CH_3), 2.63 (m, 2H, $\text{C}(\text{O})\text{CH}_2$), 2.88 (hept, J = 6.9, 1H, $\text{CH}(\text{CH}_3)_2$), 2.97 (t, J = 7.8, 2H, CH_2Ph), 3.50 (br m, 2H, 2 x $\text{CH}(\text{CH}_3)_2$), 6.56 (q, J = 6.9, 1H, CH), 7.04 (s, 2H, phenyl), 7.19-7.32 (m, 5H, phenyl); ^{13}C NMR δ 22.2, 24.0, 24.4, 24.9 (CH_3), 29.5 (*o*- $\text{CH}(\text{CH}_3)_2$), 31.2 (CH_2Ph), 34.2 (*p*- $\text{CH}(\text{CH}_3)_2$), 36.5 ($\text{C}(\text{O})\text{CH}_2$), 68.4 (CH), 121.2, 126.4, 128.4, 128.6, 132.2, 140.6, 148.2 (phenyl), 172.4 ($\text{C}=\text{O}$); HRMS calcd for $\text{C}_{26}\text{H}_{36}\text{O}_2\text{Na}$ $[\text{M}+\text{Na}]^+$ 403.2613. Found: 403.2461. The enantiomers could not be separated using GC or HPLC.



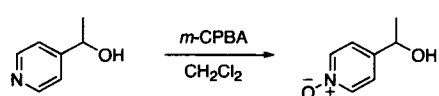
Chloroacetic acid 1-(2,4,6-triisopropylphenyl) ethyl ester (12b). Purification on silica gel (100% hexanes to 98:2 hexanes/EtOAc) to give a white solid (562 mg, 86%): mp 47-49 °C; ^1H NMR δ 1.25 (d, J = 6.9, 6H, $\text{C}(\text{CH}_3)_2$), 1.26 (d, J = 6.9, 6H, $\text{C}(\text{CH}_3)_2$), 1.31 (d, J = 6.9, 6H, $\text{C}(\text{CH}_3)_2$), 1.69 (d, J = 6.9, 3H, CH_3), 2.92 (hept, J = 6.9, 1H, $\text{CH}(\text{CH}_3)_2$), 3.50 (br m, 2H, 2 x $\text{CH}(\text{CH}_3)_2$), 4.07 (d, J = 6.6, 2H, $\text{C}(\text{O})\text{CH}_2\text{Cl}$), 6.62 (q, J = 6.9, 1H, CH), 7.04 (s, 2H, phenyl); ^{13}C NMR δ 22.2, 23.9, 24.0, 24.3, 24.9 (CH_3), 29.5 (*o*- $\text{CH}(\text{CH}_3)_2$), 34.2 (*p*- $\text{CH}(\text{CH}_3)_2$), 41.3 (CH_2Cl), 70.8 (CH), 121.3, 131.3, 148.6 (phenyl), 166.8 ($\text{C}=\text{O}$); HRMS calcd for $\text{C}_{19}\text{H}_{29}^{35}\text{ClO}_2\text{Na}$ $[\text{M}+\text{Na}]^+$ 347.1753. Found: 347.1645. The enantiomers could not be separated using GC or HPLC.

**Dihydrocinnamic acid 1,2,2-trimethyl-propyl ester (13a).**

Purification on silica gel (100% hexanes to 99:1 hexanes/EtOAc) to give a clear liquid (866 mg, 74%): ^1H NMR δ 0.88 (s, 9H, $\text{C}(\text{CH}_3)_3$), 1.11 (d, $J = 6.6$, 3H, CH_3), 2.65 (m, 2H, $\text{C}(\text{O})\text{CH}_2$), 2.98 (t, $J = 7.8$, 2H, CH_2Ph), 4.70 (q, $J = 6.6$, 1H, CH), 7.21-7.33 (m, 5H, phenyl); ^{13}C NMR δ 14.9 (CH_3), 25.7 ($\text{C}(\text{CH}_3)_3$), 31.1 (CH_2Ph), 34.1 ($\text{C}(\text{CH}_3)_3$), 36.3 ($\text{C}(\text{O})\text{CH}_2$), 77.7 (CH), 126.3, 128.4, 128.6, 140.7 (phenyl), 172.6 ($\text{C}=\text{O}$); HRMS calcd for $\text{C}_{15}\text{H}_{22}\text{O}_2\text{Na}$ $[\text{M}+\text{Na}]^+$ 257.1517. Found: 257.1156. The enantiomers were separated using GC (program A; (*R* or *S*)-**13a**, $t_R = 31.1$ min; (*R* or *S*)-**13a**, $t_R = 31.2$ min).

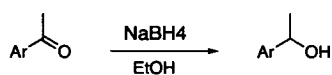
**Dihydrocinnamic acid 1-(1-oxy-pyridin-4-yl)-ethyl ester**

(5a). *m*-CPBA (77%, 670 mg, 2.96 mmol) was added portion-wise to a stirred solution of **2a** (757 mg, 2.99 mmol) in CH_2Cl_2 (25 mL) at 0°C .⁵ The ice bath was removed and the reaction solution was stirred overnight at RT. The solution was concentrated *in vacuo* and the crude residue was purified on silica gel (95:5 $\text{CHCl}_3/\text{MeOH}$) to give a viscous, clear liquid (710 mg, 89%): ^1H NMR δ 1.48 (d, $J = 6.6$, 3H, CH_3), 2.72 (m, 2H, $\text{C}(\text{O})\text{CH}_2$), 2.97 (t, $J = 7.5$, 2H, CH_2Ph), 5.79 (q, $J = 6.6$, 1H, CH), 7.08 (d, $J = 6.9$, 2H, pyridyl), 7.18-7.32 (m, 7H, phenyl), 8.16 (d, $J = 6.9$, 2H, pyridyl); ^{13}C NMR δ 21.6 (CH_3), 31.8 (CH_2Ph), 36.6 ($\text{C}(\text{O})\text{CH}_2$), 71.3 (CH), 125.4, 127.4, 129.4, 129.5, 140.2, 141.6, 146.2, (aromatic), 173.4 ($\text{C}=\text{O}$); HRMS calcd for $\text{C}_{16}\text{H}_{18}\text{NO}_3$ $[\text{M}+\text{H}]^+$ 272.1292. Found: 272.1298. The enantiomers were separated using GC (program B; (*S*)-**5a**, $t_R = 59.5$ min; (*R*)-**5a**, $t_R = 60.2$ min).

**1-(1-Oxy-pyridin-4-yl)-ethanol (5).**⁶ *m*-

CPBA (77%, 1.82 g, 8.13 mmol) was added portion-wise to a stirred solution of 1-(pyrid-4-yl) ethanol (1.03 g, 8.13 mmol) in CH_2Cl_2 (50mL) at 0°C .⁵ The ice bath was removed and the reaction solution was stirred overnight at RT. The solution was concentrated *in vacuo* and the crude residue was purified on silica gel (4:1 $\text{CHCl}_3/\text{MeOH}$) to give a white, hygroscopic solid (1.07 g, 95%): mp $79-81^\circ\text{C}$; ^1H NMR δ 1.49 (d, $J = 6.6$, 3H, CH_3), 4.87 (q, $J = 6.6$, 1H, CH), 7.26 (d, $J = 6.6$, 2H, pyridyl) 8.01 (d, $J = 6.9$, 2H, pyridyl); ^{13}C NMR (CD_3OD) δ 24.9 (CH_3), 68.4 (CH), 124.9, 140.0, 151.7 (pyridyl); HRMS calcd for $\text{C}_7\text{H}_{10}\text{NO}_2$ $[\text{M}+\text{H}]^+$ 140.0717. Found: 140.0710. The enantiomers were separated using GC (program B; (*R*)-**4**, $t_R = 20.7$ min;

(*S*)-4, $t_R = 21.0$ min).



Synthesis of racemic secondary alcohols 4, 6-10.

General procedure. NaBH₄ (555 mg, 15 mmol) was added portion-wise to a stirred solution of ketone (10 mmol) in EtOH (10 mL) at 0°C. The ice bath was removed and the reaction solution was stirred for 3 h at RT. The solution was cooled to 0 °C and quenched with 1 N HCl (10 mL) and extracted with CH₂Cl₂ (3 x 20 mL). The combined organic layers were washed with sat. NaHCO₃ (25 mL) (except 8), sat. NaCl (25 mL) and dried over Na₂SO₄. The organic layer was concentrated *in vacuo* to give the crude alcohol. The relevant analytical data are given below:

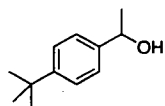
1-(4-Trifluorophenyl)-ethanol (4).⁷ Obtained as clear liquid (1.74 g, 97%): ¹H NMR δ 1.52 (d, $J = 6.3$, 3H, CH₃), 1.87 (br s, 1H, OH), 4.99 (q, $J = 6.6$, 1H, CH), 7.50-7.64 (m, 4H, phenyl); ¹³C NMR δ 25.4 (CH₃), 69.8 (CH), 125.5 (q, CF₃), 125.6, 125.7, 149.8 (phenyl). The enantiomers were separated using GC (program C; (*R*)-4, $t_R = 10.6$ min; (*S*)-4, $t_R = 10.9$ min).

1-(4-Isopropylphenyl)-ethanol (6). Obtained as clear liquid (2.82 g, 85%): ¹H NMR δ 1.27 (d, $J = 6.9$, 6H, CH(CH₃)₂), 1.51 (d, $J = 6.3$, 3H, CH₃), 1.86 (br s, 1H, OH), 2.93 (hept, $J = 6.9$, 1H, CH(CH₃)₂), 4.89 (q, $J = 6.3$, 1H, CH), 7.23-7.34 (m, 4H, phenyl); ¹³C NMR δ 24.1 (CH₃), 25.0 (C(CH₃)₂), 33.9 (CH(CH₃)₂), 70.3 (CH), 125.6, 126.6, 143.4, 148.2 (phenyl); HRMS calcd for C₁₁H₁₆ONa [M+Na]⁺ 187.1098. Found: 187.1100. The enantiomers were separated using GC (program A; (*R*)-6, $t_R = 24.9$ min; (*S*)-6, $t_R = 25.4$ min).

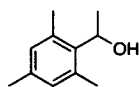
1-(4-Nitrophenyl)-ethanol (7).⁸ Obtained as yellow liquid (2.98 g, 90%): ¹H NMR δ 1.54 (d, $J = 6.6$, 3H, CH₃), 1.97 (br s, 1H, OH), 5.04 (q, $J = 6.6$, 1H, CH), 7.55-8.24 (m, 4H, phenyl); ¹³C NMR δ 25.6 (CH₃), 69.6 (CH), 123.8, 126.2, 147.2, 153.2 (phenyl). The enantiomers were separated using GC (program A; (*R*)-7, $t_R = 42.1$ min; (*S*)-7, $t_R = 43.1$ min).

4-(1-Hydroxyethyl)-benzoic acid (8). Obtained as white solid (1.49 g, 90%): mp 137-139 °C; ¹H NMR (CD₃OD) δ 1.53 (d, $J = 6.3$, 3H, CH₃), 4.92 (m, 1H, CH), 7.49-8.04 (m, 4H, phenyl); ¹³C NMR (CD₃OD) δ 26.4 (CH₃), 71.3 (CH), 127.3, 131.4, 131.7, 154.0 (phenyl), 170.7 (COOH); HRMS

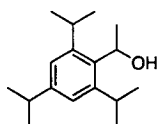
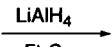
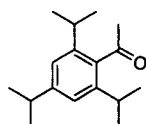
calcd for $C_9H_{10}O_3Na$ $[M+Na]^+$ 189.0527. Found: 189.0264. The enantiomers were separated using HPLC (Chiralpak AD-H column, 75:25 hexanes/EtOH, 0.5 mL/min, 254 nm; (*R*)-**8**, t_R = 13.9 min; (*S*)-**8**, t_R = 15.3 min).



1-(4-*tert*-Butylphenyl)-ethanol (9). Obtained as white solid (1.74 g, 97%): mp 60–62 °C; 1H NMR δ 1.34 (s, 9H, $C(CH_3)_3$), 1.52 (d, J = 6.0, 3H, CH_3), 4.90 (q, J = 6.3, 1H, CH), 7.32–7.42 (m, 4H, phenyl); ^{13}C NMR δ 25.0 (CH_3), 31.5 ($C(CH_3)_3$), 34.6 ($C(CH_3)_3$), 70.3 (CH), 125.3, 125.5, 142.9, 150.5 (phenyl); HRMS calcd for $C_{12}H_{18}ONa$ $[M+Na]^+$ 201.1255. Found: 201.1007. The enantiomers were separated using GC (program A; (*R*)-**9**, t_R = 28.1 min; (*S*)-**9**, t_R = 28.4 min).

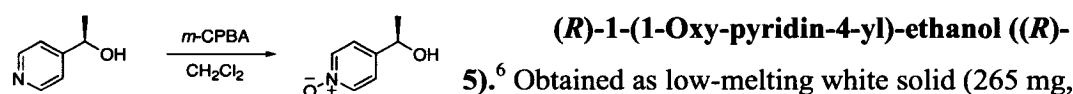


1-(2,4,6-trimethylphenyl)-ethanol (10).⁷ Obtained as white solid (3.01 g, 92%): mp 66–68 °C; 1H NMR δ 1.53 (d, J = 6.6, 3H, CH_3), 2.25 (s, 3H, *p*- CH_3), 2.42 (s, 6H, *o*- CH_3), 5.37 (q, J = 6.9, 1H, CH), 6.82 (s, 2H, phenyl); ^{13}C NMR δ 20.6 (CH_3), 20.8 (CH_3), 21.6 (CH_3), 67.5 (CH), 130.2, 135.8, 136.5, 137.8 (phenyl). The enantiomers were separated using GC (program C; (*R*)-**10**, t_R = 12.9 min; (*S*)-**10**, t_R = 13.3 min).



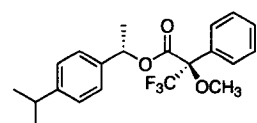
Synthesis of 1-(2,4,6-triisopropylphenyl)-ethanol (12).⁹ 2,4,6-Triisopropylacetophenone (2.46 g, 10 mmol) in anhydrous Et_2O (10 mL) was added drop-wise to a stirred slurry of $LiAlH_4$ (570 mg, 15 mmol) in anhydrous Et_2O (20 mL) at 0 °C. The ice bath was removed and the reaction solution was stirred for 3 h at RT. The solution was then cooled to 0 °C and quenched with 1N HCl (10 mL) and extracted with EtOAc (3 x 25 mL). The combined organic layers were washed with sat. $NaHCO_3$ (25 mL), sat. NaCl (25 mL) and dried over Na_2SO_4 . The organic layer was concentrated *in vacuo* to give a white solid (1.62 g, 65%): mp 85–87 °C (lit.⁹ 84–85 °C); 1H NMR δ 1.27 (d, J = 6.9, 12H, 2 x $C(CH_3)_2$), 1.29 (d, J = 6.9, 6H, $C(CH_3)_2$), 1.63 (d, J = 6.6, 3H, CH_3), 1.76 (br s, 1H, OH), 2.88 (hept, J = 6.9, 1H, $CH(CH_3)_2$), 3.61 (m, 2H, 2 x $CH(CH_3)_2$), 5.55 (q, J = 6.9, 1H, CH), 7.05 (s, 2H, phenyl); ^{13}C NMR δ 23.7, 24.0, 24.1, 24.7, 24.8 (CH_3), 29.1 (*o*- $CH(CH_3)_2$), 34.2 (*p*- $CH(CH_3)_2$), 66.2 (CH), 121.1, 122.2, 136.0, 147.7 (phenyl). The enantiomers were separated using GC (program C; (*R*)-**11**, t_R = 14.2 min; (*S*)-**11**, t_R = 14.5 min).

Determination of absolute configuration. Enantiopure alcohols (*R*)-1, (*R*)-2 and (*R*)-11 were purchased from Sigma-Aldrich Corporation. Absolute configurations of alcohols 3, 4, 7 and 10 were assigned by similarity in the order of elution of enantiomers of previously reported GC analyses.^{7,8} Enantiopure (*R*)-4 was synthesized via *m*-CPBA oxidation⁵ of (*R*)-3, as described above for (+/-)-4. Absolute configurations of alcohols 6, 8 and 9 were assigned using the configurational correlation model for the corresponding (*R*)-MTPA derivatives, which were synthesized using (*S*)-(+)- α -methoxy- α -(trifluoromethyl)-phenylacetyl chloride in pyridine.¹⁰ Enantiopure (*S*)-6 and (*S*)-9 were prepared via PCL-catalyzed acylation of racemic alcohol with vinyl acetate and (*S*)-8 was prepared by PCL-catalyzed hydrolysis of 8a followed by hydrolysis of the remaining starting material. The relevant analytical data are below:

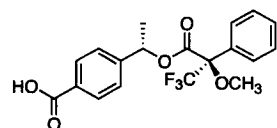


95%, 98% ee): ¹H NMR δ 1.46 (d, J = 6.6, 3H, CH₃), 4.85 (q, J = 6.6, 1H, CH), 7.26 (d, J = 7.2, 2H, pyridyl) 8.00 (d, J = 7.2, 2H, pyridyl); ¹³C NMR (CD₃OD) δ 24.9 (CH₃), 68.4 (CH), 124.9, 140.0, 151.7 (pyridyl); HRMS calcd for C₇H₁₀NO₂ [M+H]⁺ 140.0717.

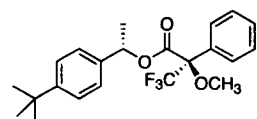
Found: 140.0710.



(*R,S*)-1-(4-Isopropylphenyl)-ethyl MTPA ester. ¹H NMR δ 1.26 (d, J = 6.9, 6H, CH(CH₃)₂, *S*-enantiomer), 1.27 (d, J = 6.9, 6H, CH(CH₃)₂, *R*-enantiomer), 1.59 (d, J = 6.6, 3H, CH₃), *R*-enantiomer), 1.65 (d, J = 6.6, 3H, CH₃), *S*-enantiomer), 2.91 (hept, J = 6.6, 1H, CH(CH₃)₂), 3.50 (q, J = 1.5, 3H, OCH₃, *R*-enantiomer), 3.58 (q, J = 1.5, 3H, OCH₃, *S*-enantiomer), 6.10 (q, J = 6.6, 1H, CH, *S*-enantiomer), 6.14 (q, J = 6.6, 1H, CH, *R*-enantiomer), 7.15-7.43 (m, 9H, phenyl).

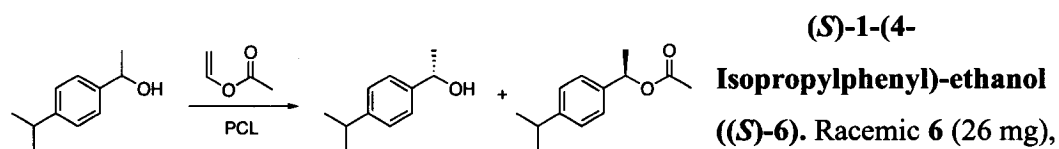


(*R,S*)-4-(1-Hydroxyethyl)-benzoic acid MTPA ester. ¹H NMR δ 1.61 (d, J = 6.6, 3H, CH₃, *R*-enantiomer), 1.66 (d, J = 6.6, 3H, CH₃, *S*-enantiomer), 3.50 (q, J = 1.5, 3H, OCH₃, *R*-enantiomer), 3.59 (q, J = 1.5, 3H, OCH₃, *S*-enantiomer), 6.14 (q, J = 6.6, 1H, CH, *S*-enantiomer), 6.18 (q, J = 6.6, 1H, CH, *R*-enantiomer), 7.21-8.13 (m, 9H, phenyl).

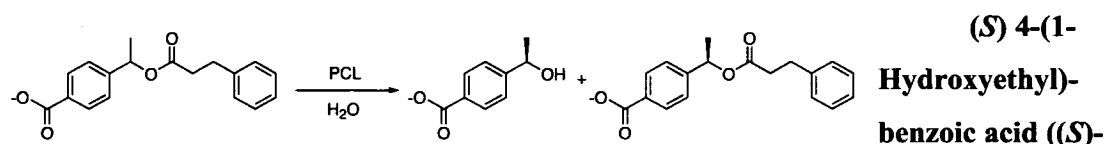


(*R,S*)-1-(4-*tert*-Butylphenyl)-ethyl MTPA ester. ¹H NMR δ 1.33 (s, 9H, C(CH₃)₃, *S*-enantiomer), 1.34 (s, 9H, CH₃)₃, *R*-

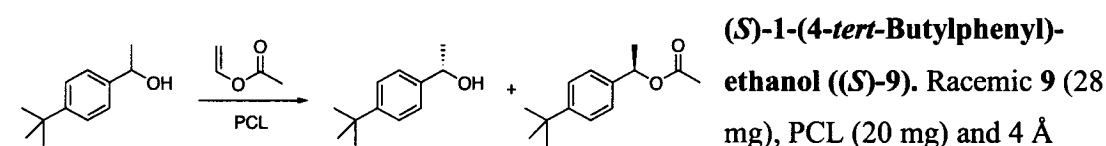
enantiomer), 1.59 (d, $J = 6.6$, 3H, CH_3 , R -enantiomer), 1.65 (d, $J = 6.6$, 3H, CH_3 , S -enantiomer), 3.50 (q, $J = 1.5$, 3H, OCH_3 , R -enantiomer), 3.58 (q, $J = 1.5$, 3H, OCH_3 , S -enantiomer), 6.10 (q, $J = 6.6$, 1H, CH , S -enantiomer), 6.14 (q, $J = 6.6$, 1H, $\text{CH}(\text{CH}_3)$, R -enantiomer), 7.19-7.43 (m, 9H, phenyl).



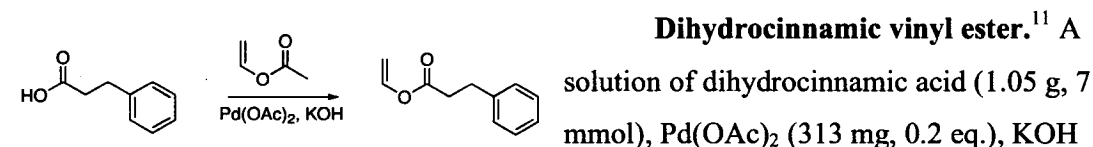
PCL (20 mg) and 4 Å molecular sieves were stirred together in vinyl acetate (1 mL) at RT. After 72 h, the reaction solution was concentrated and product and starting material were separated on silica gel (100% hexanes to 9:1 hexanes/EtOAc). Unreacted starting material was isolated as a clear liquid (12 mg, 46%, 99% ee).



8). A solution of racemic **8a** (61 mg) in CH_3CN (200 μL) was added to a solution of PCL (50 mg) in 50 mM BES (pH 7.2, 1.8 mL) and stirred at RT. After 72 h, the reaction solution was acidified with 1 N HCl (1 mL) and extracted with EtOAc (3 x 2 mL). The combined organic layers were concentrated and product and starting material were separated on silica gel (4:1 hexanes/EtOAc to 100% EtOAc). Remaining starting material was hydrolyzed in 1 N KOH (1:1 H_2O /EtOH) to give a white solid (21 mg, 63%, 15% ee).



molecular sieves were stirred together in vinyl acetate (1 mL) at RT. After 72 h, the reaction solution was concentrated and product and starting material were separated on silica gel (100% hexanes to 9:1 hexanes/EtOAc). Unreacted starting material was isolated as a clear liquid (13 mg, 46%, 99% ee).



(40 mg, 0.1 eq.) and vinyl acetate (65 mL, 100 eq.) was stirred at RT for 3 h. The reaction mixture was diluted with Et₂O (100 mL) and filtered through Celite. The reaction solution was concentrated *in vacuo* and the residue was purified on silica gel (95:5 hexanes/EtOAc) to give a clear liquid (692 mg, 56%): 2.74 (m, 2H, C(O)CH₂), 3.01 (t, *J* = 7.5, 2H, CH₂Ph), 4.60 (dd, *J* = 6.3, 1.8, 1H, H₂C=C), 4.90 (dd, *J* = 14.1, 1.8, 1H, H₂C=C), 7.22-7.34 (m, 6H); ¹³C NMR δ 30.7 (CH₂Ph), 35.6 (C(O)CH₂), 97.9 (H₂C=), 126.5, 128.4, 128.7, 140.2 (phenyl), 141.2 (=CH), 170.1 (C=O).

Large-scale fermentation and purification of subtilisin BPN' and subtilisin E.

Protease deficient *B. subtilis* DB104 was transformed with vector pBE3, as previously described.^{2,12} Transformed cells were grown in 2XSG¹² media (500 mL) with shaking for 10 h at 37 °C. This culture was used to inoculate 14 L of 2XSG media in a 20 L fermentor. After 42 hours (OD₆₀₀ = 9.1), the culture was cooled and centrifuged. The cell pellet was discarded and the supernatant was concentrated using a 0.45 μm cartridge (8,000 MW cutoff) equipped with a 1.2 μm prefilter. The concentrate was brought to 70% saturation with NH₄SO₄ (472 g/L), stirred overnight and then centrifuged at 8,000 rpm for 1.5 h. The precipitate was resuspended and dialyzed for 48 h against 8 L of 10 mM HEPES (pH 7.5, 1 mM CaCl₂). The sample was passed through a bed of DE-52 anion exchange cellulose with vacuum. The clarified solution was then concentrated by passage through an 8,000 MW ultra filtration cartridge. The retentate was brought to 1.8 M NH₄SO₄, centrifuged and the supernatant was passed through a 0.45 μm filter to give crude subtilisin.

Subtilisin E or BPN' was purified on a BioCad purification system (Applied Biosystems, Foster, USA) using a Poros 20HP2 (10 x 100) column.¹³ The sample was loaded and washed with 1.8 M NH₄SO₄ in 20 mM HEPES (pH 7.0) and then eluted with a linear gradient of 1.8 M to 0 M NH₄SO₃ in 20 mM HEPES (pH 7.0). The enzyme activity was monitored by adding 90 μL of assay solution [0.2 mM succinyl-AAPF-*p*-nitroanilide (suc-AAPF-*p*NA) / 100 mM Tris pH 8.0 / 10 mM CaCl₂] to 10 μL of eluent and following the reaction at 410 nm at 37 °C for 15 min. The specific activity toward suc-AAPF-*p*NA was ca. 20 U/mg (lit.² 17.2 U/mg). Fractions containing protein were concentrated by passage through an 8,000 MW cutoff ultrafiltration cartridge and diafiltered in 10 mM

HEPES (pH 7.5, 1 mM CaCl₂). The final retentate was frozen and lyophilized to give ca. 300 mg of subtilisin.

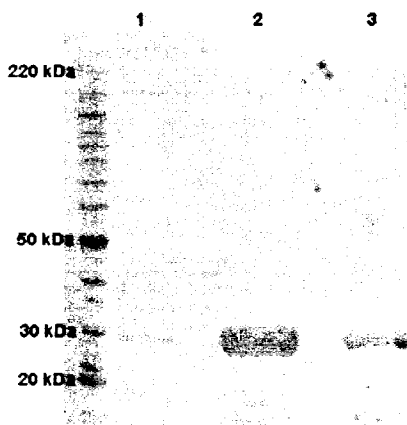
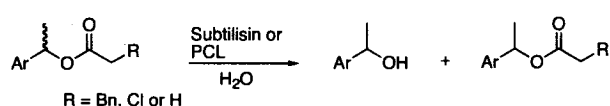


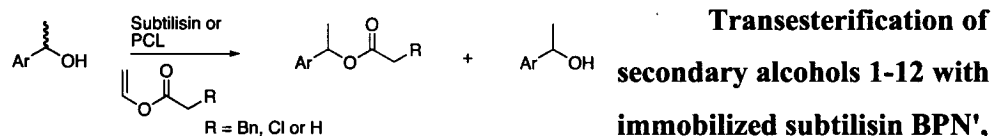
Figure A3.1. SDS-polyacrylamide gel electrophoresis of subtilisin BPN' and E from *B. subtilis* DB104 carrying pBE3 and subtilisin Carlsberg (Sigma-Aldrich). The gel was stained by Coomassie Blue. To prevent autolysis, subtilisin was treated with PMSF (phenylmethylsulfonylfluoride) before denaturation. Purified PMSF-inhibited subtilisin BPN' is shown in *lane 1*. PMSF-inhibited subtilisin Carlsberg is shown in *lane 2*. Purified PMSF-inhibited subtilisin E is shown in *lane 3*.



Hydrolysis of esters 1a-13a with subtilisin BPN', subtilisin Carlsberg, subtilisin E or PCL.

Subtilisin BPN', subtilisin Carlsberg, subtilisin E or PCL (solution in 50 mM BES buffer (pH 7.2, 395 μL), CaCl₂ (1 M, 5 μL), 100 mM BES buffer (pH 7.2, 50 μL) and substrate (100 mM in CH₃CN, 50 μL) were mixed in a 1.5 mL polypropylene conical tube or 1.5 mL glass vial. The reaction was shaken at 30 °C for 48 h with **1a**, **3a**, **4a**, **6a**, **7a**, **8a**, **9a**, **10a**, **11a**, **11c**, **12a** and **13a**, 2 h with **2a** and **5a** and 3 h with **10b** and **12b**. The reaction was terminated with the addition of CH₂Cl₂ (500 μL). The phases were separated by centrifugation, and the organic layers were collected. The aqueous phase was extracted with CH₂Cl₂ (2 x 500 μL) and the combined organics were evaporated under a stream of air. The residue was diluted with EtOAc or EtOH (150 μL) and analyzed by GC or HPLC. The enantiomers were separated using the conditions described above.

Immobilization of subtilisin BPN', subtilisin Carlsberg, subtilisin E and PCL.¹¹ Subtilisin BPN' (54.5 mg), subtilisin Carlsberg (52.5 mg) and subtilisin E (52.5 mg) or PCL (57.5 mg) was dissolved in 50 mM phosphate buffer (pH 7.5, 30 mL) and KCl (10.78 g) was added with swirling. The solution was frozen in liquid N₂ and lyophilized for 48 h.



Transesterification of secondary alcohols 1-12 with immobilized subtilisin BPN', subtilisin Carlsberg, subtilisin E or PCL. KCl-subtilisin or KCl-PCL powder (ca. 500 mg, ca. 2.5 mg protein), dihydrocinnamic vinyl ester (18 mg, 100 μ mol), chloroacetic vinyl ester (12 mg, 100 μ mol) or vinyl acetate (9 mg, 100 μ mol), secondary alcohol (500 μ mol) and 4 Å molecular sieves (100 mg) were added to a glass vial. Anhydrous dioxane (2 mL) was added and the mixture was stirred at 30 °C for at least 48 h. A small amount of the solution was removed, filtered through a 0.45 μ m nylon filter and analyzed by GC or HPLC. The enantiomers were separated using the conditions described above.

Modelling of tetrahedral intermediates bound to subtilisin E. All modelling was performed using *Insight II 2000.1 / Discover* (Accelrys, San Diego, USA) on a SGI Octane UNIX workstation using the AMBER force field.¹⁴ We used a nonbonded cutoff distance of 8 Å, a distance-dependent dielectric of 1.0 and scaled the 1-4 van der Waals interactions by 50%. Protein structures in Figure A3.2 were created using PyMOL (Delano Scientific, San Carlos, CA, USA). The x-ray crystal structure of subtilisin E (entry 1SCJ)¹⁵ from the Protein Data Bank is a Ser221Cys subtilisin E-propeptide complex. Using the Builder module of *Insight II*, we replaced the Cys221 with a serine and removed the propeptide region. The hydrogen atoms were added to correspond to pH 7.0. Histidines were uncharged, aspartates and glutamates were negatively charged, and arginines and lysines were positively charged. The catalytic histidine (His64) was protonated. The positions of the water hydrogens and then the enzyme hydrogens were optimized using a consecutive series of short (1 ps) molecular dynamic runs and energy minimizations.¹⁶ This optimization was repeated until there was <2 kcal/mol in the energy

of the minimized structures. Thereafter, an iterative series of geometry optimizations were performed on the water hydrogens, enzyme hydrogens and full water molecules. Finally, the whole system was geometry optimized.

The tetrahedral intermediates were built manually and covalently linked to Ser221. Nonstandard partial charges were calculated using a formal charge of -1 for the substrate oxyanion. Energy minimization proceeded in three stages. First, minimization of substrate with only the protein constrained ($25 \text{ kcal mol}^{-1} \text{ \AA}^{-2}$); second, minimization with only the protein backbone constrained ($25 \text{ kcal mol}^{-1} \text{ \AA}^{-2}$) and for the final stage the minimization was continued without constraints until the rms value was less than $0.0005 \text{ kcal mol}^{-1} \text{ \AA}^{-1}$. A catalytically productive complex required all five hydrogen bonds within the catalytic machinery. We set generous limits for a hydrogen bond: a donor to acceptor atom distance of less than 3.1 \AA with a nearly linear arrangement ($>120^\circ$ angle) of donor atom, hydrogen, and acceptor atom. Structures lacking any of the five catalytically relevant hydrogen bonds or encountering severe steric clash with enzyme were deemed nonproductive.

Molecular modelling details for (*R*)-1a and (*S*)-1a tetrahedral intermediates bound to subtilisin E. Modelling 1a with subtilisin E gave one productive conformation for each enantiomer. The two other plausible conformations encountered severe steric clash with the protein. Similar to previous modelling studies with subtilisin Carlsberg,¹⁷ the productive conformation of the (*S*)-1a binds with the methyl group in the leaving-group S_1' pocket and the productive conformation of the (*R*)-1a has the phenyl group in this pocket.

Productive conformer of (*R*)-1a (Figure A3.2). (*R*)-1a fit well in the active site, but S_1' pocket residues bumped the phenyl group ($C_{\text{ortho}} - C_{\epsilon}$ (Met222) distance = 3.77 \AA , $C_{\text{meta}} - C_{\gamma}$ (Tyr217) distance = 3.68 \AA , $C_{\text{para}} - C_{\beta}$ (Tyr217) distance = 3.72 \AA and $C_{\text{ortho}} - C_{\alpha}$ (Gly219) distance = 3.72 \AA).¹⁸ The increased steric interaction between S_1' residues and the phenyl group may hinder binding of (*R*)-1a and account for the enantioselectivity of subtilisin E for (*S*)-1a in organic solvent. However, this tight fit also suggests a favourable hydrophobic interaction - tendency of nonpolar compounds to transfer from an aqueous phase to an organic phase - between the phenyl group and S_1' pocket residues.¹⁹ This favourable hydrophobic interaction may improve binding of the phenyl group and

account for the enantioference with secondary alcohols in water. In nonpolar media, this favourable hydrophobic effect is expected to be negligible, thus the increased steric hindrance experienced by the phenyl group versus the methyl group in the S_1' pocket would favour reaction of (*S*)-1a.

Non-productive conformer of (*R*)-1a (not shown). The methyl group of non-productive (*R*)-1a bumped catalytic His 64 (CH_3 - $\text{C}_{\delta 2}$ distance = 3.58 Å and the phenyl group encountered steric clash with the oxyanion hole Asn155 (C_{ipso} - $\text{N}_{\delta 2}$ distance = 3.41 and C_{ortho} - $\text{N}_{\delta 2}$ distance = 3.29 Å).¹⁸ The methyl group was forced out of the S_1' leaving-group pocket because of this steric clash with active site residues.

Productive conformer of (*S*)-1a (Figure A3.2). (*S*)-1a fit well in the active site and S_1' residues did not hinder the methyl group.

Non-productive conformer of (*S*)-1a (not shown). The phenyl group of non-productive (*S*)-1a encountered steric clash with catalytic His 64 (C_{ipso} - $\text{C}_{\delta 2}$ distance = 3.53 Å, C_{ortho} - $\text{N}_{\delta 2}$ distance = 3.53 Å, C_{ortho} - $\text{C}_{\delta 2}$ distance = 3.44 Å and C_{meta} - $\text{C}_{\delta 2}$ distance = 3.52 Å) and the methyl group bumped the oxyanion hole Asn 155 (C_{methyl} - $\text{N}_{\delta 2}$ distance = 3.68 Å).¹⁸ The phenyl group was forced out of the S_1' leaving-group pocket because of this steric clash with active site residues.

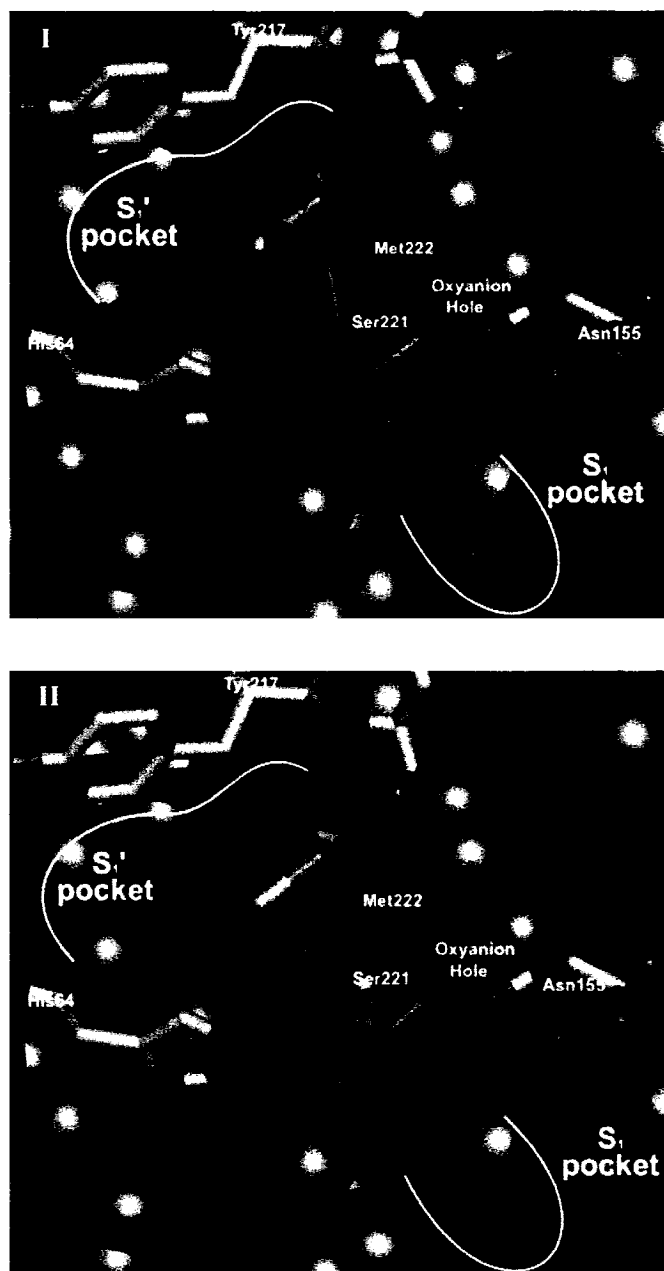


Figure A3.2. Catalytically competent orientation of the tetrahedral intermediates for the subtilisin E catalyzed hydrolysis of (*R*)-**1a** (I) and (*S*)-**1a** (II) as identified by molecular modelling. The important active site and substrate atoms are shown as sticks. The atoms are coloured as follows: green (substrate carbon), grey (enzyme carbon), red (oxygen), blue (nitrogen) and orange (sulfur). Surrounding atoms (space fill) of subtilisin are shown in the colour blue. For clarity, all hydrogen atoms and water molecules are hidden. The binding modes of I and II maintain all catalytically essential hydrogen bonds and the ben-

zyl moiety of the dihydrocinnamoyl group was bound in the S_1 pocket, as expected based on its similarity to phenylalanine. On the basis of previous work with secondary alcohols, the phenyl group (Large) or methyl group (Medium) was bound in the leaving-group S_1' pocket.¹⁷ In the fast-reacting enantiomer, (*R*)-**1a** (I), the phenyl group is bound in the hydrophobic S_1' pocket and the methyl group is exposed to solvent water. In the slow-reacting enantiomer, (*S*)-**1a** (II), the methyl group is bound in the hydrophobic S_1' pocket and the phenyl group is exposed to solvent water. The non-productive conformations (not shown) encountered severe steric clash with the active site residues of the protein.

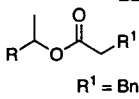
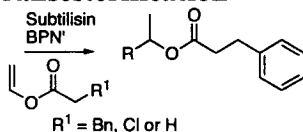
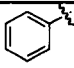
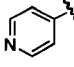
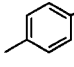
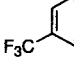
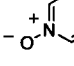
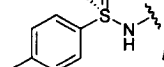
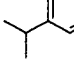
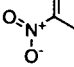
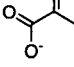
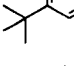
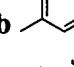
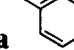
Table A3.1. Minimized structures for the tetrahedral intermediate for the subtilisin E-catalyzed hydrolysis of **1a**

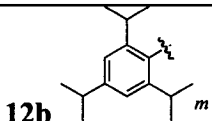
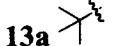
Conformation	Group in $S_1'^a$	H-bond $N_{\epsilon 2}-O_\gamma$ distance (Å) (N-H-O $_\gamma$ angle, deg) ^b	Comments
(<i>R</i>)- 1a (Figure A3.2)	phenyl	2.94 (136)	Steric contact with Tyr 217, Gly 219 and Met 222 in S_1' pocket
(<i>R</i>)- 1a (not shown)	methyl ^c	2.99 (134)	Steric clash with catalytic residues His 64 and Asn 155
(<i>S</i>)- 1a (Figure A3.2)	methyl	2.95 (138)	Unhindered in S_1' pocket
(<i>S</i>)- 1a (not shown)	phenyl ^c	3.11 (135)	Steric clash with catalytic residues His 64 and Asn 155

^aNarrow, hydrophobic pocket where leaving-group alcohol binds. ^bUnless otherwise noted, hydrogen bonds (His 64 $N_{\epsilon 2} - O$, Ser 221 $NH - O^-$, and Asn155 $NH_{\delta 2} - O^-$) were present in all structures (N - O distance 2.7 – 3.1 Å, N-H-O angle 120- 175°). ^cGroup is forced out of S_1' because of steric clash with active site residues.

Tables of Enantioselectivity. Tables A3.2-A3.5 support Table 3.1. They provide the enantiomer excess and enantioselectivity data for subtilisin BPN', Carlsberg and E-catalyzed hydrolysis of esters **1a-13a**, **10b** and **12b** and transesterification of secondary alcohols **1-12**. Table A3.5 provides the enantiomer excess and enantioselectivity data for PCL-catalyzed hydrolysis of esters **1a-13a** and **10b**, **11c** and **12b** and transesterification of **1-12**.

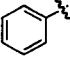
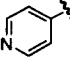
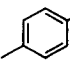
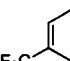
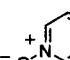
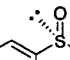
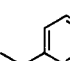
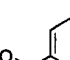

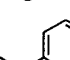
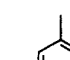
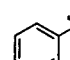
Table A3.2. Enantioselectivity of BPN¹-catalyzed hydrolysis of **1a-13a** and transesterification of **1-13** with a vinyl ester in dioxane

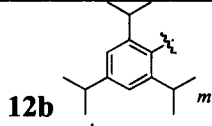
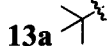
Hydrolysis					Transesterification ^a				
									
R	ee _s (%) ^b	ee _p (%) ^b	E ^c (ΔΔG [‡]) ^d	E _{pref} ^e	ee _s (%) ^b	ee _p (%) ^b	E ^c (ΔΔG [‡]) ^d	E _{pref} ^e	
1a 	21	85	15 (1.6)	R ^f	1	66	4.9 (1.0)	S	
2a 	29	33	2.6 (0.6)	R ^f	2	89	18 (1.7)	S	
3a 	31	93	37 (2.2)	R ^g	1	49	3.0 (0.7)	S	
4a 	4	81	9.9 (1.4)	R ^g	1	87	15 (1.6)	S	
5a 	42	27	2.5 (0.6)	S ^h	3	82	10 (1.4)	S	
	44	94	50 (2.4)	R	n.r. ^j	n.r.	n.r.	n.r.	
6a 	10	98	109 (2.8)	R ^k	1	4	1.1 (0.1)	R	
7a 	5	60	4.2 (0.9)	R ^l	4	82	11 (1.4)	S	
8a 	13	69	6.2 (1.1)	S ^k	n.r.	n.r.	n.r.	n.r.	
9a 	2	89	18 (1.7)	R ^k	n.r.	n.r.	n.r.	n.r.	
10b 	38 ⁿ	55	4.9 (1.0)	R ^g	3	41 ⁿ	2.5 (0.6)	R	
11a 	4	49	3.0 (0.7)	S ^f	19	51	3.7 (0.8)	S	

	n.r.	n.r.	n.r.	n.r.	n.r.	n.r.	n.r.	n.r.
	n.r.	n.r.	n.r.	n.r.	n.p. ^o	n.p.	n.p.	n.p.

^aEnzyme immobilized on KCL. ^bEnantiomeric excess: enantiomeric excess of substrate and product were determined by GC analysis on 25 m x 0.25 mm Chrompack CP-Chiralsil-Dex CB column (Varian Inc., Palo Alto, CA, USA) using He as a carrier gas or HPLC analysis performed on a 4.6 x 250 mm Daicel Chiralcel OD or Chiralpak AD-H column (Chiral Technologies, Exton, USA) and monitored at 254 nm. ^cEnantioselectivity: the enantiomeric ratio *E* measures the relative rate of hydrolysis of the fast enantiomer as compared to the slow enantiomer as defined by Sih (Chen, C.S.; Fujimoto, Y.; Girdaukas, G.; Sih, C.J. *J. Am. Chem. Soc.* **1982**, *104*, 7294-7299). ^d $\Delta\Delta G^\ddagger = -RT \ln V_A/V_B$, where V_A and V_B are the reaction rates of enantiomers A and B, respectively. $\Delta\Delta G^\ddagger$ is the difference in activation energy of the enantiomeric substrates. This is a direct measure for the selectivity of reaction, which in turn depends on the ratio of the individual reaction rates of the enantiomers (see Faber, K. *Biotransformations in Organic Chemistry*; Springer-Verlag: Berlin, 1997; pp 17-20.). ^eEnantiopreference. ^fAbsolute configuration determined by comparison with an authentic sample (Sigma-Aldrich). ^gAbsolute configuration determined by similarity in the order of elution in the GC analysis (Doucet, H.; Fernandez, E.; Layzell, T. P.; Brown, J. M. *Chem. Eur. J.* **1999**, *5*, 1320-1330.). ^hAbsolute configuration determined by comparison with an authentic sample prepared as described above. ⁱ*N*-Dihydrocinnamoyl-*p*-toluenesulfinamide. From Mugford, P. F.; Magloire, V. M.; Kazlauskas, R. J. *J. Am. Chem. Soc.* **2005**, *127*, 6536-6537. ^jNo reaction. ^kAbsolute configuration determined using the configurational correlation model for the corresponding (*R*)-MTPA derivatives (Dale, J. A.; Mosher, H. S. *J. Am. Chem. Soc.* **1973**, *95*, 512-519.). ^lAbsolute configuration determined by similarity in the order of elution in the GC analysis (Uray, G.; Stampfer, W.; Fabian, W. M. F. *J. Chromatogr. A* **2003**, *992*, 151-157.). ^mReaction as chloroacetate. ⁿ**10b** could not be separated by GC or HPLC. To facilitate analysis, **10b** was purified on silica gel (100% hexanes to 90:10 hexanes/EtOAc) and hydrolyzed in 1 N KOH (1:1 EtOH/H₂O) to **10** for GC analysis. ^oNot performed.

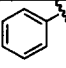
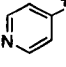
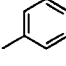
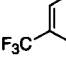
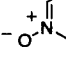
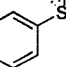
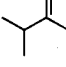
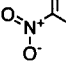
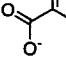
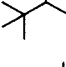
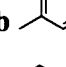
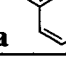
Table A3.3. Enantioselectivity of subtilisin Carlsberg-catalyzed hydrolysis of **1a-13a** and transesterification of **1-13** with a vinyl ester in dioxane

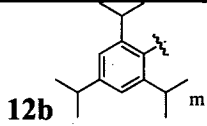
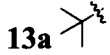
R	Hydrolysis				Transesterification ^a			
	ee _s (%) ^b	ee _p (%) ^b	E ^c (ΔΔG°) ^d	E _{pref} ^e	ee _s (%) ^b	ee _p (%) ^b	E ^c (ΔΔG°) ^d	E _{pref} ^e
1a 	9	5	1.2 (0.1)	R ^f	4	92	25 (1.9)	S
2a 	9	24	1.7 (0.3)	S ^f	3	89	18 (1.7)	S ^e
3a 	1	6	1.1 (0.1)	S ^g	1	94	33 (2.1)	S ^f
4a 	4	36	2.2 (0.5)	S ^g	1	97	66 (2.5)	S ^f
5a 	30	40	3.1 (0.7)	S ^h	1	94	32 (2.1)	S ^g
6a 	82	64	11 (1.4)	R	n.r. ^j	n.r.	n.r.	n.r.
7a 	7	40	2.5 (0.6)	R ^k	2	83	11 (1.4)	S
8a 	20	31	2.3 (0.5)	S ^l	4	60	4.2 (0.9)	S
9a 	41	43	3.6 (0.8)	S ^k	n.r.	n.r.	n.r.	n.r.
10b 	3	32	2.0 (0.4)	R ^k	1	73	6.5 (1.1)	S
11a 	5 ⁿ	23	1.7 (0.3)	S ^g	3	55 ⁿ	3.6 (0.8)	S
11a 	2	51	3.1 (0.7)	S ^f	11	89	19 (1.8)	S

	n.r.	n.r.	n.r.	n.r.	n.r.	n.r.	n.r.	n.r.
	n.r.	n.r.	n.r.	n.r.	n.p. ^o	n.p.	n.p.	n.p.

^aEnzyme immobilized on KCL. ^bEnantiomeric excess: enantiomeric excess of substrate and product were determined by GC analysis on 25 m x 0.25 mm Chrompack CP-Chiralsil-Dex CB column (Varian Inc., Palo Alto, CA, USA) using He as a carrier gas or HPLC analysis performed on a 4.6 x 250 mm Daicel Chiralcel OD or Chiralpak AD-H column (Chiral Technologies, Exton, USA) and monitored at 254 nm. ^cEnantioselectivity: the enantiomeric ratio *E* measures the relative rate of hydrolysis of the fast enantiomer as compared to the slow enantiomer as defined by Sih (Chen, C.S.; Fujimoto, Y.; Girdaukas, G.; Sih, C.J. *J. Am. Chem. Soc.* **1982**, *104*, 7294-7299). ^d $\Delta\Delta G^\ddagger = -RT \ln V_A/V_B$, where V_A and V_B are the reaction rates of enantiomers A and B, respectively. $\Delta\Delta G^\ddagger$ is the difference in activation energy of enantiomeric substrates. This is a direct measure for the selectivity of reaction, which in turn depends on the ratio of the individual reaction rates of the enantiomers (see Faber, K. *Biotransformations in Organic Chemistry*; Springer-Verlag: Berlin, 1997; pp 17-20.). ^eEnantiopreference. ^fAbsolute configuration determined by comparison with an authentic sample (Sigma-Aldrich). ^gAbsolute configuration determined by similarity in the order of elution in the GC analysis (Doucet, H.; Fernandez, E.; Layzell, T. P.; Brown, J. M. *Chem. Eur. J.* **1999**, *5*, 1320-1330.). ^hAbsolute configuration determined by comparison with an authentic sample prepared as described above. ⁱ*N*-Dihydrocinnamoyl-*p*-toluenesulfinamide. From Savile, C. K.; Magloire, V. M.; Kazlauskas, R. J. *J. Am. Chem. Soc.* **2005**, *127*, 2104-2113. ^jNo reaction. ^kAbsolute configuration determined using the configurational correlation model for the corresponding (*R*)-MTPA derivatives (Dale, J. A.; Mosher, H. S. *J. Am. Chem. Soc.* **1973**, *95*, 512-519.). ^lAbsolute configuration determined by similarity in the order of elution in the GC analysis (Uray, G.; Stampfer, W.; Fabian, W. M. F. *J. Chromatogr. A* **2003**, *992*, 151-157.). ^mReaction as chloroacetate. ⁿ**10b** could not be separated by GC or HPLC. To facilitate analysis, **10b** was purified on silica gel (100% hexanes to 90:10 hexanes/EtOAc) and hydrolyzed in 1 N KOH (1:1 EtOH/H₂O) to **10** for GC analysis. ^oNot performed.

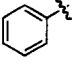
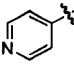
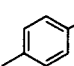
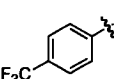
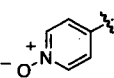
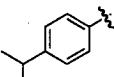
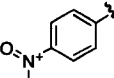
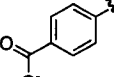
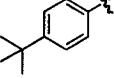
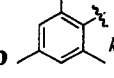
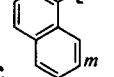
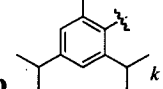
Table A3.4. Enantioselectivity of subtilisin E-catalyzed hydrolysis of **1a-13a** and transesterification of **1-13** with a vinyl ester in dioxane

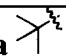
R	Hydrolysis				Transesterification ^a			
	ee _s (%) ^b	ee _p (%) ^b	E ^c (ΔΔG°) ^d	E _{pref} ^e	ee _s (%) ^b	ee _p (%) ^b	E ^c (ΔΔG°) ^d	E _{pref} ^e
1a 	22	70	7.0 (1.2)	R ^f	2	36	2.2 (0.7)	S
2a 	18	11	1.5 (0.2)	R ^f	5	90	20 (1.8)	S
3a 	31	84	16 (1.7)	R ^g	1	17	1.5 (0.2)	S
4a 	10	75	7.7 (1.2)	R ^g	1	75	7.1 (1.2)	S
5a 	31	83	4.5 (0.9)	S ^h	1	84	12 (1.5)	S
6a 	89	99	>150 (>3.0)	R	n.r. ^j	n.r.	n.r.	n.r.
7a 	11	98	110 (2.8)	R ^k	1	84	12 (1.5)	S
8a 	5	45	2.8 (0.6)	R ^l	4	85	13 (1.5)	S
9a 	23	63	5.5 (1.0)	S ^k	n.r.	n.r.	n.r.	n.r.
10b 	4	90	20 (1.8)	R ^k	1	37	2.2 (0.5)	S
11a 	17	87	17 (1.7)	R ^g	1	24	1.7 (0.3)	R
11a 	6	26	1.8 (0.4)	R ^f	6	58	4.0 (0.8)	S

	n.r.	n.r.	n.r.	n.r.	n.r.	n.r.	n.r.	n.r.
	n.r.	n.r.	n.r.	n.r.	n.p. ^o	n.p.	n.p.	n.p.

^aEnzyme immobilized on KCL. ^bEnantiomeric excess: enantiomeric excess of substrate and product were determined by GC analysis on 25 m x 0.25 mm Chrompack CP-Chiralsil-Dex CB column (Varian Inc., Palo Alto, CA, USA) using He as a carrier gas or HPLC analysis performed on a 4.6 x 250 mm Daicel Chiralcel OD or Chiralpak AD-H column (Chiral Technologies, Exton, USA) and monitored at 254 nm. ^cEnantioselectivity: the enantiomeric ratio *E* measures the relative rate of hydrolysis of the fast enantiomer as compared to the slow enantiomer as defined by Sih (Chen, C.S.; Fujimoto, Y.; Girdaukas, G.; Sih, C.J. *J. Am. Chem. Soc.* **1982**, *104*, 7294-7299). ^d $\Delta\Delta G^\ddagger = -RT \ln V_A/V_B$, where V_A and V_B are the reaction rates of enantiomers A and B, respectively. $\Delta\Delta G^\ddagger$ is the difference in activation energy of enantiomeric substrates. This is a direct measure for the selectivity of reaction, which in turn depends on the ratio of the individual reaction rates of the enantiomers (see Faber, K. *Biotransformations in Organic Chemistry*; Springer-Verlag: Berlin, 1997; pp 17-20.). ^eEnantiopreference. ^fAbsolute configuration determined by comparison with an authentic sample (Sigma-Aldrich). ^gAbsolute configuration determined by similarity in the order of elution in the GC analysis (Doucet, H.; Fernandez, E.; Layzell, T. P.; Brown, J. M. *Chem. Eur. J.* **1999**, *5*, 1320-1330.). ^hAbsolute configuration determined by comparison with an authentic sample prepared as described above. ⁱ*N*-Dihydrocinnamoyl-*p*-toluenesulfinamide. From Savile, C. K.; Magloire, V. M.; Kazlauskas, R. J. *J. Am. Chem. Soc.* **2005**, *127*, 2104-2113. ^jNo reaction. ^kAbsolute configuration determined using the configurational correlation model for the corresponding (*R*)-MTPA derivatives (Dale, J. A.; Mosher, H. S. *J. Am. Chem. Soc.* **1973**, *95*, 512-519.). ^lAbsolute configuration determined by similarity in the order of elution in the GC analysis (Uray, G.; Stampfer, W.; Fabian, W. M. F. *J. Chromatogr. A* **2003**, *992*, 151-157.). ^mReaction as chloroacetate. ⁿ**10b** could not be separated by GC or HPLC. To facilitate analysis, **10b** was purified on silica gel (100% hexanes to 90:10 hexanes/EtOAc) and hydrolyzed in 1 N KOH (1:1 EtOH/H₂O) to **10** for GC analysis. ^oNot performed.

Table A3.5. Enantioselectivity of PCL-catalyzed hydrolysis of **1a-13a** or transesterification of **1-13** with a vinyl ester in dioxane

R	Hydrolysis				Transesterification ^a			
	ee _s (%) ^b	ee _p (%) ^b	E ^c (ΔΔG [‡]) ^d	E _{pref} ^e	ee _s (%) ^b	ee _p (%) ^b	E ^c (ΔΔG [‡]) ^d	E _{pref} ^e
1a 	94	99	>150 (>3.0)	R ^f	2	99	>150 (>3.0)	R
2a 	89	94	97 (2.8)	R ^f	3	99	>150 (>3.0)	R
3a 	47	92	38 (2.2)	R ^g	3	99	>150 (>3.0)	R
4a 	62	98	>150 (3.0)	R ^g	1	99	>150	R
5a 	18	79	10 (1.4)	R ^h	1	79	8.6 (1.3)	R
6a 	64	99	>150 (>3.0)	R ⁱ	1	99	>150 (>3.0)	R
7a 	37	98	142 (3.0)	R ^j	1	99	>150 (>3.0)	R
8a 	41	98	148 (3.0)	R ⁱ	n.r.	n.r.	n.r.	n.r.
9a 	75	99	>150 (>3.0)	R ⁱ	1	99	>150 (>3.0)	R
10b 	n.r. ^l	n.r.	n.r.	n.r.	n.r.	n.r.	n.r.	n.r.
11c 	14	99	>150 (>3.0)	R ^f	1	99	>150 (>3.0)	R
12b 	n.r.	n.r.	n.r.	n.r.	n.r.	n.r.	n.r.	n.r.

13a 	n.r.	n.r.	n.r.	n.r.	n.p. ⁿ	n.p.	n.p.	n.p.
---	------	------	------	------	-------------------	------	------	------

^aEnzyme immobilized on KCL. ^bEnantiomeric excess: enantiomeric excess of substrate and product were determined by GC analysis on 25 m x 0.25 mm Chrompack CP-Chiralsil-Dex CB column (Varian Inc., Palo Alto, CA, USA) using He as a carrier gas or HPLC analysis performed on a 4.6 x 250 mm Daicel Chiralcel OD or Chiralpak AD-H column (Chiral Technologies, Exton, USA) and monitored at 254 nm. ^cEnantioselectivity: the enantiomeric ratio *E* measures the relative rate of hydrolysis of the fast enantiomer as compared to the slow enantiomer as defined by Sih (Chen, C.S.; Fujimoto, Y.; Girdaukas, G.; Sih, C.J. *J. Am. Chem. Soc.* **1982**, *104*, 7294-7299). ^d $\Delta\Delta G^\ddagger = -RT \ln V_A/V_B$, where V_A and V_B are the reaction rates of enantiomers A and B, respectively. $\Delta\Delta G^\ddagger$ is the difference in activation energy of enantiomeric substrates. This is a direct measure for the selectivity of reaction, which in turn depends on the ratio of the individual reaction rates of the enantiomers (see Faber, K. *Biotransformations in Organic Chemistry*; Springer-Verlag: Berlin, 1997; pp 17-20.). ^eEnantiopreference. ^fAbsolute configuration determined by comparison with an authentic sample (Sigma-Aldrich). ^gAbsolute configuration determined by similarity in the order of elution in the GC analysis (Doucet, H.; Fernandez, E.; Layzell, T. P.; Brown, J. M. *Chem. Eur. J.* **1999**, *5*, 1320-1330.). ^hAbsolute configuration determined by comparison with an authentic sample prepared as described above. ⁱAbsolute configuration determined using the configurational correlation model for the corresponding (*R*)-MTPA derivatives (Dale, J. A.; Mosher, H. S. *J. Am. Chem. Soc.* **1973**, *95*, 512-519.). ^jAbsolute configuration determined by similarity in the order of elution in the GC analysis (Uray, G.; Stampfer, W.; Fabian, W. M. F. *J. Chromatogr. A* **2003**, *992*, 151-157.). ^kReaction as chloroacetate. ^lNo reaction. ^mReaction as acetate. ⁿNot performed.

References (Chapter 3 – Appendix)

1. Lipase from *Burkholderia cepacia* was formerly known as lipase from *Pseudomonas cepacia*.
2. Zhao, H.; Arnold, F. H. *Proc. Natl. Acad. Sci. USA* **1997**, *94*, 7997-8000.
3. Kawamura, F.; Doi, R. H. *J. Bacteriol.* **1984**, *160*, 442-444.
4. Lin, Y. Y.; Palmer, D. N.; Jones, J. B. *Can. J. Chem.* **1974**, *52*, 469-476.
5. Craig, J. C.; Purushothaman, K. K. *J. Org. Chem.* **1970**, *35*, 1721-1722.

6. Taylor, R. *J. Chem. Soc., Perkin Trans. 2* **1975**, 277-281.
7. Doucet, H.; Fernandez, E.; Layzell, T. P.; Brown, J. M. *Chem. Eur. J.* **1999**, 5, 1320-1330.
8. Uray, G.; Stampfer, W.; Fabian, W. M. F. *J. Chromatogr. A* **2003**, 992, 151-157.
9. Delair, P.; Kanazawa, A. M.; de Azevedo, M. B. M.; Greene, A. E. *Tetrahedron: Asymmetry* **1996**, 7, 2707-2710.
10. Dale, J. A.; Mosher, H. S. *J. Am. Chem. Soc.* **1973**, 95, 512-519.
11. Lloyd, R. C.; Dickman, M.; Jones, J. B. *Tetrahedron: Asymmetry* **1998**, 9, 551-561.
12. Harwood, C. R.; Cutting, S. M. *Molecular Biological Methods for Bacillus*, John Wiley & Sons: Chichester, U.K., 1990; pp 33-35 and 391-402.
13. Cho, S.-J.; OH, S.-H.; Pridmore, R. D.; Juillerat, M. A.; Lee, C.-H. *J. Agric. Food Chem.* **2003**, 51, 7664-7670.
14. (a) Weiner, S. J.; Kollman, P. A.; Case, D. A.; Singh, U. C.; Ghio, C.; Alagona, G.; Profeta, S.; Weiner, P. *J. Am. Chem. Soc.* **1984**, 106, 765-784. (b) Weiner, S. J.; Kollman, P. A.; Nguyen, D. T.; Case, D. A. *J. Comp. Chem.* **1986**, 7, 230-252.
15. Jain, S. C.; Shinde, U.; Li, Y.; Inouye, M.; Berman, H. M. *J. Mol. Biol.* **1998**, 284, 137-144.
16. Raza, S.; Fransson, L.; Hult, K. *Protein Sci.* **2001**, 10, 329-338.
17. Fitzpatrick, P. A.; Ringe, D.; Klibanov, A. M. *Biotechnol. Bioeng.* **1992**, 40, 735-742.
18. The van der Waals distance for CH-C = 3.99 Å, CH-N = 3.84 Å and O-HC = 3.81 Å. These were estimated from the van der Waals radii of carbon (1.70 Å), nitrogen (1.55 Å) or oxygen (1.52 Å) and hydrogen (1.20 Å) and the C-H bond length (1.09 Å) or O-H bond length (0.96 Å) from Bondi, A. *J. Phys. Chem.* **1964**, 68, 441-451.
19. The energy of a hydrophobic interaction is from the regaining of entropy by water after it is removed from a hydrophobic group and can be estimated using the incremental Gibbs free energy of transfer.^{20,21} The incremental Gibbs free energy of transfer of the phenyl group from *n*-octanol to water was estimated to be ca. +2.9 kcal/mol, using $\Delta G_{\text{trans}} = 2.303RT\pi$, where π is the hydrophobicity constant of the phenyl group ($\pi = 2.1$)²² relative to hydrogen,²⁰ whereas the methyl group was ca. +1.5 kcal/mol. Thus, the energy difference between the two groups is ca. 1.4 kcal/mol in favour of the phenyl group when in an aqueous medium.

20. Fersht, A. *Structure and Mechanism in Protein Science*; W.H. Freeman and Company: New York, 1998; pp 324-348.
21. Leo, A.; Hansch, C.; Elkins, D. *Chem. Rev.* **1971**, *71*, 525-616.
22. Hydrophobicity partition coefficients (LogP) values were calculated using a computer program, *ClogP* (BioByte, Claremont, USA).

Chapter 4

Developing efficient routes for large-scale preparation of enantiopure compounds is the foundation of commercial biocatalysis. In this chapter we use our anchor group strategy to extend two readily available proteases, α -chymotrypsin and subtilisin Carlsberg, to *N*-acyl sulfinamides and sterically hindered secondary alcohols, respectively. We design a new anchoring acyl group that increases protease activity, increases substrate solubility in aqueous solutions and facilitates separation of product and substrate without using chromatography. This strategy will be useful for large-scale preparation of enantiopure sulfinamides and sterically hindered secondary alcohols.

The 3-(3-pyridyl)propionyl anchor group for large-scale protease-catalyzed resolution of *p*-toluenesulfinamide and sterically hindered secondary alcohols

Abstract

The 3-(3-pyridyl)propionyl acyl group serves as an anchor to increase binding to proteases, increase solubility of substrate and simplify separation of substrate and product. Proteases react up to six-hundred-fold faster with 1-phenethyl 3-(3-pyridyl)propionate versus 1-phenethyl acetate. The 3-(3-pyridyl)propionyl group increases reactivity by increasing substrate binding to active site and increasing substrate solubility in aqueous solutions. The 3-(3-pyridyl)propionyl group permits facile separation of substrate and product via mild acid extraction. To demonstrate the synthetic usefulness of this strategy, we resolve multi-gram quantities of (*R*)- and (*S*)-*p*-toluenesulfinamide with α -chymotrypsin and gram quantities of (*R*)- and (*S*)-2,2-dimethylcyclopentanol with subtilisin Carlsberg. The 3-(3-pyridyl)propionyl group is better with these protease-catalyzed resolutions than the corresponding acetate or dihydrocinnamate because it decreases reaction time by increasing reactivity, it decreases reaction volume by increasing substrate solubility and it facilitates purification without chromatography. Molecular modelling suggests the enantioselectivity of α -chymotrypsin toward (*R*)-*p*-toluenesulfinamide is high ($E = 52$) because of a favourable hydrophobic interaction between the *p*-tolyl group of the fast-reacting (*R*)-enantiomer and leaving group pocket. The enantioselectivity of subtilisin Carlsberg toward (*S*)-2,2-dimethylcyclopentanol is high ($E = 43$) because the 2,2-dimethyl quaternary carbon of the slow-reacting (*R*)-enantiomer is too large to bind in the S_1' leaving group pocket.

4.1 Introduction

Synthetic chemists often use lipases and proteases as enantioselective catalysts for resolution of secondary alcohols, amines and related compounds.¹ The lipases attract more attention than proteases because of their higher reactivity and enantioselectivity toward secondary alcohols.² The reactivity and enantioselectivity of lipases and proteases differ because their structure and substrate preference differ. Lipases have deep active site pockets for two alcohol substituents³ and bind substrate in a folded conformation.⁴ Proteases, on the other hand, have a shallow active site on the surface of the protein and bind substrate in an extended conformation.⁵ They have only one alcohol recognition pocket – the medium-sized S₁' pocket – to bind one substituent, while the other substituent is open to solvent.⁶ Since the active site of proteases is on the surface of the protein and only one substituent is bound, they accept polar⁷ and sterically hindered substrates,⁸ whereas many lipases do not. Unlike lipases, however, proteases need an anchoring acyl group to bind substrate^{9,10} and can only hydrolyze soluble substrates – most compounds of interest for organic synthesis are usually nonpolar and thus, poorly soluble in aqueous solutions.

Choice of acyl group can influence the reactivity and enantioselectivity of proteases.¹¹ While the most common acyl group, acetate, is useful for lipases, it reacts slowly with proteases such as subtilisin and α -chymotrypsin. These proteases require a large acyl group to bind substrate and catalyze hydrolysis.^{9,10} The dihydrocinnamoyl group is an effective acyl group for binding substrate. Jones and coworkers⁹ showed α -chymotrypsin binds dihydrocinnamoyl esters as tightly as *N*-acetyl phenylalanine esters and reacts at least one-hundred-fold faster than *N*-acetyl glycine esters. We previously used this group to extend subtilisin E to a new class of substrates, *N*-acyl arylsulfonamides, to give a variety of enantiopure sulfonamides.^{7b} Subtilisin E did not catalyze hydrolysis of *N*-acetyl arylsulfonamides, but it did catalyze hydrolysis of *N*-dihydrocinnamoyl arylsulfonamides. While the dihydrocinnamoyl group is useful for binding substrate, it is poorly soluble in aqueous solutions.

Large-scale resolution of racemic compounds using hydrolases is a simple and cost-effective strategy to produce enantiopure materials.¹² However, separation of substrate and product can be tedious and expensive. Thus, to successfully apply proteases to large-scale resolutions, three key requirements must be achieved: the substrate must have

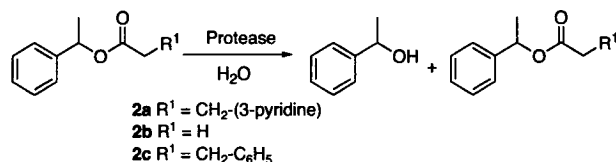
an acyl group that anchors it to the active site, the substrate should be water-soluble, and the substrate should facilitate rapid and simple separation of product and unreacted starting material.

We sought to optimize a protease-catalyzed strategy to facilitate large-scale preparation of *p*-toluenesulfinamide. To improve the solubility in aqueous solutions and increase the reactivity, we replace the dihydrocinnamoyl group with a 3-(3-pyridyl)-propionyl group. We show *N*-3-(3-pyridyl)propionyl-*p*-toluenesulfinamide **1a** is efficiently resolved to give enantiopure *p*-toluenesulfinamide, which is easily separated from unreacted substrate by washing with mild acid solution. We also resolve two sterically hindered secondary alcohol esters, 2,2-dimethylcyclopentyl 3-(3-pyridyl)-propionate **3a** and 1-(2-mesityl)ethyl 3-(3-pyridyl)propionate **4a**. This acyl group increases protease reactivity through enhanced binding, increases substrate solubility in aqueous solutions and provides a facile route for separation of product and substrate.

4.2 Results and discussion

We synthesized 1-phenethyl 3-(3-pyridyl)propionate **2a** by treating 1-phenethyl alcohol and 3-(3-pyridyl)propionic acid with *N*-(3-dimethylaminopropyl)-*N*-ethylcarbodiimide hydrochloride (EDC•HCl). Like the corresponding acetate **2b**, **2a** was stable in buffered solutions (pH 7.2) for >5 days. However, the reactivity of 1-phenethyl 3-(3-pyridyl)propionate **2a** with six commonly-used proteases was up to six-hundred-fold higher than corresponding acetate **2b** (Table 4.1). Subtilisin BL, *Aspergillus melleus* protease, subtilisin Carlsberg and *Streptomyces griseus* protease showed a fifteen to seventy-fold increase, α -chymotrypsin from bovine pancreas showed a six-hundred-fold increase, and *Aspergillus oryzae* showed no increase in activity.

Proteases showed lower activity toward the less polar dihydrocinnamate **2c** versus 3-(3-pyridyl)propionate **2a** (Table 4.1). The activity of proteases toward **2c** was similar to acetate **2b**, except for *Aspergillus oryzae* protease, which showed ten-fold lower activity toward **2c**, and α -chymotrypsin, which showed two-hundred-fold higher activity toward **2c**. The large increase for α -chymotrypsin toward **2a** and **2c** is consistent with its preference for phenylalanine as acyl group.¹³

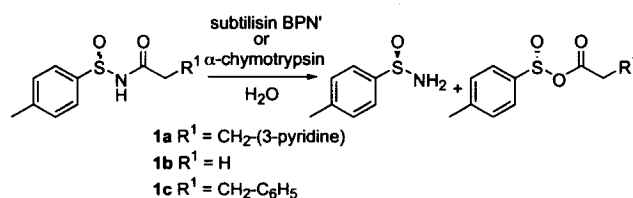
Table 4.1. Specific activity of proteases toward secondary alcohol esters **2a**, **2b** and **2c**

Protease	Prot. conc. (mg/mL) ^a	Specific activity ^b		
		2a	2b	2c
<i>Bacillus lentus</i> subtilisin ^c	2.4	10	0.6	0.7
<i>Aspergillus melleus</i> ^c	4.4	4.6	0.3	0.3
<i>Aspergillus oryzae</i> ^c	5.1	1.0	1.0	0.1
subtilisin Carlsberg ^d	9.0	20	0.5	0.5
α -chymotrypsin ^d	8.6	19	0.03	5.4
<i>Streptomyces griseus</i> ^d	6.6	7	0.1	0.3

^aProtein concentration was determined by the method of Bradford using bovine serum albumin (BSA) as standard (Bradford, M. M. *Anal. Biochem.* **1976**, *72*, 248-254.).

^bSpecific activity is calculated in $\mu\text{mol}/\text{min}/\text{mg}$ protein. ^cAltus Biologics (Cambridge, USA). ^dSigma-Aldrich (St. Louis, USA).

A different leaving group showed a similar trend. The activity of α -chymotrypsin and subtilisin BPN' toward *N*-3-(3-pyridyl)-propionyl-*p*-toluenesulfinamide **1a** and *N*-dihydrocinnamoyl-*p*-toluenesulfinamide **1c** is at least one hundred-fold higher than *N*-acetyl-*p*-toluenesulfinamide **1b** (Table 4.2).¹⁴ α -Chymotrypsin showed no reaction with **1b** after 24 h, but high reactivity toward **1a** (42% conv. after 3h) and **1c** (39% conv. after 3 h). Similarly, subtilisin BPN' did not react with *N*-acetyl **1b** after 24 h, but showed moderate reactivity toward *N*-3-(3-pyridyl)propionyl **1a** (21% conv. after 24 h) and *N*-dihydrocinnamoyl **1c** (19% conv. after 24 h). The lack of activity increase for **1a** versus **1c** may reflect the higher water-solubility of *N*-acyl sulfinamides versus nonpolar secondary alcohol esters. While both **1a** and **1c** are useful for small-scale synthesis of *p*-toluenesulfinamide **1**, **1a** is more suitable for large-scale resolution because of its higher solubility in aqueous solutions – the solubility limit of **1a** is ca. 50 mM in 10% DMF versus ca. 5 mM for **1c** – and the pyridine moiety allows for facile separation of substrate and product.

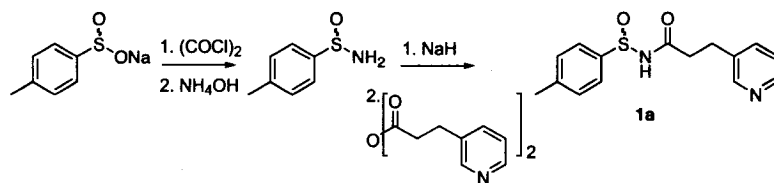
Table 4.2. Reactivity and enantioselectivity of α -chymotrypsin and subtilisin BPN' toward **1a**, **1b** and **1c**

Protease	1a		1b		1c	
	%c ^a	E ^b	%c	E	%c	E
α -chymotrypsin ^c	42 ^e	52	n.r. ^f	n.d. ^g	39 ^e	56
subtilisin BPN' ^d	21	125	n.r.	n.d.	19	75

^a% Conversion: amount of sulfinamide formed after 24 h except where noted. ^bEnantiomeric ratio: the enantiomeric ratio *E* measures the relative rate of hydrolysis of the fast-reacting enantiomer as compared to the slow-reacting enantiomer as defined by Sih (Chen, C. S.; Fujimoto, Y.; Girdaukas, G.; Sih, C. J. *J. Am. Chem. Soc.* **1982**, *104*, 7294-7299.). ^cSigma-Aldrich (St. Louis, USA). ^dFor protein expression and purification details see ref. 6. ^eReaction for 3h. ^fNo reaction. ^gNot determined.

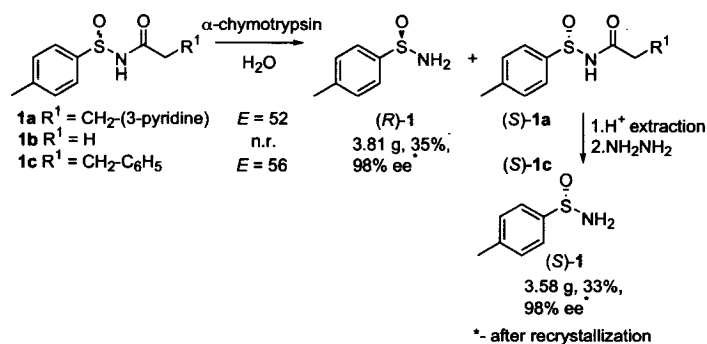
The 3-(3-pyridyl)propionyl group showed the same high enantioselectivity as the dihydrocinnamoyl group (Table 4.2). Small-scale reactions show α -chymotrypsin catalyzes the enantioselective hydrolysis of *N*-dihydrocinnamoyl-*p*-toluenesulfinamide **1c** (*E* = 56) to give (*R*)-**1**. Similarly, α -chymotrypsin catalyzed the enantioselective hydrolysis of **1a** (*E* = 52) to give (*R*)-**1**. Subtilisin BPN' and E catalyze the highly enantioselective hydrolysis of **1c** to give (*R*)-*p*-toluenesulfinamide (*R*)-**1** with *E* = 75 and *E* > 150, respectively.^{7b,15} Subtilisin BPN' showed even higher enantioselectivity toward **1a** (*E* = 125). Both subtilisin BPN' and E are inexpensive to produce by fermentation,¹⁶ but fermentation facilities are usually not available in a typical organic chemistry laboratory. Thus, to be useful for organic chemistry we opted to use a commercially available hydrolase. The structural features of the active site of α -chymotrypsin are similar to those of subtilisin,¹⁷ so it is not surprising that it also shows good enantioselectivity. However, we found that the enantioselectivity of α -chymotrypsin toward sulfinamides varied depending on the purity and supplier of enzyme. The enantioselectivity ranged from *E* = 21 to 63

with **1a** and $E = 18$ to 87 with **1c**. If one has access to fermentation facilities, we recommend using subtilisin BPN^a or E as both show consistently high enantioselectivity.



Scheme 4.1. Synthesis of racemic *N*-3-(3-pyridyl)propionyl-*p*-toluenesulfinamide **1a**.

To prepare substrate **1a**, we treated *p*-toluenesulfinic acid with oxalyl chloride, followed by ammonolysis to give *p*-toluenesulfinamide in 86% yield (Scheme 4.1).¹⁸ Acylation using a mixed anhydride prepared from isobutylchloroformate, 1-methylmorpholine and 3-(3-pyridyl)propionic acid gave poor <10% yield,¹⁸ so we used the symmetrical anhydride of 3-(3-pyridyl)propionic acid. We prepared the acid via KMnO_4 oxidation¹⁹ of 3-(3-pyridyl)propanol and prepared the symmetrical anhydride using EDC.¹⁸ Thus, treating *p*-toluenesulfinamide with NaH, followed by addition of the symmetrical anhydride of 3-(3-pyridyl)propionic acid yielded crude **1a**. Trituration with hexanes/ethyl acetate removed unreacted *p*-toluenesulfinamide **1** and gave **1a** in 73% yield. This synthetic strategy is simple, inexpensive and does not require low temperatures, special equipment or chromatography.

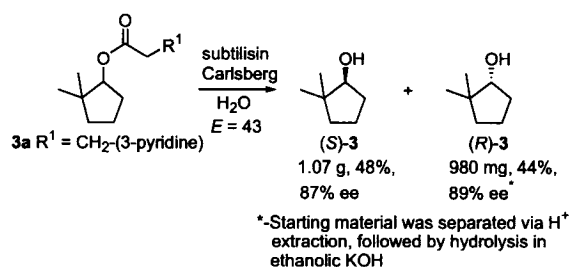


Scheme 4.2. α -Chymotrypsin-catalyzed resolution of **1a** and **1c**.

We resolved **1a** (20.2 g, 70 mmol) with α -chymotrypsin (12 g) to give (*R*)-**1** (4.48 g, 41% yield; the maximum yield is 50% in a resolution) with 87% ee at 51% conversion

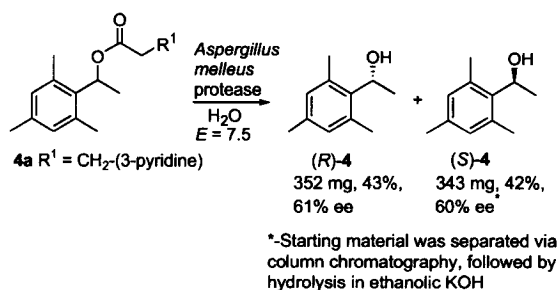
after 4 d (Scheme 4.2). The substrate was conveniently separated from the product via acid extraction (0.1 N HCl). Treating (*S*)-**1a** with hydrazine hydrate²⁰ gave (*S*)-**1** (4.29 g, 40% yield) with 92% ee. Recrystallization from hexanes/ethyl acetate gave (*R*)-**1** (3.81 g, 35% yield) with 98% ee and (*S*)-**1** (3.58 g, 33% yield) with 98% ee. The enantioselectivity ($E = 47$) was slightly lower than with small-scale reactions.

To demonstrate the usefulness of the 3-(3-pyridyl)propionyl group for resolving hindered secondary alcohols, we resolved 2,2-dimethylcyclopentanol **3** using subtilisin Carlsberg. 2,2-Dimethylcyclopentanol **3** can be prepared via asymmetric reduction using chiral organoborane reagents, but it requires long reaction times and low temperatures, and the selectivity is variable.^{21,22,23} Subtilisin Carlsberg previously showed high enantioselectivity with a structurally related substrate, *cis,cis*-6-(2,2-dimethylpropamido)spiro[4.4]nonan-1-ol.⁸ Subtilisin Carlsberg also showed good enantioselectivity toward 2,2-dimethylcyclopentyl 3-(3-pyridyl)propionate **3a** ($E = 43$). Thus, we resolved **3a** (4.95 g, 20 mmol) with subtilisin Carlsberg (4.5 g) to give (*S*)-**3** (1.07 g, 48% yield) with 87% ee at 51% conversion after 2 d (Scheme 4.3). The product and substrate were conveniently separated via acid extraction (0.1 N HCl) of remaining starting material. Subsequent hydrolysis of the remaining starting material gave (*R*)-**3** (980 mg, 44% yield) with 89% ee (Scheme 4.3). Lipases from *Candida rugosa* (CRL) and *Pseudomonas cepacia* (PCL) did not catalyze hydrolysis of **3a**; however, lipase B from *Candida antarctica* (CALB) catalyzed the enantioselective hydrolysis of **3a** ($E = 108$) to give the (*R*)-enantiomer. This discovery provides an enantiocomplementary strategy for synthesizing **3**. Although kinetic resolution yields both enantiomers, enantiocomplementary enzymes are useful for organic synthesis because they can simplify the next synthetic steps by providing the necessary enantiomer without further manipulation.⁸



Scheme 4.3. Subtilisin Carlsberg-catalyzed resolution of **3a**.

We also resolved 1-(2-mesityl)ethanol **4**, a useful chiral inductor for cycloaddition reactions,²⁴ with moderate enantioselectivity on a milligram-scale using the 3-(3-pyridyl)propionyl group. Derivative **4** cannot be resolved using lipases because of steric hindrance between the ortho methyl substituents with active site residues²⁵ and the acetate and dihydrocinnamate derivatives react only slowly with proteases (<1% conv. in 24 h). All proteases tested catalyzed the hydrolysis of **4a**. *Aspergillus melleus* protease was selected because it showed the highest enantioselectivity ($E = 7.5$). Thus, we resolved **4a** (1.48 g, 5 mmol) with *Aspergillus melleus* protease (ca. 1.5 g) to give (*R*)-**4** (352 mg, 43% yield) with 61% ee at 49% conversion after 5 d (Scheme 4.4). Product and substrate could not be quantitatively separated via acid extraction, so they were purified using chromatography. Subsequent hydrolysis of the remaining starting material gave (*S*)-**4** (343 mg, 42% yield) with 60% ee.



Scheme 4.4. *Aspergillus melleus* protease-catalyzed resolution of **4a**.

Molecular modelling of the first tetrahedral intermediate of **1a** showed α -chymotrypsin binds the sulfinamide moiety of the fast-reacting (*R*)-enantiomer similar to subtilisin E, but binds the slow-reacting (*S*)-enantiomer different than subtilisin E.^{7b} Briefly, molecular modelling of **1a** with α -chymotrypsin gave one productive conformation for each enantiomer (Figure 4.1). The two other plausible conformations lacked catalytically essential hydrogen bonds or encountered severe steric clash with the protein.²⁶ The productive conformation of both (*R*)-**1** and (*S*)-**1** have the 3-(3-pyridyl)propionyl group bound in the hydrophobic acyl pocket (specificity pocket)²⁷ of α -chymotrypsin, based on its similarity to phenylalanine.¹³ The productive conformation of (*R*)-**1a** has the *p*-tolyl group in the hydrophobic leaving group pocket (*n*-site)²⁷ and the

hydrophilic sulfoxide oxygen in solvent. The (*R*)-enantiomer fit tightly in the active site, but leaving group pocket residues bumped the *p*-tolyl group ($C_{\text{ipso}} - S_{\gamma}$ (Cys42) distance = 3.79 Å, $C_{\text{ortho}} - S_{\gamma}$ (Cys42) distance = 3.79 Å, $C_{\text{ortho}} - C_{\delta 2}$ (His57) distance = 3.67 Å, $C_{\text{ortho}} - C_{\delta}$ (Phe41) distance = 4.42 Å, $C_{\text{meta}} - C_{\alpha}$ (Cys58) distance = 3.92 Å).²⁸ This tight fit suggests a favourable hydrophobic interaction – tendency of nonpolar compounds to transfer from an aqueous phase to an organic phase – between the *p*-tolyl group and leaving group pocket residues.²⁹ This favourable hydrophobic interaction may improve binding of the *p*-tolyl group and account for the enantiopreference with sulfinamides. The productive conformation of (*S*)-**1** also fit well in the active site, but the sulfinamide was hindered by Met192 ($S_{\text{sulfinamide}} - S_{\delta}$ distance = 3.41 Å, $S_{\text{sulfinamide}} - C_{\epsilon}$ distance = 3.60 Å and $C_{\text{ipso}} - C_{\epsilon}$ distance = 3.65 Å) and forced out of the active site. This productive conformation is different than the productive conformation of (*S*)-**1b** with subtilisin E.^{7b} With subtilisin E, the substituents at stereocentre exchanged, which put the sulfoxide oxygen in the S_1' pocket and the *p*-tolyl group in solvent. With α -chymotrypsin, the entire sulfinamide moiety of (*S*)-**1a** is forced out of the active site and exposed to solvent, where it makes no favourable contact with active site residues.

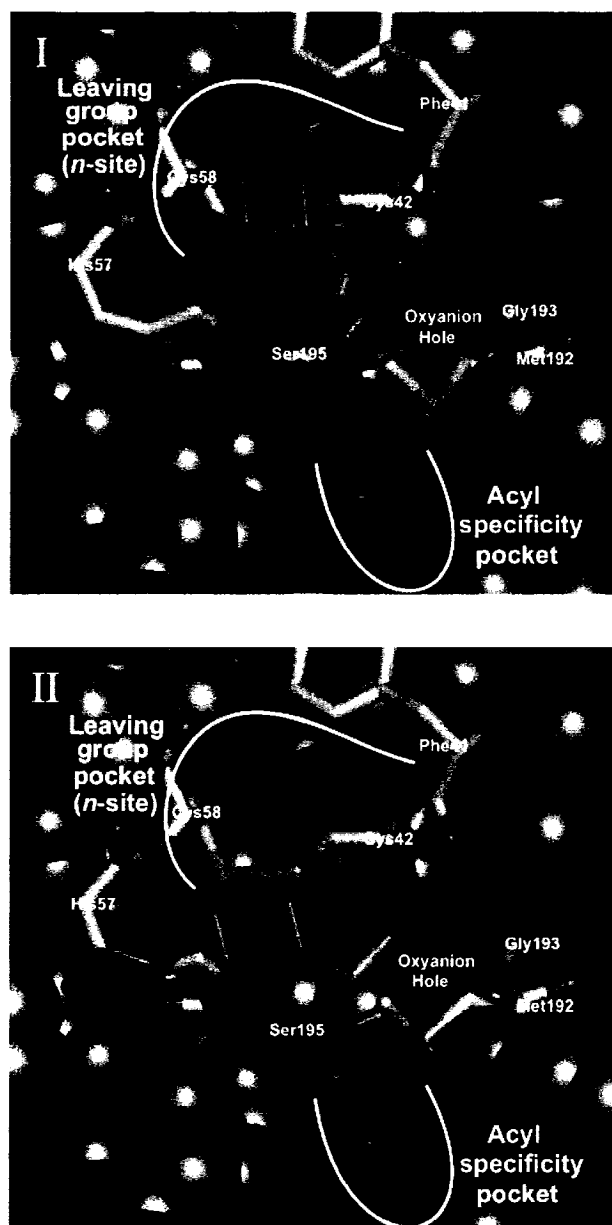


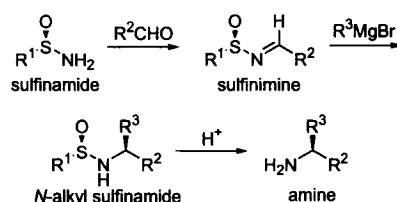
Figure 4.1. Catalytically productive tetrahedral intermediates for the α -chymotrypsin-catalyzed hydrolysis of (*R*)-**1a** (I) and (*S*)-**1a** (II) as identified by molecular modelling. The important active site and substrate atoms (sticks) are coloured as follows: green (substrate carbon), grey (enzyme carbon), red (oxygen), blue (nitrogen) and orange (sulfur). Surrounding atoms (space fill) of α -chymotrypsin are shown in blue. For clarity, all hydrogen atoms and water molecules are hidden and Ser219 is hidden to expose the acyl group pocket. Both I and II maintain all catalytically essential hydrogen bonds and the 3-(3-pyridyl)methyl moiety of the 3-(3-pyridyl)propionate group binds in the S_1 pocket, as

expected based on its similarity to phenylalanine.^{13,27} In the fast-reacting enantiomer, (*R*)-**1a** (I), the *p*-tolyl group binds in the hydrophobic leaving group pocket and sulfoxide oxygen is exposed to solvent water. In the slow-reacting enantiomer, (*S*)-**1a** (II), the sulfoxide oxygen is forced out of the hydrophobic leaving group pocket because of steric interaction between the sulfinamide moiety and active site residues. This interaction places both the *p*-tolyl group and sulfoxide oxygen in solvent where this is no favourable hydrophobic interaction with leaving group pocket residues. The non-productive conformations of (*R*)-**1** and (*S*)-**1** (not shown) encountered severe steric clash with the active site residues and lacked catalytically essential hydrogen bonds.

The enantiopreference of subtilisin toward (*S*)-2,2-dimethylcyclopentanol (*S*)-**3** agrees with predictive models for subtilisin.^{6,30} The enantiopreference of subtilisin toward secondary alcohol esters is dependent on relative substituent polarity⁶ and size.³⁰ The (*R*)-enantiomer of secondary alcohols is favoured when the large substituent is approximately the size of phenyl because of a favourable hydrophobic interaction with S₁' leaving-group pocket residues of subtilisin. The (*S*)-enantiomer is favoured when the large substituent is polar (hydrophilic) or too large to bind in the S₁' leaving-group pocket. In this case, the large substituent is the 2,2-dimethyl quaternary carbon, which is too large to bind in the S₁' pocket. This poor fit destabilizes reaction of the (*R*)-enantiomer and thus, the smaller methylene group binds in the S₁' pocket, favouring reaction of the (*S*)-enantiomer.

We developed an efficient enzyme-catalyzed route for preparation of enantiopure *p*-toluenesulfinamide **1** using the 3-(3-pyridyl)propionyl group. Sulfinamides, such as *p*-toluenesulfinamide, are useful chiral auxiliaries for synthesis of amines (Scheme 4.5).³¹ When condensed with an aldehyde or ketone to give the sulfinimine, the *N*-sulfinyl group directs nucleophilic addition across the C=N bond. This yields the *N*-alkyl sulfinamide, which upon hydrolysis of the S-N link yields an amine. Enantioselective syntheses using *p*-toluenesulfinimine include preparations of amines,³² α- and β-amino acids,³¹ aziridines³³ and amino phosphonic acids.³⁴ This protease strategy compares well with synthetic routes to sulfinamides. The standard synthetic route to enantiopure *p*-toluenesulfinamide is via menthyl-*p*-toluenesulfinate (Andersen's reagent).³⁵ Preparation of Andersen's reagent relies on the availability of both enantiomers of menthol – the unnatural (+)-

enantiomer is ca. six times as expensive as the natural (-)-enantiomer. The other synthetic route to enantiopure *p*-toluenesulfinamide is a double displacement strategy using a chiral auxiliary derived from indanol.³⁶ This route includes complicated steps requiring low temperatures and moisture- and air-sensitive reagents. Our protease-catalyzed resolution is simple, convenient, avoids the use of costly auxiliaries and allows facile separation of product and substrate.



Scheme 4.5. Synthesis of enantiopure amines from sulfinamides.

Proteases are also useful for resolving sterically hindered substrates, such as 2,2-dimethylcyclopentanol **3** and 1-(2-mesityl)ethanol **4**, that can not be easily prepared through chemical routes and are slow-reacting substrates with lipases. Proteases show higher reactivity toward these large substrates when 3-(3-pyridyl)propionic acid is used as acyl group and the enantioselectivity can be high when there is a large difference in the relative size³⁰ or polarity⁶ of the alcohol substituents.

One limitation of this method is that kinetic resolution comes with a maximum of 50% yield. However, the proteases and the racemic starting materials utilized here are inexpensive and thus, would be economic and practical for large-scale production. As well, this method provides fast and simple access to both enantiomers, which is important for preparation of chiral auxiliaries because both are needed for organic synthesis. This protease route is attractive for large-scale production because it avoids chromatographic separation of product and substrate. Other strategies utilizing succinate groups also provide a facile route for purification. For example, Fukui and co-workers^{37,38} resolved L-menthol by lipase-catalyzed resolution of the corresponding succinate monoester and separated product and substrate via base-extraction of remaining starting material. While the succinate group facilitates separation of product and substrate without chromatography, water-soluble substrates such as succinates usually react slowly with lipases. Lipases

are activated by lipid interfaces and thus, show higher activity toward nonpolar, insoluble substrates.³⁹ The succinate group may increase the reactivity of proteases by increasing substrate solubility. However, subtilisin E showed lower enantioselectivity toward the mono-methylester succinyl ($E = 52$) derivative of *p*-toluenesulfinamide than the dihydrocinnamoyl derivative ($E = >150$).^{7b} The 3-(3-pyridyl)propionyl group maintains reactivity and enantioselectivity with subtilisin and α -chymotrypsin by mimicking phenylalanine and anchoring substrate to the active site, and the pyridine moiety facilitates separation of product and substrate through mild acid extraction.

4.3 Conclusion

In summary, the 3-(3-pyridyl)propionyl group increases substrate binding to proteases, increases substrate solubility in aqueous solutions, and provides a facile route for separation of substrate and product. This is a cost-effective route for large-scale preparation of the useful chiral auxiliary, *p*-toluenesulfinamide **1**, and sterically hindered secondary alcohols that are poor substrates for other hydrolases.

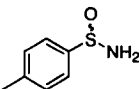
4.4 Experimental Section

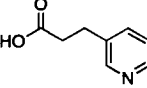
4.4.1 General

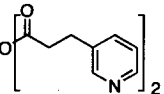
¹H- and ¹³C-NMR spectra were obtained as CDCl₃ solutions at 300 MHz and 75 MHz, respectively. Chemical shifts are expressed in ppm (δ) and are referenced to tetramethylsilane or solvent signal. Coupling constants are reported in Hertz (Hz). GC analyses were performed on a 25 m x 0.25 mm Chrompack CP-Chiralsil-Dex CB column (Varian Inc., Palo Alto, USA) with He as carrier gas using one of the two following temperature programs: **A** 17.5 psi, 50 °C, 5 °C min⁻¹, 150 °C held for 5 min, 2.5 °C min⁻¹; 175 °C held for 5 min, 5 °C min⁻¹, 200 °C held for 30 min; **B** 17.5 psi, 100 °C, held for 15 min, 25 °C min⁻¹; 200 °C held for 21 min). HPLC analyses were performed on a 4.6 x 250 mm Daicel Chiralcel OD column (Chiral Technologies, Exton, USA) and monitored at 254 nm. Subtilisin Carlsberg was purchased from Sigma-Aldrich (St. Louis, USA) and α -chymotrypsin was purchased from Sigma-Aldrich (St. Louis, USA) or Amresco (Solon, USA). Other hydrolases were a generous gift from Altus Biologics (Cambridge, USA). All reagents, buffers, starting materials and anhydrous solvents were purchased from

Sigma-Aldrich (Milwaukee, USA) and used without purification. All air- and moisture-sensitive reactions were performed under Ar. Substrates **1b**, **1c**, **2c** and **4c** were available from previous studies.^{6,7b}

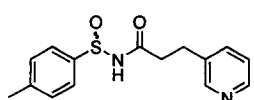
4.4.2 Synthesis of substrates

 ***p*-Toluenesulfinamide, 1.** Oxalyl chloride (67.2 g, 530 mmol) was added drop-wise to *p*-toluenesulfinic acid sodium salt (89.0 g, 500 mmol) in toluene at 0 °C.¹⁸ After 1 h at RT, the reaction mixture was added to a biphasic mixture of NH₄OH (500 mL) and EtOAc (500 mL) at 0 °C and then stirred at RT. After 1 h, the reaction mixture was diluted with EtOAc (500 mL) and the two layers were separated. The aqueous layer was extracted with EtOAc (2 x 500 mL). The combined EtOAc layers were washed with sat. NaCl (500 mL) and dried over Na₂SO₄. The aqueous layer was then extracted with CH₂Cl₂ (2 x 500 mL). The combined CH₂Cl₂ layers were washed with sat. NaCl (500 mL) and dried over Na₂SO₄. The combined organic layers were concentrated *in vacuo* to give a white powder (66.7 g, 86%): mp 115-117 °C (lit.¹⁸ 117-118 °C); ¹H NMR δ 2.42 (s, 3H, PhCH₃), 4.30 (br s, 2H, -NH₂), 7.30 (d, *J* = 8.1, 2H, phenyl), 7.62 (d, *J* = 8.1, 2H, phenyl); ¹³C NMR δ 21.7 (PhCH₃), 125.6, 129.7, 141.5, 143.6 (phenyl). The enantiomers were separated using HPLC (Chiralcel OD-H column, 85:15 hexanes/EtOH, 0.75 mL/min, 254 nm; (*R*)-**1**, *t*_R = 9.8 min; (*S*)-**1**, *t*_R = 11.1 min).

 **3-(3-Pyridyl)propionic acid.** Solid KMnO₄ (256 g, 1.62 mol) was added portion-wise to a solution of 3-(3-pyridyl)propanol (200 g, 1.46 mol) in 3 N H₂SO₄ (1.5 L) at 0 °C.¹⁹ The reaction was stirred at RT. After 24 h, the reaction mixture was adjusted to pH 6 by addition of solid KOH. Insoluble MnO₂ was pelleted by centrifugation and the clear solution was decanted. Water was removed *in vacuo* to yield 3-(3-pyridyl)propionic acid⁴⁰ (153 g, 70% yield): ¹H NMR δ 2.72 (t, *J* = 7.2, 2H, C(O)CH₂), 3.03 (t, *J* = 7.5, 2H, CH₂Ph), 7.34 (m, 1H, pyridyl), 7.68 (m, 1H, pyridyl), 8.52 (m, 2H, pyridyl).

 **3-(3-Pyridyl)propionic acid anhydride.** *N*-(3-Dimethylaminopropyl)-*N'*-ethylcarbodiimide hydrochloride (EDC•HCl) (25.2 g, 132 mmol) was added to a solution of 3-(3-pyridyl)propionic acid (40.0 g, 265

mmol) in CH_2Cl_2 (750 mL) and NEt_3 (37 mL) at 0°C and stirred at RT.¹⁸ After 24 h, the reaction was washed with ice-cold sat. NaHCO_3 (3 x 500 mL), dried over MgSO_4 and concentrated *in vacuo* to give a pale yellow oil (34.1 g, 91%): ^1H NMR δ (t, $J = 7.2$, 2H, C(O)CH_2), 3.03 (t, $J = 7.5$, 2H, CH_2Ph), 7.24 (m, 1H, pyridyl), 7.58 (m, 1H, pyridyl), 8.50 (m, 2H, pyridyl).

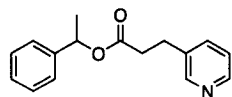


***N*-3-(3-Pyridyl)propionyl-*p*-toluene sulfonamide, 1a.**

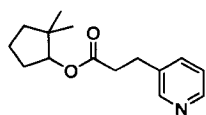
Sodium hydride (60% dispersion in oil; 12.0 g, 300 mmol) was added portion-wise over 15 min to a solution of *p*-toluenesulfonamide (15.5 g, 100 mmol) in THF (750 mL) at 0°C . The symmetric anhydride of 3-(3-pyridyl)propionic acid (32.1 g, 113 mmol) was added drop-wise over 15 min at 0°C and the reaction mixture was then stirred at RT for 3h.¹⁸ The reaction mixture was diluted with EtOAc (400 mL) and sat. NaHCO_3 (400 mL) was added slowly. The layers were separated and the aqueous layer was extracted with EtOAc (3 x 250 mL). The combined EtOAc layers were washed with sat. NaHCO_3 (500 mL) and dried over MgSO_4 . The aqueous layer was extracted with CH_2Cl_2 (2 x 250 mL). The combined CH_2Cl_2 layers were washed with NaHCO_3 (250 mL) and dried over MgSO_4 . The combined organic layers were concentrated *in vacuo* to give a pale yellow solid. Trituration with hexane/ethyl acetate gave a white powder (21.1 g, 73%): mp $161\text{--}163^\circ\text{C}$; ^1H NMR δ 2.39 (s, 3H, PhCH_3), 2.72 (m, 2H, C(O)CH_2), 3.01 (t, $J = 7.2$, 2H, CH_2Pyr), 4.78 (br s, 1H, NH), 7.25–7.48 (m, 3H, phenyl or pyridyl), 7.47 (m, 2H, phenyl or pyridyl), 7.68 (m, 1H, phenyl or pyridyl), 8.25 (m, 2H, pyridyl); ^{13}C NMR (DMSO-d_6) δ 21.4 (PhCH_3), 27.9 (CH_2Pyr), 36.9 (C(O)CH_2), 124.0, 125.4, 130.2, 136.4, 136.6, 140.9, 142.1, 147.9, 150.2 (phenyl or pyridyl), 173.8 (C=O); HRMS calcd for $\text{C}_{15}\text{H}_{17}\text{N}_2\text{O}_2\text{S}$ $[\text{M}+\text{H}]^+$ 289.1010. Found: 289.0989. The enantiomers were separated using HPLC (Chiralcel OD-H column, 85:15 hexanes/EtOH, 0.75 mL/min, 254 nm; (*R*)-**1a**, $t_R = 20.0$ min; (*S*)-**1a**, $t_R = 22.5$ min).

General procedure for synthesis of racemic esters 2a-4a. EDC•HCl (7.5 mmol) was added portion-wise to a stirred solution of secondary alcohol (5 mmol), 3-(3-pyridyl)propionic acid (7.5 mmol), 4-(dimethylamino)-pyridine (0.5 mmol) and NEt_3 (7.5 mmol) in CH_2Cl_2 (25 mL) at 0°C . The ice bath was removed and the reaction was stirred RT for 48 h. The reaction was quenched with the addition of sat. NaHCO_3 (25 mL). The layers were separated and the aqueous layer was extracted with CH_2Cl_2 (2 x 25 mL). The

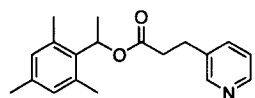
combined organic layers were washed with sat. NaHCO_3 (2 x 25 mL) and dried over MgSO_4 . The organic layer was concentrated *in vacuo* to give the crude ester. The relevant analytical data are given below:



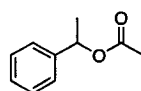
3-(3-Pyridyl)propionic acid 1-phenyl-ethyl ester, 2a. Purification on silica gel (100% hexanes to 60:40 hexanes/acetone) to give a clear liquid (1.10 g, 87%): ^1H NMR δ 1.51 (d, $J = 6.6$, 3H, CH_3), 2.70 (m, 2H, C(O)CH_2), 2.98 (t, $J = 7.5$, 2H, CH_2Pyr), 5.88 (q, $J = 6.6$, 1H, CH), 7.32-7.39 (m, 6H, phenyl), 7.54-7.58 (m, 1H, phenyl), 8.46-8.50 (m, 2H, pyridyl); ^{13}C NMR δ 22.2 (CH_3), 28.1 (CH_2Pyr), 35.6 (C(O)CH_2), 72.7 (CH), 123.5, 126.1, 128.0, 128.6, 135.9, 136.1, 141.5, 147.7, 149.8 (phenyl or pyridyl), 171.6 (C=O); HRMS calcd for $\text{C}_{16}\text{H}_{18}\text{NO}_2$ $[\text{M}+\text{H}]^+$ 256.1337. Found: 256.1336. The enantiomers were separated using GC (program A; (*S*)-**2a**, $t_R = 52.3$ min; (*R*)-**2a**, $t_R = 52.5$ min).



3-(3-Pyridyl)propionic acid 2,2-dimethylcyclopentanol, 3a. Purification on silica gel (100% hexanes to 75:25 hexanes/acetone) to give a clear liquid (1.05 g, 86%): ^1H NMR δ 0.90 (s, 3H, CH_3), 0.93 (s, 3H, CH_3), 1.43 (m, 2H, CH_2), 1.52 (m, 2H, CH_2), 1.67 (m, 2H, CH_2), 2.08 (m, 2H, CH_2), 4.73 (m, 1H, CH), 7.27 (m, 1H, phenyl), 7.61 (m, 1H, phenyl), 8.49 (m, 2H, phenyl); ^{13}C NMR δ 20.6 (CH_2), 22.2 (CH_2), 26.6 (CH_2), 28.2 (CH_2Pyr), 30.5 (CH_2), 35.6 (C(O)CH_2), 38.0 (CH_2), 41.9 (C), 123.4, 135.9, 147.7, 149.8 (pyridyl), 172.1 (C=O). HRMS calcd for $\text{C}_{15}\text{H}_{21}\text{NO}_2$ $[\text{M}+\text{H}]^+$ 248.1655. Found: 248.1650. The enantiomers could not be separated using GC.



3-(3-Pyridyl)propionic acid 2-mesityl-ethyl ester, 4a. Purification on silica gel (100% hexanes to 60:40 hexanes/acetone) to give a clear liquid (1.27 g, 86%): ^1H NMR δ 1.53 (d, $J = 6.9$, 3H, CH_3), 2.26 (s, 3H, *p*- CH_3), 2.40 (s, 6H, *o*- CH_3), 2.68 (m, 2H, C(O)CH_2), 2.97 (t, $J = 7.5$, 2H, CH_2Pyr), 6.28 (q, $J = 6.9$, 1H, CH), 6.83 (s, 2H, phenyl), 7.24-7.28 (m, 1H, pyridyl), 7.56-7.60 (m, 1H, pyridyl), 8.46-8.50 (m, 2H, pyridyl); ^{13}C NMR δ 19.6 (CH_3), 20.5 (CH_3), 20.9 (CH_3), 28.1 (CH_2Pyr), 35.6 (C(O)CH_2), 69.9 (CH), 123.5, 130.1, 134.2, 135.9, 136.0, 136.1, 137.2, 147.7, 149.8 (phenyl or pyridyl), 171.7 (C=O); HRMS calcd for $\text{C}_{17}\text{H}_{24}\text{NO}_2$ $[\text{M}+\text{H}]^+$ 298.1807. Found: 298.1813. The enantiomers could not be separated using GC.



Acetic acid 1-phenyl-ethyl ester, 2b. Acetyl chloride (15 mmol) was added drop-wise to a stirred solution of 1-phenethyl alcohol (10 mmol) and pyridine (15 mmol) in CH_2Cl_2 (50 mL) at 0 °C. The ice bath was removed and stirred until the reaction was complete by TLC. The reaction was quenched with the addition of sat. NaHCO_3 (25 mL). The layers were separated and the aqueous layer was extracted with CH_2Cl_2 (2 x 25 mL). The combined organic layers were washed with 1N HCl (2 x 25 mL), sat. NaHCO_3 (2 x 25 mL), sat. NaCl (25 mL) and dried over Na_2SO_4 . The organic layer was concentrated *in vacuo* to give the crude ester. Purification on silica gel (100% hexanes to 95:5 hexanes/EtOAc) gave the **2b** as a clear liquid (1.80 g, 73%): ^1H NMR δ 1.55 (d, J = 6.6, 3H, CH_3), 2.09 (m, 3H, $\text{C}(\text{O})\text{CH}_3$), 5.90 (q, J = 6.6, 1H, CH), 7.36-7.38 (m, 5H, phenyl); ^{13}C NMR δ 21.4 (CH_3), 22.3 (CH_3), 72.4 (CH), 126.2, 128.0, 128.6, 141.8 (phenyl), 170.4 ($\text{C}=\text{O}$). The enantiomers were separated using GC (program **B**; (*S*)-**2b**, t_R = 9.7 min; (*R*)-**2b**, t_R = 11.9 min).



2,2-Dimethylcyclopentanol, 3. NaBH_4 (3.42 g, 90 mmol) was added portion-wise to a stirred solution of 2,2-dimethylcyclopentanone (6.72 g, 60 mmol) in EtOH (100 mL) at 0 °C. The ice bath was removed and the reaction solution was stirred for 3 h at RT. The solution was cooled to 0 °C and quenched with 1 N HCl (50 mL) and extracted with EtOAc (3 x 50 mL). The combined organic layers were washed with sat. NaHCO_3 (50 mL), sat. NaCl (50 mL), dried over MgSO_4 and concentrated *in vacuo* to give a clear liquid (5.87 g, 86%): ^1H NMR δ 0.95 (s, 3H, CH_3), 0.97 (s, 3H, CH_3), 1.40 (m, 2H, CH_2), 1.57 (m, 2H, CH_2), 1.72 (m, 2H, CH_2), 2.03 (m, 2H, CH_2), 3.69 (t, J = 6.3, 1H, CH); ^{13}C NMR δ 19.9 (CH_2), 21.3 (CH_2), 26.7 (CH_2), 32.7 (CH_2), 37.5 (CH_2), 42.1 ($\text{C}(\text{CH}_3)_2$), 81.4 (CHOH). The enantiomers were separated using GC (program **B**; (*R*)-**3**, t_R = 5.6 min; (*S*)-**3**, t_R = 5.8 min).

4.4.3 Small-scale protease-catalyzed hydrolysis of **2a** and **3a**

Bacillus lentus subtilisin (subtilisin BL), *Aspergillus melleus* protease, *Aspergillus oryzae* protease, subtilisin Carlsberg, α -chymotrypsin from bovine pancreas, *Streptomyces griseus* protease (10 mg/mL; solution in 50 mM BES buffer (pH 7.2, 450 μL)) and substrate (100 mM in CH_3CN , 50 μL) containing 50 mM *n*-decane as internal standard were mixed in a 1/2 dram glass vial. The reaction mixture was shaken at 30 °C for 6 h with

2a and 24 h with **2b**, **2c**, **3a** and **4a**. For specific activity measurements the reaction was stopped at a conversion below 10%. The reaction was terminated with the addition of CH_2Cl_2 (500 μL). The phases were separated by centrifugation, and the organic layers were collected. The aqueous phase was extracted with CH_2Cl_2 (2 x 500 μL) and the combined organics were evaporated under a stream of Air. The residue was diluted with EtOAc (150 μL) and analyzed by GC. The enantiomers were separated using the conditions described above.

4.4.4 Large-scale protease-catalyzed hydrolysis of **1a**, **3a** and **4a**

α -Chymotrypsin-catalyzed hydrolysis of **1a.** α -Chymotrypsin (12 g) was added to a solution of BES buffer (3.15 L, 1 mM, pH 7.2) and 100 mM KCl and stirred for 15 min to ensure complete dissolution. Substrate **1a** (20.2 g, 70 mmol) was dissolved in dimethylformamide (350 mL) and added drop-wise to the enzyme solution. The rate of hydrolysis was monitored by pH stat., which maintained the pH at 7.2 by automatic titration with 1 N NaOH. At ca. 50% conversion (4 d), the reaction was terminated by extraction of substrate and product with CH_2Cl_2 (3 x 500 mL). The combined organic layers were washed with dH_2O (3 x 500 mL), sat. NaCl (1 x 500 mL), dried over MgSO_4 and concentrated *in vacuo*. The crude mixture was dissolved in EtOAc (250 mL) and unreacted starting material was extracted with ice-cold 0.1 N HCl (2 x 100 mL). The combined aqueous layers were then back-extracted with EtOAc (50 mL). The combined EtOAc layers were washed with sat. NaHCO_3 (100 mL), sat. NaCl (100 mL), dried over MgSO_4 and concentrated *in vacuo* to give (*R*)-**1** as a white solid (4.48 g, 41% yield) with 87% ee. The combined aqueous layers were neutralized with solid NaHCO_3 and extracted with CH_2Cl_2 (2 x 200 mL). The combined CH_2Cl_2 layers were washed with sat. NaHCO_3 (100 mL), sat. NaCl (100 mL) and dried over MgSO_4 . The solution was concentrated *in vacuo* to give (*S*)-**1a**, which was subsequently treated with hydrazine hydrate (35 mL). After stirring for 3 h, the reaction solution was diluted with CH_2Cl_2 (100 mL) and washed with 1 N HCl (50 mL), sat. NaHCO_3 (50 mL), sat. NaCl (50 mL) and concentrated *in vacuo* to give (*S*)-**1** (4.29 g, 40% yield) with 92% ee. Recrystallization from hexanes/ethyl acetate gave (*R*)-**1** (3.81 g, 35% yield) with 98% ee and (*S*)-**1** (3.58 g, 33% yield) with 98% ee.

Subtilisin Carlsberg-catalyzed hydrolysis of 3a. Protease from *Bacillus licheniformis* (subtilisin Carlsberg; 50 mL of 92 mg/mL solution; 4.5 g) was added to BES buffer (400 mL, 1 mM, pH 7.2) and stirred for 15 min. Substrate **3a** (4.95 g, 20 mmol) was dissolved in MeCN (50 mL) and added to the enzyme solution. The rate of hydrolysis was monitored by pH stat., which maintained the pH at 7.2 by automatic titration with 1 N NaOH. After 2 d, the reaction was terminated by extraction of substrate and product with EtOAc (3 x 75 mL). The organic layer was extracted with ice-cold 0.1 N HCl (3 x 50 mL). The combined aqueous layers were then extracted with EtOAc (25 mL). The combined EtOAc layers were dried over MgSO₄ and concentrated *in vacuo* to give (*S*)-**3** (1.07 g, 48% yield) with 87% ee. The aqueous layer was neutralized with solid Na₂HCO₃ and extracted with EtOAc (3 x 50 mL). The combined organic layers were dried over Na₂SO₄ and concentrated *in vacuo* to give (*R*)-**3a**, which was subsequently hydrolyzed in ethanolic KOH (1 N, 1:1: ethanol/water) to give (*R*)-**3** (**3**) (980 mg, 44% yield) with 89%.

***Aspergillus melleus* protease-catalyzed hydrolysis of 4a.** *Aspergillus melleus* protease (1.5 g) was added to BES buffer (180 mL, 1 mM, pH 7.2) and stirred for 30 min to ensure complete dissolution. Substrate **4a** (1.49 g, 5 mmol) was dissolved in DMF (20 mL) and added to the enzyme solution. The rate of hydrolysis was monitored by pH stat., which maintained the pH at 7.2 by automatic titration with 1 N NaOH. After 5 d, the reaction was terminated by extraction of substrate and product with EtOAc (3 x 50 mL). Product and substrate were difficult to separate via acid extraction. Thus, product and substrate were purified using column chromatography (100% hexanes to 4:1 hexanes/acetone) to give (*R*)-**4** (352 mg, 43%) with 61% ee and (*S*)-**4a**, which was subsequently hydrolyzed in ethanolic KOH (1 N, 1:1: ethanol/water) to give (*S*)-**4** (343 mg, 42%) with 60% ee.

4.4.5 Absolute configuration of 2,2-dimethylcyclopentanol, **3**

Absolute configuration of alcohol **3** was assigned using the configurational correlation model for the corresponding (*R*)-MTPA derivatives, which were synthesized using (*R*)-(+)- α -methoxy- α -(trifluoromethyl)-phenylacetyl chloride in pyridine.⁴¹ ¹H NMR δ 0.91 (s, 3H, CH₃, *R*-enantiomer), 0.93 (s, 3H, CH₃, *R*-enantiomer), 0.98 (s, 3H, CH₃, *S*-enantiomer), 1.00 (s, 3H, CH₃, *S*-enantiomer), 1.46 (m, 2H, CH₂), 1.57 (m, 2H,

CH_2), 1.68 (m, 2H, CH_2), 2.18 (m, 2H, CH_2), 3.54 (s, 3H, OCH_3 , *S*-enantiomer), 3.57 (s, 3H, OCH_3 , *R*-enantiomer), 4.90 (m, 1H, CH), 7.42 (m, 3H, phenyl), 7.52 (m, 2H, phenyl).

4.4.6 Modelling of tetrahedral intermediates bound to α -chymotrypsin

All modelling was performed using *Insight II 2000.1 / Discover* (Accelrys, San Diego, USA) on a SGI Tezro UNIX workstation using the AMBER force field.⁴² We used a nonbonded cutoff distance of 8 Å, a distance-dependent dielectric of 1.0 and scaled the 1-4 van der Waals interactions by 50%. Protein structures in Figure 4.1 were created using PyMOL (Delano Scientific, San Carlos, CA, USA). The x-ray crystal structure of α -chymotrypsin (entry 6CHA)⁴³ is from the Protein Data Bank. The hydrogen atoms were added to correspond to pH 7.0. Histidines were uncharged, aspartates and glutamates were negatively charged, and arginines and lysines were positively charged. The catalytic histidine (His64) was protonated. The positions of the water hydrogens and then the enzyme hydrogens were optimized using a consecutive series of short (1 ps) molecular dynamic runs and energy minimizations.⁴⁴ This optimization was repeated until there was <2 kcal/mol in the energy of the minimized structures. Thereafter, an iterative series of geometry optimizations were performed on the water hydrogens, enzyme hydrogens and full water molecules. Finally, the whole system was geometry optimized.

The tetrahedral intermediates were built manually and covalently linked to Ser195. Nonstandard partial charges were calculated using a formal charge of -1 for the substrate oxyanion. Energy minimization proceeded in three stages. First, minimization of substrate with only the protein constrained (25 kcal mol⁻¹ Å⁻²); second, minimization with only the protein backbone constrained (25 kcal mol⁻¹ Å⁻²) and for the final stage the minimization was continued without constraints until the rms value was less than 0.0005 kcal mol⁻¹ Å⁻¹. A catalytically productive complex required all five hydrogen bonds within the catalytic machinery. We set generous limits for a hydrogen bond: a donor to acceptor atom distance of less than 3.1 Å with a nearly linear arrangement (>120° angle) of donor atom, hydrogen, and acceptor atom. Structures lacking any of the five catalytically relevant hydrogen bonds or encountering severe steric clash with enzyme were deemed nonproductive.

Acknowledgments

C.K.S. thanks McGill University for a fellowship. We thank the University of Minnesota for financial support and the Minnesota Supercomputing Institute for access to molecular modelling computers and software.

References

- ¹ (a) Faber, K. *Biotransformations in Organic Chemistry*, 5th ed. Springer-Verlag, Berlin, 2004; (b) Drauz, K.; Waldman, H., Eds. *Enzyme Catalysis in Organic Synthesis*; Wiley-VCH: Weinheim, 2002 (c) Wong, C.-H.; Whitesides, G. M. *Enzymes in Synthetic Organic Chemistry*; Pergamon: New York, 1994.
- ² Bornscheuer, U. T.; Kazlauskas, R. J. *Hydrolases in Organic Synthesis – Regio- and Stereoselective Biotransformations*; Wiley-VCH: Weinheim, 1999; pp. 17-18.
- ³ Cygler, M.; Grochulski, P.; Kazlauskas, R. J.; Schrag, J. D.; Bouthillier, F.; Rubin, B.; Serreqi, A. N.; Gupta, A. K. *J. Am. Chem. Soc.* **1994**, *116*, 3180-3186.
- ⁴ Mezzitti, A.; Schrag, J.; Cheong, C. S.; Kazlauskas, R. J. *Chem. Biol.* **2005**, *12*, 427-437.
- ⁵ Tyndall, J. D. A.; Tessa Nall, T.; Fairlie, D. P. *Chem. Rev.* **2005**, *105*, 973-1000.
- ⁶ Savile, C. K.; Kazlauskas, R. J. *J. Am. Chem. Soc.* **2005**, *127*, 12228-12229.
- ⁷ (a) Muchmore, D. C. *US Patent* US 5,215,918; (b) Savile, C. K.; Magloire, V. P.; Kazlauskas, R. J. *J. Am. Chem. Soc.* **2005**, *127*, 2104-2113.
- ⁸ Mugford, P. F.; Lait, S. M.; Keay B. A.; Kazlauskas, R. J. *ChemBioChem*, **2004**, *5*, 980-987.
- ⁹ (a) Lin, Y. Y.; Palmer, D. N.; Jones, J. B. *Can. J. Chem.* **1974**, *52*, 469-476.
- ¹⁰ (a) Estell, D. A.; Graycar, T. P.; Miller, J. V.; Powers, D. B.; Burnier, J. P.; Ng, P. G.; Wells, J. A. *Science* **1986**, *233*, 659-663. (b) Wells, J. A.; Powers, D. B.; Bott, R. R.; Graycar, T. P.; Estell, D. A. *Proc. Natl. Acad. Sci. USA*, **1987**, *84*, 1219-1223.
- ¹¹ Pohl, T.; Waldmann, H. *Tetrahedron Lett.* **1995**, *36*, 2963-2966.
- ¹² Breuer, M.; Ditrich, K.; Habicher, T.; Hauer, B.; Keßeler, M.; Stürmer, R.; Zelinski, T. *Angew. Chem. Int. Ed.* **2004**, *43*, 788-824.

- ¹³ Kundu, N.; Roy, S.; Maenza, F. *Eur. J. Biochem.* **1972**, *28*, 311-315.
- ¹⁴ Based on a limit of detection of 0.1% conversion.
- ¹⁵ Mugford, P. F.; Magloire, V. P.; Kazlauskas, R. J. *J. Am. Chem. Soc.* **2005**, *127*, 6536-6537.
- ¹⁶ (a) Harwood, C. R.; Cutting, S. M. *Molecular Biological Methods for Bacillus*; John Wiley & Sons: Chichester, U.K., 1990; pp 33-35 and 391-402. (b) Cho, S.-J.; OH, S.-H.; Pridmore, R. D.; Juillerat, M. A.; Lee, C.-H. *J. Agric. Food Chem.* **2003**, *51*, 7664-7670.
- ¹⁷ Branden, C.; Tooze, J. *Introduction to Protein Structure*; Garland: New York, 1991; pp 241-243.
- ¹⁸ Backes, B. J.; Dragoli, D. R.; Ellman, J. A. *J. Org. Chem.* **1999**, *64*, 5472-5478.
- ¹⁹ Crombie, L.; Harper, S. H. *J. Am. Chem. Soc.* **1950**, 2685-2689.
- ²⁰ Keith, D. D.; Tortora, J. A.; Yang, R. *J. Org. Chem.* **1978**, *43*, 3711-3713.
- ²¹ Brown, H. C.; Cho, B. T.; Park, W. S. *J. Org. Chem.* **1988**, *53*, 1231-1238.
- ²² Brown, H. C.; Srebnik, M.; Ramachandran, P. V. *J. Org. Chem.* **1989**, *54*, 1577-1583.
- ²³ Cho, B. T.; Chun, Y. S. *Tetrahedron: Asymmetry* **1992**, *3*, 1539-1542.
- ²⁴ Delair, P.; Kanazawa, A. M.; de Azevedo, M. B. M.; Greene, A. E. *Tetrahedron: Asymmetry* **1996**, *7*, 2707-2710.
- ²⁵ Naemura, K.; Murata, M.; Tanaka, R.; Yano, M.; Hirose, K.; Tobe, Y. *Tetrahedron: Asymmetry* **1996**, *7*, 3285-3294.
- ²⁶ The sulfoxide oxygen of non-productive (*R*)-**1a** bumped catalytic His57 ($O - C_{\delta 2}$ distance = 3.04 Å and the *p*-tolyl group was hindered by Met192 ($C_{ortho} - C_{\gamma}$ distance = 3.33 Å and $C_{meta} - C_{\gamma}$ distance = 3.73 Å), Gly193 ($C_{para} - N$ distance = 3.96 Å) and Phe41 ($CH_3 - C_{\epsilon}$ distance = 3.75 Å). As well, the *p*-tolyl group forms an unfavourable *syn*-pentane interaction with the oxyanion. This intramolecular interaction and severe steric clash between *p*-tolyl group and active site residues significantly distorts the substrate and results in the loss of two catalytically relevant hydrogen bonds ($N_{\delta 2} - O_{\gamma}$ distance = 4.49 Å and $N_{\delta 2} - N_{sulfonamide}$ distance = 5.13 Å). The *p*-tolyl group of non-productive (*S*)-**1a** was hindered by catalytic His57 ($C_{ortho} - N_{\epsilon 2}$ distance = 3.38 Å, $C_{ortho} - C_{\delta 2}$ distance = 3.27 Å, $C_{meta} - C_{\delta 2}$ distance = 3.73 Å and $C_{meta} - C_{\gamma}$ distance = 3.90 Å) and the sulfonamide

bumped the Met192 ($S_{\text{sulfonamide}} - S_{\delta}$ distance = 3.33 Å and $S_{\text{sulfonamide}} - C_{\epsilon}$ distance = 3.52 Å). The steric hindrance between *p*-tolyl group and active site residues results in the loss of one catalytically relevant hydrogen bond ($N_{\delta 2} - N_{\text{sulfonamide}}$ distance = 3.20 Å).

²⁷ Cohen, S. G. *Trans. N. Y. Acad. Sci.* **1969**, *31*, 705-719.

²⁸ The van der Waals distance for CH-C = 3.99 Å, CH-N = 3.84 Å, CH-S = 4.09 Å and O-HC = 3.81 Å. These were estimated from the van der Waals radii of carbon (1.70 Å), nitrogen (1.55 Å), sulfur (1.80 Å) or oxygen (1.52 Å) and hydrogen (1.20 Å) and the C-H bond length (1.09 Å) from Bondi, A. *J. Phys. Chem.* **1964**, *68*, 441-451.

²⁹ The energy of a hydrophobic interaction is from the regaining of entropy by water after it is removed from a hydrophobic group and can be estimated using the incremental Gibbs free energy of transfer. The incremental Gibbs free energy of transfer of the *p*-tolyl group from *n*-octanol to water is estimated to be ca. +3.4 kcal/mol, using $\Delta G_{\text{trans}} = 2.303RT\pi$, where π is the hydrophobicity constant of the *p*-tolyl group ($\pi = 2.5$, using *ClogP* (Bio-Byte, Claremont, USA)) relative to hydrogen, whereas the sulfoxide oxygen is ca. -1.8 kcal/mol. Switching from (*S*)-**1a** to (*R*)-**1a** places the *p*-tolyl group into the hydrophobic leaving-group pocket and removes the sulfoxide oxygen for a total of ca. 5.2 kcal/mol in favour of placing the *p*-tolyl group in the hydrophobic leaving-group pocket when in an aqueous medium. The energy difference may be higher if one includes the hydrophobic surface of the leaving-group pocket. For details, see: (a) Fersht, A. *Structure and Mechanism in Protein Science*; W.H. Freeman and Company: New York, 1998; pp 324-348. (b) Leo, A.; Hansch, C.; Elkins, D. *Chem. Rev.* **1971**, *71*, 525-616.

³⁰ Fitzpatrick, P. A.; Klibanov, A. M. *J. Am. Chem. Soc.* **1991**, *113*, 3166-3171.

³¹ Davis, F. A.; Zhou, P.; Chen, B.-C. *Chem. Soc. Rev.* **1998**, *27*, 13-18.

³² Moreau, P.; Essiz, M.; Merour, J.-Y.; Bouzard, D. *Tetrahedron: Asymmetry* **1997**, *8*, 591-598.

³³ Davis, F. A.; Zhou, P.; Reddy, G. V. *J. Org. Chem.* **1994**, *59*, 3243-3245.

³⁴ Lefebvre, I. M.; Evans, S. A. *J. Org. Chem.* **1997**, *62*, 7532-7533.

³⁵ (a) Anderson, K. K. in *The Chemistry of Sulphones and Sulphoxides*, Patai, S.; Rapoport, Z.; Stirling, C. J. M., eds.; John Wiley & Sons: New York, **1988**, pp 55-94. (b)

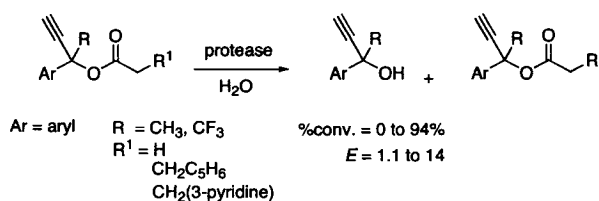
- Phillips, H. J. *Chem. Soc.* **1925**, *127*, 2552-2587. (b) Hulce, M.; Mallamo, J. P.; Frye, L. L.; Kogan, T. P.; Posner, G. A. *Org. Synth.* **1986**, *64*, 196-206.
- ³⁶ Han, Z.; Krishnamurthy, D.; Grover, P.; Fang, Q. K.; Senanayake, C. H. *J. Am. Chem. Soc.* **2002**, *124*, 7880-7881.
- ³⁷ Omata, T.; Iwamoto, N.; Kimura, T.; Tanaka, A.; Fukui, S. *Eur. J. Appl. Microbiol. Biotechnol.* **1981**, *11*, 199-204.
- ³⁸ Fukui, S.; Tanaka, A. *Methods Enzymol.* **1987**, *136*, 293-302.
- ³⁹ Bornscheuer, U. T.; Kazlauskas, R. J. *Hydrolases in Organic Synthesis – Regio- and Stereoselective Biotransformations*; Wiley-VCH: Weinheim, 1999; pp. 17-18, 65-87, 179-182.
- ⁴⁰ Walker, F. A.; Benson, M. *J. Am. Chem. Soc.* **1980**, *102*, 5530-5538.
- ⁴¹ Dale, J. A.; Mosher, H. S. *J. Am. Chem. Soc.* **1973**, *95*, 512-519.
- ⁴² (a) Weiner, S. J.; Kollman, P. A.; Case, D. A.; Singh, U. C.; Ghio, C.; Alagona, G.; Profet, S.; Weiner, P. *J. Am. Chem. Soc.* **1984**, *106*, 765-784. (b) Weiner, S. J.; Kollman, P. A.; Nguyen, D. T.; Case, D. A. *J. Comp. Chem.* **1986**, *7*, 230-252.
- ⁴³ Tulinsky, A.; Blevins, R. A. *J. Biol. Chem.* **1987**, *262*, 7737-7743.
- ⁴⁴ Raza, S.; Fransson, L.; Hult, K. *Protein Sci.* **2001**, *10*, 329-338.

Chapter 5

Resolving sterically hindered substrates such as tertiary alcohols is a great challenge in biocatalysis. Most hydrolases show low activity toward tertiary alcohols and their esters. In this chapter we extend several proteases to tertiary alcohol esters by tailoring anchor group. We show proteases catalyze hydrolysis of esters of tertiary alcohols when substrate has an anchor group that binds it to the protease active site. This is the first protease-catalyzed resolution of chiral tertiary alcohols.

Tailoring anchor group extends proteases to tertiary alcohol esters

Abstract



Although hydrolases can resolve many chiral primary and secondary alcohols, only a few resolutions of tertiary alcohols have been reported. We show proteases, which have a large open binding site for alcohols, catalyze hydrolysis of esters of tertiary alcohols when substrate has an anchor group that binds it to the protease active site. We show that a *syn*-pentane-like interaction destabilizes the transition state for reaction of tertiary alcohols, but that the addition of an anchor group that binds substrate to the protease stabilizes transition state and enables proteases to catalyze hydrolysis of tertiary alcohol esters. We then rationalize this hypothesis using molecular modelling and propose strategies to increase the enantioselectivity of these new reactions. Further, we show dihydrocinnamates are resistant to chemical hydrolysis and that proteases catalyze hydrolysis of sterically demanding allylic and alkyl tertiary alcohol esters that do not react with other hydrolases.

5.1 Communication

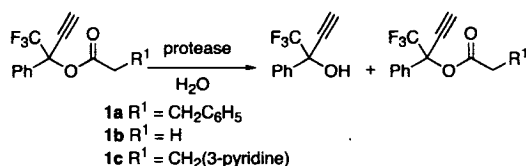
Although hydrolases can resolve many chiral primary and secondary alcohols,¹ only a few resolutions of tertiary alcohols have been reported.^{2,3,4} Most researchers assume that the problem with tertiary alcohols is that they are too large to fit in the active site. Indeed, Bornscheuer and coworkers⁵ found that lipases with a larger alcohol binding site, as indicated by a GGGX sequence motif, are more likely to accept esters of tertiary alcohols as substrates. In this communication, we focus on proteases, which already have a large open binding site for alcohols,^{6,7} but still do not catalyze reaction with tertiary alcohols.⁸ We hypothesize that internal strain destabilizes the transition state for this reaction. We demonstrate that the addition of anchor groups that bind the substrate to the protease to stabilize the transition state enables proteases to catalyze hydrolysis of esters of tertiary alcohols. We further rationalize this hypothesis using molecular modelling and propose strategies to increase the enantioselectivity of these new reactions.

Enzymes often use an anchoring group to bind and orient a substrate for reaction. For example, orotidine 5'-monophosphate decarboxylase is an efficient catalyst.⁹ Although reaction occurs entirely in the orotic acid base, the ribosyl phosphate moiety is essential for activity. Orotic acid ($2.5 \times 10^{-5} \text{ M}^{-1} \text{ s}^{-1}$) alone shows twelve orders of magnitude lower activity than orotidine 5'-monophosphate ($6.3 \times 10^7 \text{ M}^{-1} \text{ s}^{-1}$), even though orotic acid ($K_i = 9.5 \text{ mM}$) binds to the active site. In a few cases, researchers have used anchoring groups to enhance biocatalytic reactions. For example, the fungus *Beauveria bassiana* did not hydroxylate cyclopentanone, but did hydroxylate the *N*-benzoylspirooxazolidine derivative with moderate yield and diastereoselectivity.¹⁰

We started by investigating the reactivity of several commercial proteases toward α -trifluoromethyl- α -acetylenic esters **1a–1c** (Table 5.1). The CF_3 group reduces spontaneous hydrolysis via alkyl oxygen cleavage, which otherwise prevents reaction in water.^{2,3} Subtilisin BL, subtilisin Carlsberg, α -chymotrypsin and protease from *Streptomyces griseus* catalyzed hydrolysis of dihydrocinnamate **1a**.¹¹ However, protease from *Aspergillus melleus* showed low reactivity toward **1a** (<1% conv.) and protease from *Aspergillus oryzae* showed no reaction with **1a**. All proteases tested, except α -chymotrypsin, hydrolyzed the corresponding acetate **1b** and subtilisin Carlsberg, α -chymotrypsin and protease from *Streptomyces griseus* reacted with 3-(3-pyridyl)propionate **1c**. Thus, using acetate

instead of dihydrocinnamate extends proteases from *Aspergillus melleus* and *Aspergillus oryzae* to tertiary alcohol esters and increases the reactivity of subtilisin BL, subtilisin Carlsberg, and protease from *Streptomyces griseus*. α -Chymotrypsin does not react with **1a**, which is not surprising considering its preference for large acyl groups; thus, using the dihydrocinnamate instead of acetate extends α -chymotrypsin to tertiary alcohol esters. The reactivity of subtilisin Carlsberg and protease from *Streptomyces griseus* increased toward **1b** and **1c**, as compared to **1a**. This increased reactivity may reflect better binding or higher solubility of these substrates in aqueous solutions.

Table 5.1. Reactivity and enantioselectivity of proteases toward **1a-1c**^a



Protease	1a		1b		1c	
	%c ^b	E ^c	%c	E	%c	E
<i>Aspergillus melleus</i> protease	<1	n.d. ^d	38	14 (R)	n.p. ^e	n.p.
<i>Aspergillus oryzae</i> protease	n.r. ^f	n.r.	15	6.4 (R)	n.p.	n.p.
subtilisin BL	15	1.5 (R)	46	2.7 (R)	n.p.	n.p.
subtilisin Carlsberg	27	1.3 (S)	84	2.5 (R)	31	1.1 (S)
α -chymotrypsin	51	1.9 (S)	n.r.	n.d.	63	1.1 (S)
<i>Streptomyces griseus</i> protease	7	2.4 (S)	14	2.4 (R)	26	1.3 (S)

^aSee Chapter 5 - Appendix Table A5.2 for complete details. ^bConversion: reaction for 48 h. ^cEnantioselectivity: the enantiomeric ratio *E* measures the relative rate of hydrolysis of the fast enantiomer as compared to the slow enantiomer as defined by Sih.¹² ^dNot determined. ^eNot performed. ^fNo reaction.

The enantioselectivity of proteases toward alcohol **1** is low to moderate. Proteases from *Aspergillus melleus* (*E* = 14) and *Aspergillus oryzae* (*E* = 6.4) showed moderate enantioselectivity toward **1**, but only with the acetate derivative **1b**. The acetate group, however, readily hydrolyzes without an electron-withdrawing group, such as CF₃, on the

alcohol portion.¹³ Thus, it is only useful for resolving tertiary alcohols with electron-withdrawing or insulating substituents. Dihydrocinnamate esters of tertiary alcohols are chemically stable (<1% chemical hydrolysis in buffered solutions after 48 h) and show moderate to high reactivity with subtilisin Carlsberg and α -chymotrypsin. Although the enantioselectivities of these proteases toward tertiary alcohol **1** are lower than proteases from *Aspergillus melleus* and *Aspergillus oryzae*, the stability of the dihydrocinnamate group and reactivity with subtilisin Carlsberg and α -chymotrypsin make them promising enzyme-substrate pairs for resolving a wider range of tertiary alcohols (e.g., tertiary alcohols without electron-withdrawing or insulting groups).

Thus, we investigated the reactivity and enantioselectivity of subtilisin Carlsberg and α -chymotrypsin toward tertiary alcohol dihydrocinnamate esters **2a-9a** (Table 5.2). Subtilisin Carlsberg and α -chymotrypsin showed high reactivity, but low enantioselectivity, toward tertiary acetylenic dihydrocinnamate esters **2a-6a**. Subtilisin Carlsberg showed its highest enantioselectivity with **2a** ($E = 2.8$) to give (*R*)-**2** and α -chymotrypsin showed its highest enantioselectivity with **6a** ($E = 5.8$). In addition to acetylenic derivatives, subtilisin Carlsberg and α -chymotrypsin catalyzed the hydrolysis of allylic derivative **7a** and alkyl derivative **8a** – sterically hindered substrates that do not react with lipases.² Subtilisin Carlsberg showed low reactivity toward **7a** (%c = ~5%) and α -chymotrypsin showed moderate reactivity toward **7a** (%c = ~25%) – decomposition of the allylic alcohol product prevented accurate determination of conversion and E . Both subtilisin Carlsberg (%c = <1%) and α -chymotrypsin (%c = 1%) showed low reactivity toward **8a** and no reaction with **9a**.

Table 5.2. Reactivity and enantioselectivity of subtilisin Carlsberg and α -chymotrypsin toward **1a-9a**^a

1 R¹ = Ph; R² = CF₃; R³ = CCH
 2 R¹ = Ph; R² = CH₃; R³ = CCH
 3 R¹ = 4-tolyl; R² = CH₃; R³ = CCH
 4 R¹ = 4-O₂NPh; R² = CH₃; R³ = CCH
 5 R¹ = 4-*i*-PrPh; R² = CH₃; R³ = CCH
 6 R¹ = 1-Naphthyl; R² = CH₃; R³ = CCH
 7 R¹ = Ph; R² = CH₃; R³ = CH=CH₂
 8 R¹ = Ph; R² = CH₃; R³ = CH₂CH₃
 9 R¹ = Ph; R² = CH₃; R³ = CH(CH₃)₂

^a R¹ = CH₂-C₆H₅
^b R¹ = H
^c R¹ = CH₂(3-pyridine)

substrate	subtilisin Carlsberg		α -chymotrypsin	
	% ^c	<i>E</i> ^c	% ^c	<i>E</i>
1a	27	1.3 (<i>S</i>)	51	1.9 (<i>S</i>)
2a	22	2.8 (<i>R</i>)	94	1.6 (<i>R</i>)
3a	27	1.2	32	1.1
4a	27	1.1	22	2.4
5a	63	1.1	68	1.7
6a	20	1.6	25	5.8
7a	~5	n.d. ^d	~25	n.d.
8a	<1	~5 ^e	1	~3 ^e
9a	n.r. ^f	n.r.	n.r.	n.r.

^aSee Chapter 5 - Appendix Table A5.3 for complete details. ^bConversion: reaction for 48 h. ^cEnantioselectivity: the enantiomeric ratio *E* measures the relative rate of hydrolysis of the fast enantiomer as compared to the slow enantiomer as defined by Sih.¹² ^dNot determined. ^eThe enantioselectivity may be inaccurate because of low conversion. ^fNo reaction.

To understand the molecular basis for protease reactivity toward tertiary alcohol esters, we modelled the first tetrahedral intermediate of protease-catalyzed hydrolysis. The reactivity of proteases toward tertiary allylic and alkyl alcohols is lower than with tertiary acetylenic alcohols and secondary alcohols. Molecular modelling suggests a *syn*-pentane-like interaction as the reason why tertiary alcohol esters hydrolyze more slowly than secondary alcohol esters. The orientation within the enzyme places the smallest group (H for secondary alcohols) in a *syn-syn* orientation to the oxyanion (Figure 5.1a). A hydrogen fits in this orientation easily, but a larger group such as methyl creates a *syn*-pentane-like interaction. A methyl/methyl *syn*-pentane interaction destabilizes a conformation by ~3.6 kcal/mol.¹⁴ Molecular mechanics calculations suggest acetylene adopts this *syn*-pentane-like orientation with oxyanion. A methyl/oxyanion *syn*-pentane-like in-

teraction is ~ 2.5 kcal/mol higher in energy than an acetylene/oxyanion *syn*-pentane-like interaction (Figures 5.1b and 5.1c). Our results are consistent with this hypothesis. While subtilisin Carlsberg and α -chymotrypsin show high reactivity toward 1-phenethyl dihydrocinnamate¹⁵ and tertiary acetylenic ester **2a**, they show a two- to four-fold decrease in conversion toward the more sterically hindered tertiary allylic ester **7a**, at least a fifty-fold decrease toward the sterically demanding tertiary alkyl ester **8a** and no reaction with **9a**.

To overcome this destabilizing *syn*-pentane-like interaction a stabilizing interaction of equal or greater energy must be added. An anchoring group adds a stabilizing interaction through improved binding and helps to stabilize the transition state. The inability of an acyl group to anchor substrate to the active site and stabilize transition state may account for the low activity or inactivity of proteases toward tertiary alcohol esters (e.g., proteases from *Aspergillus melleus* and *Aspergillus oryzae* toward **1a** and α -chymotrypsin toward **1b**).¹⁶

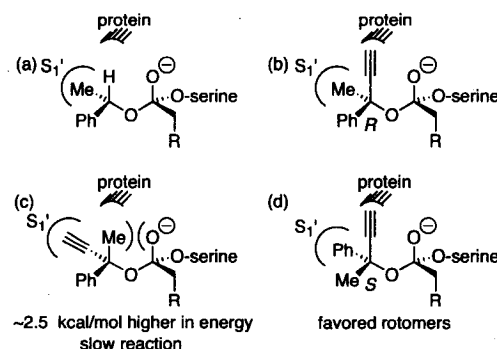


Figure 5.1. Schematic representation of the proposed conformation of the first tetrahedral intermediate of protease-catalyzed ester hydrolysis. (a) For a secondary alcohol, the hydrogen orients to form a *syn-syn* interaction with oxyanion. (b) For a tertiary acetylenic ester, the smallest substituent (acetylene) forms the *syn*-pentane-like interaction with oxyanion. The fast-reacting (*R*)-enantiomer binds with the medium-sized methyl group in the S_1' pocket and the larger phenyl group open to solvent (c) When the substituent forming the *syn*-pentane-like interaction with oxyanion is methyl or larger the transition state is destabilized and the reaction is slow. Phenyl does not adopt this orientation because it encounters steric hindrance with protein. (d) The slow-reacting (*S*)-enantiomer binds with the large phenyl group in the S_1' pocket and the medium-sized methyl group open to solvent.

The enantioselectivity of proteases toward tertiary alcohols is low. X-Ray crystal structures of subtilisin reveal one pocket – the S_1' pocket – that binds one substituent of an alcohol.⁶ The S_1' pocket of subtilisin Carlsberg is a narrow, shallow crevice that can barely accommodate a *para*-substituted aryl group. Molecular modelling of the first tetrahedral intermediate for subtilisin Carlsberg-catalyzed hydrolysis of **2a** reveals that (*R*)-**2a** places the methyl group in the S_1' pocket, while (*S*)-**2a** places the phenyl group in this pocket (see Figures 5.1b, 5.1d and Chapter 5 - Appendix Figure A5.1). In both cases, the other substituent remains in the solvent and the acetylene group forms the *syn*-pentane-like orientation with oxyanion. Binding the methyl group of (*R*)-**2a** in the S_1' pocket avoids some steric interactions between the pocket and the phenyl group, while binding the phenyl group of (*S*)-**2a** adds a good hydrophobic interaction between the pocket and the phenyl group. The enantioselectivity is low because of this competing hydrophobic interaction.

Consistent with this explanation for enantioselectivity, the enantioselectivity of subtilisin Carlsberg-catalyzed hydrolysis of **2a** increased from $E = 2.8$ in 90:10 water-acetonitrile to $E = 4.2$ in 40:60 water-acetonitrile (no reaction with >60% acetonitrile). The high concentration of acetonitrile favours the phenyl group in the solvent; thus, the enantiomer preference shifts toward the (*R*)-enantiomer, which orients with the methyl group in the S_1' pocket (Figure 5.1b). This result suggests that the enantioselectivity for acylation of tertiary alcohols in organic solvent would also be higher. Unfortunately, we did not detect any reaction. Presumably, proteases do not catalyze transesterification of tertiary alcohols because there is no acyl group to anchor and orient substrate for reaction. Also consistent with our explanation for enantioselectivity is the reverse enantiopreference of subtilisin Carlsberg toward **1a** ($E = 1.3$) to give (*S*)-**1**, where the more polar CF_3 group prefers a water-exposed orientation.^{6,17}

Although the enantioselectivities are low, this is the first hydrolase-catalyzed resolution of tertiary alcohol esters that do not contain electron-withdrawing or insulating groups and the first protease-catalyzed resolution. Unlike acetates, dihydrocinnamates are chemically stable and show high reactivity with subtilisin and α -chymotrypsin. Subtilisin BPN' and E also show high reactivity toward dihydrocinnamate esters and may show higher enantioselectivity toward tertiary alcohol esters **2a-6a** because of an increased hy-

drophobic interaction between aryl group and the larger S₁' alcohol-binding pocket.⁶ Substrates with a large difference in alcohol substituent polarity^{6,18} or size¹⁹ may also show higher enantioselectivity.

In conclusion, we show that addition of an anchor group that binds substrate to the protease active site stabilizes transition state and enables proteases to catalyze hydrolysis of esters of tertiary alcohols. Further, we show dihydrocinnamate esters are resistant to chemical hydrolysis and that proteases catalyze hydrolysis of sterically demanding allylic and alkyl tertiary alcohol esters when one alcohol substituent is methyl or smaller.

Acknowledgements

We thank McGill University and University of Minnesota for financial support and the Minnesota Supercomputing Institute for access and support for molecular modeling computers and software.

References

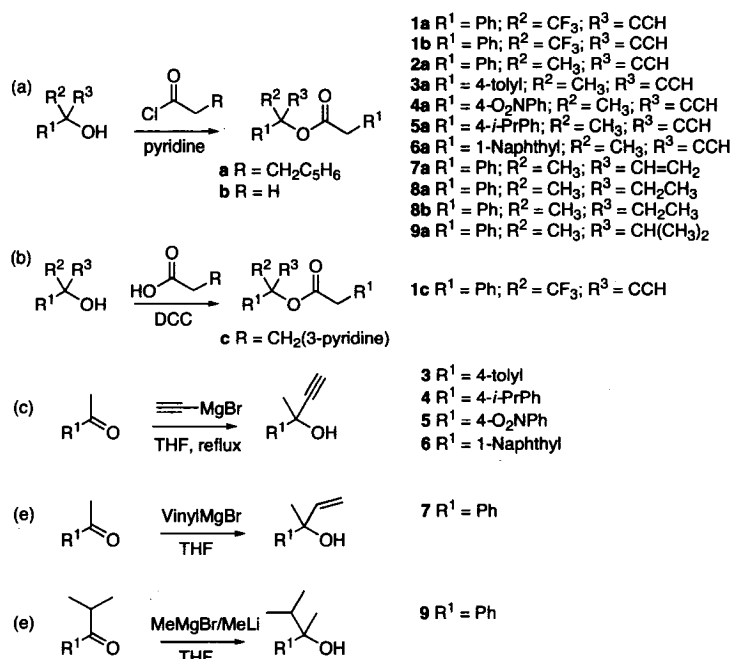
- ¹ Bornscheuer, U. T.; Kazlauskas, R. J. *Hydrolases in Organic Synthesis*; Wiley-VCH: Weinheim, 1999.
- ² O'Hagan, D.; Zaidi, N. A. *J. Chem. Soc., Perkin Trans. 1* **1992**, 947-949.
- ³ O'Hagan, D.; Zaidi, N. A. *Tetrahedron: Asymmetry* **1994**, 5, 1111-1118.
- ⁴ Krishna, S. H.; Persson, M.; Bornscheuer, U. T. *Tetrahedron: Asymmetry* **2002**, 13, 2693-2696.
- ⁵ (a) Henke, E.; Pleiss, J.; Bornscheuer, U. T. *Angew. Chem. Int. Ed.* **2002**, 41, 3211-3213.
(b) Henke, E.; Bornscheuer, U. T.; Schmid, R. D.; Pleiss, J. *ChemBioChem* **2003**, 4, 485-493.
- ⁶ Savile, C. K.; Kazlauskas, R. J. *J. Am. Chem. Soc.* **2005**, 127, 12228-12229.
- ⁷ Tyndall, J. D. A.; Tessa Nall, T.; Fairlie, D. P. *Chem. Rev.* **2005**, 105, 973-999.
- ⁸ Bordusa, F. *Chem. Rev.* **2002**, 102, 4817-4867.
- ⁹ Miller, B. G.; Snider, M. J.; Short, S. A.; Wolfenden, R. *Biochemistry* **2000**, 39, 8113-8118.

- ¹⁰ (a) Braunegg, G.; de Raadt, A.; Feichtenhofer, S.; Griengl, H.; Kopper, I.; Lehman, A.; Weber, H. -J. *Angew. Chem. Int. Ed.* **1999**, *38*, 2763-2766. (b) de Raadt, A.; Griengl, H.; Weber, H. *Chem. Eur. J.* **2001**, *7*, 27-31.
- ¹¹ Proteases, such as subtilisin and α -chymotrypsin, show preference for large acyl groups. For example, see: (a) Lin, Y. Y.; Palmer, D. N.; Jones, J. B. *Can. J. Chem.* **1974**, *52*, 469-476. (b) Estell, D. A.; Graycar, T. P.; Miller, J. V.; Powers, D. B.; Burnier, J. P.; Ng, P. G.; Wells, J. A. *Science* **1986**, *233*, 659-663.
- ¹² Chen, C. S.; Fujimoto, Y.; Girdaukas, G.; Sih, C. J. *J. Am. Chem. Soc.* **1982**, *104*, 7294-7299.
- ¹³ Attempted resolution of **8b** with *Aspergillus melleus* protease showed >50% chemical hydrolysis.
- ¹⁴ Eliel, E. L.; Wilen, S. H. *Stereochemistry in Organic Compounds*; Wiley: New York, 1994; p. 602.
- ¹⁵ Subtilisin Carlsberg: %conv. = 31%; $E = 1.2$. α -Chymotrypsin: %conv. = 82%; $E = 1.4$.
- ¹⁶ Fersht, A. *Structure and Mechanism in Protein Science*; W. H. Freeman and Co.: New York, 1999; pp. 349-376.
- ¹⁷ Howard, J. A. K.; Hoy, V. J.; O'Hagan, D.; Smith, G. T. *Tetrahedron* **1996**, *38*, 12613-12622.
- ¹⁸ Savile, C. K.; Magloire, V. P.; Kazlauskas, R. J. *J. Am. Chem. Soc.* **2005**, *127*, 2104-2113.
- ¹⁹ Fitzpatrick, P. A.; Klibanov, A. M. *J. Am. Chem. Soc.* **1991**, *113*, 3166-3171.

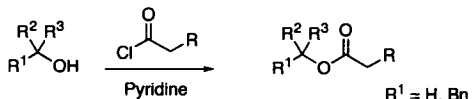
Chapter 5 – Appendix

General. ^1H - and ^{13}C -NMR spectra were obtained as CDCl_3 solutions at 300 MHz and 75 MHz, respectively. Chemical shifts are expressed in ppm (δ) and are referenced to tetramethylsilane or solvent signal. Coupling constants are reported in Hertz (Hz). GC analyses were performed on a 25 m x 0.25 mm Chrompack CP-Chiralsil-Dex CB column (Varian Inc., Palo Alto, USA) with He as carrier gas using one of the two following temperature programs: **A** 17.5 psi, 50 °C, 5 °C min⁻¹, 150 °C held for 5 min, 2.5 °C min⁻¹; 175 °C held for 5 min, 5 °C min⁻¹, 200 °C held for 30 min); **B** 17.5 psi, 120 °C held for 10 min, 20 °C min⁻¹, 200 °C held for 20 min. HPLC analyses were performed on a 4.6 x 250 mm Daicel Chiralcel OD column (Chiral Technologies, Exton, USA) and monitored at 254 nm. Flash chromatography with silica gel (35-75 mesh) was used to purify all intermediates and substrates. All reagents, buffers, starting materials and anhydrous solvents were purchased from Sigma-Aldrich (Milwaukee, USA) and used without purification. All air- and moisture-sensitive reactions were performed under Ar. Subtilisin Carlsberg, protease from *Streptomyces griseus* and α -chymotrypsin were purchased from Sigma-Aldrich (St. Louis, USA). Lipase from *Candida rugosa* (CRL), lipase A from *Candida antarctica*, protease from *Aspergillus melleus* and protease from *Aspergillus oryzae* were a generous gift from Altus Biologics (Cambridge, USA).

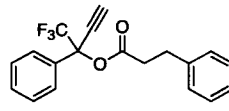
Synthesis of substrates. We synthesized esters **1a-9a**, **1b** and **8b** by treating the corresponding tertiary alcohol with the appropriate acid chloride in the presence of pyridine (Scheme A5.1a). We synthesized ester **1c** using dicyclohexylcarbodiimide (DCC) with 3-(3-pyridyl)propionic acid and the tertiary alcohol (Scheme A5.1b). We synthesized tertiary α -acetylenic alcohols via alkynyl magnesium bromide addition¹ to the appropriate ketone (Scheme A5.1c), tertiary alkenyl alcohols via vinyl magnesium bromide addition¹ to the appropriate ketone (Scheme A5.1d) and tertiary alkyl alcohols via modified alkyl addition of magnesium ate complexes derived from Grignard and alkyllithium reagents² to the appropriate ketone (Scheme A5.1e).



Scheme A5.1. Synthesis of esters **1a-9a**, **1b** and **6b**, **1c** and tertiary alcohols **3-6**, **7** and **9**.

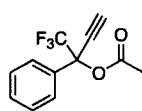


Synthesis of racemic esters 1a-9a, 1b and 8b. General procedure. Dihydrocinnamoyl chloride (7.5 mmol) was added drop-wise to a stirred solution of tertiary alcohol (5 mmol) and pyridine (7.5 mmol) in CH₂Cl₂ (25 mL) at 0 °C. The ice bath was removed and stirred until the reaction was complete by TLC (2-3 d). The reaction was quenched with the addition of sat. NaHCO₃ (25 mL). The layers were separated and the aqueous layer was extracted with CH₂Cl₂ (2 x 25mL). The combined organic layers were washed with sat. NaHCO₃ (2 x 25 mL), sat. NaCl (25 mL) and dried over MgSO₄. The organic layer was concentrated *in vacuo* to give the crude ester. All substrates were purified on silica gel. The relevant analytical data are given below:



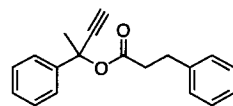
3-Dihydrocinnamic acid 1-phenyl-1-trifluoromethyl-prop-2-ynyl ester (1a). Purification on silica gel (1:1 hexanes/CH₂Cl₂) white solid (550 mg, 43%); mp 71-72 °C; ¹H NMR δ 2.81 (m, 2H, C(O)CH₂), 2.89 (s, 1H, CCH), 2.97 (t, *J* = 7.4, 2H, CH₂Ph), 7.30 (m, 8 H, phenyl), 7.48 (d, *J* = 6.9 Hz, 2 H, phenyl); ¹³C NMR δ 30.5 (CH₂Ph), 36.0

(C(O)CH₂), 75.2 (CCH), 78.9 (CCH), 120.4 (C), 124.1 (CF₃), 126.6, 126.9, 128.5, 128.6, 128.7, 129.8, 132.3, 139.9 (phenyl), 168.9 (C=O); HRMS calcd for C₁₉H₁₅F₃O₂Na [M+Na]⁺ 355.0898. Found: 355.0921. The enantiomers were separated using GC (program A; (*R*)-**1a**, *t_R* = 42.9 min; (*S*)-**1a**, *t_R* = 43.1 min).



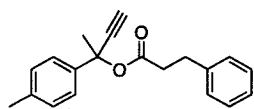
Acetic acid 1-phenyl-1-trifluoromethyl-prop-2-ynyl ester (1b).³

Purification on silica gel (100% hexanes to 80:20 hexanes/acetone) to give a low melting white solid (288 mg, 51%): ¹H NMR δ 2.20 (s, 3H, C(O)CH₃), 2.93 (s, 1H, CCH), 7.38-7.44 (m, 3H, phenyl), 7.62-7.65 (m, 2H, phenyl); ¹³C NMR δ 21.3 (C(O)CH₃), 75.5 (CCH), 78.8 (CCH), 120.3 (C), 124.1 (CF₃), 126.9, 128.6, 129.9, 132.4 (phenyl), 166.9 (C=O). The enantiomers were separated using GC (program B; (*R*)-**1a**, *t_R* = 5.2 min; (*S*)-**1a**, *t_R* = 5.5 min).



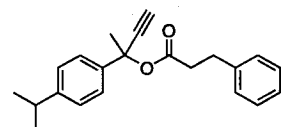
3-Dihydrocinnamic acid 1-methyl-1-phenyl-prop-2-ynyl

ester (2a). Purification on silica gel (100% hexanes to 95:5 hexanes/EtOAc) to give a clear liquid (927 mg, 67%): ¹H NMR δ 1.85 (s, 3H, CH₃), 2.65 (m, 2H, CH₂), 2.79 (s, 1H, CCH), 2.92 (t, *J* = 7.8, 2H, CH₂Ph), 7.15-7.34 (m, 8H, phenyl), 7.47-7.49 (m, 2H, phenyl); ¹³C NMR δ 30.8 (CH₂Ph), 32.2 (CH₃), 36.5 (C(O)CH₂), 75.6 (C), 75.8 (CCH), 83.1 (CCH), 124.9, 126.4, 128.0, 128.5, 128.6, 140.6, 142.2 (phenyl), 170.6 (C=O); HRMS calcd for C₁₉H₁₈O₂Na [M+Na]⁺ 301.1224. Found: 301.1204. The enantiomers were separated using GC (program A; (*S*)-**2a**, *t_R* = 46.7 min; (*R*)-**2a**, *t_R* = 46.9 min).



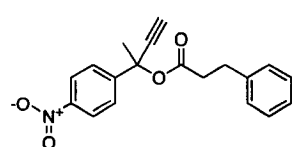
Dihydrocinnamic acid 1-methyl-1-*p*-tolyl-prop-2-ynyl

ester (3a). Purification on silica gel (100% hexanes to 95:5 hexanes/EtOAc) to give a clear liquid (336 mg, 23%): ¹H NMR δ 1.86 (s, 3H, CH₃), 2.33 (s, 3H, PhCH₃), 2.66 (m, 2H, CH₂), 2.79 (s, 1H, CCH), 2.93 (t, *J* = 7.8, 2H, CH₂Ph), 7.11-7.31 (m, 7H, phenyl), 7.47-7.49 (m, 2H, phenyl); ¹³C NMR δ 21.2 (PhCH₃), 30.8 (CH₂Ph), 32.0 (CH₃), 36.5 (C(O)CH₂), 75.5 (C), 75.6 (CCH), 83.2 (CCH), 124.9, 126.3, 128.5, 128.6, 129.2, 137.8, 139.2, 140.6 (phenyl), 170.7 (C=O); HRMS calcd for C₂₀H₂₀O₂Na [M+Na]⁺ 315.1340. Found: 315.1360. The enantiomers could not be separated using GC.



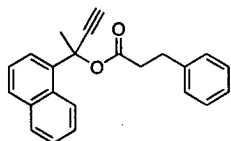
Dihydrocinnamic acid 1-(4-isopropyl-phenyl)-1-methyl-prop-2-ynyl ester (4a). Purification on silica gel (100%

hexanes to 95:5 hexanes/EtOAc) to give a clear liquid (507 mg, 32%): ^1H NMR δ 1.24 (d, $J = 7.2$, 6H, $\text{CH}(\text{CH}_3)_2$), 1.86 (s, 3H, CH_3), 2.67 (m, 2H, $\text{C}(\text{O})\text{CH}_2$), 2.79 (s, 1H, CCH), 2.91 (sept, $J = 6.9$, 1H, $\text{CH}(\text{CH}_3)_2$), 2.97 (t, $J = 7.5$, 2H, CH_2Ph), 7.15-7.42 (m, 9H, phenyl); ^{13}C NMR δ 24.0 ($\text{CH}(\text{CH}_3)_2$), 30.8 (CH_2Ph), 32.0 (CH_3), 33.8 ($\text{CH}(\text{CH}_3)_2$), 36.5 ($\text{C}(\text{O})\text{CH}_2$), 75.5 (C), 75.5 (CCH), 83.2 (CCH), 124.9, 126.3, 126.5, 128.5, 128.6, 139.4, 140.6, 148.5 (phenyl), 170.7 ($\text{C}=\text{O}$); HRMS calcd for $\text{C}_{22}\text{H}_{24}\text{O}_2\text{Na}$ $[\text{M}+\text{Na}]^+$ 343.1671. Found: 343.1673. The enantiomers could not be separated using GC.



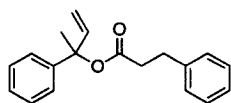
Dihydrocinnamic acid 1-methyl-1-(4-nitro-phenyl)-prop-2-ynyl ester (5a). Purification on silica gel (95:5 to 75:25 hexanes/EtOAc) to give a yellow solid (608 mg, 38%): mp 65-

66 °C; ^1H NMR δ 1.85 (s, 3H, CH_3), 2.72 (m, 2H, $\text{C}(\text{O})\text{CH}_2$), 2.88 (s, 1H, CCH), 2.96 (t, $J = 7.5$, 2H, CH_2Ph), 7.18-7.31 (m, 5H, phenyl), 7.56 (d, $J = 9.0$, 2H, phenyl), 8.15 (d, $J = 9.0$, 2H, phenyl); ^{13}C NMR δ 30.7 (CH_2Ph), 32.0 (CH_3), 36.1 ($\text{C}(\text{O})\text{CH}_2$), 74.6 (C), 76.7 (CCH), 81.8 (CCH), 123.8, 125.9, 126.5, 128.5, 128.6, 140.1, 147.5, 149.2 (phenyl), 170.5 ($\text{C}=\text{O}$); HRMS calcd for $\text{C}_{19}\text{H}_{17}\text{NO}_4\text{Na}$ $[\text{M}+\text{Na}]^+$ 346.1047. Found: 346.1055. The enantiomers could not be separated using GC.



Dihydrocinnamic acid 1-methyl-1-naphthalen-1-yl-prop-2-ynyl ester (6a). Purification on silica gel (100% hexanes to 95:5 hexanes/EtOAc) to give a clear liquid (974 g, 59%): ^1H NMR δ 1.97 (s, 3H, CH_3), 2.72 (m, 2H, $\text{C}(\text{O})\text{CH}_2$), 2.91 (s, 1H, CCH), 2.97 (t, J

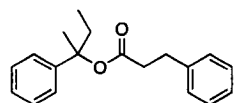
$= 7.5$, 2H, CH_2Ph), 7.21-8.06 (m, 12H, phenyl); ^{13}C NMR δ 30.8 (CH_2Ph), 32.0 (CH_3), 36.4 ($\text{C}(\text{O})\text{CH}_2$), 75.7 (C), 76.0 (CCH), 83.0 (CCH), 122.6, 124.3, 126.4, 127.7, 128.4, 128.5, 128.6, 133.0, 133.1, 139.4, 140.5 (phenyl), 170.7 ($\text{C}=\text{O}$) HRMS calcd for $\text{C}_{23}\text{H}_{20}\text{O}_2\text{Na}$ $[\text{M}+\text{Na}]^+$ 351.1359. Found: 351.1360. The enantiomers could not be separated using GC.



Dihydrocinnamic acid 1-methyl-1-phenyl-allyl ester (7a). Purification on silica gel (100% hexanes to 95:5 hexanes/EtOAc) to give a clear liquid (493 mg, 35%): ^1H NMR δ 1.87 (s, 3H, CH_3),

2.69 (m, 2H, $\text{C}(\text{O})\text{CH}_2$), 2.97 (t, $J = 7.5$, 2H, CH_2Ph), 5.24 (dd, $J = 0.9$, 10.5, 1H, $\text{C}=\text{CH}_2$), 5.26 (dd, $J = 0.9$, 17.4, 1H, $\text{C}=\text{CH}_2$), 6.25 (dd, $J = 10.8$, 17.4, 1H, $\text{C}=\text{CH}_2$), 7.21-7.34 (m, 10H, phenyl); ^{13}C NMR δ 25.5 (CH_3), 31.0 (CH_2Ph), 36.9 ($\text{C}(\text{O})\text{CH}_2$), 83.3 (C),

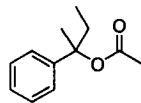
114.5 (C=CH₂), 125.3, 126.3, 127.3, 128.3, 128.5, 128.6, 140.7 (phenyl), 141.5 (C=CH₂), 143.7 (phenyl), 171.2 (C=O); HRMS calcd for C₁₉H₂₀O₂Na [M+Na]⁺ 303.1373. Found: 303.1360. The enantiomers could not be separated using GC or HPLC.



Dihydrocinnamic acid 1-methyl-1-phenyl-propyl ester

(8a). Purification on silica gel (1:1 hexanes/CH₂Cl₂) to give a clear liquid (1.13 g, 61%): ¹H NMR δ 0.72 (t, *J* = 7.5, 3H, CH₂CH₃), 1.76

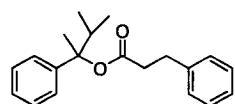
(s, 3H, CH₃), 1.96 (q, *J* = 7.2, 2H, CH₂CH₃), 2.63 (t, *J* = 7.5, 2H, C(O)CH₂), 2.92 (t, *J* = 7.8, 2H, CH₂Ph), 7.15-7.27 (m, 10H, phenyl); ¹³C NMR δ 8.3 (CH₂CH₃), 24.5 (CH₃), 31.2 (CH₂Ph), 35.4 (CH₂CH₃), 37.0 (C(O)CH₂), 84.6 (C), 124.9, 126.4, 127.0, 128.3, 128.6, 128.7, 140.9, 145.0 (phenyl), 171.6 (C=O); HRMS calcd for C₁₉H₂₂O₂Na [M+Na]⁺ 305.1523. Found: 305.1517. The enantiomers could not be separated using GC.



Acetic acid 1-methyl-1-phenyl-propyl ester (8b). Purification on

silica gel (100% hexanes to 95:5 hexanes/EtOAc) to give a clear liquid (518 mg, 54%): ¹H NMR δ 0.78 (t, *J* = 7.2, 3H, CH₂CH₃), 1.81 (s, 3H, CH₃),

2.02 (q, *J* = 7.5, 2H, CH₂CH₃), 2.07 (s, 3H, C(O)CH₃), 7.20-7.35 (m, 5H, phenyl); ¹³C NMR δ 8.2 (CH₂CH₃), 22.3 (C(O)CH₃), 24.5 (CH₃), 35.4 (CH₂CH₃), 84.4 (C), 124.7, 126.9, 128.2, 145.0 (phenyl), 169.8 (C=O); HRMS calcd for C₁₂H₁₆O₂Na [M+Na]⁺ 215.1049. Found: 215.1047. The enantiomers were separated using GC (program B; (*S*)-**8b**, *t*_R = 6.6 min; (*R*)-**8b**, *t*_R = 6.8 min).

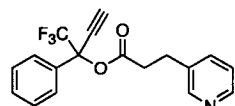


Dihydrocinnamic acid 1,2-dimethyl-1-phenyl-propyl

ester (9a). Purification on silica gel (100% hexanes to 90:10

hexanes/EtOAc) to give a clear liquid (536 mg, 36%): ¹H NMR δ

0.64 (d, *J* = 6.9, C(CH₃)₂), 0.91 (d, *J* = 6.9, C(CH₃)₂), 1.77 (s, 3H, CH₃), 2.02 (sept, 1H, *J* = 6.8, CH(CH₃)₂), 2.60 (t, *J* = 7.5, 2H, C(O)CH₂), 2.91 (t, *J* = 7.5, 2H, CH₂Ph), 7.10-7.28 (m, 10H, phenyl); ¹³C NMR δ 17.2 (CH(CH₃)₂), 17.7 (CH(CH₃)₂), 19.0 (CH₃), 31.1 (CH₂Ph), 37.0 (C(O)CH₂), 39.8 (CH(CH₃)₂), 85.6 (C), 125.4, 126.4, 126.9, 128.0, 128.6, 128.7, 140.9, 144.1, 171.5 (phenyl), 171.5 (C=O); HRMS calcd for C₂₀H₂₄O₂Na [M+Na]⁺ 319.1662. Found: 319.1673. The enantiomers could not be separated using GC.



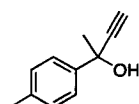
Synthesis of 3-(3-pyridyl)propionic acid 1-phenyl-1-

trifluoromethyl-prop-2-ynyl ester (1c). Dicyclohexylcarbodiimide (3 mmol) was added to a stirred solution of 1-phenyl-1-

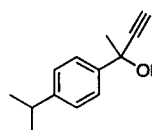
trifluoromethyl-prop-2-ynol (2 mmol), 3-(3-pyridyl)propionic acid (3 mmol), 4-dimethylaminopyridine (0.2 mmol) and NEt_3 (3 mmol) in CH_2Cl_2 (15 mL) at 0°C . The ice bath was removed and the reaction was stirred RT for 48 h. The reaction was quenched with the addition of sat. NaHCO_3 (25 mL). The layers were separated and the aqueous layer was extracted with CH_2Cl_2 (2 x 25 mL). The combined organic layers were washed with sat. NaHCO_3 (2 x 25 mL), dried over MgSO_4 and concentrated *in vacuo* to give the crude ester. Purification on silica gel (100% hexanes to 75:25 hexanes/acetone) gave the title compound as a white solid (340 mg, 51%): mp $121\text{--}122^\circ\text{C}$; ^1H NMR δ ^1H NMR δ 2.85 (m, 2H, $\text{C}(\text{O})\text{CH}_2$), 2.95 (s, 1H, CCH), 3.00 (t, $J = 7.5$, 2H, CH_2Pyr), 7.30–7.41 (m, 5H, phenyl or pyridyl), 7.50–7.63 (m, 2H, phenyl or pyridyl), 8.51 (m, 2H, pyridyl); ^{13}C NMR δ 27.7 ($\text{CH}_2\text{Pyridine}$), 35.5 ($\text{C}(\text{O})\text{CH}_2$), 76.7 (CCH), 79.1 (CCH), 120.2 (C), 123.6 (pyridyl), 124.1 (CF_3), 126.8, 128.6, 129.9, 132.1, 135.4, 136.4, 147.9, 149.7 (phenyl or pyridyl), 168.4 ($\text{C}=\text{O}$); HRMS calcd for $\text{C}_{18}\text{H}_{15}\text{F}_3\text{NO}_2$ $[\text{M}+\text{H}]^+$ 334.1057. Found: 334.1054. The enantiomers could not be separated using GC.

Synthesis of racemic tertiary α -acetylenic alcohols 3 - 6. General procedure.¹

Alkynyl Magnesium Bromide (0.5 M; 48 mL, 24 mmol) was added to a solution of the appropriate ketone (20 mmol) in THF (10 mL) and refluxed for 4 h or until complete by TLC. The solution was cooled to RT and quenched with dH_2O (25 mL) and extracted with EtOAc (3 x 25 mL). The combined organic layers were washed with sat. NaCl (25 mL) and dried over MgSO_4 . The organic layer was concentrated *in vacuo* to give the crude tertiary alcohol. The relevant analytical data are given below:

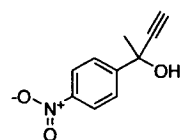


2-*p*-Tolyl-but-3-yn-2-ol (3). Obtained as yellow liquid (7.71 g, 96%): ^1H NMR δ 1.78 (s, 3H, CH_3), 2.36 (s, 3H, PhCH_3), 2.66 (s, 1H, CCH), 7.18 (d, $J = 7.8$, 2H, phenyl), 7.55 (d, $J = 8.4$, 2H, phenyl); ^{13}C NMR δ 21.1 (PhCH_3), 33.2 (CH_3), 67.9 (CCH), 69.7 (C), 87.7 (CCH), 125.0, 129.1, 137.5, 142.4 (phenyl). The enantiomers were separated using GC (program B; (*R* or *S*)-3, $t_R = 11.7$ min; (*R* or *S*)-3, $t_R = 11.9$ min).

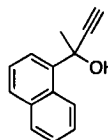


2-(4-Isopropyl-phenyl)-but-3-yn-2-ol (4). Obtained as yellow liquid (1.89 g, 85%): ^1H NMR δ 1.27 (d, $J = 6.9$, 6H, $\text{CH}(\text{CH}_3)_2$), 1.81 (s, 3H, CH_3), 2.69 (s, 1H, CCH), 2.94 (sept, $J = 7.2$, 1H, $\text{CH}(\text{CH}_3)_2$), 7.25 (d,

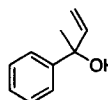
$J = 8.4$, 2H, phenyl), 7.60 (d, $J = 8.4$, 2H, phenyl); ^{13}C NMR δ 24.1 ($\text{CH}(\text{CH}_3)_2$), 33.0 (CH_3), 33.8 ($\text{CH}(\text{CH}_3)_2$), 69.7 (C), 72.9 (CCH), 87.6 (CCH), 125.0, 126.5, 142.6, 148.6 (phenyl). The enantiomers were separated using GC (program B; (*R* or *S*)-4, $t_{\text{R}} = 13.3$ min; (*R* or *S*)-4, $t_{\text{R}} = 13.5$ min).



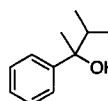
2-(4-Isopropyl-phenyl)-but-3-yn-2-ol (5). Obtained as bright yellow liquid (2.86 g, 75%): ^1H NMR δ 1.81 (s, 3H, CH_3), 2.76 (s, 1H, CCH), 7.84 (d, $J = 8.7$, 2H, phenyl), 8.23 (d, $J = 9.0$, 2H, phenyl); ^{13}C NMR δ 33.5 (CH_3), 69.4 (C), 74.2 (CCH), 86.1 (CCH), 123.7, 126.1, 147.5, 152.2 (phenyl). The enantiomers were separated using GC (program B; (*R* or *S*)-5, $t_{\text{R}} = 15.8$ min; (*R* or *S*)-5, $t_{\text{R}} = 16.0$ min).



2-Naphthalen-1-yl-but-3-yn-2-ol (6). Obtained as orange liquid (4.45 g, 91%): ^1H NMR δ 1.90 (s, 3H, CH_3), 2.76 (s, 1H, CCH), 7.50-8.16 (m, 7H, phenyl); ^{13}C NMR δ 33.1 (CH_3), 70.1 (C), 73.5 (CCH), 87.4 (CCH), 123.5, 123.6, 126.3, 126.4, 127.7, 128.4, 128.5, 133.0, 133.1, 142.4 (phenyl). The enantiomers were separated using GC (program B; (*R* or *S*)-6, $t_{\text{R}} = 15.8$ min; (*R* or *S*)-6, $t_{\text{R}} = 15.9$ min).

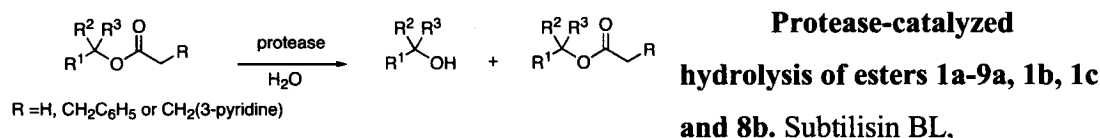


Synthesis of 2-phenyl-but-3-en-2-ol (7). Vinyl Magnesium Bromide (0.5 M; 48 mL, 24 mmol) was added to a solution of acetophenone (20 mmol) in THF (10 mL) and refluxed for 4 h. The solution was cooled to RT and quenched with dH_2O (25 mL) and extracted with EtOAc (3 x 25 mL). The combined organic layers were washed with sat. NaCl (25 mL) and dried over MgSO_4 . The organic layer was concentrated *in vacuo* to give a clear liquid (2.67 g, 90%): ^1H NMR δ 1.68 (s, 3H, CH_3), 5.17 (dd, $J = 0.9$, 10.5, 1H, $\text{C}=\text{CH}_2$), 5.32 (dd, $J = 1.2$, 17.4, 1H, $\text{C}=\text{CH}_2$), 6.20 (dd, $J = 10.8$, 17.4, 1H, $\text{C}=\text{CH}_2$), 7.30-7.51 (m, 5H, phenyl); ^{13}C NMR δ 29.4 (CH_3), 74.8 (C), 112.4 ($\text{C}=\text{CH}_2$), 125.3, 127.1, 128.3 (phenyl), 144.9 ($\text{C}=\text{CH}_2$), 146.6 (phenyl). The enantiomers were separated using HPLC (Chiralcel OD-H column, 98:2 hexanes/*i*-PrOH, 1.0 mL/min, 254 nm; (*R* or *S*)-7, $t_{\text{R}} = 12.7$ min; (*R* or *S*)-7, $t_{\text{R}} = 16.2$ min).

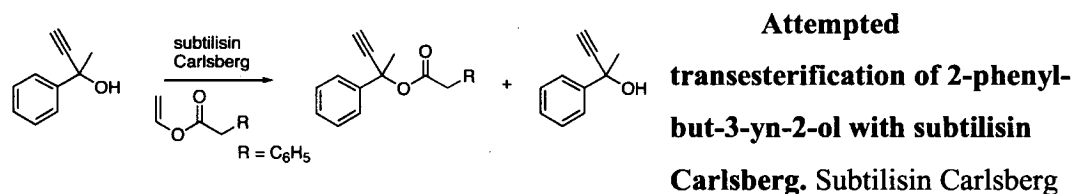


Synthesis of 3-methyl-2-phenyl-butan-2-ol (9). Methyllithium (1.5 M; 50 mmol, 33 mL) was added to methylmagnesium bromide (3.0 M, 10 mL, 30 mmol) at -78°C and stirred at this temperature for 1 h. A solution of isobutyl acetophenone (3.70 g, 25 mmol) in THF ((40 mL) was then added drop-wise and stirred for 6 h at -78°C .² The reaction was quenched with addition of sat. NH_4Cl

(100mL) and extracted with Et₂O (3 x 50 mL). The combined organic layers were washed with sat. NaCl (50 mL) and concentrated *in vacuo* to give a clear liquid (4.05 g, 96%): ¹H NMR δ 0.82 (d, *J* = 6.9, C(CH₃)₂), 0.91 (d, *J* = 6.9, C(CH₃)₂), 1.55 (br s, 1H, OH), 1.65 (s, 3H, CH₃), 2.04 (sept, 1H, *J* = 6.9, CH(CH₃)₂), 7.22-7.45 (m, 5H, phenyl); ¹³C NMR δ 17.3 (CH₃), 17.5 (CH₃), 38.7 (CH), 125.4, 126.5, 127.9, 147.9 (phenyl). The enantiomers were separated using GC (program B; (*R* or *S*)-9, *t*_R = 9.2 min; (*R* or *S*)-9, *t*_R = 9.9 min).



Aspergillus melleus protease, *Aspergillus oryzae* protease, subtilisin Carlsberg, α-chymotrypsin and protease from *Streptomyces griseus* in 50 mM BES buffer (10 mg/mL, pH 7.2, 450 μL) and substrate (100 mM in CH₃CN, 50 μL) were mixed in a 1.5 mL glass vial at 30 °C for 24 h to 48 h. The reaction was terminated with the addition of CH₂Cl₂ (500 μL). The phases were separated by centrifugation, and the organic layers were collected. The aqueous phase was extracted with CH₂Cl₂ (2 x 500 μL) and the combined organics were evaporated under a stream of air. The residue was diluted with EtOAc or EtOH (150 μL) and analyzed by GC or HPLC. The enantiomers were separated using the conditions described above. In cases where GC could not separate the substrate, it was purified using flash chromatography, hydrolyzed in ethanolic KOH and the enantiomeric excess was determined as the alcohol.



(50 mg), dihydrocinnamic vinyl ester (18 mg, 100 μmol), 2-phenylbut-3-yn-2-ol (73 mg, 500 μmol) and 4 Å molecular sieves (100 mg) were added to a glass vial. Anhydrous dioxane (2 mL) was added and the mixture was stirred at 30 °C for at least 48 h. A small amount of the solution was removed, filtered through a 0.45 μm nylon filter and analyzed

by GC. The enantiomers were separated using the conditions described above.

Modelling of tetrahedral intermediates bound to subtilisin Carlsberg. All modelling was performed using *Insight II 2000.1 / Discover* (Accelrys, San Diego, USA) on a SGI Octane UNIX workstation using the AMBER force field.⁴ We used a nonbonded cutoff distance of 8 Å, a distance-dependent dielectric of 1.0 and scaled the 1-4 van der Waals interactions by 50%. Protein structures in Figure A5.1 were created using PyMOL (Delano Scientific, San Carlos, USA). The x-ray crystal structure of subtilisin Carlsberg (entry 1CSE)⁵ is from the Protein Data Bank. Using the Builder module of *Insight II*, we removed the inhibitor, Eglin C. The hydrogen atoms were added to correspond to pH 7.0. Histidines were uncharged, aspartates and glutamates were negatively charged, and arginines and lysines were positively charged. The catalytic histidine (His64) was protonated. The positions of the water hydrogens and then the enzyme hydrogens were optimized using a consecutive series of short (1 ps) molecular dynamic runs and energy minimizations.⁶ This optimization was repeated until there was <2 kcal/mol in the energy of the minimized structures. Thereafter, an iterative series of geometry optimizations were performed on the water hydrogens, enzyme hydrogens and full water molecules. Finally, the whole system was geometry optimized.

The tetrahedral intermediates were built manually and covalently linked to Ser221. Nonstandard partial charges were calculated using a formal charge of -1 for the substrate oxyanion. Energy minimization proceeded in three stages. First, minimization of substrate with only the protein constrained (25 kcal mol⁻¹ Å⁻²); second, minimization with only the protein backbone constrained (25 kcal mol⁻¹ Å⁻²) and for the final stage the minimization was continued without constraints until the rms value was less than 0.0005 kcal mol⁻¹ Å⁻¹. A catalytically productive complex required all five hydrogen bonds within the catalytic machinery. We set generous limits for a hydrogen bond: a donor to acceptor atom distance of less than 3.1 Å with a nearly linear arrangement (>120° angle) of donor atom, hydrogen, and acceptor atom. Structures lacking any of the five catalytically relevant hydrogen bonds or encountering severe steric clash with enzyme were deemed nonproductive.

To calculate the intramolecular substrate interactions, we extracted the substrate coordinates for **2a** from the appropriate enzyme-substrate complex PDB file and performed a short molecular mechanics minimization to calculate energy.

Molecular modelling details for (*R*)-2a and (*S*)-2a tetrahedral intermediates bound to subtilisin Carlsberg. Molecular mechanics calculations with **2a** show the methyl/oxyanion *syn*-pentane-like and phenyl/oxyanion *syn*-pentane-like interactions are ca. 2.5 kcal/mol higher in energy than the acetylene/oxyanion *syn*-pentane-like interaction. These calculations combined with the lower reactivity toward substrates **7a**, **8a** and **9a** suggest the acetylene group occupies the same site as hydrogen of secondary alcohols, and forms the *syn*-pentane-like interaction with the oxyanion. Thus, modelling **2a** with subtilisin Carlsberg gave one productive conformation for each enantiomer (Table A5.1 and Figure A5.1). The four other plausible conformations lost catalytically essential hydrogen bonds and/or encountered steric clash with the protein (Table A5.1). Similar to previous modelling studies with secondary alcohols with subtilisin Carlsberg,⁷ the productive conformation of the (*R*)-**2a** binds with the methyl group in the leaving-group S₁' pocket and the productive conformation of the (*S*)-**2a** has the phenyl group in this pocket.

Productive conformer of (*R*)-2a (Figure A5.1). The acetylene group forms the *syn*-pentane-like interaction with the oxyanion. (*S*)-**2a** fit well in the active site and S₁' residues did not hinder the methyl group.

Non-productive conformer of (*R*)-2a (not shown). The methyl group forms the *syn*-pentane-like interaction with the oxyanion. The phenyl group of non-productive (*R*)-**2a** encountered steric clash with Met222 (C_{ortho} - S distance = 3.62 Å, C_{meta} - S distance = 3.88 Å and C_{meta} - C_ε distance = 3.78 Å).⁸

Non-productive conformer of (*R*)-2a (not shown). The phenyl group forms the *syn*-pentane-like interaction with the oxyanion. The phenyl group of non-productive (*R*)-**2a** encountered steric clash with oxyanion hole Asn155 (C_{ortho} - N_{δ2} distance = 3.29 Å, C_{ortho} - C_γ distance = 3.39 Å, C_{meta} - N_{δ2} distance = 3.73 Å, C_{meta} - C_γ distance = 3.40 Å) and G219 (C_{meta} - C_α distance = 3.69 Å).⁸

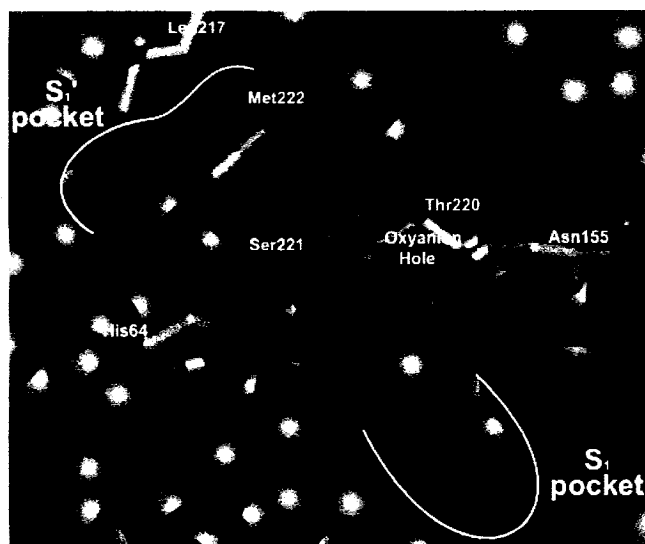
Productive conformer of (*S*)-2a (Figure A5.1). The acetylene group forms the *syn*-pentane-like interaction with the oxyanion. (*R*)-**2a** fit well in the active site, but the

phenyl group bumped Met222 ($C_{\text{meta}} - C_{\epsilon}$ distance = 3.98 Å) and His64 ($C_{\text{meta}} - C_{\delta 2}$ distance = 3.72 Å) in the S_1' pocket.⁸ This tight fit suggests a favourable hydrophobic interaction – tendency of nonpolar compounds to transfer from an aqueous phase to an organic phase – between the phenyl group and S_1' pocket residues.⁹ Consistent with this hypothesis, higher concentrations of organic co-solvent decreased this hydrophobic interaction and increased the enantioselectivity of subtilisin Carlsberg toward (*R*)-**2a**.

Non-productive Conformer of (*S*)-2a** (not shown).** The methyl group forms the *syn*-pentane-like interaction with the oxyanion. The phenyl group of non-productive (*S*)-**2a** encountered steric clash with catalytic His64 ($C_{\text{ortho}} - N_{\delta 2}$ distance = 3.64) and the methyl group bumped oxyanion hole Asn155 ($\text{CH}_3 - N_{\delta 2}$ distance = 3.74 Å).⁸

Non-productive Conformer of (*S*)-2a** (not shown).** The phenyl group forms the *syn*-pentane-like interaction with the oxyanion. The phenyl group of non-productive (*S*)-**2a** encountered steric clash with oxyanion hole Asn155 ($C_{\text{ortho}} - N_{\delta 2}$ distance = 3.38 and $C_{\text{meta}} - N_{\delta 2}$ distance = 3.45 Å and $C_{\text{para}} - N_{\delta 2}$ distance = 3.51 Å, $C_{\text{para}} - C_{\gamma}$ distance = 3.42 Å) and Gly219 ($C_{\text{ortho}} - C_{\alpha}$ distance = 3.53 and $C_{\text{meta}} - C_{\alpha}$ distance = 3.63 Å).⁸

I



II

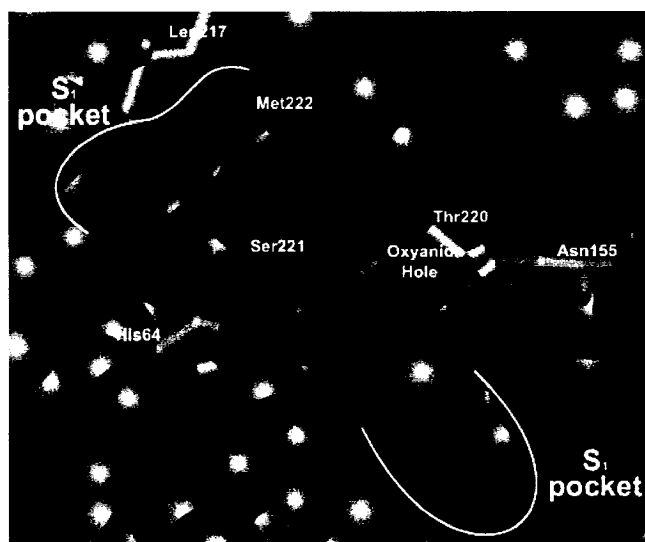


Figure A5.1. Catalytically competent orientation of the tetrahedral intermediates for the subtilisin Carlsberg catalyzed hydrolysis of (*R*)-**2a** (I) and (*S*)-**2a** (II) as identified by molecular modelling. The important active site and substrate atoms are shown as sticks. The atoms are coloured as follows: green (substrate carbon and Ser221), grey (enzyme carbon), red (oxygen), blue (nitrogen) and orange (sulfur). Surrounding atoms (space fill) of subtilisin are shown in the colour blue. For clarity, all hydrogen atoms and water molecules are hidden. The binding modes of I and II maintain all catalytically essential hydrogen bonds and the benzyl moiety of the dihydrocinnamoyl group was bound in the S_1

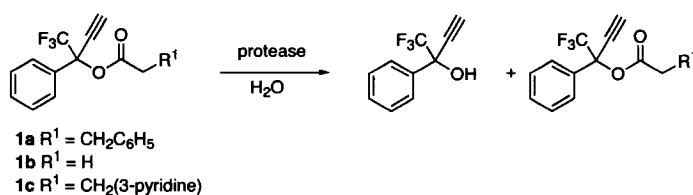
pocket, as expected based on its similarity to phenylalanine. On the basis of previous work with secondary alcohols, the phenyl group (Large) or methyl group (Medium) was bound in the leaving-group S_1' pocket.⁷ The acetylene occupied the same site as hydrogen of a secondary alcohol, based on molecular mechanics calculations and lower reactivity toward substrates **7a**, **8a** and **9a**. In the fast-reacting enantiomer, (*R*)-**2a** (I), the methyl group is bound in the hydrophobic S_1' pocket and the phenyl group is exposed to solvent water. In the slow-reacting enantiomer, (*S*)-**2a** (II), the phenyl group is bound in the hydrophobic S_1' pocket and the methyl group is exposed to solvent water. The non-productive conformations (not shown) lost catalytically essential hydrogen bonds and/or encountered severe steric clash with the active site residues of the protein.

Table A5.1. Minimized structures for tetrahedral intermediates of subtilisin Carlsberg-catalyzed hydrolysis of **2a**

Conformation	Group in S_1' ^a	Group syn-pentane-like to oxyanion	H-bond $N_{\alpha 2}-O_{alc}$ distance (Å) (N-H-O _γ angle, deg) ^b	Comments
(<i>R</i>)- 2a (Figure A5.1)	methyl	acetylene	3.03 (150)	Unhindered in S_1' pocket
(<i>R</i>)- 2a (not shown)	phenyl	methyl	2.98 (153)	Steric clash between phenyl and Met222
(<i>R</i>)- 2a (not shown)	acetylene	phenyl	3.21 (155)	Steric clash between phenyl and Asn155 and Gly219
(<i>S</i>)- 2a (Figure A5.1)	phenyl	acetylene	3.07 (156)	Steric contact between phenyl and Met222 and His64
(<i>S</i>)- 2a (not shown)	acetylene	methyl	2.86 (130)	Steric clash between phenyl and His64
(<i>S</i>)- 2a (not shown)	methyl	phenyl	3.02 (153)	Steric clash between phenyl and Asn155

^aNarrow, hydrophobic pocket where one substituent of leaving-group tertiary alcohol can bind. ^bUnless otherwise noted, hydrogen bonds ($His64N_{\alpha 2} - O$, $S221NH - O^-$, and $Asn155 NH_2 - O^-$) were present in all structures (N - O distance 2.7 – 3.1 Å, N-H-O angle 120–175°).

Table A5.2. Reactivity and enantioselectivity of proteases toward 1,1,1-trifluoro-2-phenyl-but-3-yn-2-ol esters **1a**, **1b** and **1c**



	1a		1b		1c	
Protease	%c^a	E^b (E_{pref})^c	%c	E (E_{pref})	%c	E (E_{pref})
<i>Aspergillus melleus</i> protease	3	2.0 (R)	38	14 (R)	n.p. ^d	n.p.
<i>Aspergillus oryzae</i> protease	n.r. ^e	n.r.	15	6.4 (R)	n.p.	n.p.
Subtilisin BL	15	1.5 (R)	46	2.7 (R)	n.p.	n.p.
Subtilisin Carlsberg	8	1.3 (S)	84	2.5 (R)	31	1.1 (S)
α-Chymotrypsin	51	1.9 (S)	<1	n.d.	63	1.1 (S)
<i>Streptomyces griseus</i> protease	7	2.4 (S)	14	2.4 (R)	26	1.3 (S)

^aConversion: reaction for 48 h. ^bEnantioselectivity: the enantiomeric ratio *E* measures the relative rate of hydrolysis of the fast enantiomer as compared to the slow enantiomer as defined by Sih (Chen, C. S.; Fujimoto, Y.; Girdaukas, G.; Sih, C. J. *J. Am. Chem. Soc.* **1982**, *104*, 7294-7299). The enantioselectivity was determined using the enantiomeric excess of substrate and product, which were determined by GC analysis on 25 m x 0.25 mm Chrompack CP-Chiralsil-Dex CB column (Varian Inc., Palo Alto, CA, USA) using He as a carrier gas. ^cEnantiopreference. The absolute configuration was determined by *Candida cylindracea* (*rugosa*) lipase (CRL)-catalyzed hydrolysis of **1b**, which has previously been shown to give (*R*)-**1** by O'Hagan (O'Hagan, D.; Zaidi, N. A. *Tetrahedron: Asymmetry* **1994**, *5*, 1111-1118.). ^dNot performed. ^eNo reaction.

Table A5.3. Enantioselectivity of subtilisin Carlsberg and α -chymotrypsin catalyzed hydrolysis of **2a-9a**

$R^1 = \text{CH}_2\text{C}_6\text{H}_5$

$R^1 = \text{CH}_2\text{C}_6\text{H}_5$	Subtilisin Carlsberg					α -Chymotrypsin				
	%c ^a	ee _s (%) ^b	ee _p (%) ^b	E ^c	E _{pref} ^d	%c ^a	ee _s (%) ^b	ee _p (%) ^b	E ^c	E _{pref} ^d
1a	27	4	11	1.3	S ^e	51	23	22	1.9	S ^e
2a	22	12	42	2.8	R ^f	94	61	4	1.6	R ^f
3a	27	3 ^g	8	1.2 ^h	n.d. ⁱ	32	1 ^g	3	1.1	n.d.
4a	27	2 ^g	4	1.1	n.d.	22	10 ^g	37	2.4	n.d.
5a	63	3 ^g	5	1.1	n.d.	68	14 ^g	30	1.7	n.d.
6a	20	5 ^g	20	1.6	n.d.	25	22 ^g	65	5.8	n.d.
7a	~5	n.d. ^j	n.d. ^k	n.d.	n.d.	~25	n.d. ^j	n.d. ^k	n.d.	n.d.
8a	1	1 ^g	64	4.6 ^l	n.d.	1	1	50	3.0 ^l	n.d.
9a	n.r. ^m	n.r.	n.r.	n.r.	n.r.	n.r.	n.r.	n.r.	n.r.	n.r.

^aConversion: reaction for 48 h. ^bEnantiomeric excess: enantiomeric excess of substrate and product were determined by GC analysis on 25 m x 0.25 mm Chrompack CP-Chiralsil-Dex CB column (Varian Inc., Palo Alto, CA, USA) using He as a carrier gas.

^cEnantioselectivity: the enantiomeric ratio *E* measures the relative rate of hydrolysis of the fast enantiomer as compared to the slow enantiomer as defined by Sih (Chen, C. S.; Fujimoto, Y.; Girdaukas, G.; Sih, C. J. *J. Am. Chem. Soc.* **1982**, *104*, 7294-7299). ^dEnantiopreference. ^eThe absolute configuration was determined by *Candida cylindracea* (*rugosa*) (CRL)-catalyzed hydrolysis of **1b**, which has previously been shown to give (*R*)-**1** by O'Hagan (O'Hagan, D.; Zaidi, N. A. *Tetrahedron: Asymmetry* **1994**, *5*, 1111-1118.). ^fThe absolute configuration was determined by *Candida antarctica* lipase A (CALA)-catalyzed acylation of **2** with vinyl acetate, which has previously been shown to proceed with *R*-selectivity by Bornscheuer (Krishna, S. H.; Persson, M.; Bornscheuer, U. T. *Tetrahedron: Asymmetry* **2002**, *13*, 2693-2696). ^gSubstrates **3a-9a** could not be separated by GC. To facilitate analysis, the ester was purified on silica gel (100% hexanes to 90:10 hexanes/EtOAc) and hydrolyzed in 1 N KOH (1:1 EtOH/H₂O) to the corresponding alcohol for GC analysis. ^hComplicated by ca. 1% chemical hydrolysis. ⁱNot determined. ^jThe enantiomers could not be separated by GC or HPLC. ^kWe could not detect the product allylic alcohol as it readily decomposed in aqueous solutions. However, we observed loss of substrate in the presence of enzyme. ^lThe enantioselectivity may be inaccurate because of low conversion. ^mNo reaction.

References (Chapter 5 – Appendix)

- ¹ O'Hagan, D.; Zaidi, N. A. *Tetrahedron: Asymmetry* **1994**, *5*, 1111-1118.
- ² Hatano, M.; Matsumura, T.; Ishihara, K. *Org. Lett.* **2005**, *7*, 573-574.
- ³ O'Hagan, D.; Zaidi, N. A. *J. Chem. Soc., Perkin Trans. 1* **1992**, 947-949.
- ⁴ (a) Weiner, S. J.; Kollman, P. A.; Case, D. A.; Singh, U. C.; Ghio, C.; Alagona, G.; Profeta, S.; Weiner, P. *J. Am. Chem. Soc.* **1984**, *106*, 765-784. (b) Weiner, S. J.; Kollman, P. A.; Nguyen, D. T.; Case, D. A. *J. Comp. Chem.* **1986**, *7*, 230-252.
- ⁵ Bode, W.; Papamokos, E.; Musil, D. *Eur. J. Biochem.* **1987**, *166*, 673-682.
- ⁶ Raza, S.; Fransson, L.; Hult, K. *Protein Sci.* **2001**, *10*, 329-338.
- ⁷ Fitzpatrick, P. A.; Ringe, D.; Klibanov, A. M. *Biotechnol. Bioeng.* **1992**, *40*, 735-742.
- ⁸ The van der Waals distance for CH-C = 3.99 Å, CH-N = 3.84 Å, CH-S = 4.09 Å. These were estimated from the van der Waals radii of carbon (1.70 Å), nitrogen (1.55 Å), sulfur (1.80 Å).

(1.80 Å) or oxygen (1.52 Å) and hydrogen (1.20 Å) and the C-H bond length (1.09 Å) from Bondi, A. *J. Phys. Chem.* **1964**, *68*, 441-451.

⁹ The energy of a hydrophobic interaction is from the regaining of entropy by water after it is removed from a hydrophobic group and can be estimated using the incremental Gibbs free energy of transfer. The incremental Gibbs free energy of transfer of the phenyl group from *n*-octanol to water was estimated to be ca. +2.9 kcal/mol, using $\Delta G_{trans} = 2.303RT\pi$, where π is the hydrophobicity constant of the phenyl group ($\pi = 2.1$, using *ClogP* (BioByte, Claremont, USA)) relative to hydrogen, whereas the methyl group was ca. +1.5 kcal/mol. Switching from (*R*)-**2a** to (*S*)-**2a** places the phenyl group into the hydrophobic S₁' leaving-group pocket and removes the methyl group for a total of ca. 1.4 kcal/mol in favour of placing the phenyl group in the hydrophobic leaving-group pocket when in an aqueous medium. The energy difference may be higher if one includes the hydrophobic surface of the leaving-group pocket. For details, see: (a) Fersht, A. *Structure and Mechanism in Protein Science*; W.H. Freeman and Company: New York, 1998; pp 324-348. (b) Leo, A.; Hansch, C.; Elkins, D. *Chem. Rev.* **1971**, *71*, 525-616.

Chapter 6

In this chapter, we apply our anchor group strategy in reverse. That is, instead of tuning substrate to increase the hydrolase-catalyzed reaction rate, we alter the chromogenic reference compound structure to slow its reaction. We show Quick E using our new chromogenic reference compounds can measure high enantioselectivities and simplify screening.

New chromogenic reference compounds for Quick E

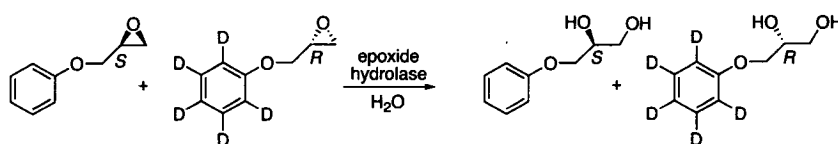
Abstract

Modern molecular biology methods such as directed evolution have boosted the number of enzyme libraries. Consequently, methods are required for their rapid and reliable characterization. Quick E is a technique previously developed in our lab for high-throughput screening of hydrolase enantioselectivity. This colourimetric method measures the reaction rate of enantiopure esters by pH-indicator in the presence of a chromogenic reference compound. The reference compound is present to account for competitive binding by the antipode and allows for quantitative determination of enantioselectivity. However, Quick E cannot measure high enantioselectivities because it is difficult to measure slow-reacting enantiomer hydrolysis before the reference compound hydrolyzes. We tune the chromogenic reference compound structure to slow its reaction and increase its solubility in aqueous solutions. We show resorufin 11-sulfoundecanoate is soluble under our conditions and reacts twenty to two-hundred-fold slower with four lipases versus our standard reference compound, resorufin acetate. We also show resorufin 3-(3-pyridyl)propionate reacts twelve-fold and twenty-fold slower with a lipase and an esterase, respectively. We then use these reference compounds to measure Quick E of six different hydrolases and compare them to the true *E* determined via the endpoint method. In all cases, the Quick E value using our new chromogenic reference compounds was closer to the true *E* value than the Quick E value using resorufin acetate.

6.1 Introduction

Currently, the best method to measure enantioselectivity E is the endpoint method developed by Sih and coworkers.¹ To measure E , researchers run a small-scale resolution, work-up the reaction and measure the conversion and enantiomeric purity of the substrate or product. This strategy is time-consuming and is not practical for screening hundreds of enzymes.

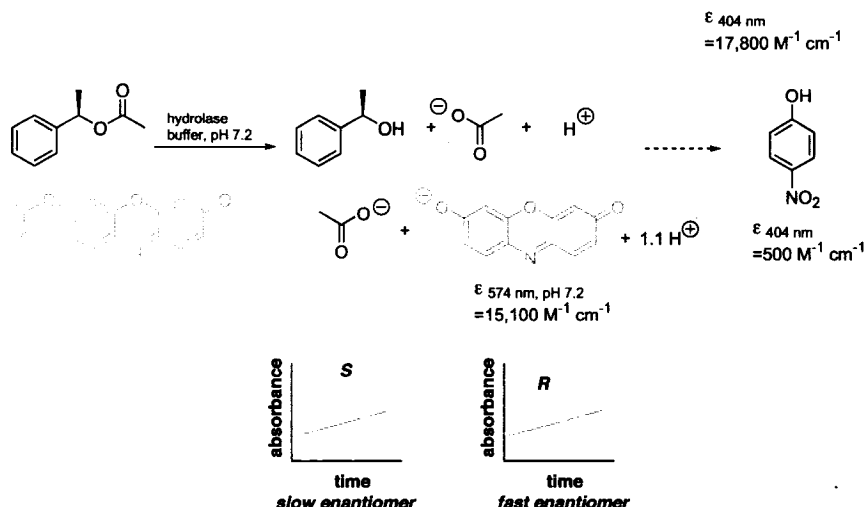
Several high-throughput assays exist for rapid determination of enantioselectivity.^{2,3} For example, Reetz and coworkers⁴ developed a MS-based high-throughput screening system for enzyme enantioselectivity using deuterated pseudo-enantiomers (Scheme 6.1). The different mass-to-charge ratio allows quantitative determination of their respective signals via MS and thus, the pseudo-enantiomeric excess. This system can screen up to 10,000 mutants per day. The draw back, however, is that this system requires enantio-pure non-deuterated and deuterated substrates and specialized equipment.



Scheme 6.1. Enzymatic hydrolysis of the pseudo-enantiomers (S)-glycidyl phenyl ether and (R)- d_5 -glycidyl phenyl ether. The substrates are chemically similar, but their masses differ. MS is used to determine enantioselectivity, where the two different pseudo-enantiomer signals yield the pseudo-enantiomeric excess.

Janes and Kazlauskas^{5,6} developed a fast colourimetric method called Quick E to measure enantioselectivity. This colourimetric method measures the reaction rate of enantiopure esters by pH-indicator in the presence of a chromogenic reference compound (Scheme 6.2). The reference compound is present to account for competitive binding by the antipode and allows for quantitative determination of enantioselectivity. To understand the importance of competitive binding in enzyme selectivity, imagine a hypothetical case where both substrates have the same k_{cat} values, but different K_M values. In a competitive experiment, the enzyme will bind and transform the better binding substrate. However, if the hydrolysis of the two substrates occurs in separate vessels, the result depends

on the substrate concentration. At saturating amounts of substrate, both reactions will proceed at the same rate and the measured selectivity will incorrectly indicate that the reaction is nonselective. At substrate concentrations well below K_M , the estimated selectivity will be close to the true selectivity. In the first case, however, one requires a competitive experiment to measure the true enantioselectivity. The chromogenic reference compound adds competition to the reaction.



Scheme 6.2. The Quick E screening method for rapid determination of hydrolase enantioselectivity. Hydrolysis of substrate (1-phenethyl acetate) and reference compound (resorufin acetate) releases acid that protonates the pH-indicator (*p*-nitrophenoxide) and decreases its absorbance at 404 nm. Hydrolysis of resorufin acetate yields resorufin anion, a pink chromophore that absorbs at 574 nm. The increase in resorufin anion absorbance at 574 nm and the decrease in absorbance at 404 nm for the pH indicator are measured simultaneously.

In a typical Quick E experiment we measure hydrolysis of an individual enantiomer (true substrate) by using a pH-indicator and a chromogenic reference compound by formation of chromophore whose colour is different than the pH-indicator. For example, hydrolase-catalyzed hydrolysis of an enantiomeric ester releases protons, which protonate *p*-nitrophenol (pH-indicator) and decrease its absorbance at 404 nm. Hydrolysis of the resorufin acetate (chromogenic reference compound) is simultaneously detected by meas-

uring the release of resorufin anion, a pink chromophore that absorbs at 574 nm (Scheme 6.2). Such an experiment yields the correct selectivity for true substrate one and the reference compound, eq. 6.1.

$$\frac{\text{substrate 1}}{\text{reference}} \text{selectivity} = \frac{\text{rate of substrate 1 reaction}}{\text{rate of reference reaction}} \cdot \frac{[\text{reference}]}{[\text{substrate 1}]} \quad \text{eq. 6.1}$$

In a second experiment, the other enantiomer (true substrate two) competes against the same reference compound to yield the correct selectivity for true substrate two and the reference compound, eq. 6.2.

$$\frac{\text{substrate 2}}{\text{reference}} \text{selectivity} = \frac{\text{rate of substrate 2 reaction}}{\text{rate of reference reaction}} \cdot \frac{[\text{reference}]}{[\text{substrate 2}]} \quad \text{eq. 6.2}$$

Finally, dividing these two selectivities yields the desired selectivity of substrate one vs. substrate two, eq. 6.3.

$$\frac{\text{substrate 1}}{\text{substrate 2}} \text{selectivity} = \frac{\frac{\text{substrate 1}}{\text{reference}} \text{selectivity}}{\frac{\text{substrate 2}}{\text{reference}} \text{selectivity}} \quad \text{eq. 6.3}$$

Quick selectivity methods (Quick E for enantioselectivity, Quick D for diastereoselectivity, Quick S for substrate selectivity) are defined as all methods that, instead of letting the substrates compete directly against one another, do so indirectly by competing each substrate against a reference compound.

The main advantage of Quick E over other methods is its speed. Traditional methods involve chromatographic analysis of product and substrate by chiral HPLC or GC columns; analysis of one reaction can often take an hour or more. With Quick E, 96 reactions can be monitored simultaneously using a microplate reader.

A disadvantage of Quick E is that it requires pure enantiomers, albeit in small amounts. Often, small amounts are available from preparative HPLC with chiral stationary phases or other methods. Another disadvantage is that it is often difficult to determine high enantioselectivity values because the slow-reacting enantiomer reacts much slower than the reference compound. Once the reference compound is completely hydrolyzed, there is no competitive binding between the two substrates. If the K_M values of the enanti-

omers are different, the Quick E will underestimate the enzyme enantioselectivity. Practically, however, the researcher will discontinue data collection and repeat the experiment using a higher concentration of substrate and/or enzyme. Often, one cannot measure the Quick E of highly enantioselective enzymes because the disfavoured enantiomer reacts much slower than the reference compound. In this chapter, we apply our structure-based substrate design in reverse. That is, instead of tuning substrate to improve reaction rate, we alter the reference compound structure to slow its reaction. In addition, we increase its solubility in aqueous solutions – colourimetric assays require clear solutions – to reduce the concentration of detergent and/or organic co-solvent. We show that our new chromogenic reference compounds allow measurement of higher enantioselectivities (e.g., $E = >200$) than previously.

6.2 Results and discussion

Choice of reference compound is important for Quick E screening. Since this system relies on competitive binding by a chromogenic reference compound, the reference compound should be present throughout the course of substrate reaction. Thus, reference compound and substrate should have comparable reaction rates. Often, substrate hydrolysis cannot be measured before the chromogenic reference compound hydrolyzes. This is an especially important issue when the enzyme enantioselectivity is high (e.g., $E > 100$), because the slow-reacting enantiomer hydrolyzes much slower than reference compound. For this reason, different reference compounds are needed for different hydrolase-substrate combinations. We sought to design new reference compounds that would react slowly with a variety of hydrolases so we could measure the initial rate of the slow-reacting enantiomers by adding more enzyme or extending reaction time.

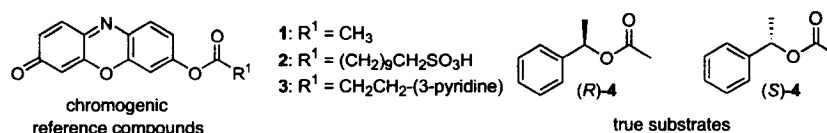


Figure 6.1. Structures of achiral chromogenic reference compounds 1-3 and enantiomeric substrates (R)-4 and (S)-4.

The typical chromogenic reference compound resorufin acetate **1** reacts quickly with many hydrolases (Figure 6.1). Sterically hindered acyl groups such as pivaloate and isobutyrate react slower, but are poorly soluble in aqueous solutions. Sulfoundecanoate esters are more hindered than acetate and are water-soluble. The sulfoundecanoyl group has been previously used to solubilize nonpolar prodrugs such as corticosteroids.⁷ Polar, water-soluble substrates often react slowly with lipases (see Introduction 1.6) and thus, may be ideal reference compounds for screening lipase enantioselectivity. We prepared 11-sulfoundecanoic acid by treating 11-bromoundecanoic acid with sodium sulfite in 0.5 N NaOH. Treating resorufin sodium salt and 11-sulfoundecanoic acid with *N*-(3-dimethylaminopropyl)-*N'*-ethylcarbodiimide (EDC) gave resorufin sulfoundecanoate **2** in 25% yield.

Resorufin 11-sulfoundecanoate **2** was soluble under our conditions and reacted slowly with most lipases, hydrolases that prefer nonpolar substrates,⁸ as compared to resorufin acetate **1** (Table 6.1). Resorufin 11-sulfoundecanoate **2** reacted one-hundred-ninety-eight-fold slower with *Pseudomonas cepacia* lipase (PCL), ninety-four-fold slower with *Rhizopus oryzae* lipase (ROL), eighty-eight-fold slower with *Alcaligenes species* lipase (ASL) and twenty-two-fold slower with *Candida rugosa* lipase (CRL), as compared to resorufin acetate **1**. It was only two-fold slower with *Pseudomonas fluorescens* esterase (PFE) and *Aspergillus oryzae* protease (AOP), but four-fold faster with subtilisin Carlsberg and nine-fold faster with *Candida antarctica* lipase B (CALB). The high reactivity of subtilisin Carlsberg toward **2** is not surprising, given its preference for water-soluble substrates.⁸ CALB, unlike other lipases, reacts quickly with soluble substrates.⁹

Given the high reactivity of CALB and PFE toward reference compounds **1** and **2**, we also investigated resorufin esters containing aryl groups – both CALB and PFE prefer short-chain linear acyl groups such as acetate or butyrate.^{8,10} In chapter 4, we showed the 3-(3-pyridyl)propionyl group increased the water solubility of ester substrates. Thus, we synthesized resorufin 3-(3-pyridyl)propionate **3** in 33% yield by treating resorufin sodium salt and 3-(3-pyridyl)propionic acid with EDC.

Resorufin 3-(3-pyridyl)propionate **3** was soluble under our reaction conditions and reacted twelve-fold slower with CALB and twenty-one-fold slower with PFE, as compared to resorufin acetate **1**. AOP showed similar activity toward **3** as compared to **1**.

Subtilisin Carlsberg showed four-fold higher activity toward **3** as compared to **1**. Subtilisin usually shows higher activity toward water-soluble substrates with large acyl groups.¹¹ Thus, the slowest reacting reference compound for subtilisin Carlsberg is **1** because of its small acyl group. The bold lettering in Table 6.1 indicates the slowest reacting reference compound for that hydrolase.

Table 6.1. Specific activity of hydrolases toward different reference compounds

Hydrolase	Weight ^a (protein) ^b	Specific Activity ($\mu\text{mol}/\text{min}/\text{mg}$) ^c		
		1	2	3
<i>Pseudomonas cepacia</i> lipase ^d (PCL)	1.11 (0.10)	12.1	0.06	2.06
<i>Candida antarctica</i> lipase B ^d (CALB)	1.16 (0.21)	2.57	19.96	0.22
<i>Rhizopus oryzae</i> lipase ^d (ROL)	1.16 (0.07)	13.52	0.14	17.50
porcine pancreatic lipase ^d (PPL)	1.40 (0.10)	0.06	0.30	1.18
<i>Alcaligenes species</i> lipase ^d (ASL)	1.12 (0.07)	8.79	0.09	0.86
<i>Candida rugosa</i> lipase ^d (CRL)	0.97 (0.07)	4.02	0.18	1.18
<i>Pseudomonas fluorescens</i> esterase ^e (PFE)	0.84 (0.45)	0.57	0.26	0.03
<i>Aspergillus oryzae</i> protease ^d (AOP)	1.02 (0.23)	1.79	0.73	2.26
subtilisin Carlsberg ^f	0.93 (0.40)	4.29	17.24	19.41

^a Amount (mg) of solid enzyme per mL of buffer in the stock solutions used for initial rate measurements. ^b Protein concentration of stock solutions in mg/mL determined by the Bio-Rad assay using BSA as the standard. ^c Final concentration in the microplate wells during assay: 0.05 mM reference compound **1**, **2** or **3**, 8.4% MeCN, 0.79 mM 4-nitrophenol, 4.58 mM BES buffer, pH 7.2. Rates of hydrolysis are reported in $\mu\text{mol}/\text{min}/\text{mg}$ protein and are calculated using the Beer-Lambert Law with $\epsilon = 15,100 \text{ M}^{-1}\text{cm}^{-1}$, $l = 1 \text{ cm}$. ^d Altus Biologics (Cambridge, USA). ^e see ref.¹². ^f Sigma-Aldrich (St. Louis, USA).

These slower reacting reference compounds should be useful for measuring the enantioselectivity of slow-reacting substrates. To validate this modification, we determined the Quick E of six hydrolases that show varying reactivity and enantioselectivity toward 1-phenethyl acetate **4**. We measured the quick E of these hydrolases toward **4** using reference compounds **1** - **3** and compared these values to the endpoint *E*.

Table 6.2. Enantioselectivity of hydrolases toward 1-phenethyl acetate **4** using Quick E with reference compound **1**, **2** or **3**

Hydrolase	Quick E ^a (time (s)) ^b			<i>E</i> end-point ^{c,d} (enantiopreference)
	1	2	3	
<i>Pseudomonas cepacia</i> lipase (PCL)	>5.0 (10-100)	250±16 (100-1500)	n.p.	>200 (<i>R</i>)
<i>Candida antarctica</i> lipase B (CALB)	>25 (10-100)	n.p. ^f	613±38 (100-1000)	>200 (<i>R</i>)
<i>Rhizopus oryzae</i> lipase (ROL)	n.d. ^e	37±5 (10-1500)	n.p.	38 (<i>S</i>)
<i>Alcaligenes species</i> lipase (ASL)	n.d.	99±12 (100-2000)	n.p.	94 (<i>R</i>)
<i>Candida rugosa</i> lipase (CRL)	6.6±1.9 (50-300)	2.8±0.3 (10-1000)	n.p.	1.2 (<i>R</i>)
<i>Pseudomonas fluorescens</i> esterase (PFE)	>6.0 (100-3000)	n.p.	>30±1 (10-1000)	126 (<i>R</i>)

^aFinal concentration in the microplate wells during assay: 0.05 mM resorufin acetate, 0.61 mM or 12.52 mM (*R*)- or (*S*)- 1-phenethyl acetate **5**, 8.4% MeCN, 0.79 mM 4-nitrophenol, 4.58 mM BES buffer, pH 7.2. Changes in absorbance at 404 nm and 574 nm were monitored simultaneously. Rates were calculated in $\mu\text{mol}/\text{min}/\text{mg}$ protein taking into account the amounts of protein in each well as determined by the Bio-Rad assay using BSA as a standard. Reported error is the standard deviation of four measurements.

^bData collection time. ^cEndpoint values were determined using the identical conditions as in the microplate wells during screening but with no pH indicator: Janes, L. E; Löwen-dahl, A. C.; Kazlauskas, R. J. *Chem. Eur. J.* **1998**, *4*, 2317-2324. ^dEnantiomeric ratio calculated from ee_s and ee_p as defined by Chen, C. S.; Fujimoto, Y.; Girdaukas, G.; Sih, C. J. *J. Am. Chem. Soc.* **1982**, *104*, 7294-7299. ^enot determined. ^fnot performed.

We measured the Quick E of four lipases toward **4** using resorufin acetate **1** or resorufin 11-sulfoundecanoate **2** as reference compound (Table 6.2). We could measure high enantioselectivities with resorufin 11-sulfoundecanoate **2**, but not with resorufin acetate **1**. In cases where both reference compounds yielded enantioselectivities, the Quick E using **2** was closer to the true E than Quick E using **1**. The Quick E of PCL toward **4** using **1** (Quick E = >5.0) as reference compound was at least forty-fold lower than the end-point E ($E = >200$). However, the Quick E using **2** (Quick E = 250 ± 16) as reference compound agreed well with the endpoint E . The Quick E of ROL and ASL toward **4** using **2** as reference compound (Quick E = 37 ± 5 and 99 ± 12 , respectively) also agreed with the end point E ($E = 38$ and 94 , respectively). We did not determine the Quick E of ROL and ASL toward **4** using **1** as reference compound because the slow-reacting enantiomer showed no reaction before resorufin acetate **1** hydrolyzed (ca. 60 sec.). The Quick E of CRL toward **4** using **2** as reference compound (Quick E = 2.8 ± 0.3) was two-fold higher than the end point E ($E = 1.2$), but was closer than the Quick E using **1** (Quick E = 6.6 ± 1.9) as reference compound.

We measured the Quick E of CALB and PFE toward **4** using resorufin acetate **1** or resorufin 3-(3-pyridyl)propionate **3** as reference compound. In both cases, the Quick E using **3** was closer to the true E than Quick E using **1**. The Quick E of CALB lipase toward **4** using **1** (Quick E = 25) as reference compound was at least eight-fold lower than the end-point E ($E = >200$). However, using **3** as reference compound, one could easily measure this high enantioselectivity (Quick E = 613 ± 38). The Quick E of PFE using **3** (Quick E = 31 ± 1) as reference compound was four-fold lower than the end point E ($E = 126$), but was closer than the Quick E using **1** (Quick E = >6) as reference compound.

Using slower-reacting, water-soluble reference compounds has three advantages. First, you can measure high enantioselectivities because you can add more enzyme or extend measurement time and measure the reaction rate of slow reacting substrates. Second, you can avoid the use of detergents and organic co-solvents that can alter the enantioselectivity. Last, fewer manipulations are required. Using a slower-reacting reference compound avoids having to alter substrate or enzyme concentrations to increase reaction rate, as one can simply allow the reaction to proceed for a longer period of time.

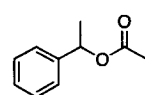
Measuring high enantioselectivity is challenging for both the true E methods and the Quick E methods. For true-E methods, measuring high enantioselectivity requires detecting the slow-reacting enantiomer accurately. For Quick-E methods, measuring high enantioselectivity requires measuring the rate of reaction of the slow-reacting enantiomer and chromogenic reference compound. We designed new reference compounds that react slowly with a variety of hydrolases. Using these new reference compounds, we can now measure reaction rate of slow-reacting enantiomers in the presence of reference compound by adding more enzyme or extending reaction time. Thus, we can now measure high enantioselectivities using Quick E.

6.3 Experimental Section

6.3.1 General

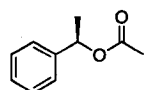
^1H - and ^{13}C -NMR spectra were obtained as CDCl_3 solutions at 300 MHz and 75 MHz, respectively. Chemical shifts are expressed in ppm (δ) and are referenced to tetramethylsilane or solvent signal. Coupling constants are reported in Hertz (Hz). GC analyses were performed on a 25 m x 0.25 mm Chrompack CP-Chiralsil-Dex CB column (Varian Inc., Palo Alto, USA) with He as carrier gas using the following temperature programs: 17.5 psi, 100 °C, held for 15 min, 25 °C min^{-1} ; 200 °C held for 21 min. Subtilisin Carlsberg was purchased from Sigma-Aldrich (St. Louis, USA). Altus Biologics (Cambridge, USA) provided other hydrolases. All reagents, buffers, starting materials and anhydrous solvents were purchased from Sigma-Aldrich (Milwaukee, USA) and used without purification. All air- and moisture-sensitive reactions were performed under Ar.

6.3.2 Synthesis of substrates

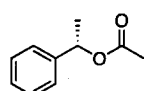


1-Phenethyl acetate, 4. A solution of acetyl chloride (7.85 g, 100 mmol) in CH_2Cl_2 (20 mL) was added drop-wise to a stirred solution of 1-phenethyl alcohol (6.10 g, 50 mmol) and pyridine (4 mL, 50 mmol) in CH_2Cl_2 (75 mL) at 0 °C. The ice bath was removed and the solution was stirred overnight at RT. The reaction was quenched with the addition of sat. NaHCO_3 (75 mL). The layers were separated and the aqueous layer was extracted with CH_2Cl_2 (2 x 50 mL). The combined organic layers were washed with 1 N HCl (2 x 50 mL), sat. NaHCO_3 (2 x 50 mL) and dried over

MgSO₄. The organic layer was concentrated *in vacuo* to give the crude ester. Purification on silica gel (95:5 hexanes/EtOAc) gave the title compound as a clear liquid (5.73 g, 35 mmol, 70%): ¹H NMR δ 1.55 (d, *J* = 6.6, 3H, CH₃), 2.09 (m, 3H, C(O)CH₃), 5.90 (q, *J* = 6.6, 1H, CH), 7.36-7.38 (m, 5H, phenyl); ¹³C NMR δ 21.4 (CH₃), 22.3 (CH₃), 72.4 (CH), 126.2, 128.0, 128.6, 141.8 (phenyl), 170.4 (C=O). The enantiomers were separated using GC ((*S*)-4, *t*_R = 9.7 min; (*R*)-4, *t*_R = 11.9 min).

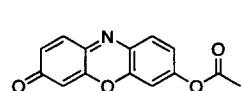


(*R*)-1-Phenethyl acetate, (*R*)-4. The procedure was similar to the racemic acetate. Purification on silica gel (95:5 hexanes/EtOAc) gave the title compound as a clear liquid (463 mg, 69%, 99.8% ee).

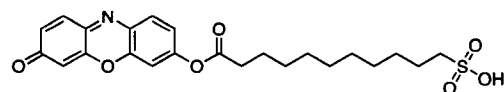


(*S*)-1-Phenethyl acetate, (*S*)-4. The procedure was similar to the racemic acetate. Purification on silica gel (95:5 hexanes/EtOAc) gave the title compound as a clear liquid (431 mg, 64%, 99.9% ee).

6.3.3 Synthesis of reference compounds

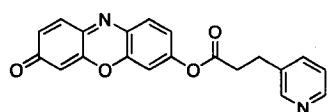


Resorufin acetate, 1.¹³ Acetyl chloride (0.6 mL, 8.6 mmol) was added drop-wise to a slurry of resorufin sodium salt (1.02 g, 4.3 mmol) in anhydrous CH₂Cl₂ (60 mL) and pyridine (0.4 mL, 4.3 mmol) over 10 min at 0 °C. The reaction was warmed to RT and stirred overnight. The reaction was diluted with CH₂Cl₂ (300 mL) and filtered to remove unreacted resorufin. The solvent was removed *in vacuo* and the residue was purified on silica gel (98:2 CHCl₃/MeOH) to give the title compound as an orange solid (0.48 g, 44% yield): mp = 217 – 220 °C (decomp.) (lit.¹³ = 223-225 °C); ¹H-NMR δ 2.37 (s, 3H), 6.34 (d, *J* = 1.8, 1H), 6.84-6.90 (dd, *J* = 2.1, 9.9, 1 H), 7.11-7.16 (dd, *J* = 2.2, 7.3, 1H), 7.16 (s, 1H), 7.44 (d, *J* = 9.7, 1H), 7.81 (d, *J* = 4.4, 1H); ¹³C-NMR (d₆-DMSO) δ 22.2, 106.3, 110.1, 119.7, 130.8, 130.9, 134.6, 135.0, 143.8, 147.9, 149.2, 152.9, 168.2, 184.9.



Resorufin 11-sulfooundecanoate, 2. 11-Sulfooundecanoic acid was prepared by treating 11-bromoundecanoic acid (10.6 g, 40 mmol) with sodium sulfite in 0.5 N NaOH (75 mL) and EtOH (10 mL).⁷ After refluxing overnight, the solution was cooled and acidified, resulting in precipitation of the acid. The precipitate was filtered and dried under vacuum overnight to give 11-sulfooundecanoic

acid (9.02 g, 34 mmol, 85%). To a solution 11-sulfoundecanoic acid (2.10 g, 8 mmol) in 2:1 CH₂Cl₂/MeCN (30 mL) was added EDC (1.25 g, 8 mmol) drop-wise at 0 °C. After stirring for 5 min., resorufin sodium salt (940 mg, 4 mmol) was added in one portion. After stirring at 0 °C for 3 h, the reaction was diluted with CH₂Cl₂ (100 mL) and filtered to remove unreacted resorufin. The solvent was removed *in vacuo* and the resulting residue was purified silica gel (9:1 CHCl₃/MeOH to 4:1 CHCl₃/MeOH) to give the title compound as a dark red paste (480 mg, 1.0 mmol, 25%): ¹H-NMR (d₆-DMSO) δ 1.23 (br s, 12H), 1.63 (m, 2H), 1.86 (m, 2H), 2.33 (m, 2H), 3.36 (m, 2H), 6.29 (d, *J* = 1.8, 1H), 6.81-6.85 (dd, *J* = 2.1, 9.9, 1H), 7.21-7.24 (dd, *J* = 2.4, 8.4, 1H), 7.38 (d, *J* = 2.1, 1H), 7.54 (d, *J* = 9.3, 1H), 7.89 (d, *J* = 8.7, 1H). ¹³C-NMR (d₆-DMSO) δ 26.9, 29.4, 34.6, 37.2, 55.9, 104.0, 109.2, 119.5, 133.7, 133.8, 137.5, 148.0, 152.9, 158.9, 164.0, 194.2. HRMS under EI showed no molecular ion.



Resorufin 3-(3-pyridyl)propionate, 3. To prepare

the 3-(3-pyridyl)propionic acid anhydride, *N*-(3-dimethylaminopropyl)-*N'*-ethylcarbodiimide EDC•HCl

(1.91 g, 10 mmol) was added to a solution of 3-(3-pyridyl)propionic acid (3.02 g, 20 mmol) in CH₂Cl₂ (50 mL) at 0 °C and stirred at RT.¹⁴ After 24 h, the reaction was washed with ice-cold sat. NaHCO₃ (3 x 25 mL), dried over MgSO₄ and concentrated *in vacuo* to give a pale yellow oil (1.62 g, 57%): ¹H NMR δ 2.72 (t, *J* = 7.2, 2H), 3.03 (t, *J* = 7.5, 2H), 7.24 (m, 1H), 7.58 (m, 1H), 8.50 (m, 2H). A solution of 3-(3-pyridyl)propionic acid anhydride (1.14 g, 4 mmol) in CH₂Cl₂ (10 mL) was then added drop-wise to a slurry of resorufin sodium salt (590 mg, 2.5 mmol) in CH₂Cl₂ (20 mL) and pyridine (250 μL, 3 mmol) at 0 °C. After stirring at RT for 3 h, the reaction was diluted with CH₂Cl₂ (100 mL) and filtered to remove unreacted resorufin. The solvent was removed *in vacuo*. Purification on silica (95:5 CHCl₃/MeOH) gave the title compound as an orange solid (280 mg, 33%): mp = 186-188 °C (decomp.); ¹H-NMR δ 3.00 (t, *J* = 6.9, 2H), 3.14 (t, *J* = 7.2, 3H), 6.34 (d, *J* = 2.1, 1H), 6.85-6.89 (dd, *J* = 2.1, 9.9, 1H), 7.05-7.10 (dd, *J* = 2.4, 8.4, 1H), 7.09 (s, 1H), 7.36-7.46 (m, 2H), 7.71-7.81 (m, 2H), 8.55-8.62 (m, 2H); ¹³C-NMR (d₆-DMSO) δ 27.7, 35.1, 106.6, 110.3, 120.0, 124.0, 131.4, 135.2, 135.7, 136.1, 136.5,

144.6, 148.2, 148.7, 149.9, 150.3, 153.6, 171.1, 186.2; HRMS calcd for $C_{20}H_{15}N_2O_4$ ($M+H^+$) 347.1007. Found: 347.1034.

6.3.4. Quick E measurements

1-Phenethyl acetate 4 with reference compounds 1, 2 or 3. These measurements were carried out using 96-well microplates and a microplate reader. The assay solutions were prepared by mixing the pH-indicator, 4-nitrophenol (6560 μ L of a 0.9115 mM solution in 5.0 mM BES, pH 7.2) and MeCN (370 μ L), then vortexing the solution. (*R*)-1-Phenethyl acetate (*R*)-4 (46 μ L of a 100 mM solution in MeCN), and reference compound, 1, 2 or 3 (224 μ L of a 1.69 mM solution in MeCN) were added drop-wise. Hydrolase solutions (5 μ L/well) were added to the wells and the assay solution (95 μ L/well) was added quickly using an 8-channel pipette. The final concentration in each well was 0.61 mM (*R*)-4, 0.05 mM reference compound, 4.58 mM BES buffer, 0.79 mM 4-nitrophenol, 8.4% acetonitrile. The plate was placed in the microplate reader, shaken for 3 s and the simultaneous decrease in absorbance at 404 nm and increase at 574 nm was monitored at 25 °C as often as permitted by the microplate software, typically every 11 seconds. Data were collected for 60 minutes. Each hydrolysis was carried out in quadruplicate and was averaged. The procedure was repeated for the other enantiomer (*S*)-4; however, the final concentration of substrate in each well was 12.5 mM. Activities were calculated using the slopes of the linear, initial portions of the curves where $\epsilon_{404\text{ nm}} = 17,300\text{ M}^{-1}\text{ cm}^{-1}$ and $\epsilon_{574\text{ nm}} = 15,140\text{ M}^{-1}\text{ cm}^{-1}$ and $l = 0.306\text{ cm}$. To calculate specific activities ($\mu\text{mol/min/mg protein}$), we took into account the total amount of protein in each well as determined by the Bio-Rad protein Assay.

Acknowledgements

We thank McGill University and University of Minnesota for financial support.

References

- ¹ Chen, C.-S.; Fujimoto, Y.; Girdaukas, G.; Sih, C. J. *J. Am. Chem. Soc.* **1982**, *104*, 7294-7299.
- ² Reetz, M. T. *Angew. Chem. Int. Ed.* **2001**, *40*, 284-310.
- ³ Bornscheuer, U. T. *Eng. Life Sci.* **2004**, *4*, 539-542.
- ⁴ Schrader, W.; Eipper, A. Pugh, D. J.; Reetz, M. T. *Can. J. Chem.* **2002**, *80*, 626-632.
- ⁵ Janes, L. E.; Kazlauskas, R. J. *J. Org. Chem.* **1997**, *62*, 4560-4561.
- ⁶ Janes, L. E.; Cimpioia, A.; Kazlauskas, R. J. *J. Org. Chem.* **1999**, *64*, 9019-9029.
- ⁷ Anderson, B. D.; Conradi, R. A.; Knuth, K. E. *J. Pharma. Sci.* **1985**, *74*, 365-374.
- ⁸ Bornscheuer, U. T.; Kazlauskas, R. J. *Hydrolases in Organic Synthesis*; Wiley-VCH: Weinheim, 1999; pp. 1-31.
- ⁹ Martinelle, M.; Holmquist, M.; Hult, K. *Biochim. Biophys. Acta* **1995**, *1258*, 272-276.
- ¹⁰ Horsman, G. P.; Liu, A. M. F.; Henke, E.; Bornscheuer, U. T.; Kazlauskas, R. J. *Chem. Eur. J.* **2003**, *9*, 1933-1939.
- ¹¹ Hedstrom, L. *Chem. Rev.* **2002**, *102*, 4501-4503.
- ¹² Krebsfänger, N.; Zocher, F.; Altenbuchner, J.; Bornscheuer, U. T. *Enzyme Microb. Technol.* **1998**, *22*, 641-646.
- ¹³ Kramer, D. N.; Guilbault, G. G. *Anal. Chem.* **1964**, *36*, 1662-1663.
- ¹⁴ Backes, B. J.; Dragoli, D. R.; Ellman J. A. *J. Org. Chem.* **1999**, *64*, 5472-5478.

Summary, conclusions and future work

Hydrolases are excellent catalysts for production of enantiopure compounds. Although strategies exist for lipase-catalyzed resolution of secondary alcohols, there are few strategies using proteases such as subtilisin. Researchers often overlook subtilisin for resolving secondary alcohols because its reactivity and enantioselectivity toward nonpolar secondary alcohol esters is lower than the lipases. Lipases show higher reactivity because they prefer water-insoluble (nonpolar) substrates. The enantioselectivity of lipases is higher because they bind substrate in a folded conformation and they have a deep active site that places both substituents of the secondary alcohol in well-defined hydrophobic pockets. The active site of subtilisin, on the other hand, is on its surface. It binds substrate in an extended conformation and reacts only with water-soluble (polar) substrates. Subtilisin has a large nonpolar pocket (the S_1 pocket) to bind acyl group and a shallow crevice (the S_1' pocket) to bind one substituent of a secondary alcohol group, while the other substituent remains in solvent. First, we hypothesized that subtilisin would be highly reactive if acyl group anchored the substrate to the active site. Second, we hypothesized that subtilisin would be highly enantioselective if there was a large hydrophobicity difference between alcohol substituents.

To test our first hypothesis, we showed that an anchoring acyl group increases protease reactivity and extends subtilisin E to a new class of substrates, *N*-acyl sulfinamides. Subtilisin E did not catalyze hydrolysis of *N*-acetyl arylsulfinamides, but did catalyze hydrolysis of *N*-dihydrocinnamoyl arylsulfinamides. Molecular modelling of the first tetrahedral intermediate for subtilisin E-catalyzed hydrolysis of *N*-dihydrocinnamoyl-*p*-toluenesulfinamide suggested the *N*-dihydrocinnamoyl group mimics phenylalanine and thus binds the sulfinamide to the active site.

We then further increased the reactivity of proteases by tuning acyl group. By replacing the dihydrocinnamoyl group with the 3-(3-pyridyl)propionyl group, we increased substrate solubility and hence, the reactivity with subtilisin and α -chymotrypsin. We used this group to resolve a polar substrate, *p*-toluenesulfinamide, and a sterically hindered substrate, 2,2-dimethylcyclopentanol, on a large-scale and purified product and substrate without using chromatography. The selectivity and mildness of this biocatalytic route

make it the preferred route for preparation of enantiopure sulfinamides and sterically hindered secondary alcohols because it is amenable to scale up, environmentally acceptable and performed under mild conditions.

Next, we used different anchoring acyl groups to extend several proteases to tertiary alcohol esters, sterically hindered substrates that react slowly with lipases. We investigated proteases because they have a large open binding site that can accept sterically hinder alcohols, but still do not catalyze reactions of tertiary alcohols. We showed that internal strain destabilizes the transition state for this reaction, but that the addition of an anchor group that binds substrate to the protease stabilizes transition state and enables proteases to catalyze hydrolysis of tertiary alcohol esters. For example, α -chymotrypsin did not react with tertiary alcohol acetates, but showed high reactivity toward the dihydrocinnamate. Further, we showed dihydrocinnamate esters are resistant to chemical hydrolysis and that proteases catalyze hydrolysis of sterically demanding allylic and alkyl tertiary alcohols that do not react with lipases.

Last, we applied our anchoring group strategy to improve our colourimetric screening method, Quick E. Instead of tuning substrate to increase the hydrolase-catalyzed reaction rate, we altered the chromogenic reference compound structure to slow its reaction. We could measure reaction rate of slow reacting enantiomers using our new chromogenic reference compounds and thus, measure higher enantioselectivities ($E = >200$) than previously. Currently, we are using resorufin 3-(3-pyridyl)propionate as reference compound to screen CALB enzyme libraries for increased enantioselectivity toward slow-reacting carboxylic acid esters.

To test our second hypothesis, we showed subtilisin enantioselectivity stems from a favourable hydrophobic interaction between nonpolar substituent and S_1' pocket residues and favourable solvation of polar substituent in water. The enantioselectivity of a series of secondary alcohols in water varied linearly with the difference in hydrophobicity ($\log P/P_0$) of the substituents. The larger the $\log P/P_0$ difference the higher the enantioselectivity. Based on our results, we proposed a new structure-based model for predicting the enantiopreference of subtilisin toward secondary alcohol esters and related substrates. This revised model of the enantioselectivity of subtilisin toward secondary alcohols is consistent with the structure of subtilisin, rationalizes why enantioselectivity changes and

even reverses with changes in solvent, and provides a strategy to increase enantioselectivity by modifying the substrate.

Consistent with our hypothesis, the enantioselectivity of subtilisin toward *N*-acyl arylsulfonamides is high because the difference in substituent hydrophobicity is large. The (*R*)-enantiomer reacts faster because of preferential binding of the nonpolar *p*-tolyl group in the hydrophobic S₁' pocket versus the polar sulfoxide oxygen, which prefers to be exposed to solvent water.

Also consistent with our hypothesis, the enantioselectivity toward nonpolar tertiary alcohols was low because the medium-sized substituent and the large substituent compete for the S₁' leaving group pocket, where binding methyl group avoids some steric interactions and binding of phenyl group adds a good hydrophobic interaction. Molecular modelling also suggested the reactivity is limited to tertiary alcohols with a methyl or smaller substituent because this substituent adopts an unfavourable *syn*-pentane-like orientation with the oxyanion of the first tetrahedral intermediate. We plan to increase the enantioselectivity by modifying substrate to increase the difference in substituent hydrophobicity. We also plan to use saturation mutagenesis at key amino acid positions in the S₁' pocket to alter the shape, size and polarity of this pocket.

Thus, we confirmed our first hypothesis by showing that we could increase protease reactivity by tailoring the anchoring acyl group. By doing so, we extended proteases to two new classes of substrates, *N*-acyl arylsulfonamides and tertiary alcohol esters. Further, by optimizing acyl group to increase solubility and simplify purification, we developed a new strategy for large-scale preparation of sulfonamides and sterically hindered secondary alcohols.

We confirmed our second hypothesis by showing that protease enantioselectivity increases with increasing substituent hydrophobicity difference. This effect stems from a favourable hydrophobic interaction between nonpolar substituent and S₁' pocket residues and favourable solvation of polar substituent in water. This finding provides a strategy to increase enantioselectivity by modifying the substrate.

For chemists to solve the next generation of synthetic problems for production of chemicals, fuels and fine chemicals requires new chemical reactions. Catalytic promiscuity – the ability of a single active site to catalyze more than one chemical transformation –

has potential application in biocatalysis by enabling discovery of new catalysts. Protein engineering can add or enhance new catalytic activities in existing enzymes. However, the new catalytic activity is usually very low. We showed that anchoring groups can increase reactivity by at least one-hundred-fold. We believe that our anchoring group strategy will also accelerate these new reactions and enable the discovery of new catalytic activities.

Contributions to knowledge

- i. We developed a strategy to increase the reactivity of proteases using structure-based anchoring acyl groups that bind substrate to active site. This facilitated protease-catalyzed reaction of otherwise unreactive substrates and extended proteases to two new substrates, *N*-acyl arylsulfonamides and tertiary alcohol esters.
- ii. We showed protease enantioselectivity was high if there was a large difference in substituent hydrophobicity. The high enantioselectivity stems from favourable hydrophobic interaction between nonpolar substituent and S₁' pocket residues and favourable solvation of polar substituent in water. This provided a new strategy to increase protease enantioselectivity by modifying the substrate, where a large difference in substituent hydrophobicity = high enantioselectivity. Based on our results, we refined the current rule for predicting subtilisin enantiopreference toward secondary alcohols to show subtilisin binds only one substituent and leaves the other in solvent. Our revised model for the enantioselectivity of subtilisin toward secondary alcohols is consistent with the structure of subtilisin and rationalizes why enantioselectivity changes and even reverses with changes in solvent.
- iii. Using our anchoring acyl group strategy, we extended proteases to polar substrates, *N*-acyl arylsulfonamides. Enantiopure sulfonamides are useful chiral auxiliaries for asymmetric synthesis of amines. Our new protease-catalyzed route to enantiopure sulfonamides is amenable to scale up, environmentally acceptable and performed under mild conditions. This was the first reported biocatalytic route to these useful chiral auxiliaries.
- iv. Using different anchoring acyl groups, we extended several proteases to sterically hindered substrates, tertiary alcohol esters. We showed proteases catalyzed hydrolysis of a wide range of tertiary alcohol esters with high reactivity and low to moderate enantioselectivity. We showed that internal strain destabilizes the transition state for this reaction, but that addition of an anchor group that binds substrate to active site enables proteases to catalyze hydrolysis of tertiary alcohol esters. This was the first reported protease-catalyzed resolution of tertiary alcohols.

v. We designed a new acyl group that increased the reactivity of proteases toward secondary alcohol esters and allowed for separation of product and substrate via mild acid extraction. The 3-(3-pyridyl)propionyl group is the best acyl group for large-scale protease-catalyzed resolutions because it shows high water solubility, increases reactivity with proteases and allows for purification without using chromatography.

vi. We used our anchor group strategy to develop new slower reacting reference compounds for Quick E. We can now measure higher enantioselectivities ($E = >200$) than previously.

Appendix I
Copyright waivers

ACS PUBLICATIONS DIVISION GUIDELINES

FOR THESES AND DISSERTATIONS

ATTENTION: STUDENTS, STUDENT ADVISORS, AND TEACHERS

Permission is automatically granted to include your paper(s) or portions of your paper(s) in your thesis; please pay special attention to the implications paragraph below. The Copyright Subcommittee of the Joint Board/Council Committees on Publications approved the following:

Copyright permission for published and submitted material from theses and dissertations

ACS extends blanket permission to students to include in their theses and dissertations their own articles, or portions thereof, that have been published in ACS journals or submitted to ACS journals for publication, provided that the ACS copyright credit line is noted on the appropriate page(s).

Publishing implications of electronic publication of theses and dissertation material

Students and their mentors should be aware that posting of theses and dissertation material on the Web prior to submission of material from that thesis or dissertation to an ACS journal may affect publication in that journal. Whether Web posting is considered prior publication may be evaluated on a case-by-case basis by the journal's editor. If an ACS journal editor considers Web posting to be "prior publication", the paper will not be accepted for publication in that journal. If you intend to submit your unpublished paper to ACS for publication, check with the appropriate editor prior to posting your manuscript electronically.

If your paper has not yet been published by ACS, we have no objection to your including the text or portions of the text in your thesis/dissertation in **print and microfilm formats**; please note, however, that electronic distribution or Web posting of the unpublished paper as part of your thesis in electronic formats might jeopardize publication of your paper by ACS. Please print the following credit line on the first page of your article: "Reproduced (or 'Reproduced in part') with permission from [JOURNAL NAME], in press (or 'submitted for publication'). Unpublished work copyright [CURRENT YEAR] American Chemical Society." Include appropriate information.

If your paper has already been published by ACS and you want to include the text or portions of the text in your thesis/dissertation in **print or microfilm formats**, please print the ACS copyright credit line on the first page of your article: "Reproduced (or 'Reproduced in part') with permission from [FULL REFERENCE CITATION.] Copyright [YEAR] American Chemical Society." Include appropriate information.

Note: If you plan to submit your thesis to UMI or to another dissertation distributor, you should not include the unpublished ACS paper in your thesis if the thesis will be disseminated electronically, until ACS has published your paper. After publication of the paper by ACS, you may release the entire thesis (**not the individual ACS article by itself**) for electronic dissemination; ACS's copyright credit line should be printed on the first page of the ACS paper.

SUMMARY: The inclusion of your ACS unpublished or published manuscript is permitted in your thesis in print and microfilm formats. If ACS has published your paper you may include the manuscript in your thesis on an intranet that is not publicly available. Your ACS article cannot be posted electronically on a publicly available medium, such as but not limited to, electronic archives, Internet, intranet, library server, etc. The only material from your paper that can be posted on a public electronic medium is the article abstract, figures, and tables and you may link to the article's DOI.

Questions? Please contact the ACS Publications Division Copyright Office at copyright@acs.org or at 202-872-4368.

August 1998, March 2003, October 2003

Appendix II
Reprints of published manuscripts

Subtilisin-Catalyzed Resolution of *N*-Acyl Arylsulfinamides

Christopher K. Savile,[†] Vladimir P. Magloire, and Romas J. Kazlauskas^{*†}

Contribution from the Department of Chemistry, McGill University, 801 Sherbrooke Street West,
Montréal, Québec, Canada H3A 2K6

Received July 30, 2004; E-mail: rjk@umn.edu

Abstract: We report the first biocatalytic route to sulfinamides ($R-S(O)-NH_2$), whose sulfur stereocenter makes them important chiral auxiliaries for the asymmetric synthesis of amines. Subtilisin E did not catalyze hydrolysis of *N*-acetyl or *N*-butanoyl arylsulfinamides, but did catalyze a highly enantioselective ($E > 150$ favoring the (*R*)-enantiomer) hydrolysis of *N*-chloroacetyl and *N*-dihydrocinnamoyl arylsulfinamides. Gram-scale resolutions using subtilisin E overexpressed in *Bacillus subtilis* yielded, after recrystallization, three synthetically useful auxiliaries: (*R*)-*p*-toluenesulfinamide (42% yield, 95% ee), (*R*)-*p*-chlorobenzenesulfinamide (30% yield, 97% ee), and (*R*)-2,4,6-trimethylbenzenesulfinamide (30% yield, 99% ee). Molecular modeling suggests that the *N*-chloroacetyl and *N*-dihydrocinnamoyl groups mimic a phenylalanine moiety and thus bind the sulfinamide to the active site. Molecular modeling further suggests that enantioselectivity stems from a favorable hydrophobic interaction between the aryl group of the fast-reacting (*R*)-aryl sulfinamide and the S_1' leaving group pocket in subtilisin E.

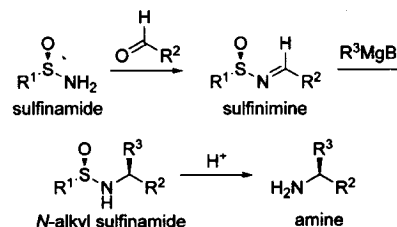
Introduction

The chiral sulfinyl group ($R-S(O)-$) is an important functional group for asymmetric synthesis because it effectively transfers chirality to a wide range of centers.^{1–3} This efficacy stems from the steric and stereoelectronic differences between the substituents: a lone pair, an oxygen, and an alkyl or aryl group. As well, the sulfinyl group is configurationally stable.²

Sulfinamides ($R-S(O)-NH_2$) are useful sulfinyl chiral auxiliaries for synthesis of amines (Scheme 1).^{4,5} When condensed with an aldehyde or ketone to give the sulfinimine, the *N*-sulfinyl group directs nucleophilic addition across the $C=N$ bond. This yields the *N*-alkyl sulfinamide, which upon hydrolysis of the $S-N$ link yields an amine. Enantioselective syntheses using sulfinimines include preparations of amines,⁶ α - and β -amino acids,⁵ amino alcohols,⁷ aziridines,⁸ and amino phosphonic acids.⁹

The best route to enantiopure aryl sulfinyl moieties is via menthyl-*p*-toluenesulfinate (Andersen's reagent).^{2,10,11} Nucleo-

Scheme 1. Synthesis of Enantiopure Amines from Sulfinamides



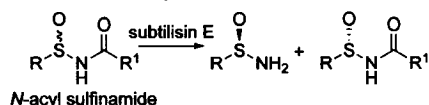
philic displacement of menthol at chiral sulfur leads to enantiopure aryl sulfinyl compounds⁴ including *p*-toluenesulfinamide.¹² However, preparation of Andersen's reagent relies on the crystallization of diastereomers epimeric at sulfur, and only *p*-toluenesulfinate and close analogues efficiently crystallize as the menthyl derivative.^{2,4,13} Thus, this route is limited to *p*-toluenesulfinamide and close analogues. Asymmetric oxidation using 1 equiv of (+)- or (–)-*N*-(phenylsulfonyl)(3,3-dichlorocamphoryl)oxaziridine also yields enantiopure aryl sulfinyl moieties.¹⁴

The two other routes to enantiopure sulfinamides use either an enantioselective oxidation of *tert*-butyl disulfide^{6,15} or a double displacement using a chiral auxiliary derived from indanol.¹⁶ The enantioselective oxidation developed by Ellman

[†] Current address: Department of Biochemistry, Molecular Biology & Biophysics and The Biotechnology Institute, University of Minnesota, 1479 Gortner Avenue, Saint Paul, MN 55108.

- (1) Carreña, M. C. *Chem. Rev.* **1995**, *95*, 1717–1760 and references therein.
- (2) Anderson, K. K. In *The Chemistry of Sulphones and Sulphoxides*; Patai, S., Rappoport, Z., Stirling, C. J. M., Eds.; John Wiley & Sons: New York, 1988; pp 55–94.
- (3) Walker, A. J. *Tetrahedron: Asymmetry* **1992**, *3*, 961–998.
- (4) Nudelman, A. In *The Chemistry of Sulphinic Acids, Esters and their Derivatives*; Patai, S., Ed.; John Wiley & Sons: New York, 1990; pp 35–85.
- (5) Davis, F. A.; Zhou, P.; Chen, B.-C. *Chem. Soc. Rev.* **1998**, *27*, 13–18.
- (6) Liu, G.; Cogan, D. A.; Ellman, J. A. *J. Am. Chem. Soc.* **1997**, *119*, 9913–9914.
- (7) Kochi, T.; Tang, T. P.; Ellman, J. A. *J. Am. Chem. Soc.* **2002**, *124*, 6518–6519.
- (8) Davis, F. A.; Zhou, P.; Reddy, G. V. *J. Org. Chem.* **1994**, *59*, 3243–3245.
- (9) Lefebvre, I. M.; Evans, S. A. *J. Org. Chem.* **1997**, *62*, 7532–7533.
- (10) (a) Phillips, H. J. *Chem. Soc.* **1925**, *127*, 2552–2587. (b) Hulce, M.; Mallamo, J. P.; Frye, L. L.; Kogan, T. P.; Posner, G. A. *Org. Synth.* **1986**, *64*, 196–206.

- (11) Drabowicz, J.; Kielbasinski, P.; Mikolajczyk, M. In *The Chemistry of Sulphones and Sulphoxides*; Patai, S., Rappoport, Z., Stirling, C. J. M., Eds.; John Wiley & Sons: New York, 1988; pp 233–378.
- (12) Davis, F. A.; Xiang, Y.; Andemichael, Y.; Fang, T.; Fanelli, D. L.; Zhang, H. *J. Org. Chem.* **1999**, *64*, 1403–1406.
- (13) Herbranson, H. F.; Cusano, C. M. *J. Am. Chem. Soc.* **1961**, *83*, 2124–2128.
- (14) Davis, F. A.; Reddy, R. T.; Reddy, R. E. *J. Org. Chem.* **1992**, *57*, 6387–6389.
- (15) Cogan, D. A.; Liu, G.; Kim, K.; Backes, B. J.; Ellman, J. A. *J. Am. Chem. Soc.* **1998**, *120*, 8011–8019.
- (16) Han, Z.; Krishnamurthy, D.; Grover, P.; Fang, Q. K.; Senanayake, C. H. *J. Am. Chem. Soc.* **2002**, *124*, 7880–7881.

Scheme 2. Subtilisin-Catalyzed Kinetic Resolution of Sulfonamides

and co-workers relies on the stability of the oxidation product, thiosulfinate (*t*-Bu-S(O)-S-*t*-Bu), to racemization and is thus limited to *tert*-butylsulfonamide. The double displacement route developed by Senanayake and co-workers uses *N*-sulfonyl-1,2,3-oxathiazolidine-2-oxide intermediates. This route yields a variety of enantiopure sulfonamides, but includes complicated steps requiring low temperatures and moisture- and air-sensitive reagents.

Many groups have reported biocatalytic routes to sulfinyl stereocenters, but not to sulfonamides. A direct biocatalytic route to sulfinyl compounds is oxidation. For example, enantioselective oxidation of unsymmetrical sulfides yields sulfoxides.^{11,17} These direct oxidation routes may not be suitable routes to sulfonamides because oxidation of unsubstituted sulfonamides (RSNH₂) can involve nitrene intermediates.¹⁸ Another biocatalytic route to enantiopure sulfinyl groups is lipase-catalyzed hydrolysis of a pendant ester group.¹⁹ Enantioselectivity can be high even when the stereocenter is remote from the reacting carbonyl. Ellman and co-workers tested the hydrolase-catalyzed acylation of the sulfonamide amino group, but did not observe any reaction.¹⁵ In this paper, we explore the reverse reaction—hydrolase-catalyzed hydrolysis of *N*-acylsulfonamides (Scheme 2) and find that subtilisin E shows high enantioselectivity toward many arylsulfonamides. Further, molecular modeling suggests that the high enantioselectivity of subtilisin toward sulfonamides compared to the moderate enantioselectivity toward the isosteric secondary alcohols likely stems from the polar nature of the oxygen substituents in sulfonamides (Figure 1).

Results

Synthesis of Substrates. We prepared racemic sulfonamides 1–8 by one of three established routes (Scheme 3). The simplest route, from the corresponding sulfonic acid, yielded *p*-toluenesulfonamide 1 and benzenesulfonamide 2. Treating the sulfonic acid with oxalyl chloride followed by ammonolysis yielded the sulfonamides in 56–59% yield.²⁰

To prepare sulfonamides for which no sulfonic acid precursors were available (*p*-chlorobenzenesulfonamide 3, *p*-methoxybenzenesulfonamide 4, 2,4,6-trimethylbenzenesulfonamide 5, 1-naphthylsulfonamide 6, and 2,4,6-triisopropylbenzenesulfonamide 7), we used the sulfonyl chlorides. Reduction of the sulfonyl chloride with P(OMe)₃ in ethanol gave the respective sulfinate ethyl esters.²¹ Displacement of ethanol with lithium bis(tri-

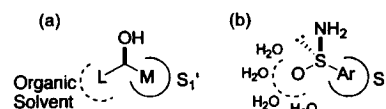


Figure 1. Empirical rules that predict the enantioselectivity of subtilisins toward secondary alcohols and sulfonamides. (a) In organic solvent, subtilisins favor the secondary alcohol enantiomer with the shape shown, where L is a large substituent, such as phenyl, and M is a medium substituent, such as methyl. (b) In water, subtilisins favor the sulfonamide enantiomer with the shape shown, where Ar is an aryl substituent. We suggest that a favorable hydrophobic interaction between the aryl substituent and S1' pocket and good solvation of the polar sulfoxide oxygen in water explain the enantioselectivity with sulfonamides.

methylsilyl)amide followed by desilylation gave the corresponding sulfonamides in 21–55% overall yield.²⁰

We prepared *tert*-butylsulfonamide 8 from *tert*-butyl disulfide in three steps. Oxidation of *tert*-butyl disulfide with 3-chloroperoxybenzoic acid followed by addition of sulfuric chloride gave *tert*-butylsulfinyl chloride,²² which reacted with NH₄OH to give 8 in 21% overall yield.²⁰

To prepare *N*-acylsulfonamides a–m, we treated the appropriate sulfonamide with 2 equiv of *n*-butyllithium in THF at –78 °C followed by rapid addition of the necessary symmetrical carboxylic acid anhydride (15–90% yield).²⁰

Initial Screening. Initial screening of the *N*-butanoyl derivative 1b with 50 hydrolases revealed no active hydrolases, but screening the more reactive *N*-chloroacetyl derivative 1c identified four moderately to highly active proteases, one lipase and one esterase (Table 1).²³ To determine enantioselectivities, we carried out small-scale reactions and measured the enantiomeric purity of the starting materials and products by HPLC using a column with a chiral stationary phase.

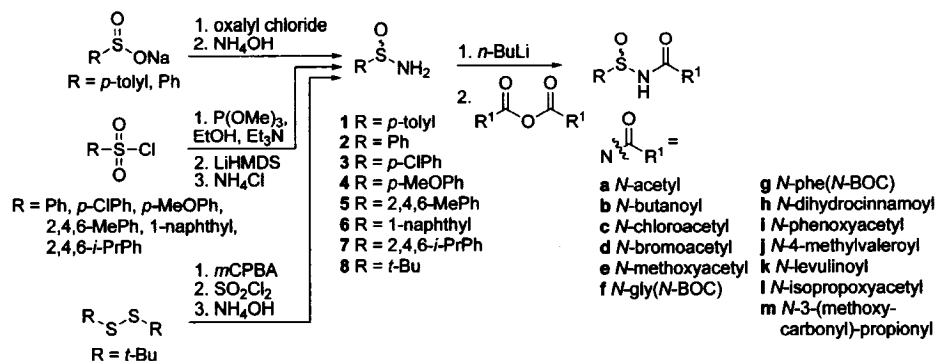
Proteinase from *Bacillus subtilis* var. biotus A showed the highest true enantioselectivity ($E_{\text{true}} > 150$). At 50% conversion, the product, (*R*)-1, had 93% ee while the unreacted starting material, (*S*)-1c, had 92% ee corresponding to an apparent enantioselectivity (E_{app}) of 90. However, this substrate also underwent ca. 1–3% spontaneous chemical hydrolysis. After correction for this chemical hydrolysis,²⁴ the true enantioselectivity (E_{true}) was > 150 .

A related protease, subtilisin Carlsberg, also catalyzed hydrolysis of 1c with low apparent enantioselectivity (E_{app}). However, the amount of product sulfonamide was much lower than the amount of 1c that disappeared. Further analysis revealed that in addition to the expected C–N bond hydrolysis, this protease also catalyzed S–N bond hydrolysis.²⁵ Details of this unprecedented reaction will be reported separately.

The two other proteases, protease from *Aspergillus oryzae* and protease/acylase from *Aspergillus melletus*, as well as a lipase, *Candida antarctica* lipase A, and bovine cholesterol esterase, also catalyzed the hydrolysis of 1c, but showed only low to moderate enantioselectivity ($E_{\text{true}} = 6$ –29). All hydrolases, except lipase A from *Candida antarctica*, favored the (*R*)-enantiomer.

- (17) (a) Kagan, H. B. In *Catalytic Asymmetric Synthesis*; Ojima, I., Ed.; VCH: New York, 1993; pp 203–226. (b) Holland, H. L. *Chem. Rev.* **1988**, *88*, 473–485. (c) ten Brink, H. B.; Holland, H. L.; Schoemaker, H. E.; van Lingen, H.; Wever, R. *Tetrahedron: Asymmetry* **1999**, *10*, 4563–4572. (18) (a) Capozzi, G.; Modena, G.; Pasquato, L. In *The Chemistry of Sulphenic Acids and Their Derivatives*; Patai, S., Ed.; Wiley: Chichester, U.K., 1990; pp 403–516. (b) Atkinson, R. S.; Judkins, B. D. *J. Chem. Soc., Perkin Trans. 1* **1981**, 2615–2619. (19) (a) Allenmark, S. G.; Andersson, A. C. *Tetrahedron: Asymmetry* **1993**, *4*, 2371–2376. (b) Burgess, K.; Henderson, I. *Tetrahedron Lett.* **1989**, *30*, 3633–3636. (c) Burgess, K.; Henderson, I.; Ho, K.-K. *J. Org. Chem.* **1992**, *57*, 1290–1295. (d) Serregi, A. N.; Kazlauskas, R. J. *Can. J. Chem.* **1995**, *73*, 1357–1367. (20) Backes, B. J.; Dragoli, D. R.; Ellman, J. A. *J. Org. Chem.* **1999**, *64*, 5472–5478. (21) Klunder, J. M.; Sharpless, K. B. *J. Org. Chem.* **1987**, *52*, 2598–2602.

- (22) (a) Netscher, T.; Prinzbach, H. *Synthesis* **1987**, 683–686. (b) Gontcharov, A. V.; Liu, H.; Sharpless, K. B. *Org. Lett.* **1999**, *1*, 783–786. (23) Jones, L. E.; Löwendahl, C. P.; Kazlauskas, R. J. *Chem.-Eur. J.* **1998**, *4*, 2324–2331. (24) A computer program, Selectivity-KRESH, was used for all calculations. For details, see: Faber, K.; Hönig, H.; Kleewein, A. In *Preparative Biotransformations*; Roberts, S. M., Ed.; John Wiley & Sons: New York, 1995; pp 0.079–0.084. (25) ¹H NMR and HRMS-ESI identified *p*-toluenesulfonic acid as the primary product in this enzymatic reaction: Mugford, P. F.; Magloire, V. P.; Kazlauskas, R. J. Manuscript in preparation.

Scheme 3. Synthesis of Sulfonamides 1–8 and *N*-Acylsulfonamides**Table 1.** Screening of Hydrolases for Enantioselective Hydrolysis of **1c**

hydrolase	wt ^a	%C _{app} ^b	ee _s (%) ^{c,d}	ee _p (%) ^{c,d}	E _{app} ^{d,e}	x(sp) ^f (%)	E _{true} ^{g,h}	enantio-preference ^h
<i>B. subtilis</i> var. biotocus A protease	16	50	92	93	90	3	>150	R
subtilisin E	n.d.	37 ⁱ	56	97	115	2	>150	R
subtilisin Carlsberg	34	56	82	64	n.d. ^j	n.d.	n.d. ^j	R
<i>A. oryzae</i> protease	90	56	88	68	14	3	17	R
<i>A. melletus</i> protease/acylase	250	29 ^k	30	75	9	10	29	R
<i>C. antarctica</i> lipase A	137	14	11	65	5	3	6	S
bovine cholesterol esterase	80	29 ^k	27	67	7	10	11	R

^a Weight of enzyme in milligrams. ^b Conversion %: amount of sulfonamide formed in 6 h, except where noted. ^c Enantiomeric excess %. Enantiomeric excess of substrate and product was determined by HPLC analysis on Daicel Chiralcel OD or AD columns at 238 or 222 nm. ^d The ee_p , ee_s , and E_{app} (apparent enantioselectivity) are with no correction for chemical hydrolysis; n.d. = not determined. ^e Enantiomeric ratio: the enantiomeric ratio E measures the relative rate of hydrolysis of the fast enantiomer as compared to that of the slow enantiomer as defined by Sih (Chen, C. S.; Fujimoto, Y.; Girdaukas, G.; Sih, C. J. *J. Am. Chem. Soc.* **1982**, *104*, 7294–7299). ^f The $x(sp)$ refers to % spontaneous chemical hydrolysis. ^g E_{true} is the enantioselectivity corrected for chemical hydrolysis.²⁴ ^h The absolute configuration was determined by comparison to authentic samples prepared by the method of Davis and co-workers.¹² ⁱ Reaction for 3 h. ^j This reaction was complicated by competing sulfinyl hydrolysis. Accurate determination of E_{app} and E_{true} was more complicated and will be reported elsewhere. ^k Reaction for 24 h.

Although this initial screen identified *B. subtilis* var. biotocus A as the best commercial enzyme for hydrolysis of **1c**, it is, unfortunately, expensive (U.S. \$725/gram), and its amino acid sequence is not available from the supplier. We suspected that subtilisin E might be a similar or even the same enzyme. Subtilisin E is an alkaline serine protease produced by *B. subtilis* that has been cloned and overexpressed,²⁶ and its structure has been elucidated by X-ray crystallography.²⁷ Confirming our hunch, subtilisin E showed similar enantioselectivity ($E_{true} > 150$) to *B. subtilis* var. biotocus A in the hydrolysis of **1c** (Table 1) as well as four other substrates (see below and Supporting Information). We focused further experiments on subtilisin E because it showed high enantioselectivity, it was inexpensive to produce by fermentation, and the X-ray crystal structure permitted a molecular-level interpretation of results.

Optimization of *N*-Acyl Group for Enantioselectivity and Reactivity. The *N*-acetyl derivative **1a** and *N*-butanoyl derivative **1b** showed no reaction with subtilisin E,²⁸ but several acyl groups with electron-withdrawing functional groups similar to those of **1c** showed enantioselective hydrolysis (Table 2). The *N*-bromoacetyl derivative **1d** reacted similarly to **1c**. It showed high enantioselectivity ($E_{true} > 150$) and conversion (53% c_{app} in 3 h), but also underwent a similar spontaneous chemical hydrolysis (4% after 3 h). The *N*-methoxyacetyl derivative **1e** showed at least 6-fold lower enantioselectivity ($E_{true} = 26$), 10-

fold lower conversion (28% c_{app} after 24 h), and a slower spontaneous chemical hydrolysis (4% after 24 h). Glycine derivative **1f** showed at least 3-fold lower enantioselectivity ($E_{true} = 54$) than did **1c**, and 11-fold lower conversion (26% c_{app} after 24 h).

Since subtilisin favors hydrolysis of peptides with aromatic or large nonpolar residues at the P₁ position,²⁹ we prepared several phenylalanine derivatives or analogues. The phenylalanine derivative **1g** demonstrated at least 3-fold lower selectivity ($D_{true} = 46$) and 6-fold lower conversion (46% c_{app} after 24 h) than **1c**. However, the *N*-dihydrocinnamoyl derivative **1h** showed very high enantioselectivity ($E_{true} > 150$) similar to that of **1c**, but with 6-fold lower conversion (47% c_{app} after 24 h).³⁰ Surprisingly, the closely related *N*-phenoxyacetyl derivative **1i** did not react with enzyme.

Three nonpolar substrates structurally related to leucine (**1j**, **1k**, and **1l**) showed at least 6-, 8-, and 21-fold lower enantioselectivity ($E_{true} = 7$ –24) and 24-, 40-, and 60-fold lower conversion (5–13% c_{app} after 24 h), respectively, than did **1c**. A similar compound, **1m**, demonstrated at least 3-fold lower enantioselectivity ($E_{true} = 52$) and 12-fold lower conversion (24% c_{app} after 24 h) than did **1c**.

(29) (a) Estell, D. A.; Graycar, T. P.; Miller, J. V.; Powers, D. B.; Burnier, J. P.; Ng, P. G.; Wells, J. A. *Science* **1986**, *233*, 659–663. (b) Wells, J. A.; Powers, D. B.; Bott, R. R.; Graycar, T. P.; Estell, D. A. *Proc. Natl. Acad. Sci. U.S.A.* **1987**, *84*, 1219–1223.

(30) Additional screening with the *N*-dihydrocinnamoyl derivative **1h** showed chymotrypsin from bovine pancreas catalyzed its hydrolysis with good enantioselectivity ($E = 45$), favoring the (*R*)-enantiomer, and high conversion ($c_{app} = 52\%$) after 6 h. This enzyme was missed in our initial activity screen because it reacted only slowly with the *N*-chloroacetyl derivative **1c**.

(26) (a) Park, S.-S.; Wong, S.-L.; Wang, L.-F.; Doi, R. H. *J. Bacteriol.* **1989**, *171*, 2657–2665. (b) Zhao, H.; Arnold, F. H. *Proc. Natl. Acad. Sci. U.S.A.* **1997**, *94*, 7997–8000.

(27) Jain, S. C.; Shinde, U.; Li, Y.; Inouye, M.; Berman, H. M. *J. Mol. Biol.* **1998**, *284*, 137–144.

(28) Based on a limit of detection of 0.1%.

Table 2. Reactivity and Enantioselectivity of Subtilisin E toward Substrates with Differing *N*-Acyl Group (1a–m)

<i>N</i> -acyl group	%c _{app} ^a	relative rate (%c _{app} /h) ^b	ee _s (%) ^c	ee _p (%) ^c	<i>E</i> _{true} ^d
	n.r.	n.a.	n.a.	n.a.	n.a.
	n.r.	n.a.	n.a.	n.a.	n.a.
	36 ^e	12	56	97	>150 ^f
	53 ^e	18	99	89	>150 ^g
	28	1.2	33	84	26 ^g
	26	1.1	34	95	54
	46	1.9	77	90	44 ^h
	47	2.0	89	99	>150
	n.r.	n.a.	n.a.	n.a.	n.a.
	13	0.5	14	91	24
	8	0.3	8	90	20
	5	0.2	4	75	7
	24	1.0	30	95	52

^a Conversion %: amount of sulfonamide formed in 24 h, except where noted. ^b Conversion % per hour (assumes linear rate throughout course of reaction); n.a. = not applicable. ^c Enantiomeric excess %. Enantiomeric excess of substrate and product was determined by HPLC analysis on Daicel Chiralcel OD or AD columns at 238 or 222 nm; n.d. = not determined. ^d Enantiomeric ratio: the enantiomeric ratio *E* measures the relative rate of hydrolysis of the fast enantiomer as compared to that of the slow enantiomer as defined by Sih (Chen, C. S.; Fujimoto, Y.; Girdaukas, G.; Sih, C. J. *J. Am. Chem. Soc.* **1982**, *104*, 7294–7299). ^e Reaction for 3 h. ^f Corrected for ca. 2% chemical hydrolysis. ^g Corrected for ca. 4% chemical hydrolysis. ^h Diastereomeric ratio.

The *N*-dihydrocinnamoyl derivative **1h** and *N*-chloroacetyl derivative **1c** were the best acyl groups for *p*-toluenesulfonamide since they showed the highest enantioselectivity and reactivity. Thus, compounds **1c** and **1h**, which contain these groups, reacted at least 100 times faster than the simplest *N*-acylsulfonamide,

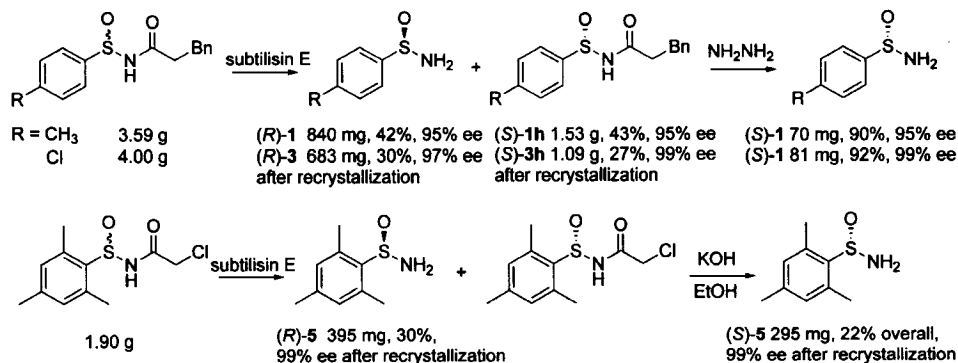
Table 3. Enantioselectivity of Subtilisin E toward Substrates with Differing Sulfonamide Aryl Group

Sulfonamide	R'	%c _{app} ^a	ee _s (%) ^b	ee _p (%) ^b	<i>E</i> _{app}	<i>E</i> _{true} ^c
	Cl	14	16	97	76	>150 ^{d,e}
	Bn	14	16	99	>150	>150
	Cl	35	52	97	110	>150 ^{d,e}
	Bn	9	10	99	>150	>150
	Cl	21	25	94	41	>150 ^{d,f}
	Bn	40	65	98	>150	>150
	Cl	41	67	94	65	98 ^{d,e}
	Bn	0.5	n.d.	n.d.	n.d.	n.d.
	Cl	19 ^g	20	73	13	13
	Bn	n.r.	n.a.	n.a.	n.a.	n.a.
	Cl	30 ^g	3	9	1.2	1.2
	Cl	n.r.	n.a.	n.a.	n.a.	n.a.
	Bn	n.r.	n.a.	n.a.	n.a.	n.a.

^a Conversion %: conversion refers to the amount of sulfonamide formed. All reactions as *N*-chloroacetyl were 3 h and as *N*-dihydrocinnamoyl were 24 h, except where noted; n.r. = no reaction. ^b Enantiomeric excess %. Enantiomeric excess of substrate and product was determined by HPLC analysis on Daicel Chiralcel OD or AD columns at 238 or 222 nm; n.d. = not determined, n.a. = not applicable. ^c Enantiomeric ratio: the enantiomeric ratio *E* measures the relative rate of hydrolysis of the fast enantiomer as compared to the slow enantiomer as defined by Sih (Chen, C. S.; Fujimoto, Y.; Girdaukas, G.; Sih, C. J. *J. Am. Chem. Soc.* **1982**, *104*, 7294–7299). ^d Similar *E* results were obtained with *B. subtilis* var. *biotus* A (see Supporting Information Table S1). ^e Corrected for ca. 1% chemical hydrolysis. ^f Corrected for ca. 3% chemical hydrolysis. ^g Reaction for 24 h.

1a.²⁸ The conversion was 6-fold lower for **1h**, as compared that of **1c**, but it did not suffer spontaneous chemical hydrolysis. Although the reactivity and enantioselectivity of **1d** were comparable to that of **1c**, its synthesis was less efficient (max yield 20% for **1d** vs 50% for **1c**).

Sulfonamide Substrate Range and Enantioselectivity. To determine the substrate range of subtilisin E, we tested seven additional arylsulfonamides with enzyme (Table 3). Subtilisin E catalyzed the hydrolysis of **2c** and para-substituted benzenesulfonamides, **3c** and **4c**, with high enantioselectivity (*E*_{true} > 150), but the enantioselectivity decreased with the more substituted sulfonamide, **5c** (*E*_{true} = 98), and the more hindered sulfonamides, **6c** (*E*_{true} = 13) and **7c** (*E*_{true} = 1.2). Compound **8c** did not react with subtilisin E.

Scheme 4. Gram-Scale Kinetic Resolution of Sulfonamides **1**, **3**, and **5**

Subtilisin E showed moderate to high conversion with **2c**, **3c**, **4c**, and **5c** ($c_{\text{app}} = 14, 35, 21$, and 41% , respectively, after 3 h), but the conversion decreased with the more hindered arylsulfonamides, **6c** and **7c** ($c_{\text{app}} = 19$ and 30% , respectively, after 24 h). Competing chemical hydrolysis (1–3%) occurred with all *N*-chloroacetyl derivatives; however, reducing the reaction temperature to 10°C reduced spontaneous hydrolysis to $<1\%$ after 24 h. *B. subtilis* var. *biotus* A gave similar conversions and enantioselectivity (see Supporting Information Table S1).

The *N*-dihydrocinnamoyl sulfonamides showed similar enantioselectivity to the *N*-chloroacetyl sulfonamides, but lower conversion and no spontaneous chemical hydrolysis. *N*-Dihydrocinnamoyl derivatives **2h**, **3h**, and **4h** showed high enantioselectivity ($E_{\text{true}} > 150$) and low to moderate conversion, $c_{\text{app}} = 14\%$ (8-fold lower than **2c**), 9% (30-fold lower than **3h**), and 40% (4-fold lower than **4c**), respectively, after 24 h. Compound **5h** reacted very slowly ($0.5\% c_{\text{app}}$ after 24 h), and **6h** and **8h** did not react. This lack of reaction may be due to either poor solubility³¹ or poor fit in the enzyme active site. We resolved the more hindered substrates using the more reactive *N*-chloroacetyl group, but used the *N*-dihydrocinnamoyl group for all other sulfonamides to avoid spontaneous chemical hydrolysis.

Comparing the HPLC traces of the product sulfonamides to samples of known absolute configuration, prepared using either Davis and co-workers' method¹² for toluenesulfonamide or Senanayake and co-workers' method¹⁶ for all other sulfonamides (see Supporting Information), established the absolute configurations. Subtilisin E favored the (*R*)-enantiomer in all cases.

Gram-Scale Resolutions. To demonstrate the synthetic usefulness of this reaction, we resolved sulfonamides **1**, **3**, and **5** on a multigram scale with subtilisin E (Scheme 4). We chose these sulfonamides for preparative reactions because sulfonamide **1** is widely used as a chiral auxiliary,⁵ the aryl group of **3** has different electronic properties than **1** and might be a useful alternative, and 2,4,6-trimethylbenzenesulfonamide **5** is more hindered than **1** and gives fewer byproducts during nucleophilic addition.³²

Resolution of **1h** (3.59 g) with subtilisin E gave (*R*)-**1** (840 mg, 42% yield; the maximum yield is 50% in a resolution) with 95% ee and (*S*)-**1h** (1.53 g, 43% yield) with 95% ee at ca. 50% conversion (3 days). If desired, both product and starting material can be recrystallized to $>99\%$ ee. The *N*-dihydrocinnamoyl group could be removed with hydrazine hydrate.³³ Treating (*S*)-**1h** (144 mg) with hydrazine hydrate gave (*S*)-**1** (70 mg, 90% yield) with 95% ee.

We resolved **3h** (4.00 g) to give (*R*)-**3** (683 mg, 30% yield) with 97% ee and (*S*)-**3h** (2.42 g, 60% yield) with 64% ee at ca. 40% conversion (3 days). For unknown reasons, this resolution stopped at 40% conversion, but recrystallization of unreacted starting material gave (*S*)-**3h** (1.09 g, 27%) with 99% ee. Treating (*S*)-**3h** (155 mg) with hydrazine hydrate gave (*S*)-**1** (81 mg, 92%) with 99% ee.

We used the *N*-chloroacetyl group to resolve 2,4,6-trimethylbenzenesulfonamide **5** (1.90 g) because the *N*-dihydrocinnamoyl derivative reacted very slowly. The resolution yielded (*R*)-**5** (520 mg, 39% yield) with 90% ee at ca. 48% conversion (6 h). Recrystallization of (*R*)-**5** gave 395 mg (30%) with 99% ee. The unreacted starting material, (*S*)-**5c**, was isolated with 45% yield (860 mg, 82% ee). The *N*-chloroacetyl group cleaved in ethanolic KOH. Hydrolysis, followed by recrystallization, gave (*S*)-**5** (295 mg, 22% yield) with 99% ee. Recrystallization was necessary because 5% of starting material spontaneously hydrolyzed during reaction. However, chemical hydrolysis could be reduced to $<1\%$ at 10°C , while the enzymatic reaction was only 3-fold slower ($c_{\text{app}} = 16\%$ at 10°C vs 41% at 37°C after 3 h).

These enzymatic resolutions are simple, convenient, and avoid costly auxiliaries.^{12,16} The current synthetic route to enantiopure **1** relies on the starting material menthyl-*p*-toluenesulfonate (U.S. \$15–40/g), and enantiopure **3** and **5** rely on the amino alcohol, *cis*-1-amino-2-indanol (U.S. \$30/g) and give low yields of the sterically hindered **5**.³⁴ This enzymatic resolution yields enantiopure *N*-acylsulfonamides as intermediates. These may be useful for diastereoselective enolate alkylation reactions as a route to enantiopure α -substituted carboxylic acids.²⁰

Molecular Basis for Higher Reactivity of **1c and **1h**.** To understand why (*R*)-**1h** and (*R*)-**1c** reacted with subtilisin E while (*R*)-**1a** did not, we modeled the first tetrahedral intermedi-

(31) The solubility of both **5h** and **6h** in 10% MeCN/buffer was <5 mM. Organic cosolvents (1,4-dioxane, EtOH, DMSO) or additives (10 mM guanidium chloride) did not significantly improve solubility. Performing the reaction experiment at 50°C or using a biphasic reaction system with *tert*-butylmethyl ether also did not increase conversion. Using MeCN or 1,4-dioxane at higher concentrations (20–90%) improved substrate solubility, but did not increase conversion.

(32) Han, Z.; Krishnamurthy, D.; Pflum, D.; Grover, P.; Wald, S. A.; Senanayake, C. H. *Org. Lett.* **2002**, *4*, 4025–4028.

(33) Keith, D. D.; Tortora, J. A.; Yang, R. J. *Org. Chem.* **1978**, *43*, 3711–3713.

(34) In our hands, the sodium bis(trimethylsilyl)amide displacement¹⁶ gave low yields of (*R*)-**2**–**4** and (*R*)-**6** (18–52%) and no yield for (*R*)-**5**. When $\text{LiNH}_2/\text{NH}_3$ was used in place of sodium bis(trimethylsilyl)amide, (*R*)-**5** formed in low yield (3%) and enantiomeric excess (68% ee).

Table 4. Minimized Structures for the Tetrahedral Intermediate of Subtilisin-E-Catalyzed Hydrolysis of **1h**, **1c**, **1a**, and **7c**

conformation	group in S ₁ ' ^a	H bond N _ε -O _γ distance (Å) (N-H-O _γ angle, deg) ^b	comments
(<i>R</i>)- 1h (Figure 2)	tolyl	2.96 (155)	steric contact with Tyr 217, His 64, and Met 222 in S ₁ ' pocket
(<i>R</i>)- 1h	OS ^c	3.08 (152)	severe steric clash with Gly219 and Asn155
(<i>S</i>)- 1h (Figure 2)	OS	3.03 (154)	unhindered in S ₁ ' pocket
(<i>S</i>)- 1h	tolyl ^c	2.99 (157)	steric clash with catalytic His 64
(<i>R</i>)- 1c	tolyl	2.98 (153)	possible hydrogen bond with Thr 220 (Cl _α -O _{γ1} distance = 3.81 Å)
(not shown)			
(<i>R</i>)- 1a	tolyl	2.97 (153)	no contact with S ₁ residues
(not shown)			
(<i>R</i>)- 7c (Figure S2)	none	2.94 (157)	binds above S ₁ ' pocket
(<i>S</i>)- 7c (Figure S2)	none	2.93 (156)	binds above S ₁ ' pocket

^a Narrow, hydrophobic pocket where leaving group alcohol, amide, or sulfonamide binds. ^b Unless otherwise noted, hydrogen bonds (His64 N_{ε2}-N or O, Ser221 NH-O⁻, and Asn155 NH_{δ2}-O⁻) were present in all structures (N-N or O distance 2.7–3.1 Å, N-H-O or N-H-N angle 120–175°). ^c Group is forced out of S₁' because of steric clash with active site residues.

ate for hydrolysis of these substrates (see Experimental Section for modeling details). The modeling identified interactions that bind the *N*-acyl group of (*R*)-**1h** and (*R*)-**1c**, but not (*R*)-**1a**, to the S₁ pocket.

The (*R*)-**1h** tetrahedral intermediate fit well in the active site, and all five catalytically relevant hydrogen bonds were normal length (<3.1 Å) (Table 4). The benzyl moiety of the dihydrocinnamoyl group bound in the S₁ pocket, as expected based on its similarity to phenylalanine.^{29,35} This benzyl moiety contacted hydrophobic portions of five out of eight residues lining this pocket (Leu126, Gly127, Gly128, Ala152, and Gly154). Using the incremental Gibbs free energy of transfer from *n*-octanol to water,^{36,37} we estimate the energy for this benzyl-S₁ pocket hydrophobic interaction to be 2.7–5.5 kcal/mol.³⁸ Thus, the hydrophobic interaction between the benzyl moiety and S₁ pocket likely improves binding of (*R*)-**1h**, as compared to (*R*)-**1a**.

The (*R*)-**1c** tetrahedral intermediate also fit well in the active site, and all five hydrogen bonds were normal length (<3.1 Å) (not shown). The α -chloro atom of (*R*)-**1c** was bound in the S₁ pocket near the hydroxyl group (O_{γ1}-H) of Thr220 (O_{γ1}-Cl distance = 3.81 Å). This O_{γ1}-Cl distance was closer than the van der Waals contact (3.91 Å),³⁹ but longer than a hydrogen bond between a hydroxyl group and chlorine (2.91–3.52 Å).⁴⁰ A typical hydrogen bond between substrate and protein lowers the energy by 0.5–1.5 kcal/mol.⁴¹ This O_{γ1}-Cl interaction

combined with the inductive effects of the α -chlorine atom, which increases the electrophilicity of the carbonyl carbon, may improve the binding and reactivity of (*R*)-**1c**.

Although the tetrahedral intermediate for (*R*)-**1a** also fits in the subtilisin active site and makes all five key hydrogen bonds, the small *N*-acyl group lacks contact with S₁ pocket residues (not shown). This lack of favorable interaction with S₁ residues to improve binding and an electron-withdrawing group to increase reactivity may account for its lack of reaction.⁴²

Molecular Basis for Enantioselectivity of Subtilisin E with **1h.** Empirical rules based on substituent size can often predict the fast-reacting enantiomer in subtilisin-catalyzed reactions of secondary alcohols (Figure 1a).⁴³ Sulfonamides mimic secondary alcohols, where the aryl group is the large substituent and the oxygen is the medium substituent, because of their similar shape. However, the solvation of the medium group of a secondary alcohol (e.g., methyl group) and the sulfoxide oxygen differs. The incremental Gibbs free energy of transfer^{36,37} from *n*-octanol to water for a methyl group is +0.56 kcal/mol, while that for sulfoxide oxygen is -3.0 kcal/mol.⁴⁴ We hypothesized that subtilisin E favors the (*R*)-enantiomer because the sulfoxide oxygen favors a water-exposed orientation, while the aryl group binds in the S₁' leaving group pocket because of a favorable hydrophobic interaction (Figure 1b).

To test this hypothesis, we modeled the first tetrahedral intermediate for hydrolysis of **1h**. The protein modeling molecular mechanics force field (AMBER) did not include parameters for the sulfonamide group, so we estimated these parameters using geometric information for methyl sulfonamide⁴⁵

(35) Lee, T.; Jones, J. B. *J. Am. Chem. Soc.* **1996**, *118*, 502–508.

(36) (a) Fujita, T.; Iwasa, J.; Hansch, C. *J. Am. Chem. Soc.* **1964**, *86*, 5175–5180. (b) Leo, A.; Hansch, C.; Elkins, D. *Chem. Rev.* **1971**, *71*, 525–616. (c) Hansch, C.; Coats, E. *J. Pharm. Sci.* **1970**, *59*, 731–743. (d) Hansch, C.; Leo, A. *Substituent Constants for Correlation Analysis in Chemistry and Biology*; John Wiley and Sons: New York, 1979; pp 48–51.

(37) Fersht, A. *Structure and Mechanism in Protein Science*; W. H. Freeman and Company: New York, 1998; pp 324–348.

(38) A hydrophobic interaction is the tendency of nonpolar compounds to transfer from an aqueous phase to an organic phase. The energy of a hydrophobic interaction is from the regaining of entropy by water after it is removed from a hydrophobic group and can be estimated using the incremental Gibbs free energy of transfer.³⁷ The incremental Gibbs free energy of transfer of a benzyl group from *n*-octanol to water is 2.7 kcal/mol using $\Delta G_{\text{trans}} = 2.303RT\pi$, where π is the hydrophobicity constant of the benzyl group ($\pi = 2.01$)^{36d} relative to hydrogen. However, binding of the benzyl group in the hydrophobic S₁ cavity removes two water-hydrophobic interfaces (i.e., substrate and protein), so the value might be as high as 5.5 kcal/mol.³⁷ Since the S₁ pocket lies on the surface of the protein and the benzyl group is not completely buried, we estimate the energy for this hydrophobic interaction to be 2.7–5.5 kcal/mol.^{36a,b,37}

(39) Estimated from the van der Waals radii of chlorine (1.75 Å) and hydrogen (1.20 Å) and the O-H bond length (0.96 Å) from: Bondi, A. *J. Phys. Chem.* **1964**, *68*, 441–451.

(40) Jeffrey, G. A.; Saenger, W. *Hydrogen Bonding in Biological Structures*; Springer-Verlag: Berlin, 1991; pp 29–31.

(41) Removal of a hydrogen bond donor or acceptor in an enzyme active site weakens binding by 0.5–1.5 kcal/mol.³⁷ Although the hydrogen bond inventory is zero (i.e., the number of hydrogen bonds is the same for both the free enzyme and the enzyme-substrate complex), hydrogen bonds between an enzyme and substrate increase the entropy due to the release of bound water molecules.

(42) This reasoning predicts lower *K_M* values for **1h** and **1c** than for **1a**, but low solubility of these substrates (<5 mM) prevented us from testing this prediction.

(43) (a) Fitzpatrick, P. A.; Klibanov, A. M. *J. Am. Chem. Soc.* **1991**, *113*, 3166–3171. (b) Kazlauskas, R. J.; Weissfloch, A. N. *E. J. Mol. Catal.* **1997**, *3*, 65–72.

from ab initio calculations and from force field parameters for a sulfonamide-based inhibitor⁴⁶ also derived from ab initio calculations (see Supporting Information for details). Using these estimates, we expect only a qualitative rationalization of the enantioselectivity of subtilisin E with *N*-acylsulfonamides.

Modeling **1h** with subtilisin E gave one productive conformation for each enantiomer (Table 4). The two other plausible conformations encountered severe steric clash with the protein.⁴⁷ The productive complex of (*R*)-**1h** had its *p*-tolyl group bound in the S₁' pocket and the sulfoxide oxygen exposed to solvent water (Figure 2). All hydrogen bond angles were >120°, and all five hydrogen bond lengths were <3.1 Å (Table 4). The *p*-tolyl group appears to just fit in the S₁' pocket: Met222 in the bottom of the S₁' pocket, Tyr217 at the back of the S₁' pocket, and catalytic His64 bumped the *p*-tolyl group.⁴⁷ This tight fit suggests a favorable hydrophobic interaction between the tolyl group and the S₁' residues.

The productive complex of the slower-reacting (*S*)-**1h** had its sulfoxide oxygen in the S₁' pocket and the tolyl group exposed to solvent water (Figure 2). All hydrogen bond angles were >120°, and all five hydrogen bond lengths were <3.1 Å (Table 4). The sulfoxide oxygen fits well in the S₁' pocket, and the protein does not hinder the *p*-tolyl group.⁴⁷ Unlike the favored enantiomer, the smaller oxygen does not make steric contact with S₁' residues. Although the slow-reacting (*S*)-enantiomer avoids steric hindrances, it also lacks favorable hydrophobic interactions between the tolyl group and the S₁' residues. Using octanol–water partitioning data, we estimate that the hydrophobic interactions favor binding of (*R*)-**1h** by ~6.4 kcal/mol over the (*S*)-enantiomer in water.⁴⁴ The (*R*)-enantiomer places the hydrophobic aryl group in the S₁' pocket and the hydrophilic sulfoxide oxygen in the solvent (water), while the (*S*)-enantiomer does the opposite.

Consistent with this explanation, the enantioselectivity of the subtilisin-E-catalyzed hydrolysis of **1h** decreased from *E* > 150 in 9:1 water/acetonitrile to *E* = 12 in 1:9 water/acetonitrile. Similarly, the enantioselectivity with **1c** decreased from *E* > 150 in 9:1 water/acetonitrile to *E* = 41 in 1:9 water/acetonitrile. The high concentration of acetonitrile favors the *p*-tolyl group in the solvent; thus, the enantiomer preference shifts toward the (*S*)-enantiomer, which orients with the oxygen in the S₁' pocket and the tolyl group in solvent. This result suggests that the enantioselectivity for acylation of sulfonamides in organic solvent would also be low, but we did not detect any acylation of *p*-toluenesulfonamide, consistent with Ellman's earlier report of no reaction.¹⁵

The decreasing enantioselectivity with the larger sulfonamides, **5c** (*E*_{true} = 98) and **6c** (*E*_{true} = 13), and the loss of enantiose-

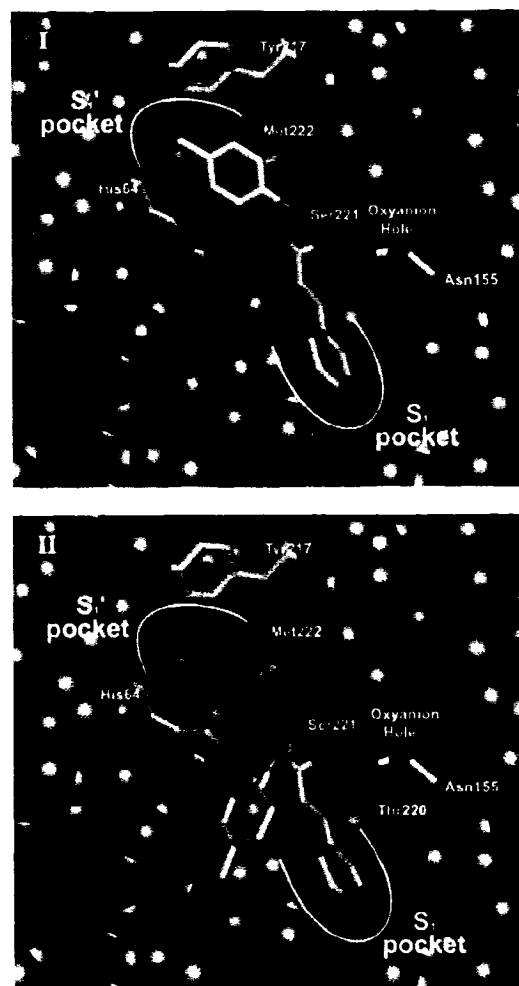


Figure 2. Catalytically productive tetrahedral intermediates for the subtilisin-E-catalyzed hydrolysis of fast-reacting (*R*)-**1h** (I) and slow-reacting (*S*)-**1h** (II), as identified by molecular modeling. The important active site and substrate atoms (sticks) are colored as follows: gray (carbon), red (oxygen), blue (nitrogen), and orange (sulfur). Surrounding atoms (space fill) of subtilisin are shown in blue. For clarity, all hydrogen atoms and water molecules are hidden. Both I and II maintain all catalytically essential hydrogen bonds, and the benzyl moiety of the dihydrocinnamoyl group binds in the S₁ pocket, as expected based on its similarity to phenylalanine.²⁹ In the fast-reacting enantiomer, (*R*)-**1h** (I), the *p*-tolyl group binds in the hydrophobic S₁' pocket and sulfoxide oxygen is exposed to solvent water. In the slow-reacting enantiomer, (*S*)-**1h** (II), the sulfoxide oxygen binds in the hydrophobic S₁' pocket and the *p*-tolyl group is exposed to solvent water. The nonproductive conformations (not shown) encountered severe steric clash with the active site residues.

lectivity with the very large sulfonamide, **7c** (*E*_{true} = 1.2), are also consistent with this explanation for enantioselectivity. Larger aryl substituents increase the steric hindrance in the S₁' pocket, which overwhelms the energy gained through a hydrophobic interaction between the pocket and the aryl group and, therefore, reduces the enantioselectivity. In other words, when either the aryl group or sulfoxide oxygen can fit in the S₁' pocket (1–4), a hydrophobic interaction favors the aryl group and the enantioselectivity is high. However, as the aryl group becomes larger, increased steric hindrance with S₁' residues oppose the hydrophobic interaction and lower the enantioselectivity (5–7). Modeling with **7c** suggests that this sulfonamide leaving group is too large for the S₁' pocket and binds above it (see Supporting Information Figure S2).

(44) The incremental Gibbs free energy of transfer from *n*-octanol to water for the tolyl group was estimated to be ca. +3.4 kcal/mol, and the sulfoxide oxygen was ca. -3.0 kcal/mol using $\Delta G_{\text{trans}} = 2.303RT\pi$, where π is the hydrophobicity constant of the group relative to hydrogen.^{36a,b,37} Switching from (*S*)-**1h** to (*R*)-**1h** places the tolyl group into a hydrophobic pocket (3.4 kcal/mol for the tolyl group) and removes the sulfoxide group from the hydrophobic pocket (3.0 kcal/mol) for a total of 6.4 kcal/mol in water. The hydrophobicity constant of the tolyl group ($\pi = 2.52$) was estimated by adding π values of a phenyl and a methyl group.^{36d} The hydrophobicity constant of the sulfoxide oxygen ($\pi = -2.19$) was estimated by subtracting π values of a methyl sulfide group from a methyl sulfoxide group.^{36d} The energy difference may be higher if one includes the hydrophobic surface of the S₁' pocket.

(45) Bharatam, P. V.; Kaur, A.; Kaur, D. J. *Phys. Org. Chem.* **2002**, *15*, 197–203.

(46) Rossi, K. A.; Merz, K. M., Jr.; Smith, G. M.; Baldwin, J. J. *J. Med. Chem.* **1995**, *38*, 2061–2069.

(47) See Supporting Information for complete molecular modeling details.

Discussion

In this paper, we identified subtilisin E as the most suitable hydrolase of those examined for preparation of enantiopure arylsulfonamides. The reactivity and enantioselectivity of subtilisin E toward *N*-acyl arylsulfonamides depend on the *N*-acyl group. Simple *N*-acyl compounds, such as *N*-acetyl and *N*-butanoyl, did not react with subtilisin E. Molecular modeling suggests that the reactive acyl groups may mimic a phenylalanine moiety. Other research groups have also modified unreactive substrates to convert them into good substrates. For example, the fungus *Beauveria bassiana* did not hydroxylate cyclopentanone, but did hydroxylate the *N*-benzoylspirooxazolidine derivative with high yield and diastereoselectivity.⁴⁸ In a second example, changing from the 2-pyridylacetyl to the 4-pyridylacetyl increased the rate 8-fold and the enantioselectivity 3-fold for a penicillin G acylase-catalyzed hydrolysis of 1-phenethyl esters.⁴⁹ In a third example, the enantioselectivity of *Pseudomonas cepacia* lipase-catalyzed acylation of 2-[(*N,N*-dimethylcarbamoyl)methyl]-3-cyclopenten-1-ol varied from *E* = 4 to 156, depending on the acylating agent.⁵⁰

There are three synthetic routes to enantiopure sulfonamides: the method of Davis and co-workers¹² for *p*-toluenesulfonamide, the method of Ellman and co-workers⁶ for *tert*-butylsulfonamide, and the method of Senanayake and co-workers¹⁶ for a variety of alkyl- and arylsulfonamides. Using subtilisin E, we resolved gram quantities of **1h**, **3h**, and **5c**. These resolutions were simple, convenient, and inexpensive. Our strategy does not provide us with as wide a variety of enantiopure sulfonamides as reported by Senanayake, but the selectivity and mildness of the biocatalytic route make it the preferred route when there is a choice. The biocatalytic route is amenable to scale-up, is environmentally acceptable, and is performed under mild conditions. As well, the catalyst, subtilisin E, is inexpensive to produce and could be recycled.

Molecular modeling of the first tetrahedral intermediate for subtilisin-E-catalyzed hydrolysis of **1h** suggests that the (*R*)-enantiomer reacts faster because of preferential binding of the nonpolar *p*-tolyl group in the hydrophobic S₁' pocket versus the polar sulfoxide oxygen, which prefers to be exposed to solvent water. Changing the solvent to 1:9 water/acetonitrile decreased the enantioselectivity. A similar decrease in enantioselectivity occurred for subtilisin-catalyzed reactions of amino acid derivatives.⁵¹ In water, subtilisin Carlsberg showed high enantioselectivity for the hydrolysis of a natural L-amino acid ester, but in organic solvent, transesterification was 1–2 orders of magnitude less enantioselective. Klivanov and co-workers suggested that the L-amino acid, but not the D-amino acid, binds to the hydrophobic S₁ pocket. Water as the solvent favors this interaction; thus, the enantioselectivity is higher in water. As expected, the difference in enzyme enantioselectivity was greater for amino acid derivatives with more hydrophobic side chains.

Subtilisins usually show only low to moderate enantioselectivity with secondary alcohols and isosteric amines, but high

enantioselectivity with the structurally related sulfonamides. For secondary alcohols and isosteric primary amines, the substituents are usually both hydrophobic, so the hydrophobic binding contribution differences are smaller than those for arylsulfonamides, where the substituents are the polar sulfoxide oxygen and the hydrophobic aryl group. This polarity difference between the two substituents appears to dominate subtilisin E's enantioselectivity of arylsulfonamides, resulting in high enantioselectivity.

Experimental Section

General. ¹H and ¹³C NMR spectra were obtained as dilute CDCl₃ solutions at 300 and 75 MHz, respectively. Chemical shifts are expressed in parts per million (δ) and are referenced to tetramethylsilane or trace CHCl₃ in CDCl₃. Coupling constants are reported in hertz (Hz). HPLC analyses were performed on a 4.6 × 250 mm Daicel Chiralcel OD or Chiralpak AD column (Chiral Technologies, Exton, U.S.A.) and monitored at 238 or 222 nm. Flash chromatography with silica gel (230–400 mesh) or preparative TLC (20 × 20 cm, 1000 μm) was used to purify all intermediates and substrates. Visualization of UV-inactive materials on TLC was accomplished using phosphomolybdic acid or ninhydrin followed by heating. All reagents, buffers, starting materials, and anhydrous solvents were purchased from Sigma-Aldrich Canada (Oakville, Canada) and used without purification. All air- and moisture-sensitive reactions were performed under N₂. The pBE3 *Escherichia coli*–*Bacillus subtilis* shuttle vector,^{26b} containing the subtilisin E gene, was kindly provided by Dr. F. Arnold (Caltech), and the *Bacillus subtilis* strain DB104⁵² was a gift from Dr. S. L. Wong (University of Calgary).

Synthesis of Substrates. Sulfonamides (1–8). We prepared racemic sulfonamides **1–8** using literature procedures (Scheme 3).^{20–22} The relevant analytical data are in the Supporting Information.

***N*-Acylsulfonamides.** We prepared *N*-acylsulfonamides by treating sulfonamides **1–8** with 2 equiv of *n*-BuLi in THF, followed by rapid addition of the symmetrical anhydride of the appropriate carboxylic acid.⁵³ The relevant analytical data are given below or in the Supporting Information.

***N*-Chloroacetyl-*p*-toluenesulfonamide (1c)** was obtained as a white solid (186 mg, 50%): mp 119–121 °C; ¹H NMR δ 2.43 (s, 3H, PhCH₃), 4.29 (s, 2H, C(O)CH₂Cl), 7.31 (d, *J* = 8.1, 2H), 7.63 (d, *J* = 8.1, 2H); ¹³C NMR δ 21.8 (PhCH₃), 42.5 (C(O)CH₂Cl), 124.8, 130.6, 139.9, 143.5 (phenyl), 167.2 (C=O); HRMS calcd for C₉H₁₀ClNO₂S (M⁺) 231.0120, found 231.0123. The enantiomers were separated by HPLC (Daicel Chiralcel OD column, 90:10 hexanes/EtOH, 0.5 mL/min, 238 nm; (*R*)-**1c**, *t*_R = 21.3 min; (*S*)-**1c**, *t*_R = 51.4 min).

***N*-Dihydrocinnamoyl-*p*-toluenesulfonamide (1h)** was obtained as a white solid (550 mg, 59%): mp 85–87 °C (lit.²⁰ mp 94–96 °C); ¹H NMR δ 2.43 (s, 3H, PhCH₃), 2.70 (m, 2H, C(O)CH₂), 3.01 (t, *J* = 7.8, 2H, CH₂Ph), 7.17–7.29 (m, 7H, phenyl), 7.41 (d, *J* = 8.1, 2H, phenyl), 7.81 (br s, 1H, NH); ¹³C NMR δ 21.9 (tolyl CH₃), 31.2 (CH₂Ph), 37.9 (C(O)CH₂), 124.9, 126.6, 128.7, 128.8, 130.1, 140.1, 140.3, 142.6 (phenyl), 173.6 (C=O). The enantiomers were separated by HPLC (Daicel Chiralcel OD column, 90:10 hexanes/EtOH, 0.5 mL/min, 238 nm; (*R*)-**1h**, *t*_R = 20.4 min; (*S*)-**1h**, *t*_R = 22.4 min).

Hydrolase Library. All screening was performed at pH 7.2. The hydrolases were dissolved in BES buffer (5.0 mM, pH 7.2) at the concentration listed in Table 1, centrifuged for 10 min at 2000 rpm, and titrated to pH 7.2. The supernatant was used for screening.

Screening of Commercial Hydrolases with pH Indicators. The assay solution was prepared by mixing **1c** (1 mL of a 440 mM solution in CH₃CN) and *p*-nitrophenol (6.71 mL of a 1.0 mM solution in 5.0 mM BES, pH 7.2) with BES buffer (5.14 mL of a 5.0 mM solution, pH 7.2). Hydrolase solutions (10 μL/well) were transferred to a 96-

(48) (a) Braunegg, G.; de Raadt, A.; Feichtenhofer, S.; Griengl, H.; Kopper, I.; Lehman, A.; Weber, H.-J. *Angew. Chem., Int. Ed.* **1999**, *38*, 2763–2766. (b) de Raadt, A.; Griengl, H.; Weber, H. *Chem.-Eur. J.* **2001**, *7*, 27–31.

(49) Pohl, T.; Waldmann, H. *Tetrahedron Lett.* **1995**, *36*, 2963–2966.

(50) Ema, T.; Maeno, S.; Takaya, Y.; Sakai, T.; Utaka, M. *J. Org. Chem.* **1996**, *61*, 8610–8616.

(51) (a) Zaks, A.; Klivanov, A. M. *J. Am. Chem. Soc.* **1986**, *108*, 2767–2768. (b) Margolin, A. L.; Tai, D.-F.; Klivanov, A. M. *J. Am. Chem. Soc.* **1987**, *109*, 7885–7887. (c) Sakurai, T.; Margolin, A. L.; Russell, A. J.; Klivanov, A. M. *J. Am. Chem. Soc.* **1988**, *110*, 7236–7237.

(52) Kawamura, F.; Doi, R. H. *J. Bacteriol.* **1984**, *160*, 442–444.

(53) Chen, F. M. F.; Kuroda, K.; Benoiton, N. L. *Synthesis* **1978**, *12*, 928–930.

well microtiter plate followed by assay solution (90 μ L/well). The final concentration in each well was 3.1 mM substrate, 4.65 mM BES, 0.46 mM *p*-nitrophenol in a total volume of 100 μ L 7% acetonitrile in buffer. The plate was shaken for 5 s on the microplate reader, and the absorbance decrease was monitored at 404 nm for 1 h. The assay was performed in quadruplicate at 25 and 37 $^{\circ}$ C.²³ The low pK_a of the *N*-acetylsulfonamide NH group (ca. pK_a 6) reduced the sensitivity of the assay by protonating the pH indicator, *p*-nitrophenoxide, but a decrease in the absorbance could still be observed at pH 7.2.

Small-Scale Reactions with Commercial Hydrolases to Determine Enantioselectivity. Reactions of *N*-chloroacetylsulfonamides with commercial enzymes were carried out at 25 $^{\circ}$ C. For example, proteinase from *B. subtilis* var. biotus A (16 mg) and substrate (5 mM in CH₃CN) in a total volume of 10 mL of buffer (20 mM BES, pH 7.2) were stirred together in reaction vials for 3–6 h. Upon completion, the aqueous phase was extracted with CH₂Cl₂ (2 \times 10 mL). The combined organic layers were dried over anhydrous Na₂SO₄ and concentrated in vacuo. The residue was dissolved in 1 mL of EtOH, filtered through a nylon filter (0.45 μ m), and analyzed by HPLC (Daicel OD column, 90:10 hexanes/EtOH, 1.0 mL/min, 238 nm).

Cultivation and Isolation of Subtilisin E. Protease-deficient *B. subtilis* DB104 was transformed with vector pBE3, as previously described.^{26b,34} Protease-deficient *B. subtilis* DB104 secretes proteases into the culture medium and accumulates them to a high level. Endogenous protease activity is less than 3%.³² Cells were grown in Schaeffer's sporulation medium (2XSG) supplemented with kanamycin (50 μ g/mL). Enzyme activity was monitored by adding 90 μ L of assay solution [0.2 mM succinyl-AAPF-*p*-nitroanilide (suc-AAPF-*p*NA)/100 mM Tris pH 8.0/10 mM CaCl₂] to 10 μ L of supernatant and following the reaction at 410 nm at 37 $^{\circ}$ C for 15 min. When maximal activity was reached (48 h), the cells were centrifuged, and the supernatant was filter sterilized and lyophilized. The residue was dissolved in 10 or 50 mM Tris buffer (pH 8.0, 10 mM CaCl₂), and the initial activity was assessed as above. Typical activity of the supernatant or prepared solution was 10–20 U/mL, with suc-AAPF-*p*NA.

Hydrolysis of *N*-Acetylsulfonamides with Subtilisin E. Reactions of *N*-acetylsulfonamides with subtilisin E were carried out at 37 $^{\circ}$ C. Each mixture consisted of subtilisin E (solution in 10 mM Tris buffer (pH 8.0, 1 mM CaCl₂), 178 μ L), CaCl₂ (1 M, 2 μ L), and substrate (50 mM in CH₃CN, 20 μ L). The reaction was allowed to continue for 3 h with *N*-bromoacetyl and *N*-chloroacetyl sulfonamides and for 24 h with all other substrates. The reaction was diluted with dH₂O (400 μ L) and terminated with the addition of CH₂Cl₂ (500 μ L). The organic layer was removed, and the aqueous layer was twice extracted with CH₂Cl₂ (500 μ L). The phases were separated by centrifugation, and the organic layers were collected. The combined organics were evaporated under a stream of N₂, and the residue was diluted with EtOH (150 μ L) for analysis by HPLC (Brownlee Si-10 silica column followed by Daicel OD column, 90:10 hexanes/EtOH, 0.6 mL/min, 238 or 222 nm). Although the chiral column separated enantiomers, it did not separate the substrate and product. This two-column system separated the substrate and product in the silica column and the enantiomers of each in the chiral column.

Gram-Scale Resolution of *N*-Acetylsulfonamides. **1h.** Substrate (3.59 g, 12.5 mmol) in CH₃CN (50 mL) was added to enzyme solution (450 mL, ca. 20 U/mL with suc-AAPF-*p*NA) and incubated at 37 $^{\circ}$ C until ca. 50% conversion (3 days), as determined by HPLC. The mixture was filtered through Celite, extracted with CH₂Cl₂ (3 \times 200 mL), dried over Na₂SO₄, and concentrated in vacuo. Separation of substrate and product on silica (1:1 EtOAc/hexanes to EtOAc) gave (*R*)-**1** (840 mg, 42%, 95% ee) and (*S*)-**1h** (1.53 g, 43%, 95% ee), as determined by HPLC. Remaining starting material (*S*)-**1h** (144 mg, 0.5 mmol) was treated with hydrazine hydrate (1 mL) at 0 $^{\circ}$ C followed by stirring at

RT until the reaction was complete by TLC (3 h). The reaction mixture was diluted with CH₂Cl₂ (15 mL) and washed with 1 N HCl (2 \times 10 mL), saturated NaHCO₃ (2 \times 10 mL), and saturated NaCl (10 mL). The organic layer was dried over Na₂SO₄ and concentrated in vacuo to give (*S*)-**1** (70 mg, 90%, 95% ee).

3h. Substrate (4.00 g, 13.0 mmol) in MeCN (100 mL) was added to enzyme solution (900 mL, ca. 15 U/mL with suc-AAPF-*p*NA) and incubated at 37 $^{\circ}$ C until ca. 40% conversion (3 days), as determined by HPLC. The mixture was filtered through Celite, extracted with CH₂Cl₂ (3 \times 200 mL), dried over Na₂SO₄, and concentrated in vacuo. Separation of substrate and product on silica (1:1 EtOAc/hexanes to EtOAc) gave (*R*)-**3** (683 mg, 30%, 97% ee) and (*S*)-**3h** (2.42 g, 60%, 64% ee). Recrystallization from EtOAc/hexanes gave (*S*)-**3h** (1.09 g, 27%, 99% ee), as determined by HPLC. Remaining starting material (*S*)-**3h** (155 mg, 0.5 mmol) was treated with hydrazine hydrate (1 mL) at 0 $^{\circ}$ C followed by stirring at RT until the reaction was complete by TLC (3 h). The reaction mixture was diluted with CH₂Cl₂ (15 mL) and washed with 1 N HCl (2 \times 10 mL), saturated NaHCO₃ (2 \times 10 mL), and saturated NaCl (10 mL). The organic layer was dried over Na₂SO₄ and concentrated in vacuo to give (*S*)-**3** (81 mg, 92%, 99% ee).

5c. Substrate (1.90 g, 7.30 mmol) in CH₃CN (30 mL) was added to enzyme solution (270 mL, ca. 20 U/mL with suc-AAPF-*p*NA) and incubated at 37 $^{\circ}$ C until ca. 49% conversion (6 h), as determined by HPLC. The mixture was filtered through Celite, extracted with CH₂Cl₂ (3 \times 200 mL), dried over Na₂SO₄, and concentrated in vacuo to give the crude mixture of substrate and product. Separation of substrate and product on silica (2:1 EtOAc/hexanes to EtOAc) gave (*R*)-**5** (520 mg, 39%, 90% ee) and (*S*)-**5c** (860 mg, 45%, 82% ee). Recrystallization from EtOAc/hexanes gave (*R*)-**5** (395 mg, 30%, 99% ee), as determined by HPLC. Remaining starting material was hydrolyzed in 1 N KOH (1:1 H₂O/EtOH) for 1 h at RT. The reaction mixture was extracted with CH₂Cl₂ (3 \times 15 mL), dried over Na₂SO₄, and concentrated in vacuo to give (*S*)-**5** (295 mg, 22%, 99% ee) after recrystallization.

Modeling of Tetrahedral Intermediates Bound to Subtilisin E. All modeling was performed using Insight II 2000.1/Discover (Accelrys, San Diego, CA) on an SGI Octane UNIX workstation using the AMBER force field.⁵⁵ We used a nonbonded cutoff distance of 8 Å and a distance-dependent dielectric of 1.0, and we scaled the 1–4 van der Waals interactions by 50%. Protein structures in Figures 2 and S1 (Supporting Information) were created using PyMOL (Delano Scientific, San Carlos, CA). The X-ray crystal structure of subtilisin E (entry 1SCJ)²⁷ from the Protein Data Bank is a Ser221Cys subtilisin E–propeptide complex. Using the Builder module of Insight II, we replaced the Cys221 with a serine and removed the propeptide region. The hydrogen atoms were added to correspond to pH 7.0. Histidines were uncharged, aspartates and glutamates negatively charged, and arginines and lysines positively charged. The catalytic histidine (His64) was protonated. The positions of the water hydrogens and then the enzyme hydrogens were optimized using a consecutive series of short (1 ps) molecular dynamic runs and energy minimizations.⁵⁶ This optimization was repeated until there was <2 kcal/mol in the energy of the minimized structures. Thereafter, an iterative series of geometry optimizations were performed on the water hydrogens, enzyme hydrogens, and full water molecules. Finally, the whole system was geometry optimized.

The tetrahedral intermediates were built manually and covalently linked to Ser221. Since the parameters for the sulfonamide group were not included in the AMBER force field, they were assigned in analogy to existing parameters.^{45–47} The geometric properties of the sulfonamide

(54) Harwood, C. R.; Cutting, S. M. *Molecular Biological Methods for Bacillus*; John Wiley & Sons: Chichester, U.K., 1990; pp 33–35 and 391–402.

(55) (a) Weiner, S. J.; Kollman, P. A.; Case, D. A.; Singh, U. C.; Ghio, C.; Alagona, G.; Profeta, S.; Weiner, P. *J. Am. Chem. Soc.* **1984**, *106*, 765–784. (b) Weiner, S. J.; Kollman, P. A.; Nguyen, D. T.; Case, D. A. *J. Comput. Chem.* **1986**, *7*, 230–252.

(56) Raza, S.; Fransson, L.; Hult, K. *Protein Sci.* **2001**, *10*, 329–338.

moiety of minimized **1h** were compared to an available X-ray crystal structure⁵⁷ and adjusted as necessary. Nonstandard partial charges were calculated using a formal charge of -1 for the substrate oxyanion. Energy minimization proceeded in three stages: first, minimization of substrate with only the protein constrained ($25 \text{ kcal mol}^{-1} \text{ \AA}^{-2}$); second, minimization with only the protein backbone constrained ($25 \text{ kcal mol}^{-1} \text{ \AA}^{-2}$); and for the final stage, the minimization was continued without constraints until the root mean square value was less than $0.0005 \text{ kcal mol}^{-1} \text{ \AA}^{-1}$. A catalytically productive complex required all five hydrogen bonds within the catalytic machinery. We set generous limits for a hydrogen bond: a donor to acceptor atom distance of less than 3.1 \AA with a nearly linear arrangement ($>120^\circ$ angle) of donor atom, hydrogen, and acceptor atom. Structures lacking any of the five catalytically relevant hydrogen bonds or encountering severe steric clash with enzyme were deemed nonproductive.

Acknowledgment. We thank the donors of the Petroleum Research Fund administered by the American Chemical Society, and McGill University for financial support. C.K.S. thanks the

Natural Sciences and Engineering Research Council (Canada) for a postgraduate fellowship. We thank Dr. Frances Arnold (California Institute of Technology, USA) for the subtilisin E plasmid, Dr. S. L. Wong (University of Calgary, Canada) for the *B. subtilis* DB104 cells, Dr. Fred Schendel and Rick Dillingham (University of Minnesota Biotechnology Institute, USA) for the large-scale fermentation and purification of subtilisin E, Dr. Ronghua Shu (McGill University) for the initial substrate synthesis and screening experiments, Linda Fransson (Royal Institute of Technology (KTH), Sweden), and the Minnesota Supercomputing Institute (University of Minnesota, USA) for assistance with the modeling software.

Supporting Information Available: Synthesis and characterization data for compounds **1–8**, enantioselectivity of *Bacillus subtilis* var. *biotecnus* A with **2c–5c**, complete molecular modeling details, and the modeling figures for **7c**. This material is available free of charge via the Internet at <http://pubs.acs.org>.

JA045397B

(57) Robinson, P. D. *Acta Crystallogr.* **1991**, *C47*, 594–596.

How Substrate Solvation Contributes to the Enantioselectivity of Subtilisin toward Secondary Alcohols

Christopher K. Savile and Romas J. Kazlauskas*

Department of Chemistry, McGill University, 801 Sherbrooke Street West, Montréal, Québec, Canada, H3A 2K6, and Department of Biochemistry, Molecular Biology & Biophysics and the Biotechnology Institute, University of Minnesota, 1479 Gortner Avenue, St. Paul, Minnesota 55108

Received May 3, 2005; E-mail: rjk@umn.edu

Enantioselective enzymes, especially hydrolases, are useful catalysts to make enantiomerically pure pharmaceuticals, agrochemicals, and fine chemicals.¹ Several empirical rules predict which substrate/hydrolase combinations work best. For example, a rule to predict the enantiopreference of subtilisin toward secondary alcohols is based on the size of the substituents at the stereocenter (Figure 1a).^{2,3} This model implies that subtilisin has two differently sized pockets for these substituents, but several experiments are inconsistent with this rule. First, the X-ray crystal structure shows only one pocket (the S_1' pocket) to bind secondary alcohols.⁴ Second, the rule often predicts the incorrect enantiomer for reactions in water. In this communication, we resolve this contradiction with a more general rule that shows subtilisin binds only one substituent of a secondary alcohol and leaves the other in solvent. This refined rule allows quantitative design of enantioselective reactions and rationalizes why solvent alters the enantioselectivity.

X-ray crystal structures of subtilisin reveal one pocket (the S_1' pocket) that binds the alcohol portion of an ester. Molecular modeling of a tetrahedral intermediate for subtilisin E-catalyzed hydrolysis of **1a** reveals that (*S*)-**1a** places the methyl group in the S_1' pocket, while (*R*)-**1a** places the phenyl group in this pocket (see SI Figure S2). In both cases, the other substituent remains in the solvent. The S_1' pocket is a shallow crevice large enough to accommodate para-substituted aryl groups, but too small for multisubstituted aryl groups.

Although the rule in Figure 1a is reliable for reactions in organic solvents,^{2,3} it is not reliable in water. In organic solvent, the subtilisin-catalyzed transesterification of secondary alcohols **1–13** with dihydrocinnamic acid vinyl ester favored the predicted (*S*)-enantiomer for 26 out of 29 reactions with varying enantioselectivity ($E = 1.5$ to 66; see SI Tables S2–S4). In water, however, subtilisin favored hydrolysis of the opposite (*R*)-enantiomer in most cases: 20 out of 33 reactions (Table 1).

To resolve these contradictions, we propose a revised rule for the enantiopreference of subtilisins with secondary alcohols (Figure 1b). This rule places one substituent in solvent and limits the size of the other substituent to approximately the size of a phenyl group. This rule predicts that solvation of one substituent contributes to the enantiopreference of subtilisin. In particular, placing a nonpolar substituent in water is unfavorable. Reactions in water involving methyl and nonpolar aryl substituents will favor the nonpolar aryl substituent in the S_1' pocket, opposite to that predicted based on size alone. Thus, the revised rule predicts that subtilisin favors the (*R*)-enantiomer of **3a** in water, but the (*S*)-enantiomer in organic solvents. On the other hand, with a polar aryl group such as that in **5a** (4-pyridine *N*-oxide), the (*S*)-enantiomer is favored both in water, where solvation of the pyridine *N*-oxide is favorable, and in organic solvent, where placing the pyridine *N*-oxide in the solvent avoids steric interactions in the S_1' pocket.

The revised rule in Figure 1b correctly predicted the (*R*)-enantiomer for reactions in water for substrates with hydrophobic

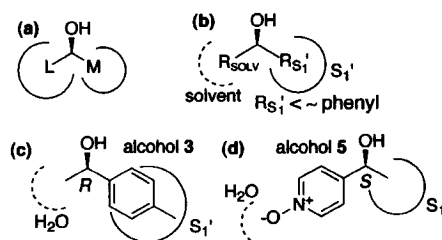


Figure 1. Empirical rules that predict the enantiopreference of subtilisins toward secondary alcohols. (a) A rule based on relative substituent size, where L is the large substituent and M is the medium substituent, is reliable in organic solvent. (b) A revised rule that is reliable in water as well. One substituent (R_{sol}) remains in solvent, while the other ($R_{S_1'}$) binds in a hydrophobic pocket. (c) In water, the nonpolar aryl group of alcohol **3** favors binding in the S_1' pocket, thus favoring the (*R*)-enantiomer. (d) An isosteric substrate alcohol **5** contains a polar aryl group that favors the water-solvated orientation, thus favoring the (*S*)-enantiomer.

Table 1. Enantioselectivity of Subtilisin BPN[−], Carlsberg[−], and E-catalyzed Hydrolysis of **1a–13a**^a

entry	substrate	log P/P_0 diff. ^c	enantioselectivity, E^b		
			subtilisin E	subtilisin Carlsberg	subtilisin BPN [−]
1	1a	+1.1	7.0 (<i>R</i>)	1.2 (<i>R</i>)	15 (<i>R</i>)
2	2a	−0.3	1.5 (<i>R</i>)	1.7 (<i>S</i>)	2.6 (<i>R</i>)
3	3a	+1.6	16 (<i>R</i>)	1.1 (<i>S</i>)	37 (<i>R</i>)
4	4a	+1.9	7.7 (<i>R</i>)	2.2 (<i>S</i>)	9.9 (<i>R</i>)
5	5a	−2.2	4.5 (<i>S</i>)	3.1 (<i>S</i>)	2.5 (<i>S</i>)
6	<i>N</i> -HCinn- <i>p</i> -TS ^d	+3.9	>150 (<i>R</i>) ^e	11 (<i>R</i>) ^f	50 (<i>R</i>) ^g
7	6a	+2.6	110 (<i>R</i>)	2.5 (<i>S</i>)	109 (<i>R</i>)
8	7a	+0.7	2.8 (<i>R</i>)	2.3 (<i>S</i>)	4.2 (<i>R</i>)
9	8a	−3.1	5.5 (<i>S</i>)	3.6 (<i>S</i>)	6.2 (<i>S</i>)
10	9a ^h		20 (<i>R</i>)	2.0 (<i>R</i>)	18 (<i>R</i>)
11	10b ^h		17 (<i>R</i>)	1.7 (<i>S</i>)	4.9 (<i>R</i>)
12	11a ^h		1.8 (<i>R</i>)	3.1 (<i>S</i>)	3.1 (<i>S</i>)
13	12b		n.r. ^h	n.r.	n.r.
14	13a		n.r.	n.r.	n.r.

^a See SI Tables S2–S5 for complete details. ^b Relative rate of the fast vs slow enantiomer. ^c Substituent hydrophobicity difference ($\log P/P_0$ Large substituent − $\log P/P_0$ Medium substituent). ^d *N*-Dihydrocinnamoyl-*p*-toluenesulfonamide. This is a secondary alcohol ester isostere with the methine replaced with sulfur and the methyl replaced with oxygen. ^e Reference 6. ^f Reference 7. ^g Not included in Figure 2 because one substituent is much larger than phenyl. ^h No reaction.

aryl groups (**1a**, **3a**, **6a**, **9a**, **10a**, and **11b**) for 14 out of 18 reactions and the (*S*)-enantiomer for substrates with hydrophilic aryl groups (**2a**, **5a** and **8a**) for eight of nine reactions. It is difficult to predict the favored enantiomer for moderately hydrophilic aryl groups (**4a** and **7a**), and indeed the enantioselectivity in these cases is low to

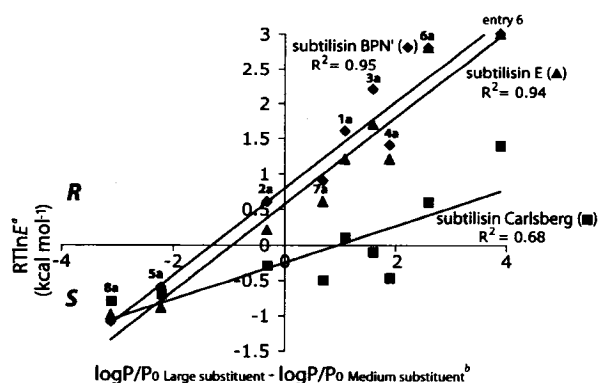


Figure 2. Differences in substituent hydrophobicity affect the enantioselectivity subtilisins toward secondary alcohols. All reactions are in water. This plot does not include substrates **9a–11a** because their substituted aryl groups are too large to fit in the S_1' pocket of subtilisins. (a) Enantioselectivity data from Table 1 is given in energy using $\Delta\Delta G^\ddagger = -RT \ln E$. (b) Hydrophobicity partition coefficient ($\log P/P_0$).

moderate ($E = 2.2$ to 9.9). With nonpolar substituents and nonpolar solvents, the rule simplifies to the previous rule in Figure 1a.

The revised rule also suggests a quantitative link between enantioselectivity and solvation of the substituents. For example, reaction of dihydrocinnamoyl esters **1a–13a** with subtilisin E showed that the enantioselectivity toward secondary alcohol esters in water varied linearly with the difference in hydrophobicity ($\log P/P_0$)⁸ between the large aryl substituent and the methyl group (Figure 2). This hydrophobicity difference accounts for the solvation of one substituent in water and the other in the hydrophobic S_1' pocket. Increases in hydrophobicity of the aryl group favored the (*R*)-enantiomer, while decreases favored the (*S*)-enantiomer. For example, subtilisin E-catalyzed hydrolysis of **6a** containing the nonpolar 4-isopropylphenyl group gave (*R*)-**6** with $E = 110$, while **7a** containing the more polar, but similar sized 4-nitrophenyl group gave (*R*)-**7** with lower enantioselectivity ($E = 2.8$), and **8a** containing the hydrophilic carboxylate group gave the opposite enantiomer (*S*)-**8** with $E = 5.5$. Subtilisin BPN' showed similar enantioselectivity toward substrates **1a–13a** consistent with the similar S_1' pocket in both cases. The enantioselectivity of subtilisin Carlsberg was lower, and the change in enantioselectivity (slope of the line in Figure 2) varied less with changes in substituent hydrophobicity, presumably due to weaker interaction between substrate and S_1' pocket.

This revised model also predicts that increasing the polarity difference between the substituents will increase the enantioselectivity of subtilisins. Consistent with this prediction, subtilisin shows high enantioselectivity toward arylsulfonamides (entry 6).⁶ This toluenesulfonamide is a polar isostere of **3a**, where a polar oxygen replaces the methyl group and thereby increases the difference in polarity between the two substituents ($\log P$ difference = +1.6 for **3a** and +3.9 for the sulfonamide). The enantioselectivity of the subtilisin-E-catalyzed hydrolysis increases from $E = 16$ for **3a** to $E = >150$ for the sulfonamide.

Increasing the hydrophobicity difference by adding nonpolar substituents to the aryl group is not a good strategy to increase enantioselectivity because it creates a substituent too large for the S_1' pocket. For example, compounds **9a–11a** contain very large aryl groups. The poor fit of this aryl group in the S_1' pocket destabilizes reaction of the (*R*)-enantiomer. Subtilisins favor the (*S*)-enantiomer in these cases, but the enantioselectivity is usually low.

This model also rationalizes how changing the organic solvent can increase the enantioselectivity of subtilisins. The enantioselectivity of subtilisin Carlsberg toward 1-phenethyl alcohol (**1**) increases

increases from $E = 3$ (*S*) in acetonitrile to $E = 54$ (*S*) in benzene, likely due to better solvation of the solvent-exposed phenyl substituent in benzene as compared to acetonitrile.² Researchers previously explained changes in enantioselectivity of subtilisins toward chiral acids using a similar rationale for solvation of the solvent-exposed groups,^{9,10} but our model is the first to use this approach for chiral alcohols.

Unlike subtilisins, which bind substrates in an extended conformation,¹¹ lipases bind substrates in a folded conformation.¹² This folding and the deeper hydrophobic pockets in lipases place both substituents of typical secondary alcohols in hydrophobic pockets that substantially shield the substituents from the solvent.¹³ For this reason, the enantioselectivity of lipase-catalyzed resolutions of secondary alcohols shows less variation with changes in substituent polarity¹⁴ or solvent.¹⁵ The SI shows that lipase from *Burkholderia cepacia* (PCL) favors the (*R*)-enantiomer for all compounds in Table 1 and shows no reversal in enantiopreference upon changing from water to organic solvent.

In conclusion, this revised model of the enantioselectivity of subtilisins toward secondary alcohols is consistent with the structure of subtilisin, rationalizes why enantioselectivity changes and even reverses with changes in solvent, and provides a strategy to increase enantioselectivity by modifying the substrate.

Acknowledgment. We thank McGill University and University of Minnesota for financial support, Dr. F. Schendel and R. Dillingham (University of Minnesota Biotechnology Institute) for the large-scale fermentation and purification of subtilisins BPN' and E and the Minnesota Supercomputing Institute for access and support for molecular modeling computers and software.

Supporting Information Available: Synthesis of compounds **1a–13a**, determination of absolute configuration, preparation of subtilisin E and BPN', molecular modeling details for **1a**, and enantioselectivity data. This material is available free of charge via the Internet at <http://pubs.acs.org>.

References

- (1) (a) Faber, K. *Biotransformations in Organic Chemistry*, 5th ed.; Springer-Verlag: Berlin, 2004. (b) Drauz, K.; Waldman, H., Eds. *Enzyme Catalysis in Organic Synthesis*; Wiley-VCH: Weinheim, Germany, 2002. (c) Bornscheuer, U. T.; Kazlauskas, R. J. *Hydrolases in Organic Synthesis: Regio- and Stereoselective Biotransformations*; Wiley-VCH: Weinheim, Germany, 1999.
- (2) Fitzpatrick, P. A.; Klivanov, A. M. *J. Am. Chem. Soc.* **1991**, *113*, 3166.
- (3) Kazlauskas, R. J.; Weissfloch, A. N. E. *J. Mol. Catal. B: Enzym.* **1997**, *3*, 65.
- (4) (a) Jain, S. C.; Shinde, U.; Li, Y.; Inouye, M.; Berman, H. M. *J. Mol. Biol.* **1998**, *284*, 137. The crystal structure of subtilisin Carlsberg, where crystals have been soaked in acetonitrile or dioxane to be nearly indistinguishable from the structure determined in water; (b) Fitzpatrick, P. A.; Steinmetz, A. C. U.; Ringe, D.; Klivanov, A. M. *Proc. Natl. Acad. Sci. U.S.A.* **1993**, *90*, 8653. (c) Schmitke, J. L.; Stern, L. J.; Klivanov, A. M. *Proc. Natl. Acad. Sci. U.S.A.* **1997**, *94*, 4250.
- (5) Chen, C. S.; Fujimoto, Y.; Girdaukas, G.; Sih, C. J. *J. Am. Chem. Soc.* **1982**, *104*, 7294.
- (6) Savile, C. K.; Magloire, V. M.; Kazlauskas, R. J. *J. Am. Chem. Soc.* **2005**, *127*, 2104.
- (7) Mugford, P. F.; Magloire, V. M.; Kazlauskas, R. J. *J. Am. Chem. Soc.* **2005**, *127*, 6536.
- (8) $\log P/P_0$ is the substituent hydrophobicity partition coefficient relative to hydrogen.
- (9) (a) Margolin, A. L.; Tai, D.-F.; Klivanov, A. M. *J. Am. Chem. Soc.* **1987**, *109*, 7885. (b) Sakurai, T.; Margolin, A. L.; Russell, A. J.; Klivanov, A. M. *J. Am. Chem. Soc.* **1988**, *110*, 7236. (c) Tawaki, S.; Klivanov, A. M. *J. Am. Chem. Soc.* **1992**, *114*, 1882.
- (10) Wangikar, P. P.; Rich, J. O.; Clark, D. S.; Dordick, J. S. *Biochemistry* **1995**, *34*, 12302.
- (11) Tyndall, J. D. A.; Tessa Nall, T.; Fairlie, D. P. *Chem. Rev.* **2005**, *105*, 973.
- (12) For example: Mezzetti, A.; Schrag, J.; Cheong, C. S.; Kazlauskas, R. J. *Chem. Biol.* **2005**, *12*, 427.
- (13) Cygler, M.; Grochulski, P.; Kazlauskas, R. J.; Schrag, J. D.; Bouthillier, F.; Rubin, B.; Serreqi, A. N.; Gupta, A. K. *J. Am. Chem. Soc.* **1994**, *116*, 3180.
- (14) Hönig, H.; Shi, N.; Polanz, G. *Biocatalysis* **1994**, *9*, 61.
- (15) (a) Parida, S.; Dordick, J. S. *J. Am. Chem. Soc.* **1991**, *113*, 2253. (b) Cernia, E.; Palocci, C.; Soro, C. *Chem. Phys. Lipids* **1998**, *93*, 157.

JA0528937